

**Microbial ecology in saline wetlands:
nitrogen, flamingos and drought as drivers**



**Universidad de Granada
Departamento de Ecología**

Gema Laura Batanero Franco

Tesis Doctoral

Julio 2019

Programa de Biología Fundamental y de Sistemas

**Microbial ecology in saline wetlands:
nitrogen, flamingos and drought as drivers**



**Universidad de Granada
Departamento de Ecología**

Gema Laura Batanero Franco

Tesis Doctoral

Julio 2019

Programa de Biología Fundamental y de Sistemas

Editor: Universidad de Granada. Tesis Doctorales
Autor: Gema Laura Batanero Franco
ISBN: 978-84-1306-294-5
URI: <http://hdl.handle.net/10481/56847>

El presente trabajo se ha desarrollado en los laboratorios del Instituto Universitario del Agua y del Departamento de Ecología en la Facultad de Ciencias de la Universidad de Granada. La investigación realizada ha sido financiada por el Ministerio de Educación y Ciencia y de Economía y de Competitividad del Gobierno de España a través de los proyectos de investigación con referencia CGL2010-15812 y CGL2014-52362-R incluyendo fondos FEDER. Durante la duración de esta tesis he disfrutado de una beca del programa de Formación de Personal Investigador con referencia BES-2011-043658, asociada al proyecto mencionado anteriormente.

Los recursos informáticos han sido facilitados por los proyectos CGL2013-47558-P y por los los proyectos CGL2017-86626-C2-2-P, incluyendo fondos FEDER.

*A mi Madre y
Miguel*

Aknowledgements/Agradecimientos

En primer lugar, mi más sincero agradecimiento a mis Directores de Tesis; Isabel Reche, por brindarme la oportunidad de adentrarme en el sorprendente mundo de la ciencia, y transmitirme como nadie, su entusiasmo y gran optimismo, durante este largo recorrido, no exento de obstáculos, y Andy Green, por su ayuda desinteresada, y estar siempre dispuesto a resolver dudas.

A mis compañeros del departamento de Ecología e Instituto del Agua, con los que he compartido muchas horas de trabajo, y me han acompañado durante este largo proceso; Nacho, Eli, Mohammad, Gaetano, Marcos, Ali, Fátima, Emilio, Ada, Ana. En especial quiero agradecer a Alba, por estar siempre dispuesta echarme una mano, acompañada con una grata sonrisa, y, por último, agradecer a mi compañera y amiga Tere, por sus visitas que me han dado fuerzas para seguir adelante.

No puedo olvidarme del equipo técnico, haciendo mención especial a Eulogio y Alejandra por la gran ayuda prestada. A Josefa Antón por ayudarnos con toda la logística durante el trabajo de campo realizado en salinas de Santa Pola. A Marion Vittecoq por ofrecernos su ayuda durante los muestreos realizados en la Camarga francesa. A Francisco Perfectti por acompañarnos y arrimar el hombro durante jornadas interminables de trabajo de campo y por ser nuestro fotógrafo oficial. A Platero, por darme un curso personalizado de Análisis de Secuenciación Masiva, del que he aprendido y obtenido enormes beneficios. Y a Domingo, por aportar sus conocimientos del ámbito de la teledetección. Sin todos ellos, esta Tesis no hubiese sido posible.

Dar las gracias a los compañeros del laboratorio en la Universidad de British Columbia, en Vancouver, por todas las facilidades que me ofrecieron durante mi estancia, agradeciendo especialmente a Curtis y Amy, por haberme hecho sentirme como en casa.

A mis amigos, por ser tan especiales, habiéndome ayudado en este proceso de Tesis, sin hablarme de ciencia;

A Paquillo por acompañar, y estar siempre dispuesto a ayudarme, mi amigo incondicional.

A Abraham, por conseguir que esta Tesis luzca mejor.

A mi primo Javi, que me ha guiado y ayudado durante toda la tesis.

A mi compañero Pablo, por su enorme paciencia y quererme tanto.

Y finalmente agradecer a mi familia más directa; mi madre ha sido el pilar fundamental en mi vida, mostrándome el camino y aunque ya no está con nosotros, es la que ha hecho posible que yo finalice este arduo camino. Gracias por enseñarme, educarme y por tu amor incondicional. Y a ti Miguel, por haber estado siempre ahí, escuchándome y aconsejándome.

INDEX

Summary (in English)	01-04
Resumen	05-09
Introduction	10-28
Chapter 1: Material and methods	29-58
1.1. Sampling and study sites	29-41
1.1.1. Regional-scale sampling in western Mediterranean saline wetlands	
1.1.2. Time-scale sampling in Fuente de Piedra lake	
1.1.3. Experimental design of guano addition	
1.2. Methodology	41-55
1.2.1 Physico - Chemical analyses	
1.2.1.1. Salinity, Temperature and pH	
1.2.1.2. Total phosphorus (TP), total dissolved phosphorus (TDP) and soluble reactive phosphorus (SRP) concentration	
1.2.1.3. Total nitrogen (TN) and total dissolved nitrogen (TDN) concentration	
1.2.1.4. Total organic carbon (TOC) and dissolved organic carbon (DOC) concentration	

1.2.2. Biological analyses	
1.2.2.1. Chlorophyll a	
1.2.2.2. Abundance of total prokaryotes, heterotrophic prokaryotes and cyanobacteria	
1.2.2.3. Abundance of viruses	
1.2.2.4. Bacterial production and archaeal production	
1.2.2.4. Bacterial production and archaeal production	
1.2.2.5. Bacterial community structure in Fuente de Piedra lake	
Collection of free-living and particle-attached bacterial assemblages	
DNA samples processing	
i. Extraction of DNA	
ii. Construction of 16S libraries and Illumina MiSeq	
iii. Processing and analysis of Illumina sequencing data in QIIME and Mothur	
iv. Alpha diversity	
v. Temporal Beta diversity	

1.3. References	56-57
------------------------	-------

Chapter 2: Alternation of bacterial and archaeal heterotrophic production along nitrogen and salinity gradients in coastal wetlands	59-86
--------------------------------------------------------------------------------------------------------------------------------------------	-------

2.1. Introduction	62-64
--------------------------	-------

2.2. Materials and methods	64-68
-----------------------------------	-------

2.3. Results	68-77
---------------------	-------

2.4. Discussion	78-79
------------------------	-------

2.5. References	80-86
------------------------	-------

Chapter 3: Flamingos and drought as drivers of nutrients and microbial dynamics in a saline lake	87-120
---------------------------------------------------------------------------------------------------------	--------

3.1. Introduction	90-91
--------------------------	-------

3.2. Materials and methods	92-97
-----------------------------------	-------

3.3. Results	98-108
---------------------	--------

3.4. Discussion	109-113
------------------------	---------

3.5. References	114-120
------------------------	---------

Chapter 4: Drought-reduction in lake area declines bacterial richness and increases temporal β diversity	121-162
4.1. Introduction	124-126
4.2. Materials and methods	126-134
4.3. Results	134-146
4.4. Discussion	146-153
4.5. References	154-162
Discussion	160-172
Conclusions (in English)	173-176
Conclusions (in Spanish)	177-180
List of abbreviations	182
Annex Chapter 1	185-192
Annex Chapter 2	193-210
Annex Chapter 4	211-216
Annex Photos	217-245

SUMMARY

Wetlands are valuable ecosystems due to their ability to reduce external nutrient loading and act as carbon sinks (Verhoeven *et al.* 2006; Li *et al.* 2017). However, this ability of wetlands to maintain water quality by reducing nitrogen loading and promoting carbon sequestration is being negatively affected by the excess nutrients associated to agriculture and urbanization taking the Earth's system to its planetary limits (Steffen *et al.* 2015). Among them, saline wetlands represent approximately 44% of the total volume of inland waters and 23% of the lake area (Messenger *et al.* 2016). Saline wetlands are classified into endorheic systems (atalasohaline waters) and coastal lagoons and marshes (talasohaline waters). Despite this global prevalence of saline wetlands and their biogeochemical relevance, microbial ecology in these systems has received little attention compared to freshwater ecosystems (Hahn 2006).

In this thesis, we have focused on the study of microbial ecology in saline wetlands located in the Mediterranean region including a wide gradient of salinity from oligosaline to hypersaline waters. We have selected nine coastal wetland complexes along the Mediterranean basin from the Odiel Marshes in Huelva (Spain) in the western side to the Sfax (Tunisia) in the eastern side, and the Fuente de Piedra lagoon, located in southern Spain, as an endorheic system. These saline wetlands are refuges, foraging sites and nesting sites for migratory waterbirds, in particular, the flamingo (Rendón *et al.* 2001, Rendón-Martos *et al.* 2000, Green and Elmberg, 2014).

In coastal wetlands, the maximum prokaryotic heterotrophic production and the cyanobacterial abundance were observed in eusaline waters. The predictor variable of the archaeal heterotrophic production (measured as the incorporation of 3H-leucine in proteins) was the concen-

tration of total dissolved nitrogen. On the contrary, bacterial heterotrophic production showed a negative correlation with total dissolved nitrogen. However, viruses that were negatively related to the heterotrophic production of bacteria probably mediated this inverse relationship. There was no correlation between archaeal heterotrophic production and virus abundance.

We have observed that coastal wetlands show values of prokaryotic heterotrophic production higher than the values in Fuente de Piedra lagoon. Phosphorus concentration seems to be the limiting factor in the growth of heterotrophic prokaryotes in this lagoon, reaching the maximum production and heterotrophic abundance in euhaline waters coupled with the dynamics of flamingos. To study this effect in depth, we analyzed the impact of high flamingo densities on both nutrient dynamics and microbial dynamics in Fuente de Piedra lagoon during a wet and a dry hydrological year. Finally, we determined experimentally the effects of the addition of guano from flamingos on the growth of heterotrophic prokaryotes. The concentration of dissolved organic carbon and total nitrogen in the lagoon was 2-3 times higher during the dry year and was positively related to salinity. On the other hand, the population dynamics of flamingos was coupled to the prokaryotic heterotrophic production, which triggered a cascading effect increasing the abundance of prokaryotes, the abundance of viruses and, finally, the concentration of dissolved nitrogen. The stimulation of heterotrophic prokaryotes was associated with soluble phosphorus inputs released from sediments by the bioturbation of flamingos within the lagoon during feeding and wading. Guano addition experiments confirmed the P-limitation of the heterotrophic prokaryotes. This study demonstrates that microbial activity in this endorheic wetland is probably limited by the availability of soluble phosphorus, which ultimately depends on the abundance of flamingos.

On the other hand, at the ecosystem level, meteorological conditions (evaporation vs. precipitation) were determinant in the nutrient dynamics and in the microbial dynamics of Fuente de Piedra lagoon. In fact, drought in endorheic wetlands can shorten the hydroperiod due to a high evaporation rate, affecting the lagoon's water level and, ultimately, the inundation area with important implications for species diversity. We have explored the effects of changes in the inundation area of Fuente de Piedra Lagoon, salinity, and flamingo population on the richness, diversity, and composition of the bacterial community, including both free-living and particle-attached communities. Statistical analyses indicated that the best predictor of the bacterial community was the inundation area. We observed a decrease in bacterial richness and diversity, in terms of observed OTUs and the Shannon index as the inundation area was smaller. A change in composition during the two hydrological years (beta temporal diversity) was also observed as a result of the reduction in the inundation area during the dry period. This effect was consistent for both free-living and particle-attached bacteria, although the magnitude of the impact was greater on free-living bacteria. Free-living bacteria are likely to be more affected by external environmental factors, while the dynamics of bacteria attached to particles may be more linked to their own organization within the biofilms. In fact, we observed that the richness, diversity and renewal rate of bacteria attached to particles was greater than their free-living equivalent, regardless of the wet or dry year.

These findings are of interest due to predictions of severe droughts, as consequences of climate change, which are likely to lead to massive salinization of wetlands (Herbert *et al.* 2015) and, subsequent, desiccation (Wurtsbaugh *et al.* 2017; Wang *et al.* 2018). In general, we have observed that the dynamics of heterotrophic prokaryotes are completely different in coastal wetlands and in an endorheic system such as Fuente de Piedra Lagoon. Nitrogen concentration is key in coastal wetlands, whereas the reduction of the inundation area is a main driver of the richness, diversity and composition of bacteria in periods of drought in Fuente de Piedra lagoon with potential effects on its ecosystem services.

RESUMEN

Los humedales son ecosistemas con valor ecológico por su gran capacidad para reducir la carga externa de nutrientes y por actuar como sumideros de carbono (Verhoeven *et al.* 2006; Li *et al.* 2017). Sin embargo, esta capacidad de los humedales de mantener la calidad del agua reduciendo la carga de nitrógeno y propiciando el secuestro de carbono se está viendo afectada negativamente debido al exceso de nutrientes procedentes sobretudo de la agricultura y la urbanización del territorio llevando al sistema Tierra a sus límites planetarios (Steffen *et al.* 2015). Entre ellos, los humedales salinos representan aproximadamente el 44% del volumen total de las aguas continentales y un 23% de la superficie lacustre (Messenger *et al.* 2016). Los humedales salinos los clasificamos en sistemas endorreicos (aguas atalasoalinas) y en lagunas costeras y marismas (aguas de talasoalinas). A pesar de esta prevalencia global de los humedales salinos y de su gran importancia a nivel biogeoquímico, su ecología microbiana ha recibido poca atención en comparación con los ecosistemas de agua dulce (Hahn 2006).

En esta tesis nos hemos centrado en el estudio de la ecología microbiana en humedales salinos ubicados en la región Mediterránea incluyendo un amplio gradiente de salinidad desde aguas oligosalinas a hipersalinas. Hemos seleccionado nueve complejos de humedales costeros a lo largo de la cuenca Mediterránea desde las Marismas de Odiel en Huelva (España) por occidente hasta las salinas de Sfax (Túnez) por oriente, y la laguna de Fuente de Piedra, localizada al sur de España, como sistema endorreico. Estos humedales salinos se caracterizan por ser refugio, lugar de forrajeo y nidificación para numerosas aves acuáticas migratorias, en particular el flamenco (Rendón *et al.* 2001, Rendón-Martos *et al.* 2000, Green y Elmberg, 2014).

En los humedales costeros, los máximos de producción heterotrófica de procariotas y de abundancia de cianobacterias fueron observados en las aguas eusalinas. La variable predictora de la producción heterotrófica de arqueas (medida como incorporación de 3H-leucina en proteínas) fue la concentración de nitrógeno total disuelto. Por el contrario, la producción heterotrófica bacteriana mostró una correlación negativa con el nitrógeno disuelto total. Sin embargo, esta relación inversa probablemente vino mediada por los virus que estuvieron negativamente relacionados con la producción heterotrófica de bacterias. No hubo una correlación entre producción heterotrófica de arqueas y la abundancia de virus.

Hemos observado que los humedales costeros muestran valores de producción heterotrófica de procariotas más elevados que la laguna de Fuente de Piedra. El fósforo parece ser el factor limitante en el crecimiento de los procariotas heterótrofos en esta laguna, alcanzado el máximo de producción y de abundancia heterotrófica en las aguas eusalinas acoplado a la dinámica de los flamencos. Para estudiar en profundidad este efecto, analizamos el impacto de las altas densidades de flamencos tanto sobre la dinámica de nutrientes como sobre la dinámica microbiana en la laguna de Fuente de Piedra durante un año hidrológico húmedo y otro año seco. Finalmente, determinamos experimentalmente los efectos de la adición de guano procedente de flamencos sobre el crecimiento de los procariotas heterotróficos. La concentración de carbono orgánico disuelto y nitrógeno total en la laguna fueron 2-3 veces más elevada durante el año seco y se relacionaron positivamente con la salinidad. Por otro lado, la dinámica poblacional de los flamencos estuvo acoplada a la producción heterotrófica de procariotas, lo que desencadenó un efecto en cascada incrementando la abundancia de procariotas, la abundancia de virus y, finalmente,

de nitrógeno disuelto. El estímulo de los procariontes heterotróficos se asoció con entradas de fósforo soluble liberado desde el sedimento por la bioturbación de los flamencos dentro de la laguna durante su alimentación y vadeo. Los experimentos de adición de guano confirmaron la limitación de P de los procariontes heterotróficos de esta laguna endorreica. Este estudio demuestra que la actividad microbiana en este humedal endorreico probablemente se ve limitada por la disponibilidad de fósforo soluble que, en última instancia, depende de la abundancia de flamencos.

Por otro lado, a nivel ecosistémico, las condiciones meteorológicas (evaporación vs. precipitación) fueron determinantes en la dinámica de nutrientes y en la dinámica microbiana de la laguna de Fuente de Piedra. De hecho, la sequía en humedales endorreicos puede acortar el hidropereodo debido a una elevada tasa de evaporación, afectando al nivel de agua de la laguna y, en última instancia, al área de inundación con importantes implicaciones para la diversidad de especies. Hemos explorado los efectos de los cambios en el área de inundación de la laguna de Fuente de Piedra, la salinidad y la población de flamencos sobre la riqueza, diversidad y composición de la comunidad bacteriana, incluyendo tanto las de vida libre como las adheridas a partículas. Los análisis estadísticos indicaron que el mejor predictor de la comunidad bacteriana era el área de la laguna. Se observó una disminución de la riqueza y diversidad bacteriana, en términos de OTUs observados y del índice de Shannon. También se apreció un cambio en la composición durante los dos años hidrológicos (beta diversidad temporal) como resultado de la reducción del área de la laguna durante el año seco. Este efecto fue consistente tanto para las bacterias de vida libre como para las adheridas a partículas, aunque la magnitud del impacto fue mayor en las bacterias de vida libre. Probablemente las bacterias de vida libre se vean más afectadas por factores externos ambientales, mientras que la dinámica de las bacterias adheridas a partículas podrían estar más vinculada a su propia organización dentro de las biopelículas. De hecho, observamos que la riqueza, diversidad y tasa de renovación de las bacterias adheridas a partículas fue mayor que su equivalente con estilo de vida libre, independientemente del año húmedo o seco.

Estos hallazgos tienen un interés debido a las predicciones de sequías severas, como consecuencias del cambio climático, que probablemente conducirán a una salinización generalizada de los humedales (Herbert *et al.* 2015) y posterior desecación (Wurtsbaugh *et al.* 2017; Wang *et al.* 2018). En general, hemos observado que la dinámica de los

procariotas heterótrofos es completamente diferente en los humedales costeros y en un sistema endorreico como la laguna de Fuente de Piedra. La concentración de nitrógeno resulta clave en humedales costeros, mientras que la reducción del área de inundación resultan determinantes de la riqueza, diversidad y composición de las bacterias en períodos de sequía en la laguna de Fuente de Piedra con posibles efectos sobre sus servicios ecosistémicos.

References

- Green, A.J., Elmberg, J. (2014). Ecosystem services provided by waterbirds. *Biol. Rev.* 89, 105–122.
- Hahn MW. (2006). The microbial diversity of inland waters. *Current Opinion in Biotechnology* 17: 256-261.
- Herbert, E.R., P. Boon, A.J. Burgin, S.C. Neubauer, R.B. Franklin, M. Ardón, K.N. Hopfensperger, L.P.M. Lamers, *et al.* 2015. A global perspective on wetland salinization: Ecological consequences of a growing threat to freshwater wetlands. *Ecosphere* 6: 1–43.
- Li Y, Zhang C, Wang N, Han Q, Zhang X, Liu Y, Xu L, Ye W. (2017). Substantial inorganic carbon sink in closed drainage basins globally. *Nat Geosci* 10:501–506.
- Messenger, M. L. Mathis Lörcher, Bernhard Lehner, Günther Grill, Irena Nedeva & Oliver Schmitt. (2016). Estimating the volume and age of water stored in global lakes using a geo-statistical approach. *Nat. Commun.* 7, 13603 doi: 10.1038/ncomms13603.
- Rendón-Martos M, Vargas JM, Rendón MA, Garrido A, Ramírez JM (2000). Nocturnal movements of breeding greater flamingos in Spain. *Waterbirds* 23(Special Publ. 1):9–19.
- Rendón, M.A., Garrido, A., Ramírez, J.M., Rendón-Martos, M. & Amat, J.A. (2001). Despotism establishment of breeding colonies of greater flamingos, *Phoenicopterus ruber*, in southern Spain. *Behavioral Ecology and Sociobiology*, 50, 55–60.
- Steffen, W., Richardson, K., Rockström, J., Cornell, S.E., Fetzer, I., Bennett, E.M., Biggs, R., Carpenter, S.R., De Vries, W., De Wit, C.A., Folke, C., Gerten, D., Heinke, J., Mace, G.M., Persson, L.M., Ramanathan, V., Reyers, B. and Sörlin, S. (2015). Planetary boundaries: guiding human development on a changing planet. *Science*, 347, doi 10.1126/science.1259855.
- Wang, J., Song, C., Reager, J.T., Yao, F., Famiglietti, J.S., Sheng, Y., MacDonald, G.M., Brun, F., Schmied, H.M., Marston, R.A., Wada, Y., 2018. Recent global decline in endorheic basin water storages. *Nat. Geosci.* 11, 926–932
- Wurtsbaugh WA, Miller C, Null SE, DeRose RJ, Wilcock P, Hahnenberger M, Howe F, Moore J. (2017). Decline of the world's saline lakes. *Nat Geosci* 10:816–821. <https://doi.org/10.1038/NGEO3052>.

Introduction

Introduction



Wetlands are among the most valuable ecosystems in the Earth characterized by an elevated biological production and spatial and temporal heterogeneity. Consequently, they contain an extremely high functional and species diversity (Mitsch & Gosselink, 2000, Mitsch *et al.* 2015). Among the ecosystem services they provide, wetlands have a water purification function, reducing the nutrient loading from through-flowing water, so much that they have been described as “the kidneys of the landscape” (Mitsch *et al.* 2015). Many of the processes involved in wetland functions are mediated by microbial activities such as denitrification and organic carbon mineralization. However, water quality functions of wetlands have been severely impaired by the nutrient enrichment derived from the agriculture, industry and urbanization. Steffen *et al.* (2015) have highlighted that the biochemical flows, in particular the nitrogen cycle, have overcome the planetary boundary (i.e. they have exceeded the safe boundaries), suggesting a high risk to suffers of irreversible damages to the Earth system (Steffen *et al.* 2015; Meier, 2017, Figure 1).

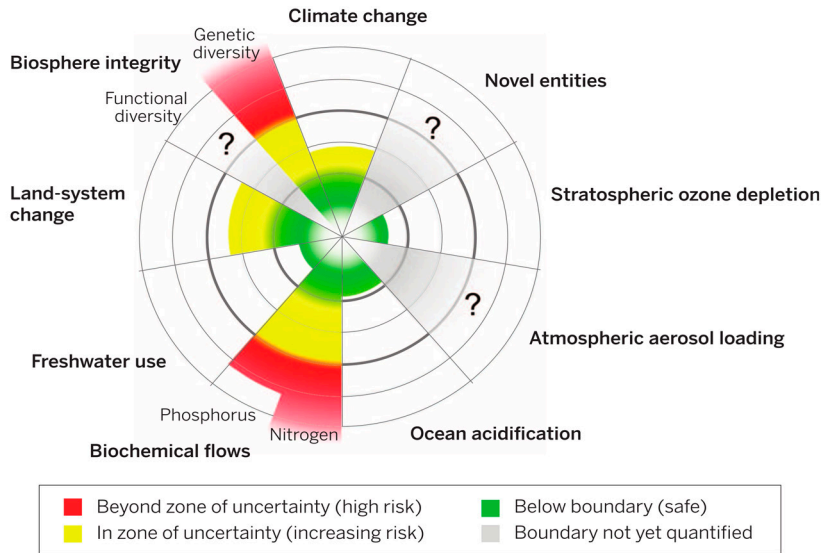


Figure 1. Planetary boundaries of seven of nine variables control according to Steffen et al. 2015. Green areas indicate the safe operating space, yellow represents the areas of uncertainty (increasing risk), red represents the areas of a high-risk and gray areas represent processes for which safe margins have not yet been determined.

Note: Nitrogen flow has crossed the high risk boundary.

These risks have promoted the restoration or construction of wetlands (Young, 1996) to control water quality through nutrient recycling and thereby protecting shorelines and biodiversity (Verhoeven et al. 2006).

In particular, saline wetlands, characterized by salinities higher than 1ppt, constitute about 44% of Earth's water volume and 23% of its lake surface (Messenger et al. 2016). Amongst saline wetlands, it is convenient to discriminate between endorheic systems (athalassic saline waters) and coastal lagoons and marshes (thalassic saline waters). Figure 2 shows a classification of water systems according to salinities, distinguishing between non-marine saline waters (athalassic) and those ones of marine origins (thalassic). Consequently, ionic composition of thalassic waters is similar to seawater (mainly Cl^- and Na^+ ions); while athalassic ones diverge from this composition, including high proportions of K^+ , Mg^{2+} and Ca^{2+} and anionic species as SO_3^{-4} , HCO_3^- and CO_3^{2-} .

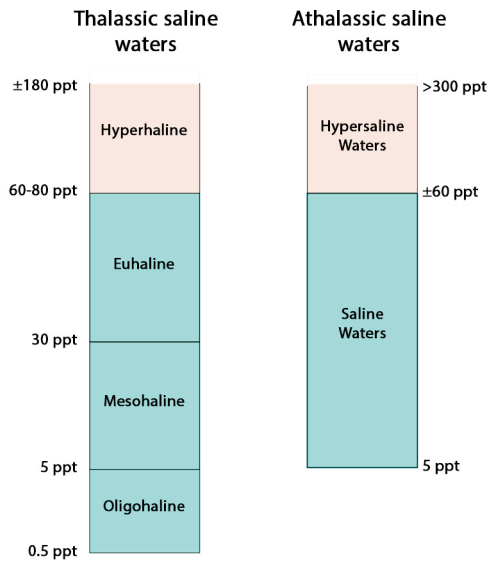


Figure 2. Categorization of waters based on salinities (modified from Por, 1972)

Endorheic systems, which constitute about 75% of saline wetlands, are located in arid and semiarid regions (Meybeck, 1995; Wurtsbaugh *et al.* 2017). They are in closed drainage basins that retain water and allow no outflow to other bodies of water such as rivers or oceans (Figure 3). Because most saline lakes are hydrologically terminal, materials (nutrients, organic matter, ions such as sulphates, Ca and Mg) largely remain within the basin resulting in high dissolved inorganic and organic carbon concentrations and high water residence times (Anderson & Stedmon 2007, Ortega-Retuerta *et al.* 2007; Figure 2). Consequently, they are extremely productive systems (Eiler *et al.* 2003, Batanero *et al.* 2017). As an example, Batanero *et al.* (2017) found extremely high prokaryotic heterotrophic abundance (296×10^6 cells ml^{-1}) and production (2.25 nmoles of leucine $\text{l}^{-1}\text{h}^{-1}$) in endorheic lake of Fuente de Piedra (Malaga, Spain; Figure 3).

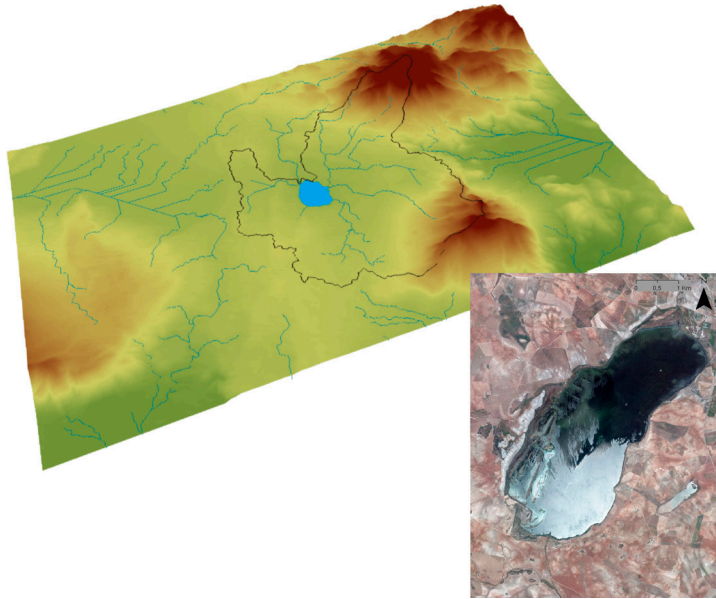


Figure 3. Illustration showing representative endorheic system (top; <https://geogeek.xyz/demarcation-of-endorheic-basins-in-arcgis.html>) and Orthophoto (<http://ws041.juntadeandalucia.es/medioambiente/dlidar/index.action>) of the endorheic Fuente de Piedra lake, Málaga, Spain (bottom right).

In contrast, coastal lagoons and marshes are located in depressions of terrain, which have been flooded by the effect of tides or due to river intrusion in estuaries zones, resulting in systems with high Cl^- and Na^+ contents. These systems present low water residence times and, consequently, high water renovation rates of nutrients and oxygen. In this case, a continuous nutrient supply promotes high biological productivities (López-Archilla *et al.* 2004a, Roehm 2005, Geertz-Hansen *et al.* 2011).

On the other hand, saline wetlands have a substantial role in the context of global carbon cycle, being recognized as potential global carbon sinks (Mcleod *et al.* 2011; Fourqurean *et al.* 2012, Li *et al.* 2017). In particular, endorheic wetlands tend to have high pH, the dissolved inorganic carbon is mostly present as HCO_3^- and CO_3^{2-} ions and not as CO_2 , counteracting atmospheric carbon dioxide emissions (Duarte *et al.* 2008). Besides, saline wetlands are characterized by having high sedimentation rates (Jellison *et al.* 1996, Finlay *et al.* 2009), which can promote flocculation process of transparent exopolymeric particles in systems with high ionic strengths (de Vicente *et al.* 2010). Therefore, coastal lagoons and marshes are considered global reservoirs for organic carbon because of their elevated primary productivity and high sedimentation rates that in the long-term minimize carbon dioxide emissions to the atmosphere.

Therefore, these are considered carbon sinks (Roehm 2005, Geertz-Hansen *et al.* 2011). However, despite their global prevalence and biogeochemical significance, the microbial ecology of saline wetlands has received little attention, in comparison with freshwaters, dynamic saline systems such as estuaries (Crump *et al.* 2004), or hypersaline solar salterns (Casamayor *et al.* 2002) (Hahn, 2006; Figure 4).

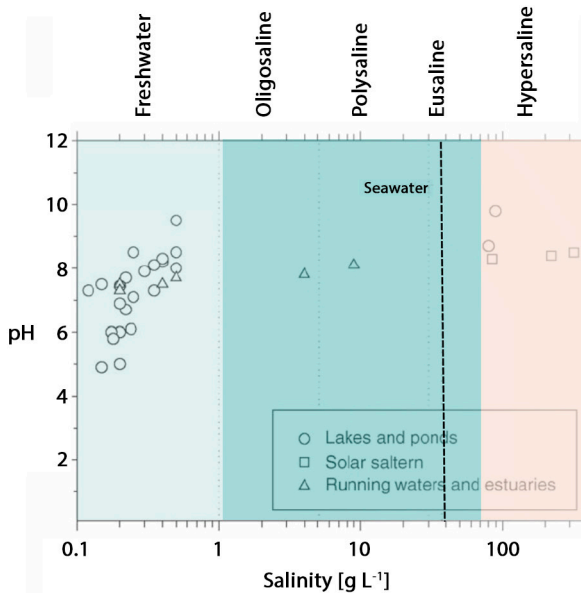


Figure 4. Underrepresentation of studies in saline waters in the range from oligosaline to eusaline (modified from Hahn, 2006).

Despite the evidence that microbial component is the compartment with the most metabolic and genetic diversity (Woese 1987) and subsequent, it plays a crucial role in global nutrient cycles (Hahn 2006), there are few studies linking their biogeochemical peculiarities with the predominant microbial community particularly in the range from oligo- to eusaline waters. Although viruses are considered to be the largest reservoir of genetic diversity on Earth (Hambly and Suttle 2005), the knowledge about viroplankton in saline inland waters is even more limited (Sandaa *et al.* 2003).

Currently, predictions of severe salinization on wetland as a consequence of anthropogenic climate change are of particular interest due to their relevant functions (Neubauer and Craft 2009, Herbert *et al.* 2015). The causes of this salinization are diverse and vary depending on the source of saline water (Herbert *et al.* 2015). For instance, the salinization

in endorheic wetlands occurs by evapoconcentration, which has increased due to climatic warming that alters the water balance. In fact, recent works have revealed world's wetlands desiccation at alarming rates, due to global warming and droughts linked to climatic change (Wurtsbaugh *et al.* 2017; Wang *et al.* 2018), leading to salinities above normal levels (Herbert *et al.* 2015; Jeppesen *et al.* 2015). In contrast, salinization in coastal lagoons and marshes occurs by saltwater intrusions linked to the sea level rise (Herbert *et al.* 2015, Park *et al.* 1989, Eliot *et al.* 1999). Recent conservative projections have pointed out that, on average, the sea level will increase by about 0.50 m by 2100 (Vousdoukas *et al.* 2018, Schuerch *et al.* 2018; Figure 5).

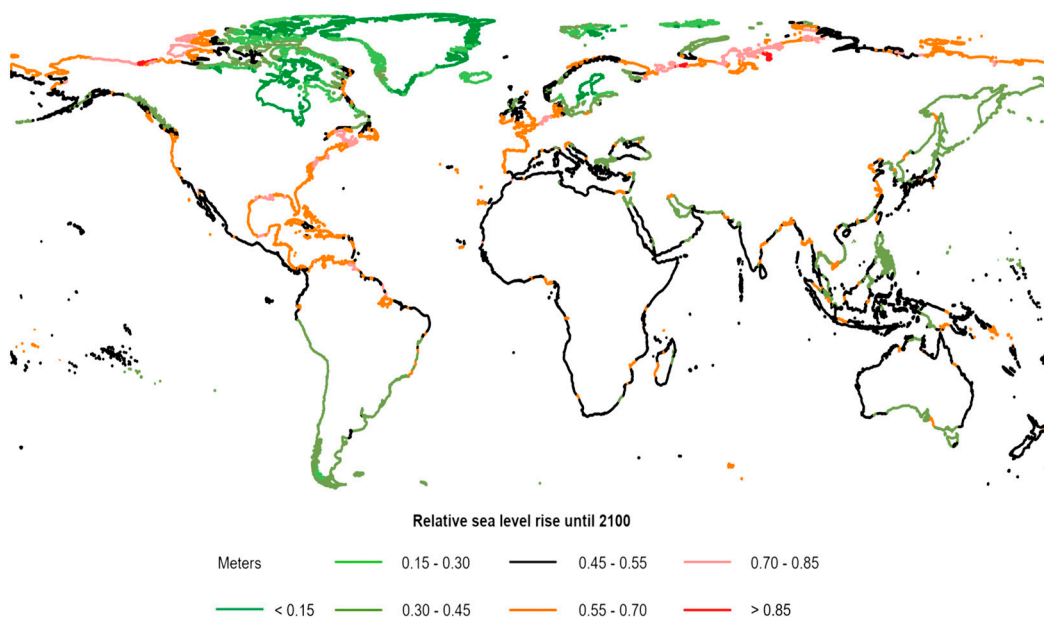


Figure 5. Simulation map of total sea-level rise in meters a moderate scenario during the period from 2010 to 2100, according to Schuerch *et al.* (2018).

Salinization alters the water and sediment chemistry, changing the dominant biogeochemical reactions at day or week scales, and induces shifts in the microbial community that drive the element cycles (Herbert *et al.* 2015; Figure 6). Although there are still great uncertainties about how salinization affects wetland biogeochemistry, it is clear that it increases the release of inorganic nitrogen (NH_4^+) and phosphorus (PO_4^{3-}) with implications for internal wetland eutrophication (Ardón *et al.* 2013, Lamers *et al.* 2001, 2002, Weston *et al.* 2006; Figure 6). In addition, salinization increases the generation of toxic sulfides (Lamers

et al. 1998; Figure 6), which play an important role in wetlands N cycling, inhibiting the final steps of denitrification and resulting in the emission of nitrogen oxides (Brunet and Garcia-Gil 1996, Laverman *et al.* 2007) with well-known implications for global nitrogen cycle. Another evidence of salinization in wetlands is the increased organic carbon mineralization by microbial pathways, promoting the atmospheric carbon dioxide emissions and, consequently, increasing their contribution to greenhouse effect (Chambers *et al.* 2011, Weston *et al.* 2011, Neubauer *et al.* 2013).

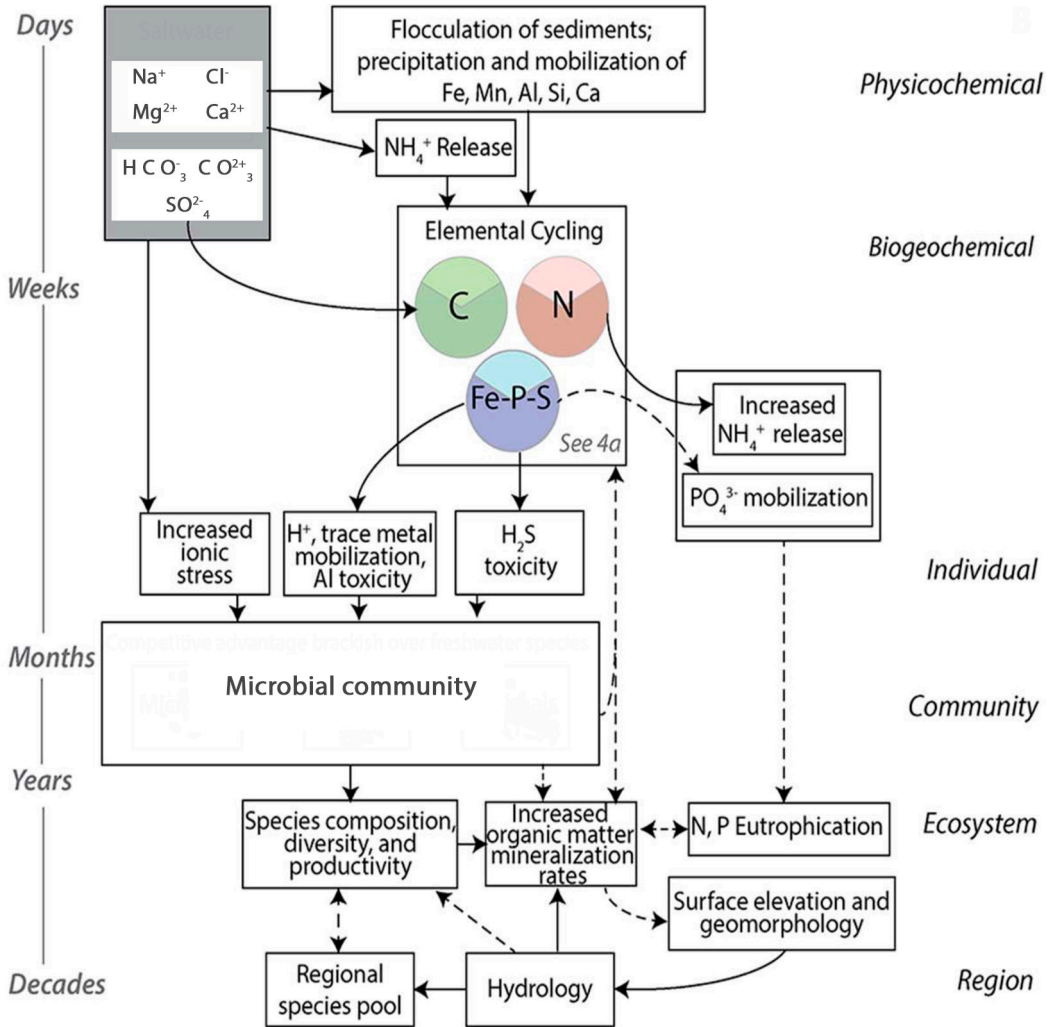


Figure 6. Predicted ecosystem effects of salinization (modified from Herbert *et al.* 2015). Composition ionic of saline waters intrusion (grey box). Solid arrows indicate pathways for which there is a high degree of consensus for the expected direction of change, while dashed lines indicate pathways for which there is little research or conflicting predictions regarding the expected direction of change.

Overall, many of the ecosystem services provided by wetlands are disrupted by salinization, such as their capacity to sequester carbon, and to remove phosphorus and nitrogen from flowing water (Herbert *et al.* 2015).

The Mediterranean region contains diverse saline wetlands including marshes such as Doñana or Odiel (Huelva, Southern Spain), coastal lagoons as Santa Guilla (Sardinia) or endorheic lakes as Fuente de Piedra (Malaga, Southern Spain), covering a wide salinity gradient, from oligi- to hypersaline waters (Alvarez-Cobelas *et al.* 2005, Beklioglu *et al.* 2007) with water residence times highly variable, sometimes even controlled by human activity as solar salterns in Santa Pola (Alicante), Cabo de Gata (Almería) or Sfax (Tunisia). This heterogeneity makes them an ideal environment to investigate the differences and similarities among systems with respect to their microbial and nutrients dynamics.

On the other hand, wetlands also provide refuge, foraging and breeding areas for diverse migratory waterbirds such as greater flamingos, gulls or shorebird species (Rendón *et al.* 2001, Rendón-Martos *et al.* 2000, Green and Elmberg, 2014). Policies for wetlands conservation (i.e. Ramsar convection) have led to waterfowl increases as, for instance, flamingos (*Phoenicopterus ruber*) in the recent decades (Figure 7). Currently, the flamingos represent the main waterbird biomass in saline Mediterranean inland waters (Rodríguez-Pérez & Green 2006, Sánchez *et al.* 2013).

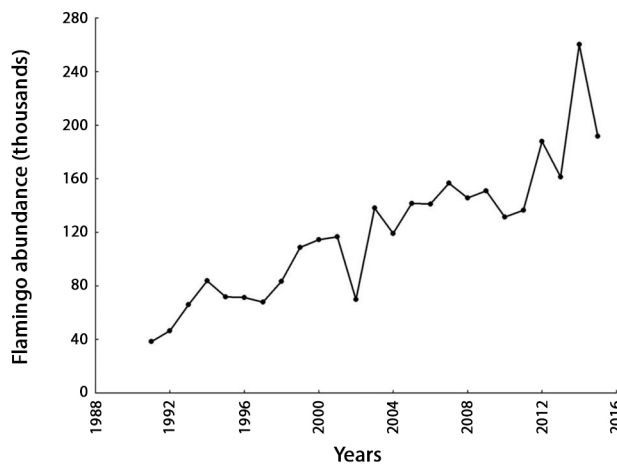


Figure 7. Population size of the flamingo (*Phoenicopterus ruber*) from 1991 to 2014 in the Mediterranean region (International Waterbird Census).

In particular, Fuente de Piedra lake houses one the most important breeding colonies of greater flamingos in the Western Mediterranean (Geraci *et al.* 2012, Rendón *et al.* 2001), enduring an overcrowding of flamingo during breeding period. However, this apparent success has a counterpart that, in many cases, is a guantrophication effect (Leentvaar 1967). Guantrophication consists of the input of nutrient from waterbirds feces; which can affect the water quality (Manny *et al.* 1994). Surprisingly, no previous studies have investigated the effects of guantrophication on aquatic microbial dynamics, despite their significant role in the biogeochemical cycles and greenhouse gas fluxes in wetlands.

Future scenarios of extreme droughts in the Mediterranean region (Giorgi, *et al.* 2008; Garcia-Ruíz, *et al.* 2011) might lead to increases in total nutrients and salts concentration in the wetlands, affecting key microbial process and ultimately, their potential value as climate stabilizers at the global scale.

In this PhD dissertation, we explore the microbial activity, dynamics and structure in coastal wetlands and marshes (Chapter 2) and in an endorheic lake (Fuente de Piedra) during two contrasting hydrological scenarios (Chapter 3 and Chapter 4) (Figure 8).

The main goals of this PhD dissertation were:

1. To improve the knowledge on the microbial ecology of the coastal wetlands by quantifying prokaryotic and cyanobacteria abundances, heterotrophic production discerning between bacterial and archaeal contribution, and the availability of nitrogen and organic carbon substrates in a large set of semi-natural and constructed wetlands covering a wide gradient of salinity from oligo- to hypersaline waters along the Western Mediterranean coast.

2. To determine the main drivers controlling the variability of prokaryotic and cyanobacteria abundances and bacterial and archaeal heterotrophic production at local (within wetland-complex) and regional (among wetland- complexes) scales and to assess the importance of nitrogen availability in coastal wetlands.

3. To determine the influence of flamingos on nitrogen, phosphorus, and microbial dynamics in an endorheic lake as Fuente de Piedra. Flamingos can increase N and P availability by guano inputs and by sediment bioturbation during feeding and trampling in the lake.

4. To test if the dissolved nutrients derived from flamingo guano would boost heterotrophic prokaryotic production performing two experiments under two contrasting (filling vs. evaporation) phases. Finally, we discuss the implications of our findings for the on-going climate change and the conservation policies on waterbirds.

5. To improve the knowledge of the bacterial structure of an endorheic system (Fuente de Piedra lake) using molecular tools and determining its operational taxonomic units (OTU) richness, diversity and composition, both in the free-living fraction and in the particle-attached assemblages, during two well-contrasted (wet and dry) hydrological years.

6. To determine the main drivers of the changes in richness, diversity and composition of bacterial community (i.e. lake area, salinity and flamingo abundance). Finally, we will discuss the implications of our findings given the threat of climate change and climate-linked impacts, such as droughts, on the microbial community, biogeochemical cycles and, consequently, on wetlands function and services.

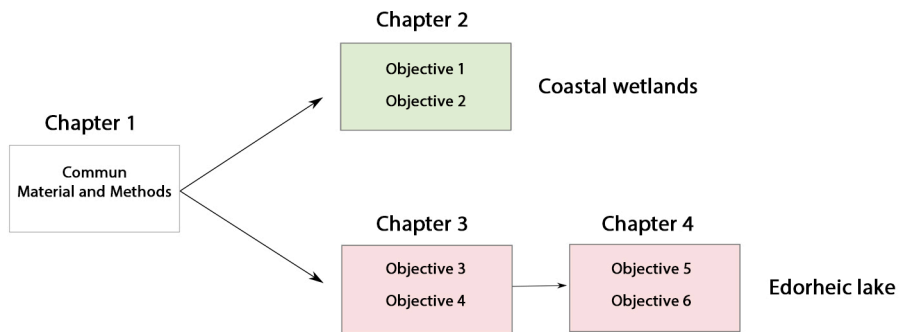


Figure 8. Simplified scheme of the structure for this PhD dissertation

References

- Alvarez-Cobelas, M., Rojo, C., Angeler, D.G., (2005). Mediterranean limnology: current status, gaps and the future. *J. Limnol.* 64 (1), 13e29.
- Anderson & Stedmon. (2007). The effects of evapoconcentration on dissolved organic carbon concentration and quality in lakes of SW Greenland. *Freshwat. Biol.* 52: 280-289.
- Ardón, M., J. L. Morse, B. P. Colman, and E. S. Bernhardt. (2013). Drought-induced saltwater incursion leads to increased wetland nitrogen export. *Global Change Biology* 19:2976–2985.
- Batanero, G.L., León-Palmero, E., Li, L., Green, A.J., Rendón-Martos, M., Suttle, C.A., Reche, I. (2017). Flamingos and drought as drivers of nutrients and microbial dynamics in a saline lake. *Scientific Reports*, 7 (1), art. no. 12173. <https://doi.org/10.1038/s41598-017-12462-9>.
- Beklioglu, M., Romo, S., Kagalou, I., Quintana, X.D., Bcares, E., (2007). State of the art in the functioning of shallow Mediterranean lakes: workshop conclusions.
- Brunet, R. C., and L. J. Garcia-Gil. (1996). Sulfide- induced dissimilatory nitrate reduction to ammonia in anaerobic freshwater sediments. *FEMS Microbiology Ecology* 21:131–138.
- Casamayor, E. O., R. Massana, S. Benlloch, L. Ovreas, B. Diez, V. J. Goddard, J. M. Gasol, I. Joint, F. Rodriguez-Valera, and C. Pedros-Alio. (2002). Changes in archaeal, bacterial and eukaryal assemblages along a salinity gradient by comparison of genetic fingerprinting methods in a multi- pond solar saltern. *Environ. Microbiol.* 4:338–348.
- Crump BC, Hopkinson CS, Sogin ML, Hobbie JE. (2004). Microbial biogeography along an estuarine salinity gradient: combined influences of bacterial growth and residence time. *Appl Environ Microbiol* 70: 1494–1505.
- Chambers, L. G., K. R. Reddy, and T. Z. Osborne. (2011). Short-term response of carbon cycling to salinity pulses in a freshwater wetland. *Soil Science Society of America Journal* 75:2000–2007.
- de Vicente I., Ortega-Retuerta E., Mazuecos IP, Pace ML, Cole JJ, Reche I. (2010). Variation in transparent exopolymer particles in relation to biological and chemical factors in two contrasting lake districts. *Aquatic Sciences* 72:443–453.
- Duarte, C. M., Y. T. Prairie, C. Montes, J., J. Cole, R. Striegl, J. Melack, and J. A. Downing. (2008). CO₂ emissions from saline lakes: A global estimate of a surprisingly large flux. *J. Geophys. Res.*, 113, G04041, doi: 10.1029/2007JG000637.

- Eiler, A., A. H. Farnleitner, T. C. Zechmeister, A. Herzig, C. Hurban, W. Wesner, R. Krachler, B. Velimirov, and A. K. T. Kirschner. (2003). Factors controlling extremely active procaryotic communities in shallow soda pools. *Microb. Ecol.* 46:43–54
- Eliot, I., C. M. Finlayson, and P. Waterman. (1999). Predicted climate change, sea-level rise and wetland management in the Australian wet-dry tropics. *Wetlands Ecology and Management* 7:63– 81.
- Finlay K, Levitt B, Wissel B, Prairie YT. (2009). Regulation of spatial and temporal variability of carbon flux in six hard-water lakes of the northern Great Plains. *Limnol. Oceanogr.* 54: 2553–2564.
- Fourqurean, J.W.; Duarte, C.M.; Kennedy, H.; Marba, N.; Holmer, M.; Mateo, M.A.; Apostolaki, E.T.; Kendrick, G.A.; Krause-Jensen, D.; McGlathery, K.J.; *et al.* (2012). Seagrass ecosystems as a globally significant carbon stock. *Nature Geoscience* 5(7): 505-509.
- García-Ruiz, J.M., López-Moreno, J.I., Vicente-Serrano, S.M., Lasanta, T., Beguería, S., (2011). Mediterranean water resources in a global change scenario. *Earth Sciences Review* 105, 121–139.
- Geertz-Hansen O, Montes C, Duarte CM, Sand-Jensen K, Marbá N, Grillas P. (2011). Ecosystem metabolism in a temporary Mediterranean marsh (Doñana National Park, SW Spain). *Biogeosciences* 8: 963–971. <http://dx.doi.org/10.5194/bg-8-963-2011>.
- Geraci, J., Béchet, A., Cézilly, F., Ficheux, S., Baccetti, N., Samraoui, B., *et al.* (2012). Greaterflamingo colonies around the Mediterranean form a single interbreeding population and share a common history. *J. Avian Biol.* 43, 341–354.
- Giorgi, F., Lionello, P., (2008). Climate change projections for the Mediterranean region. *Global and Planetary Change* 63, 90–104.
- Green, A.J., Elmberg, J. (2014). Ecosystem services provided by waterbirds. *Biol. Rev.* 89, 105–122.
- Hahn MW. (2006). The microbial diversity of inland waters. *Current Opinion in Biotechnology* 17: 256-261.
- Hambly and Suttle. (2005). The virosphere, diversity, and genetic exchange within phage communities. *Curr.Opi.Microbiol.* 8: 44-450
- Hanski I (1994) A practical model of metapopulation dynamics. *Journal of Animal Ecology* 63:151–162.

- Herbert, E.R., P. Boon, A.J. Burgin, S.C. Neubauer, R.B. Franklin, M. Ardón, K.N. Hopfensperger, L.P.M. Lamers, *et al.* (2015). A global perspective on wetland salinization: Ecological consequences of a growing threat to freshwater wetlands. *Ecosphere* 6: 1–43.
- Jellison *et al.* (1996). Organic matter accumulation in sediments of hypersaline Mono Lake during a period of changing salinity. *Limnol. Oceanogr.* 41: 1539–1544.
- Jeppesen, E., Brucet, S., Naselli-Flores, L., Papastergiadou, E., Stefanidis, K., Noges, T., *et al.* (2015). Ecological impacts of global warming and water abstraction on lakes and reservoirs due to changes in water level and related changes in salinity. *Hydrobiologia*, 750(1), 201–227.
- Lamers, L. P. M., G. E. Ten Dolle, S. T. G. Van den Berg, S. P. J. Van Delft, and J. G. M. Roelofs. (2001). Differential responses of freshwater wetland soils to sulphate pollution. *Biogeochemistry* 55:87–102.
- Lamers, L. P. M., S. J. Falla, E. M. Samborska, L. A. R. van Dulken, G. van Hengstum, and J. G. M. Roelofs. (2002). Factors controlling the extent of eutrophication and toxicity in sulfate-polluted freshwater wetlands. *Limnology and Oceanography* 47:585–593.
- Lamers, L. P., H. B. Tomassen, and J. G. Roelofs. (1998). Sulfate-induced eutrophication and phytotoxicity in freshwater wetlands. *Environmental Science and Technology* 32:199–205.
- Laverman, A. M., R. W. Canavan, C. P. Slomp, and P. V. Cappellen. (2007). Potential nitrate removal in a coastal freshwater sediment (Haringvliet Lake, The Netherlands) and response to salinization. *Water Research* 41:3061–3068.
- Leentvaar, P. (1967). Observations in guanotrophic environments. *Hydrobiologia*. 29, 441–489.
- Li Y, Zhang C, Wang N, Han Q, Zhang X, Liu Y, Xu L, Ye W. (2017). Substantial inorganic carbon sink in closed drainage basins globally. *Nat Geosci* 10:501–506.
- López-Archilla *et al.* (2004a) Ecosystem metabolism in a Mediterranean shallow lake (Laguna de Santa Olalla, Doñana National Park, SW Spain) *Wetlands* 24: 848–858.
- Manny, B. A., Johnson, W. C. & Wetzel, R. G. (1994). Nutrient additions by waterfowl to lakes and reservoirs: predicting their effects on productivity and water quality. *Hydrobiologia*. 279/280, 121–132.
- Mcleod *et al.* (2011). A blueprint for blue carbon: toward an improved understanding of the role of vegetated coastal habitats in sequestering CO₂. *Front. Ecol. Environ.* 9(10) 552–560.

- Meier. (2017). "Planetary boundaries of agriculture and nutrition – an Anthropocene approach".
 Proceedings of the Symposium on Communicating and Designing the Future of Food in the
 Anthropocene. Humboldt University Berlin, Bachmann Publisher.
- Messenger, M. L. Mathis Lóic Messenger, Bernhard Lehner, Günther Grill, Irena Nedeva & Oliver Schmitt.
 (2016). Estimating the volume and age of water stored in global lakes using a geo-statistical
 approach. *Nat. Commun.* 7, 13603 doi: 10.1038/ncomms13603.
- Meybeck (1995). Global distribution of lakes, in *Physics and Chemistry of lakes* Springer pp. 1-35.
- Mitsch, W., Bernal, B, y Hernández, M. (2015). Ecosystem services of wetlands. *International Journal of
 biodiversity Science. Ecosystem Service and Management*, 11(1): 1-4.
- Mitsch, William & G. Gosselink, James. (2000). The Value of Wetlands: Importance of Scale and
 Landscape Setting. *Ecological Economics*. 35. 25-33. 10.1016/S0921-8009(00)00165-8.
- Neubauer, S. C., and C. B. Craft. (2009). Global change and tidal freshwater wetlands: Scenarios and
 impacts. Pages 253–266 in A. Barendregt, D. F. Whigham, and A. H. Baldwin, editors. *Tidal
 freshwater wetlands*. Backhuys, Leiden, The Netherlands.
- Neubauer, S. C., R. B. Franklin, and D. J. Berrier. (2013). Saltwater intrusion into tidal freshwater marshes
 alters the biogeochemical processing of organic carbon. *Biogeosciences* 10:8171–8183.
- Ortega-Retuerta, E; Pulido-Villena, E. & Reche, I. (2007). Effects of Dissolved Organic Matter
 Photoproducts and Mineral Nutrient Supply on Bacterial Growth in Mediterranean Inland
 Waters. *Microbial Ecology*, 54 (1): 161-169.
- Park, R. A., M. S. Trehan, P. W. Mausel, and R. C. Howe. (1989). The effects of sea level rise on US coastal
 wetlands. The potential effects of global climate change on the United States. Appendix B. Sea
 level rise. U.S. EPA Office of Policy, Planning, and Evaluation, Washington, D.C., USA.
- Por, F.D. (1972). Hydrobiological notes on the high-salinity waters of the Sinai Peninsula. *Mar.
 Biol.* 14: 111–119
- Rendón, M.A., Garrido, A., Ramírez, J.M., Rendón-Martos, M. & Amat, J.A. (2001). Despotic establishment
 of breeding colonies of greater flamingos, *Phoenicopterus ruber*, in southern Spain.
Behavioral Ecology and Sociobiology, 50, 55–60.
- Rendón-Martos M, Vargas JM, Rendón MA, Garrido A, Ramírez JM (2000). Nocturnal movements of
 breeding greater flamingos in Spain. *Waterbirds* 23(Special Publ. 1):9–19.

- Rodríguez-Pérez, Green (2006). Waterbird impacts on widgeongrass *Ruppia maritima* in a Mediterranean wetland: *Oikos* 112: 525-534.
- Roehm (2005). Respiration in wetland ecosystems. In: del Giorgio PA, Williams PJ, le B, Eds. Respiration in Aquatic systems. Oxford: Oxford University Press. pp 83–102.
- Sánchez, Marta I., Pavel N. Nikolov, Darina D. Georgieva, Boyko B. Georgiev, Gergana P. Vasileva, Plamen Pankov, Mariano Paracuellos, Kevin D. Lafferty, and Andy J. Green. (2013). "High prevalence of cestodes in *Artemia* spp. throughout the annual cycle: relationship with abundance of avian final hosts." *Parasitology Research* 112, no. 5 :1913-1923.
- Sandaa, Ruth-Anne & Foss Skjoldal, Evy & Bratbak, Gunnar.(2003). Virioplankton community structure along a salinity gradient in a solar saltern. *Extremophiles* 7: 347-351. *Extremophiles: life under extreme conditions*. 7. 347-51. 10.1007/s00792-003-0328-5.
- Sanz-Aguilar, A., Béchet, A., Germain, C., Johnson, A. R. & Pradel, R. (2012). To leave or not to leave: survival trade-offs between different migratory strategies in the greater flamingo. *J. Anim. Ecol.* 81, 1171–1182.
- Schuerch, M., Spencer, T., Temmerman, S., Kirwan, M. L., Wolff, C., Lincke, D., *et al.* (2018). Future response of global coastal wetlands to sea-level rise. *Nature* 561, 231–234. doi: 10.1038/s41586-018-0476-5.
- Steffen, W., Richardson, K., Rockström, J., Cornell, S.E., Fetzer, I., Bennett, E.M., Biggs, R., Carpenter, S.R., De Vries, W., De Wit, C.A., Folke, C., Gerten, D., Heinke, J., Mace, G.M., Persson, L.M., Ramanathan, V., Reyers, B. and Sörlin, S. (2015). Planetary boundaries: guiding human development on a changing planet. *Science*, 347, doi 10.1126/science.1259855.
- Verhoeven JTA, Arheimer B, Yin CQ, Hefting MM (2006). Regional and global concerns over wetlands and water quality. *Trends Ecol Evol* 21: 96–103.
- Vousdoukas, M.I.; Mentaschi, L.; Voukouvalas, E.; Verlaan, M.; Jevrejeva, S.; Jackson, L.P.; Feyen, L. (2018). Global probabilistic projections of extreme sea levels show intensification of coastal flood hazard. *Nat. Commun.* 9, 2360.
- Wang, J., Song, C., Reager, J.T., Yao, F., Famiglietti, J.S., Sheng, Y., MacDonald, G.M., Brun, F., Schmied, H.M., Marston, R.A., Wada, Y., (2018). Recent global decline in endorheic basin water storages. *Nat. Geosci.* 11, 926–932

- Weston, N. B., M. A. Vile, S. C. Neubauer, and D. J. Velinsky. (2011). Accelerated microbial organic matter mineralization following salt-water intrusion into tidal freshwater marsh soils. *Biogeochemistry* 102:135–151.
- Weston, N. B., R. E. Dixon, and S. B. Joye. (2006). Ramifications of increased salinity in tidal freshwater sediments: Geochemistry and microbial pathways of organic matter mineralization. *Journal of Geophysical Research Biogeosciences* 111: G01009.
- Woese, CR. (1987). Bacterial evolution. *Microbiol. Rev.* 51:221-271
- Wurtsbaugh WA, Miller C, Null SE, DeRose RJ, Wilcock P, Hahnenberger M, Howe F, Moore J. (2017). Decline of the world's saline lakes. *Nat Geosci* 10:816–821. <https://doi.org/10.1038/NGEO3052>.
- Young, P., (1996). The 'new science' of wetland restoration. *Environ. Sci. Technol.* 30, 292–296.



Chapter 1

Material and methods

Material and methods

1

1.1. SAMPLING AND STUDY SITES

Two types of sampling were performed based on saline wetland type: 1) a sampling at regional spatial scale of coastal lagoons and marshes in Mediterranean area and 2) a sampling at temporal scale in an endorheic system (Fuente de Piedra lake).

1.1.1. Sampling in coastal lagoons and marshes

The regional-scale sampling design allowed us to describe microbial patterns along a vast salinity and nutrient gradient.

Study site characterization and sampling protocol

The study saline wetlands are located in the temperate zone under a semi-arid to arid Mediterranean climate with extremely dry summers with low precipitation rates. Consequently, the intense evaporation during dry period exceeds rainfall such that salts accumulate, covering a wide gradient of salinity from hypersaline (solar salterns) to oligo-mesohaline (brackish) waters. This regional-scale sampling in the West Mediterranean region was carried out in 9 wetlands complexes including 112 ponds during the summers of 2011, 2012 and 2013: Odiel marshes (Spain); Veta la Palma, Doñana (Spain); Cabo de Gata (Spain); Santa Pola (Spain); El Hondo (Spain); Ebro Delta (Spain); Giraud and Saintes-Maries-de-la-Mer, Camargue (France); Molentargius, Santa Guilla and Santa Catherine, Sardinia (Italy) and Sfax (Tunisia) (Figure 1.1). The basic physical-chemical properties and location of each pond are summarized in Table 1 in Chapter 2 and with more detail in the Table 1 in the Annex of the Chapter 2.



Figure 1.1. Location of the nine saline wetland complexes (red dots) sampled in West Mediterranean. From West to East: Odiel marshes, Veta la Palma (Doñana), Cabo de Gata, El Hondo, Santa Pola, Ebro Delta, Rhône Delta (Camargue), Santa Catterina, Santa Guilla, and Molentargius (Sardinia), and Sfax (Tunisia).

The Odiel marshes are located an estuarine complex of 7158 ha, formed at the mouths of the rivers Odiel and Tinto, near the city of Huelva (Southwestern Spain; Figure 1.2). There is evidence that Odiel River is polluted by industrial activities carried out in the surroundings of the estuary (Rodríguez-Estival *et al.*2019, Morillo *et al.* 2002). This area of natural saltmarshes also contains a multi-pond solar salterns system for commercial salt production and presents a gradient of salinity ranging from meso- to hyperhaline.

Veta La Palma is a private wetland complex divided in 37 artificial brackish ponds (total 3125 ha), located at the Guadalquivir estuary in Doñana National Park, (Southwestern Spain). These shallow ponds are managed for fish aquaculture.

The Cabo de Gata solar salterns are located in the province of Almería, southern Spain. This system covers an area of 400 ha along the coastline and separated from the Mediterranean Sea by coastal barrier. This salterns system is formed by a set of interconnecting ponds, and through them seawater is concentrated by evaporation until saturation (hyperhaline conditions).

El Hondo wetland complex is semi-artificial with a total of 2474 ha in the south of Alicante province, Spain. It includes a number of brackish ponds (meso-polyhaline waters), which are fed by the water of the Vinalopó and Segura Rivers. These ponds contain high organic matter and contaminant contents from the polluted Segura River and from agricultural and urban areas reaching periods of hypereutrophic conditions (Viñals *et al.* 2001).

Santa Pola salterns are located in the south of Alicante province (Spain). Two different multi-pond solar salterns were studied in this location: Braç del Port salterns with a superficie of 850 ha (Figure 1.3), and Bonmati salterns with 492 ha. These solar salterns are formed by a number of ponds through which seawater is pumped and evaporated, and finally the concentrated salt is used for commercial production.

Ebro Delta Natural Park is located in the Ebro mouth, in the province of Tarragona (Spain). Here, Trinidat solar salterns system was selected as sampling site, situated in the Banyà Península, on the southern end of Ebro delta (Figure 1.3). These solar salterns (total 979 ha) are operated to obtain salt commercially by evaporation of seawater.

Camargue wetlands are located between two diversions of the Rhône River, forming a delta in Southern France. Two different areas were studied in this site with a salinity gradient ranging from oligo- to hypersaline. One of them is located in the central part of the Rhône delta and consists of a complex of interconnected brackish ponds (total 6000 ha) and its surrounding area is agricultural, mostly rice crops. The other selected area was the solar salterns of Salins-de-Giraud with a total of 11000 ha (Figure 1.4), which are composed of a succession of seawater concentration ponds, situated on the eastern part of the Rhône Delta. Specifics of multi-ponds solar salterns system functioning are similar to those given by Britton and Johnson (1987) for the Saline de Giraud in the Camargue.

In Sardinia (Italy), three different areas were selected. Molentargius regional Park (total 1600 hectares), located between the coast and the cities of Cagliari and Quartu S. Elena. This area has currently become a "green" space, which includes Molentargius ponds and the former solar salterns of Cagliari, commercially inactive since the 80s. These shallow ponds are exposed to intense solar radiation favoring hyperhaline conditions by evaporation. Another selected area was the Stagno di Santa Guilla that is a coastal lagoon situated between the two diversions of the rivers Cixerri and Mannu in the Gulf of Cagliari (Figure 1.5). It was designated RAMSAR site since 1976 with 2000 ha of salt-pans. We also sampled coastal lagoons at Santa Catterina.

The Sfax solar salterns with a total of 1500 ha are located along the coast to the south of Sfax (Tunisia). This system is formed by a set of shallow ponds interconnected along the coastline and separated from the Mediterranean Sea by dykes. These solar salterns are operated for commercial salt production by evaporation of seawater reaching hyperhaline conditions. More details on this solar salterns system can be found in Ayadi *et al.* (2002).



Figure 1.2. Marismas del Odiel marshes, Huelva, Spain.



Figure 1.3. Orthophotos (<https://pnoa.ign.es>) of Santa Pola solar-salterns (left) and Ebro Delta (right).

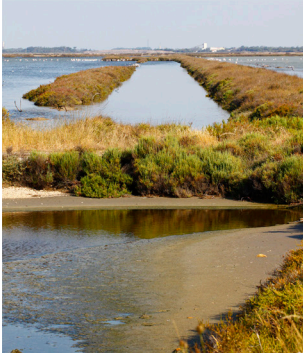


Figure 1.4. Giraud and Saintes-Maries-de-la-Mer, Camargue (France). By credit: Francisco Perfectti



Figure 1.5. Santa Guilla lagoon, Sardinia (Italy). By credit: Francisco Perfectti

1.1.2. Temporal sampling in an endorheic system: Fuente de Piedra lake

This sampling allowed us to assess the relative importance of seasonal and inter-annual changes in flamingo abundance, lake area by drought, and nutrients determining microbial activity and abundance and bacterial community structure.

Study site characterization and sampling protocol

Fuente de Piedra is an athalassohaline lake, located in an endorheic basin of karstic origin in the province of Malaga (Southern Spain; Figure 1.6). This lake covers an area of 1300 ha, is shallow with water depth not exceeding 1.5 meters. This lake houses during the summer one of the most important colonies of breeding greater flamingos (*Phoenicopterus roseus*) in the Western Mediterranean, reaching more than 50000 individuals. This lake undergoes relevant changes depending on the annual hydrological budget, with salinities that can oscillate from oligo- (< 5 ppt) to hypersaline (> 200 ppt). Each hydrological year had two phases. The filling phase occurs during the fall and the winter (September-March) and the evaporation phase during the spring and the summer (April-August). Fuente de Piedra lake was included as a Ramsar wetland in 1983 and declared Nature Reserve in 1989.

We sampled Fuente de Piedra lake biweekly during more than two hydrological years. The first hydrological year from September 2010 and August 2011 was considered wet as the lake was inundated for most time of the year and the previous hydrological year, with similar conditions, was partially sampled (from July 2010). The second hydrological year Fuente de Piedra was sampled from September 2011 and August 2012, except when the lake was completely dried out from June to October 2012. Two sampling stations were selected (Figure 1.6). The station 1 is less affected by winds and turbidity and is a flamingo foraging area, whereas the station 2 is located nearer the nesting area of the flamingos colony and is more exposed to wind, evaporation and turbidity (Figure 1.7).

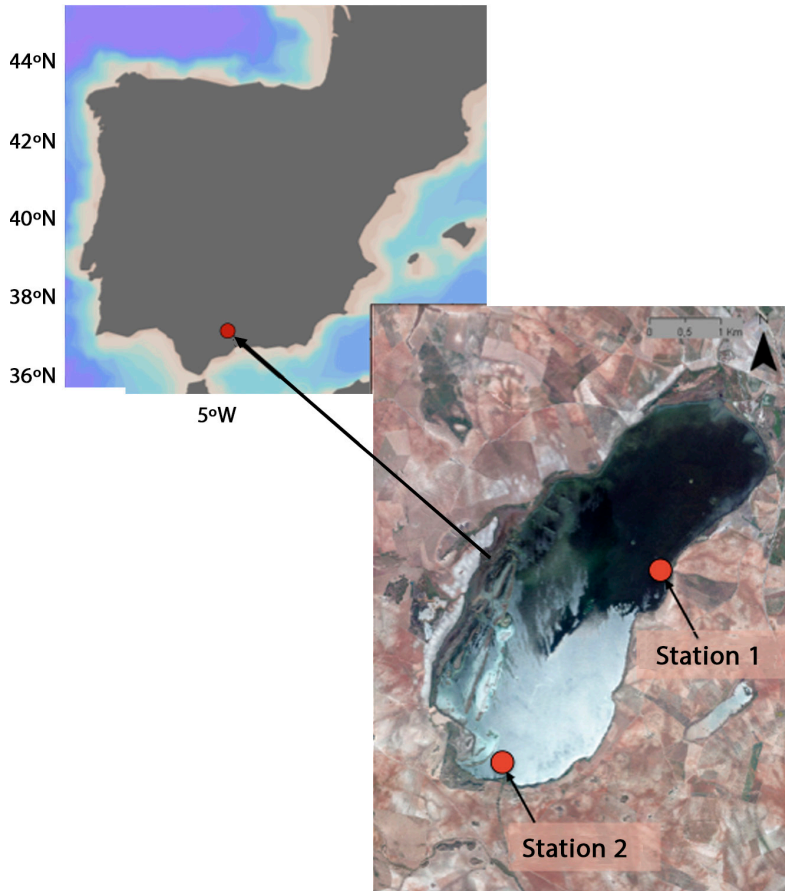


Figure 1.6. Map of the Fuente de Piedra lake and two sampling stations.



Figure 1.7. Localization of sampling Station 2 in Fuente de Piedra lake. By credit: Francisco Perfectti.

The data of rainfall, water level and flamingo abundance in Fuente de Piedra lake were provided by the “Consejería de Medio Ambiente y Ordenación del Territorio” of Junta de Andalucía, Spain.

In each study system, we took samples for dissolved and total nutrients (phosphorus, nitrogen), dissolved organic carbon (DOC), chlorophyll a concentration (chl a), prokaryotic and viral abundances and bacterial and archaeal heterotrophic production. Prior to analysis, all samples were diluted ≥ 5 -fold with Milli-Q water to avoid any interference of salinity on standard method for physicochemical and biological analysis. Microbial DNA characterization was carried out exclusively in Fuente de Piedra lake, and taxonomic diversity measured in free-living and particle-attached bacterial assemblages.

Waters samples were collected from the upper layers of the water column using a telescope sampling system with a pendulum plastic beaker scoop (VWR); Figure 1.9).

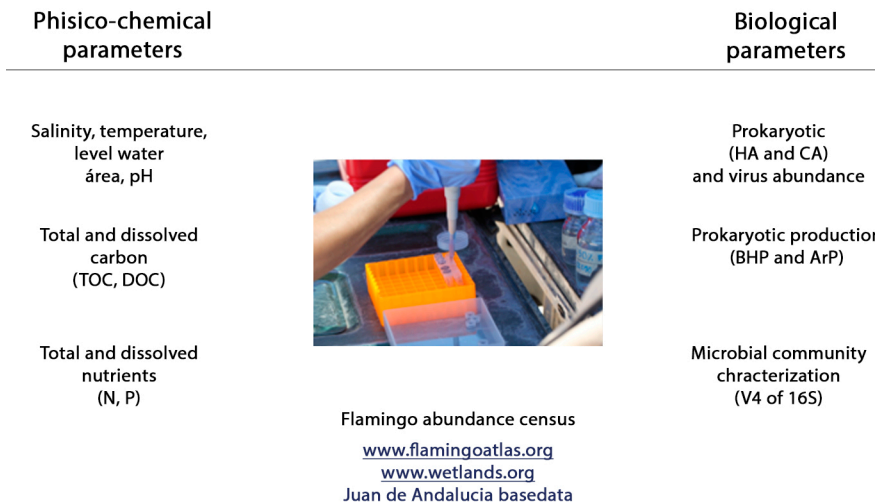


Figure 1.8. Scheme of the used chemical and biological analysis in this sampling routine.



Figure 1.9. Water samples collection in each system of sampling complex. By credit: Francisco Perfectti.

1.1.3. Experiments with guano

To determine the effects of guano on prokaryotic growth we carried out two experiments in the laboratory using previously frozen feces from flamingo chicks collected during the ringing operations in August 2010 (Figure 1.10). The details of the experimental design are described in the chapter 3.



Figure 1.10. Fresh flamingo chick feces were collected during banding operations in the Fuente de Piedra colony in August 2010. By credit: Miguel Angel Toscano.

1.2. METODOLOGY

1.2.1. Physicochemical analyses

1.2.1.1. Salinity, Temperature and pH

Salinity (ppt), temperature (°C) and pH were measured in situ using a multi-parameter probe (HANNA HI 9828). Water samples with salinity higher than 70 ppt were diluted with Milli-Q water until they were within in the operating range of the probe.

1.2.1.2. Total phosphorus (TP), total dissolved phosphorus (TDP) and soluble reactive phosphorus (SRP) concentration

TP, TDP and SRP samples (10 ml, 10 ml and 25 ml, respectively) were collected by triplicate and stored at -20 °C until analysis. TDP and SRP samples were previously filtered

through 0.7µm pore-size Whatman GF/F glass fiber filters, while TP concentrations were measured using unfiltered water. TP, TDP and SRP concentrations were measured using the molybdenum blue method proposed by Murphy & Riley (1962). The first two analysis were measured as SRP after a persulfate digestion (30° min, 120°C) following the standard protocol (APHA, 1992). This method consisted of to add ammonium molybdate in an acid medium with diluted solutions of phosphorus to form an antimony-phospho-molybdate complex, which was reduced to a blue-colored complex by ascorbic acid. The color intensity was proportional to the phosphorus concentration. The color intensity was measured by spectrophotometry at a wavelength of 885 nm. The detection limit of this method for TP and TDP concentration was 0.02 µmol-P l-1 and for SRP was 0.08 µmol-P l-1.

1.2.1.3. Total nitrogen (TN) and total dissolved nitrogen (TDN) concentration

TN and TDN samples were transferred into 40 ml glass ampoules by triplicate, sealed and stored at 4 °C until analysis. The TDN samples were previously filtered through 0.7 µm pore-size Whatman GF/F glass fiber filters. TN and TDN were analyzed by high-temperature catalytic oxidation (Álvarez-Salgado *et al.* 1998) using a total nitrogen analyzer (TNM-1, Shimadzu TOC-V CSH). TN and TDN samples were thermally decomposed at 720 °C under ultra-pure oxygen saturation and all of N forms were oxidized to nitric oxide, which was directly measured by chemiluminescence detector. The detection limit of this method was 0.002 mmol-N l-1.

1.2.1.4. Dissolved organic carbon (DOC) concentration

DOC samples were transferred into pre-combusted 40 ml glass ampoules by triplicate (Figure 1.11), acidified with 200 µl of 25 % phosphoric acid (final pH < 2), sealed and stored at 4 °C until analysis. DOC samples were collected after filtration through pre-combusted Whatman GF/F filters (2 hours at 500 °C). DOC concentrations were measured by high-Temperature Catalytic Oxidation in a Shimadzu TOC-V CSH (Benner & Strom 1993). The samples were combusted or decomposed to CO₂, which was measured with a non-dispersive infrared (NDIR) detector. The detection limit of this method was 0.004 mM. The instrument was calibrated using a four-point standard curve of potassium hydrogen phthalate. Samples were purged with phosphoric acid for 20 min to eliminate any dissolved inorganic carbon. Three to five injections were analyzed for each sample.



Figure 1.11. Glass ampoules to storage the total and dissolved organic carbon samples.

1.2.2. Biological analyses

1.2.2.1. Chlorophyll *a*

Chlorophyll *a*, concentration was analyzed spectrophotometrically after pigment extraction (APHA 1992). This pigment concentration was determined by filtering a known volume of sample through Whatman GF/F filters immediately after collection and stored at -20 °C until analysis (Figure 1.12). Once thawed, each filter was kept in a glass vial with 7 ml methanol 95% during 24 hours in dark at 4°C conditions. Then, the absorbance of the extracts was measured from 400 nm to 800 nm using a PerkinElmer Lambda 40 spectrophotometer connected to a computer equipped with UV-WINLAB software. The pigment-specific concentration was estimated according to expression proposed by Marker *et al.* (1980).

$$\text{Chl } a \text{ (}\mu\text{g/l)} = \frac{13.9 \times (\text{D665} - \text{D750}) \times V}{B}$$

Where;

- D665 is absorption of extract at 665 nm,
- D750 is absorption of extract at 750 nm (measuring turbidity in the extract)
- 13.9 is absorbance specific coefficient for Chl *a* in methanol (Talling & Driver. 1963)
- V is volume of extract
- B is volume of sample.



Figure 1.12. Particles concentrated on 0.7 μm pore-size Whatman GF/F glass fiber filters from different study ponds in Molentargius (Sardinia).

1.2.2.2. Total prokaryotic abundance (PA), heterotrophic prokaryotic abundance (HA) and cyanobacteria abundance (CyA)

Total prokaryotic (PA) and cyanobacteria (CyA) abundances were determined by flow cytometry (Gasol and Del Giorno, 2000). Triplicate samples (3 ml) were collected in cryovials, fixed with a mixture of 1% paraformaldehyde + 0.05% glutaraldehyde (30 min in the dark at 4 °C), deep frozen in liquid nitrogen, and stored at -80 °C until analysis. Once defrosted, samples were diluted with Milli-Q water (≥ 10 -fold) to avoid electronic coincidence of the prokaryotic particles. PA and CyA samples were run in a FACScalibur TM (Figure 1.13) with a laser emitting at 448nm with green fluorescence collected in the FL1 channel, orange collected in the FL2 channel, and red fluorescence collected in the FL3 channel. All parameters were collected as logarithmic signals. Prior to analysis, PA samples (500 μl) were stained for 10 min in the dark with a DMSO diluted Syber Green I (Molecular Probes) stock (1:200) at 10 μM final concentration. We added 5 μl of a solution of yellow-green 0.92 μm Polysciences latex beads as internal standard. The beads solution was sonicated (10 min) before being added to the sample. PA samples were run at low speed during 2 minutes and detected by their signature in bivariate plots Side scatter (SSC) vs. FL1 (Green fluorescence). For CyA samples, 10 μl of a solution of yellow-green 0.92 μm Polysciences latex beads were added and run at high speed during 4 minutes. The signature of CyA was detected in bivariate plots as Side scatter (SSC) vs. FL3 (Red fluorescence; Figure 2.9); FL4 (Blue fluorescence) vs FL3 (Red fluorescence) and FL2 (Red fluorescence) vs FL3 (Red fluorescence). Then, we acquired and analyzed data from flow cytometer in a computer using the BD CellQuest Pro software. We analyzed subpopulations by drawing regions around the cells of interest (Figure 1.14). Cell abundance was determined using the following expression:

$$PA \text{ (cell /ml)} = \frac{C}{T \times FR}$$

Where;

- C is average cell number by selected region
- T is acquisition time, (2 min is adequate to detect PA and HP and 4 min for CyA)
- FR is flow rate, i.e. sample volume per min ($\mu\text{l} / \text{min}$) by low speed for AP and HP, and high speed for CyA.
- Heterotrophic prokaryotic abundance (HA) was estimated subtracting cyanobacteria abundance of the total prokaryotic abundance.



Figure 1.13. BD FACScalibur TM 2 Laser, 4 Color Flow Cytometer (Becton Dickinson). (Picture obtained from BD Biosciences, USA).

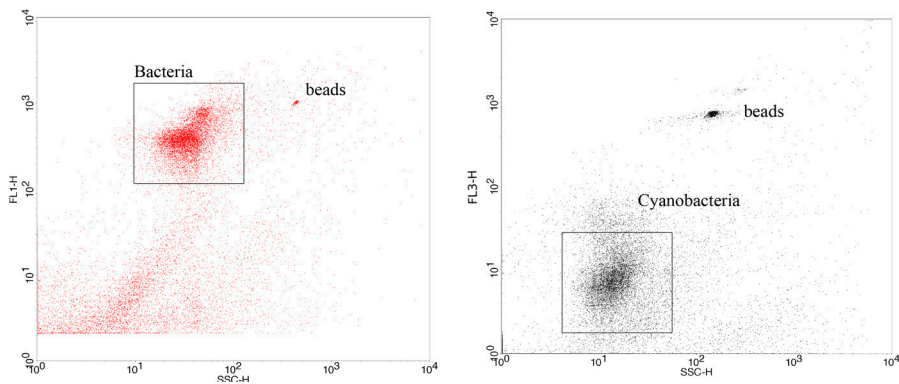


Figure 1.14. Cytograms by flow cytometry analysis of bacteria and cyanobacteria abundance sample from the Fuente de Piedra Lake: FL1-H (Green fluorescence intensity) and FL3-H (Red fluorescence intensity) for bacteria and cyanobacteria respectively vs. SSC (Side scatter; i.e. cell granularity) distributed in logarithmic scale (100 to 104). Flow Cytometer is located in Biomedical research center, University of Granada (UGR), Spain.

1.2.2.3. Virus Abundance (VA)

Virus abundance was also determined by flow cytometry (Brussaard *et al.*, 2010). Triplicate samples (1 ml) were fixed with glutaraldehyde (25% electron microscopy (EM)-grade glutaraldehyde (Sigma Aldrich) at final concentration of 0.5 % for 15-30 min at 4°C in the dark. Once fixed, samples were flash frozen in liquid nitrogen, and stored at -80 °C until analysis in the laboratory. Prior to analysis, samples were diluted with TE-buffer pH 8.0 (10 mM Trishydroxymethyl-aminomethane, Roche Diagnostics; 1 mM ethylenediaminetetraacetic acid, Sigma-Aldrich) to avoid the electronic coincidence of the virus particles. For each sample, the dilution factor was greater than 100-fold, with sample volume of 50 µl at 500 µl of final volume. Then, virus samples were stained with 5µl Syber Green I (10,000 x concentrate in DMSO; Invitrogen, Molecular Probes). Before staining, Syber Green I was diluted in molecular grade water, stock (1:200). Then, virus samples were incubated for 10 min at 80 °C in the dark. The heated samples were left to cool at room temperature during 5 min in the dark before analysis. Then, 5 µl fluorescent microspheres (FluoSpheres carboxylate modified yellow-green fluorescent microspheres; 1.0 µm diameter; Invitrogen, Molecular Probes; F8823; stored at 4°C) were added as internal standard. The beads solution was briefly sonicated before being added to the sample. After staining, samples were run through a FACScalibur TM flow cytometer (Figure 1.13) with a laser emitting with green fluorescence collected in the FL1 channel, orange collected in the FL2 channel, and red fluorescence collected in the FL3 channel, and threshold level was fixed at 52 during acquisition of the data. All parameters were collected as logarithmic signals. Samples were run at medium speed during 1 minute and data were acquired in log mode. Viruses were detected by their signature in bivariate plots of Side scatter (SSC) vs. FL1 (Green fluorescence). Viruses concentration was determined using the following expression:

$$VA \text{ (viruses/}\mu\text{L)} = \frac{V}{T \times FR}$$

Where;

- V is average viruses number by selected region
- T is acquisition time, (1 min is adequate to detect viruses)
- FR is flow rate (i.e. sample volume per min (µl/min) by medium speed)

1.2.2.4. Bacteria heterotrophic production (BP) and archaeal production (ArP)

BP and ArP were estimated as the aminoacid 3H-leucine incorporation into proteins following the micro-centrifugation technique proposed by Smith and Azam (1992). Briefly, 10 samples (5 for PHP and 5 for ArP) of 1.5ml were taken and were placed in microcentrifugation tubes. Each set includes triplicate plus two blanks (fixed immediately). Archaea production samples were previously treated with 5 µl of erythromycin (an inhibitor of bacterial activity) (Yokokawa *et al.* 2012). Then, 5 µl of 4,5-3H-L-Leucine was added to the 10 vials samples with final concentration of 54.6nM or 58.4nM, and were incubated between 2 hours to 5 hours maximum. The incubation was stopped adding 0.3 ml of 50% Trichloroacetic Acid (TCA). For blank samples the 0.3 ml of 50% trichloroacetic acid (TCA) was added before starting the incubations. Then, samples were stored at -20°C until processing in the laboratory. The sample tubes were centrifuged (10 min, 14000 rpm) and aspirated. After that, the tubes were washed with 1.5 ml of 50% TCA, vortexed, and centrifuged again. Then, 1.5 ml of scintillation cocktail (Ecoscint) was added, the tubes were placed in scintillation vials, and radio assayed in a liquid scintillation counter (Beckman). We determined leucine incorporation into protein using the following expression:

$$\text{nmoles leucine l}^{-1} \text{ h}^{-1} = \text{dpm} \cdot V \cdot t / 2.22 \cdot 10^6 \cdot \text{S.A.}$$

Where;

- dpm: desintegrations per minute
- V: sample volume (l)
- t: incubation time (h)
- 1µCi = 2.22· 10⁶ dpm
- S.A: specific activity of 3H-leucine

1.2.2.5. Bacterial community characterization in Fuente de Piedra lake

Collection of free-living and particle-attached bacterial assemblages

For DNA characterization in Fuente de Piedra lake, free-living and particle-attached bacterial assemblages were collected biweekly from July 2010 to November 2012, covering more than two hydrological years. A variable volume of lake waters was sequentially filtered through 3 µm- and 0.2 µm- membrane polycarbonate filters (Nuclepore) to discriminate the attached and the free-living bacteria, respectively. Then, each filter was placed in sterile 3-ml cryovials and covered with 1.4 ml of TES buffer (40mM EDTA; 50mM Tris pH 8.3; 0.75M sucrose) and stored at -80 °C until extraction.

DNA samples processing

DNA samples processing consisted of first the DNA extraction followed by two consecutive PCR amplifications to construct a sequencing library of the V4 hypervariable region 16S rDNA gene.

i. DNA Extraction

For total DNA, bacteria were resuspended from thawed filter by rinsing the membrane with the TES buffer and vortexed. Once resuspended, cells were centrifuged at 13,000 rpm for 5 min and the DNA was extracted from the pellets (Figure 1.15) using FavorPrep™ Genomic DNA Mini Kit (Favorgen) to manufacturer's instructions, with a final elution volume of 150 µl. Reaction products were inspected by 0.7 % agarose gel electrophoresis with in 5X TBE (45mM Tris; 44 mM boric acid; 1mM EDTA) buffer stained with ethidium bromide at final concentration of 0.5 µg/ml and DNA phage λ digested with restriction enzyme HindIII was used as electrophoresis marker.

Finally, DNA quality was assessed based on the absorbance ratios 260/280 nm and 260/230 nm using a Nanodrop 2000 Spectrophotometer (Thermo scientific).

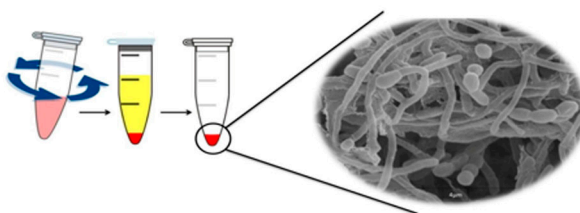


Figure 1.15. Cartoon representing the cell recovery from filters

ii. Construction of 16S libraries and Illumina MiSeq

• 1ST PCR AMPLIFICATION

The hypervariable V4 region of 16S rRNA gene from the samples was amplified by polymerase chain reaction (PCR) method, using primers 515F and 786R and Phusion flash polymerase high-fidelity PCR Master mix (Thermo Scientific).

515F - 5' - GTGCCAGCMGCCGCGTAA-3'

786R - 5' - GGACTACHVGGGTWTCTAAT-3'

Amplicons generated contained ~353 pb of length, which included specific primers and partial Illumina adapters. Table 1.1 shows the optimal mixing of reagents for the amplification carried out in the laboratory.

Table 1.1. Mix of reagents for the amplification of the 16S rDNA V4 region of 16S rRNA gene for each sample.

<i>Master Mix 1x</i>	
Phusion flash polymerase (Thermo, 2X)	10 μ l
515F (3 μ M)	1 μ l
786R (3 μ M)	1 μ l
H ₂ O	3 μ l
DNA template (2ng/ μ l)	5 μ l
Final volume	20 μ l

PCR reaction was placed in a thermal cycler (Mastercycler X50, Eppendorf; figure 1.16 and each cycle of amplification consisted of various steps at different temperatures and fixed amounts of time:

- ▷ 98°C 60" (Step1: template DNA denaturation)
- ▷ 25 cycles: 98°C 1", 52°C 5" and 72°C 5" (Step 2: denaturation, annealing, and extension cycles)
- ▷ 72°C 60" (Step 3: primer extension)
- ▷ Hold at 4°C



Figure 1.16. Mastercycler X50 Thermal cycler (Eppendorf) located in Instituto del Agua, University of Granada, Spain.

- 1ST DNA PURIFICATION

Amplicons were purified using GenElute™ PCR Clean-Up Sigma® Kit, according to manufacturer's recommendations. The purification process aims to remove excess primers, single-stranded DNA fragments, nucleotides, DNA polymerase, oil, and salts. Following this process of purification, all purified amplicons were checked by horizontal electrophoresis in 0.7 % (w/v) agarose gel electrophoresis in 5x TBE (45mM Tris; 44 mM borate acid; 1mM EDTA) containing 0.5 µg/ml ethidium bromide, to confirm both amplification and an optimum purification of DNA.

- BARCODING: ADDITION OF INDEXED ADAPTORS

The second PCR amplification adds indexed adaptors called "barcodes", which act as unique identifiers for each sample. This was achieved using Nextera XT Index (24 index - 96 samples) kit. After this procedure, amplicons showed a different combination of indexed barcodes for each sample. In our case, 15 barcodes were combined to identify 67 different DNA samples. PCR reaction was performed using a high-fidelity DNA polymerase 2 x Phusion™ Flash High-Fidelity PCR Master Mix (Thermo Scientific™) . Table 1.2. shows the mix of reagents applied in each sample to incorporate indexed barcodes to each amplicon:

Table 1.2. Mix of reagents for the amplification of the 16S rDNA V4 region of 16S rRNA gene for each sample.

<i>Master Mix</i>	
2x Phusion flash PCR Master mix	10 μ l
Nextera XT Index 1 Primers (N7XX)	2 μ l
Nextera XT Index 2 Primers (S5XX)	2 μ l
H ₂ O	3.2 μ l
DNA template (5ng/ μ l)	2.8 μ l
Final volume	20 μ l

PCR reaction was placed in a thermal cycler (Mastercycler X50, Eppendorf; figure 1.16) and each cycle of amplification consisted of various steps at different temperatures and fixed amounts of time:

- 98°C for 60" (Step1: template DNA denaturation)
- 9 cycles of 98 °C for 1", 52 °C for 5", 72 °C for 5" (Step 2: denaturation, annealing, and extension cycles)
- 72°C 60" (Step 3: primer extension)
- Hold at 4°C

• 2ND DNA PURIFICATION

PCR products were purified using GenElute™ PCR Clean-Up kit (Sigma-Aldrich), eliminating excess primers and barcodes, DNA polymerase and single-stranded DNA fragments. After this purification, second PCR products were run in a 0.7 % (w/v) agarose gel electrophoresis in 5x TBE (45mM Tris; 44 mM borate acid; 1mM EDTA) containing 0.5 μ g/ml ethidium bromide.

DNA quantification was performed employing NanoDrop™ 2000 Spectrophotometer (Thermo Scientific). Once all samples were standardized at the same final concentration, these were pooled and mixed in one single tube. Finally, this pool was diluted with Elute solution (Sigma-Aldrich), to achieve an adequate concentration (at 30 μ g/ μ l final concentration) to be sequenced on the MiSeq platform (Illumina).

Sequencing was carried out at UGR Technology Services (Granada, Spain) using Illumina MiSeq platform (Caporaso et al 2012) with 250 cycles for paired read. Both forward and reverse reads were 353 bp and full-length sequence of amplicon (V4 hypervariable region 16SrRNA, primers, partial Illumina adapters and barcodes) was approx. 427 bases paired (bp; Figure 1.17)

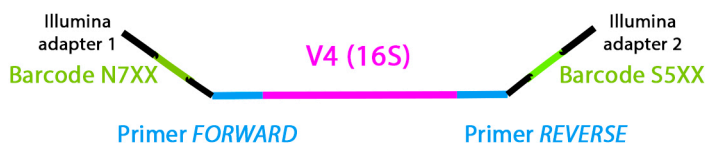


Figure 1.17. Map of the V4 sequencing library. Complete amplicon of V4 hypervariable region of 16S rDNA (427bp) prepared for sequencing on the MiSeq platform (Illumina)

iii. *Processing and analysis of Illumina sequencing data*

Paired-end data were downloaded from “Base Space” platform generated on the Illumina MiSeq machine and were provided as separate sequence files in .fastq format (two per sample – R1-forward and R2-reverse reads), which previously were de-multiplexed, de-bar-coded. Bacterial diversity analysis was carried out using the open source software package, Quantitative Insights Into Microbial Ecology (QIIME, v.1.9.0, Caporaso *et al.* (2010)) and Mothur v.1.6. (Schloss *et al.*, 2009). Before analyzing this sequence dataset, we performed some quality control (QC) using specialized FastQC application (<http://www.bioinformatics.babraham.ac.uk/projects/fastqc/>) to ensure that the raw data did not had any problems and the appropriate quality (Figure 1.18). Total number of sequences was 16,519,419, all of them of high quality (both the R1-forward and R2-reverse reads).

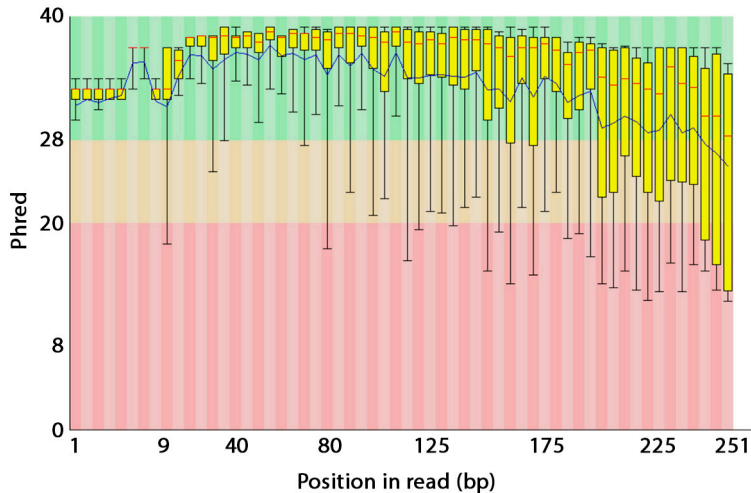


Figure 1.18. Summary per base sequences quality of forward reads. The y-axis represents Phred Quality Scores. BoxWhiskers: Red lines = Median values, Boxes = 25% and 75% percentiles and whiskers= 10% and 90% points. Blue line represents mean quality. Background of the graph: Green = calls very good quality, Orange = reasonable quality and Red = calls for poor quality.

Phred Quality Scores indices are logarithmically related to the probability of incorrect base call (Ewing & Green, 1998). Once sequences quality was displayed, paired end reads (R1-forward and R2-reverse) were combined in a single sequence per sample using Qiime. Subsequently, each sample was passed through a rigorous quality filter, resulting in a single file in Fasta format. We assigned a quality score (Phred Score) of 20 as quality threshold, which meant that the probability of incorrect base call was at least bellow a 10%. Then, the primers sequences were trimmed off using Mothur software and sequences that were larger than insert size (>251 bp) long were considered an error in sequencing and therefore excluded.

All of the remaining sequences were clustered into Operational Taxonomic Units (OTUs) using uclust v. 1.1.579 method (Edgar, 2010), with sequence similarity threshold at 99%.

Taxonomic identification of each OTUs was performed using Greengenes 13.5 reference database (<http://greengenes.secondgenome.com>). This was achieved by using pick_de_novo.py script in Qiime, whose output was a matrix (Otu_table in .biom format) with the number of reads per OTUs in each sample and their taxonomical assignment. Subsequently, a negative filtering taxa from OTU_table was performed to remove taxonomic level of Archaea, Chloroplast and Mitochondria in QIIME. Filtered OTU table contained both

0.2 µm-free-living (>0.2 µm) and particle-attached (>3 µm) bacteria samples (complete database), but our interest was to calculate separately both alpha and beta diversity of free-living and particle-attached bacteria assemblages. For this reason, two OTU table files in .biom format were generated from filtered OTU table, one for free-living (>0.2 µm) bacterial samples and another for particle-attached bacterial (>3 µm) samples.

To control uneven sequencing depth (i.e. number of sequences in each sample), datasets were standardized through multiple rarefaction analyses at different sequencing depth (to be precise at 200, 500 and then, from 1000 to 10000 sequences per sample at intervals of 1000) and 100 number of iterations in QIIME software. Several sequencing depths were explored to check the rarefaction effects and obtain a balance between costs (i.e. samples removed) and required sequencing depth to generate valid results. After the normalization step, reads detected only once (i.e. singletons) were discarded using QIIME script to reduce noise due to a potential high ratio of artifacts/real OTUs. For more details see the Annex of Chapter 1.

iv. Alpha diversity analysis

Community richness and diversity indices were calculated using Qimme software (see Annex Chapter 1). Alpha diversity was measured by counting the number of observed OTUs richness and the Shannon diversity (Shannon - Wiener index) as described by Magurran (1989) which is defined as:

$$H' = - \sum_{i=1}^S p_i \ln p_i$$

Where;

- S is the number of OTUs, pi is the proportion of the community represented by the OTU i (estimated using ni (the abundance i)/N (total abundance))

Beta Diversity

After the normalization step, community composition changes were studied using the Bray-Curtis dissimilarity matrix (Beals, 1984) to measure beta diversity. Community composition was performed using beta_diversity.py in Qiime software (see Annex Chapter 1).

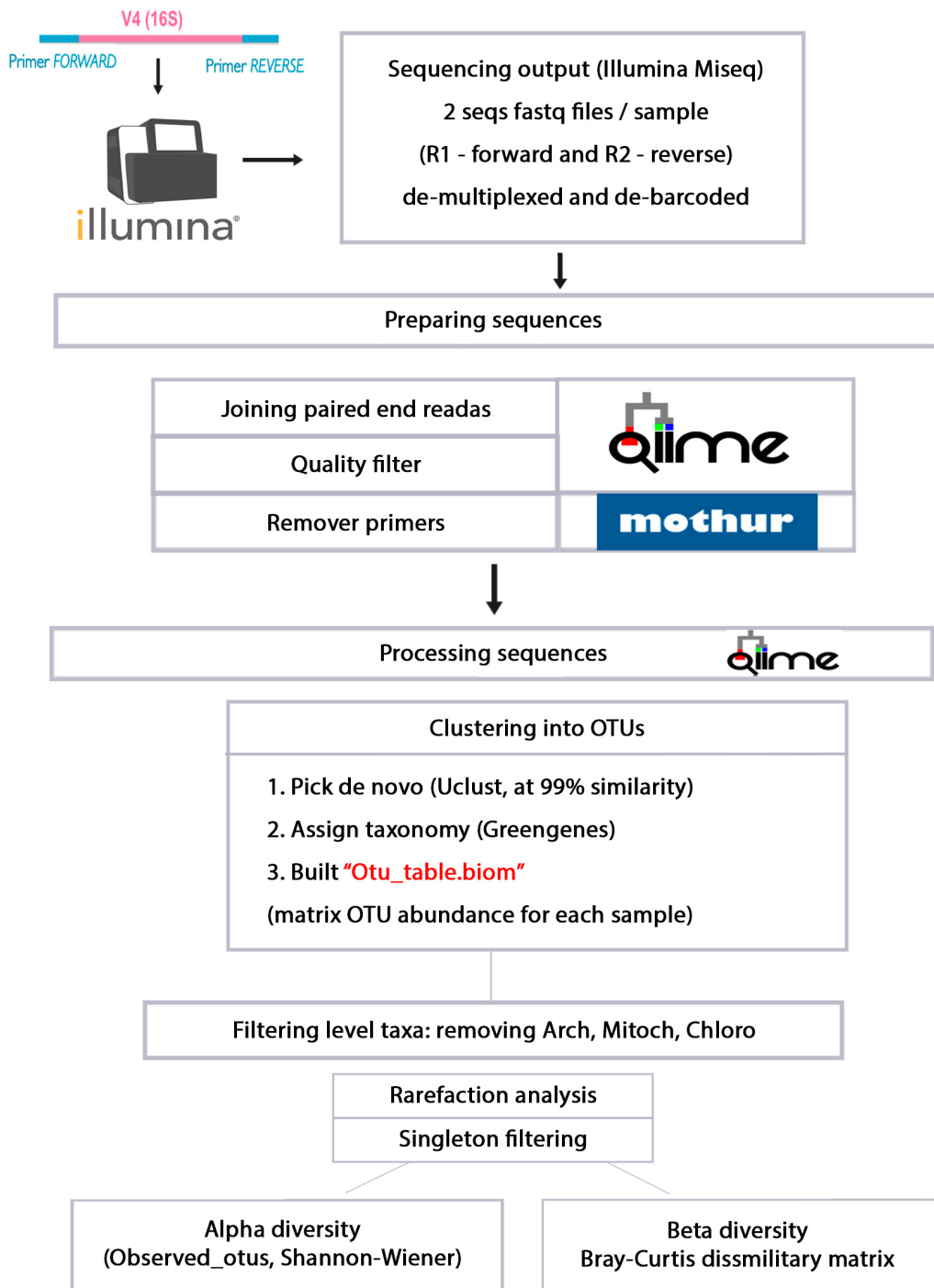


Figure 1.19. Workflow scheme of metataxonomic data analysis with Qiime and Mothur

1.3. REFERENCES

- Álvarez-Salgado, X. A. & Miller, A. E. J. (1998). Simultaneous determination of dissolved organic carbon and total dissolved nitrogen in seawater by high temperature catalytic oxidation: conditions for precise shipboard measurements. *Mar. Chem.* 62, 325–333.
- American Public Health Association (APHA). (1992). *Standard methods for the examination of water and wastewater* (ed. American Public Health Association).
- Ayadi, H., Toumi, N., Abid, O., Medhioub, K., Hammami, M., Sime-Ngando, T., Amblard, C. and Sargos, D. (2002). Etude quantitative des peuplements phytoplanctoniques et zooplanctoniques dans des bassins de la saline de Sfax en relation avec les paramètres physico-chimiques. *Journal of Water Science*, vol. 15, n° 1, 2002, p.123-135
- Beals, E.W. (1984). Bray-Curtis ordination: an effective strategy for analysis of multivariate ecological data. *Adv. Ecol. Res.* 14, 1–55.
- Britton, R.H. & Johnson, A.R. (1987). An ecological account of a Mediterranean salina: The Salin de Giraud, Camargue (S. France). *Biological Conservation*. 42. 185-230. 10.1016/0006-3207(87)90133-9.
- Brussaard, C. P. D., Payet, J. P., Winter, C. & Weinbauer, M. G. (2010). Quantification of aquatic viruses by flow cytometry. *Manual of Aquatic Viral Ecology* (ed. Wilhelm, S. W., Weinbauer, M. G. Suttle C. A.) 11, 102–109.
- Caporaso, J. G., Lauber, C. L., Walters, W. a, Berg-Lyons, D., Huntley, J., Fierer, N., ... Knight, R. (2012). Ultra-high-throughput microbial community analysis on the Illumina HiSeq and MiSeq platforms. *The ISME journal*, 6(8), 1621–4. doi:10.1038/ismej.2012.8
- Caporaso, J.G., Kuczynski, J., Stombaugh, J., Bittinger, K., Bushman, F.D., Costello, E.K., Fierer, N., Peña, A.G., Goodrich, J.K., Gordon, J.I., Huttley, G.A., Kelley, S.T., Knights, D., Koenig, J.E., Ley, R.E., Lozupone, C.A., McDonald, D., Muegge, B.D., Pirrung, M., Reeder, J., Sevinsky, J.R., Turnbaugh, P.J., Walters, W.A., Widmann, J., Yatsunenko, T., Zaneveld, J., Knight, R. (2010). QIIME allows analysis of high-throughput community sequencing data. *Nat. Methods* 7 (5), 335–336. <http://dx.doi.org/10.1038/nmeth.f.303>.
- Ewing B, Green P. (1998). Basecalling of automated sequencer traces using phred. II. Error probabilities. *Genome Research* 8:186-194.

- Gasol, J. M. & Del Giorgio, P. A. (2000). Using flow cytometry for counting natural planktonic bacteria and understanding the structure of planktonic bacterial communities. *Sci. Mar.* 64, 197–224.
- Magurran AE. (1988). *Ecological Diversity and Its Measurement*. Princeton University Press, Princeton, New Jersey.
- Marker A.F.H., Crowther C.A. & Gunn R.J.M. (1980). Methanol and acetone as solvents for estimating chlorophyll a and phaeopigments by spectrophotometry. *Arch. Hydrobiol. Beih.* 14: 52–69.
- Morillo, J., Usero, J. and Gracia, I. (2002). Partitioning of metals in sediments from the Odiel River (Spain). *Environ. Int.*, 28, 263-271.
- Murphy, J. & Riley, J. P. (1962). A modified single solution method for the determination of phosphate in natural waters. *Analytica Chimica Acta.* 27, 31–36. *Rev. Sci. Eau*, 15, 123–135.
- Rodríguez-Estival, J., Sánchez, M. I., Ramo, C., Varo, N., Amat, J. A., Garrido-Fernández, J., Hornero-Méndez, D., Ortiz-Santaliestra, M. E., Taggart, M. A., Martínez-Haro, M., Green, A. J., Mateo, R. (2019). Exposure of black-necked grebes (*Podiceps nigricollis*) to metal pollution during the moulting period in the Odiel Marshes, Southwest Spain. *Chemosphere* 216, 774-784.
- Schloss PD, Westcott SL, Ryabin T, Hall JR, Hartmann M, Hollister EB, *et al.* (2009) Introducing mothur: open-source, platform-independent, community-supported software for describing and comparing microbial communities. *Appl Environ Microbiol*; 75(23):7537–41. <https://doi.org/10.1128/AEM.01541-09> PMID: 19801464
- Smith, D. C. & Azam, F. A. (1992). Simple, economical method for measuring bacterial protein synthesis rates in seawater using 3H-leucine. *Mar Microb Food Webs* 6, 107–114.
- Viñals, M. J., W. Colom, T. Rodrigo, M. J. Dasi, J. Armengol, R. Oltra, and R. Miracle. (2001). Rasgos característicos de un humedal mediterráneo artificializado y su problemática ambiental, El Hondo de Elche (Alicante, España). *Humedales Mediterráneos* 1:147–154
- Yokokawa, T., Sintés, E., De Corte, D., Olbrich, K., and Herndl, G.J (2012). Differentiating leucine incorporation of Archaea and Bacteria throughout the water column of the eastern Atlantic using metabolic inhibitors. *Aquatic microbial ecology*. Vol. 66: 247–256. doi: 10.3354/ame01575.



Chapter 2

Alternation of bacterial and archaeal heterotrophic production along nitrogen and salinity gradients in coastal wetlands

Alternation of bacterial and archaeal heterotrophic production along nitrogen and salinity gradients in coastal wetlands

2

2.1. INTRODUCTION

Saline wetlands represent about 44% of the volume and 23 % of the area of all lakes on Earth (Messenger *et al.* 2016). They are usually very productive ecosystems and can effectively sequester carbon and in endorheic basins this process occurred even at geological time scale (Chmura *et al.* 2003; Li *et al.* 2017). These wetlands also have high heterotrophic prokaryotic production and abundance (Eiler *et al.* 2003; López-Archilla *et al.* 2004; Ortega-Retuerta *et al.* 2007; Casamayor *et al.* 2013; Sorokin *et al.* 2014). Currently, most wetlands are salinizing as a consequence of climatic warming (Herbert *et al.* 2015). On the one hand, droughts are increasing mineral evapoconcentration and reducing lake surfaces in endorheic basins (Wurtsbaugh *et al.* 2017) and, in the other hand, the rise of sea level is introducing marine waters up into the estuaries and marshes areas salinizing coastal wetlands (Herbert *et al.* 2015; Schuerch *et al.* 2018). Saline wetlands are characterized by shallow waters with high content in nutrients and dissolved organic carbon due to mineral evapoconcentration in endorheic lakes (Batanero *et al.* 2017) and in coastal wetlands due to the high water turnover (Ferrarin *et al.* 2013). How salinity can affect prokaryotic heterotrophic production might help to make more accurate projections on potential changes in carbon storage in saline wetlands in future scenarios of salinization in coastal wetlands.

Among the different aquatic ecosystems, wetlands also retain the highest proportion of anthropogenic nitrogen inputs (Saunders & Kalff, 2001) and, along with riparian zones; they improve water quality via denitrification (Verhoeven *et al.* 2006). The anthropogenic production of nitrogen fertilizer has enabled humankind to greatly increase food production; nevertheless, it has drastically disrupted the nitrogen cycle and has led to environmental problems such as eutrophication (Gruber & Galloway 2008; Canfield *et al.* 2010). This anthropogenic nitrogen production has doubled its inputs to the Earth's surface changing the

nitrogen cycle at local, regional and global scale. This change likely exceeds all the other human interventions in the cycles of nature (Gruber & Galloway 2008; Schlesinger, 2009), but in comparison with the carbon cycle has received less attention (Battye *et al.* 2017). A substantial fraction of this nitrogen, mostly derived from agricultural lands, is transported to rivers and groundwater through runoff and lost through emissions of ammonia, and other nitrogen compounds mostly by anoxic denitrification and, in oxic waters, via nitrifier denitrification (Schlesinger, 2009; Battye *et al.* 2017). Therefore, in many estuarine areas, before river discharges, natural or constructed wetlands modify the nitrogen loading into the coastal areas circumventing to some extent coastal eutrophication. These transitional waters include saline wetlands such as natural marshes and multi-pond solar salterns (Razinkovas-Baziukas & Povilanskas, 2012). In particular, multi-pond solar salterns are present all around the Mediterranean coasts and Portugal since the Phoenicians; who used ancient evaporation procedures (originally from the Emperor Huang era about 2,500 years Before Christ) to obtain salt (Baas-Becking 1931; García-Vargas & Martínez-Maganto 2006). In addition, coastal saline wetlands have also great importance for waterfowl conservation and sustainable aquaculture beyond of salt extraction (Athearn *et al.* 2009; Walton *et al.* 2015).

Despite this global prevalence of saline wetlands and their biogeochemical significance at global scale, most studies of microbial ecology in these systems have been focused on extremophile microorganisms in the hypersaline range to explore the bioenergetics and diversity constrains of microbial life associated with salinity (Antón *et al.* 2000; Pedrós-Alió *et al.* 2000a; Oren 2001; Casamayor *et al.* 2002; Gasol *et al.* 2004; Ghai *et al.* 2011). However, our understanding of moderately halophilic microorganisms in the range from oligo- to euhaline waters still remains very limited (Hahn, 2006; Herbert *et al.* 2015). The discovery that archaea are not exclusively extremophiles and they also appear in mesophilic conditions (DeLong 1992; Fuhrman 1992; Karner *et al.* 2001) has promoted studies showing that archaeal species are abundant, ubiquitous and diverse with relevant functions in both carbon cycle and nitrogen cycle (Herndl *et al.* 2005; Justice *et al.* 2012; Offre *et al.* 2013).

Archaea have relevant roles in the mineralization of organic matter in oxic conditions at least in the ocean (Herndl *et al.* 2005; Ingalls *et al.* 2006). In fact, the organo-heterotrophic nature of some archaeal groups has been recently demonstrated for specific carbohydrates (Lazar *et al.* 2016) and for dissolved proteins (Orsi *et al.* 2016). Archaea are also relevant for ammonia oxidation during nitrifier denitrification in oxic conditions and for denitrification in anoxic or suboxic conditions (Francis *et al.* 2007; Offre *et al.* 2013) with potential implications for nitrogen removal in wetlands (You *et al.* 2009). However, archaeal heterotrophic production patterns along gradients of dissolved organic carbon, nitrogen and salinity are still poorly known.

Wetlands salinization, under the projected scenario of climatic warming, and the increase of nitrogen inputs might affect ecosystem services such as carbon storage (Weston *et al.* 2011; Luo *et al.* 2017) and nitrogen removal (Franklin *et al.* 2017). In fact, these two environmental problems interact and eutrophication can boost organic carbon mineralization, reducing carbon storage, in coastal marshes (Deegan *et al.* 2012) and salinization can affect microbial nitrogen removal (Franklin *et al.* 2017). The main goal of this chapter is to describe the microbial patterns in abundance, and bacterial and archaeal heterotrophic production in a large set of semi-natural and constructed wetlands covering wide gradients of salinity, dissolved organic carbon and nitrogen along the Western Mediterranean coast. In addition, we identified the main drivers of those patterns and speculated on the potential changes in prokaryotic heterotrophic production in future scenarios of wetlands salinization and increases in nitrogen inputs.

2.2. MATERIALS AND METHODS

Study sites

We sampled a total of 112 saline ponds from nine sites during the summers of 2011, 2012 and 2013 (Table 2.1). The nine sites were: Odiel marshes (OdielM), Veta la Palma, (VPalma), Cabo de Gata (CGata), Santa Pola (SPola), El Hondo (Hondo), Ebro Delta (EbroD), Giraud and Saintes-Maries-de-la-Mer (Camargue), Molentargius, Santa Guilla and Santa Catherine (Sardinia), and Sfax (Sfax) (Fig. 2.1a). Study ponds are located in semiarid or arid areas, under typical Mediterranean climatic conditions, covering a wide gradient of salinity from hypersaline (solar salterns) to oligo-mesohaline (brackish) waters (Fig. 2.1b) and microbial productivity (Fig. 2.1c).

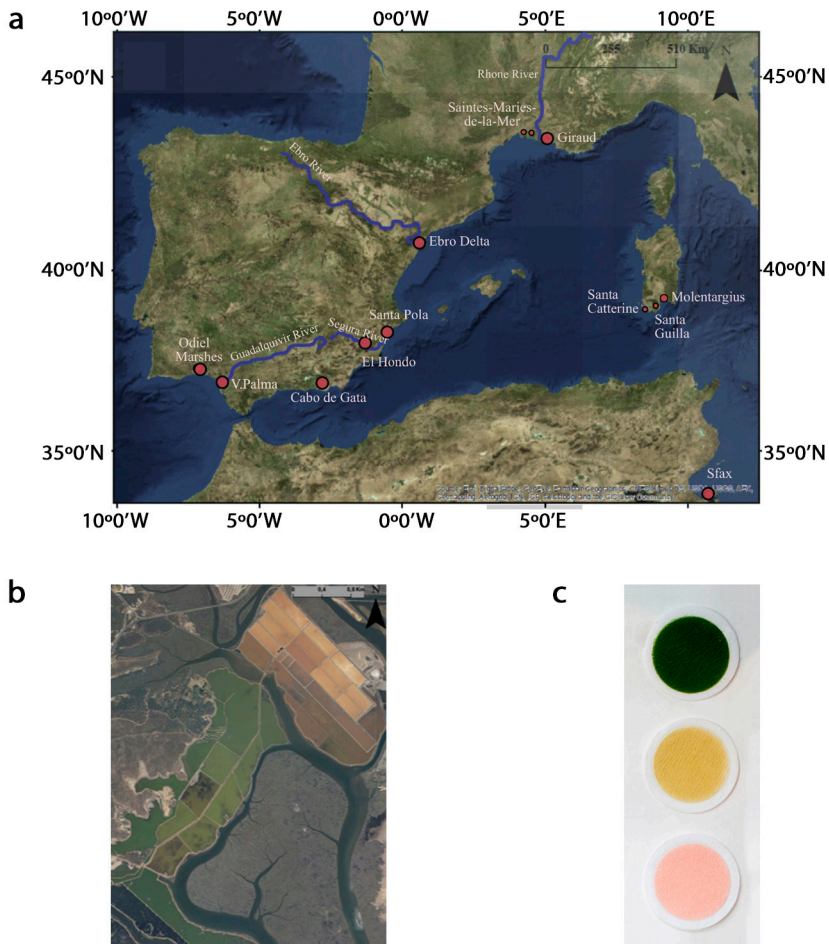


Figure 2.1. Locations of the coastal wetlands studied (a): Odiel marshes (OdielM), Veta la Palma, (VPalma), Cabo de Gata (CGata), Santa Pola (SPola), El Hondo (Hondo), Ebro Delta (EbroD), Giraud and Saintes-Maries-de-la-Mer (Camargue), Molentargius, Santa Guilla and Santa Catterine (Sardinia), and Sfax (Sfax); (b) Aerial photo of Odiel marshes, showing reservoir, evaporation and crystallizations ponds; and (c) G/F filters showing the pigment diversity of these ponds.

Solar salterns are often built as connected multi-pond systems for commercial salt production, which create a strong salinity gradient from evaporation ponds to crystallizer ponds that can be considered as natural laboratories (Fig. 2.1b) with obvious changes in microbial communities (Fig. 2.1c). In each particular pond the salinity is kept roughly constant and therefore they can be considered a stable environment (Sánchez *et al.* 2006). The brackish wetlands that we have studied are also important for sustainable aquaculture and waterfowl conservation (Sánchez *et al.* 2006). Complete physical-chemical and microbiological details for each pond are provided in Annex Chapter 2 (Table S1).

Chemical analyses

We recorded salinity with a multi-parameter probe (HANNA HI 9828). Water samples with salinity higher than 70 ppt were diluted with Milli-Q water, until they were in the operating range of the probe. Total nutrient concentrations were measured in unfiltered water, while samples for dissolved nutrient analysis were filtered through pre-combusted 0.7 μ m pore-size Whatman GF/F glass-fiber filters. Total phosphorus (TP) and total dissolved phosphorus (TDP) concentrations were measured using the molybdenum blue method (Murphy & Riley, 1962) after persulfate digestion (30 min, 120°C). Total nitrogen (TN) and total dissolved nitrogen (TDN) were analyzed by high-temperature catalytic oxidation (Álvarez-Salgado and Miller, 1998) using a total nitrogen analyzer (Shimadzu TNM-1). Standardization of the instrument was done with potassium nitrate. Dissolved organic carbon (DOC) concentration was analyzed as non-purgeable organic carbon by high-temperature catalytic oxidation using a total organic carbon analyzer (Shimadzu TOC-V CSH). Dissolved organic carbon (DOC) samples were pre-filtered through pre-combusted 0.7 μ m Whatman GF/F filters (2 hours at 500°C) and acidified with H₃PO₄ (final pH<2). The instrument was calibrated using a four-point standard curve of potassium hydrogen phthalate. Samples were purged with phosphoric acid for 20 min and three to five injections were analyzed for each sample

Biological analyses

We determined chlorophyll-a concentration filtering through 0.7 μ m pore-size Whatman GF/F glass-fiber a variable water volume from 50 ml to 2017 ml. Chlorophyll-a (chl a) was extracted with 95% methanol during 24 h in the dark at 4 °C (APHA, 1992), and was measured using a Perkin Elmer Lambda 40 spectrophotometer at 665 nm and 750 nm.

Samples for determining the abundances of prokaryotes (PA) and cyanobacteria (CyA) were taken in criovials, fixed in situ with 1% paraformaldehyde + 0.05% glutaraldehyde in the dark (30 min at 4 °C), frozen in liquid nitrogen, and stored at -80 °C until analysis with flow cytometry (Gasol and del Giorno, 2000). Once we defrosted the samples, to avoid the electronic coincidence of the prokaryotic cells, they were diluted (\geq 10-fold) with Milli-Q water. PA and CyA samples were analysed in a FACScalibur flow cytometer with a laser emitting at 448nm, and a suspension of yellow-green ca. 1 μ m latex beads (Polysciences) was added per sample as an internal standard. PA samples were stained in the dark (10 min) with a 10 μ M DMSO solution of Sybr Green I stain (Molecular Probes), run at low speed during 2 minutes and were detected by their signature in bivariate plots as side scatter (SSC) vs. FL1 (Green fluorescence). CyA samples were run at high speed during 4 minutes and were detected by their signature in bivariate plots as Side scatter (SSC) vs. FL3 (Red fluorescence). Heterotrophic prokaryotic abundance (HPA) was estimated by subtracting cyanobacteria abundance (CyA) from prokaryotic abundance (PA).

Samples for determining the virus abundance (VA) were taken in different criovials, fixed in the dark with glutaraldehyde at a final concentration of 0.5 % (15 min at 4°C), frozen in liquid nitrogen and stored at -80°C until analysis with flow cytometry (Brussard *et al.*, 2010). Prior to analysis, samples were diluted ≥ 100 -fold with TE-buffer pH 8.0 (10 mM Trihydroxymethyl-aminomethane; 1 mM ethylenediaminetetraacetic acid) to avoid electronic coincidence in virus particle counts. VA samples were stained with a working solution (1:200) of SYBR Green I (10,000X concentrate in DMSO, Molecular Probes) for 10 min in the dark and then kept at -80° until counting. Fluorescent microspheres (FluoSpheres carboxylate modified yellow-green fluorescent microspheres; 1.0 μm diameter) were added as an internal standard. Data were acquired in log mode and were detected by their signature in bivariate plots as Side scatter (SSC) vs. FL1 (Green fluorescence). Flow cytometry data were analyzed using BD CellQuest Pro software.

We measured bacterial heterotrophic production (BP) and archaeal heterotrophic production (ArP) using the 3H-Leucine incorporation into proteins (Smith and Azam, 1992). To selectively inhibit bacterial heterotrophic production we used erythromycin (Yokokawa *et al.* 2012). Two sets of three replicates (1.5 ml) and 2 trichloroacetic acid (TCA, 50%)-killed blanks (final concentration 10%) were incubated for each pond, with 54.6 nM or 58.4 nM leucine (1:2 hot: cold v/v) for 2 to 5 hours at in situ temperature. One of this set of 5 samples also contained 10 $\mu\text{g ml}^{-1}$ of erythromycin (final concentration) to inhibit bacterial production and obtain exclusively the heterotrophic production associated with archaea. The addition of TCA at a final concentration of 10% ended the incubations. In the laboratory, the samples were centrifuged (14000 rpm for 10 min), rinsed with TCA (5%), vortexed, and centrifuged again. Finally, 1.5 ml of liquid scintillation cocktail (Ecoscint A) was added to each sample and was radio-assayed using an autocalibrated scintillation counter (Beckman LS 6000 TA). Due to equipment failures or logistic problems, some parameters could not be obtained for all the study ponds. The samples for DOC were not analyzed for the ponds at the Camargue site. The HA and CyA were not determined for Camargue, Sardinia and Tunisia, and VA was not determined for El Hondo.

Statistical analyses

To determine the main drivers of the prokaryotic dynamics in the study wetlands we carried out four sets of generalized linear models (GLMs) to optimize the whole data set. In the first set of GLMs, the dependent variables considered were: prokaryotic heterotrophic abundance (PHA), cyanobacteria abundance (CyA), bacterial heterotrophic production (BP), and archaeal heterotrophic production (ArP). The predictor variables selected were: site (i.e. each wetland complex as a categorical variable), salinity, total dissolved nitrogen (TDN) and total dissolved phosphorus (TDP) (as continuous variables). We applied log and square root transformations to the dependent and predictor variables to improve the fit to a nor-

mal distribution and to avoid heteroscedasticity when it was necessary. In the second set of GLMs, we also included the concentration of dissolved organic carbon (DOC) as a predictor variable, but the data from Camargue were excluded since this variable was not available for this site. In the third set of GLMs, we determined the best predictors of the virus abundance (dependent variable) in the six sites (Odiel M, VPalma, CGata, SPola, Hondo, EbroD) where this variable was available. In this third analysis nutrients were not included as predictors because viruses are mostly dependent on host (bacterial or archaeal) density. We considered the study site as a categorical variable and salinity, PA and CyA as continuous variables. Then, to determine the potential effect of viruses on the other microbial components we performed the fourth set of GLMs considering VA as a predictor variable and BP and ArP as dependent variables. The model with the smallest value of Akaike Information Criterion (AIC) was selected as the best model for each dependent variable considered. Details of alternative “best models” for which $\Delta AIC < 2.0$ are provided in the Annex Chapter 2 (Tables S2-S6). All analyses were performed using Statistica 7.0.

2.3. RESULTS

The study ponds represented a salinity gradient that ranged more than 4 orders of magnitude from 0.22 to 343 ppt (Table 2.1) from oligo- to hyperhaline conditions, with the highest median value observed in EbroD ponds and the lowest median value in the El Hondo ponds (Fig. 2.2a). DOC concentration ranged from 0.24 to 5.76 mmol-C l⁻¹ (Table 2.1). Like for salinity, the highest median DOC concentration was observed in EbroD ponds but the lowest one was in the CGata ponds (Fig. 2.2b). TDN concentration ranged from 0.02 to 0.62 mmol-N l⁻¹ (Table 2.1). EbroD ponds also showed the highest median TDN concentration and SPola showed the lowest one (Fig. 2.2c). TDP concentration ranged from 0.50 to 40.09 μmol-P l⁻¹ (Table 2.1), with the highest median value at OdielM and the lowest at CGata (Fig. 2.2d).

Table 2.1. Ranges of basic physicochemical variables, total dissolved nitrogen (TDN), total dissolved phosphorus (TDP), dissolved organic carbon (DOC), concentration of chlorophyll *a* (Chl *a*) and virus abundance (VA) for each set of ponds in the study wetlands.

Location Sites (acronyms)	N° Ponds	Temperature (°C)	Salinity (ppt)	TDN (mmol-N l ⁻¹)	TDP (μmol-P l ⁻¹)	DOC (mmol-N l ⁻¹)	Chl <i>a</i> (μg l ⁻¹)	VA (x10 ⁹ particles ml ⁻¹)
Odiel Marshes (OdielM) Huelva, Spain	19	20.1-25.4	23.1-197.8	0.02-0.50	3.12-48.06	0.36-3.78	2.22 - 108.99	0.17 - 3.07
Veta la Palma, Doñana (VPalma) Sevilla, Spain	10	27-33.5	14.4-34.3	0.09-0.27	0.51-12.27	0.74-3.11	n.d.	0.2 - 1.14
Cabo de Gata (CGata) Almería, Spain	6	24.9-27.6	36.1-115.6	0.13-0.31	0.51-2.28	0.24-0.87	n.d.	0.04 - 0.12
Santa Pola (SPola) Alicante, Spain	14	22-27.3	35.1-162.1	0.02-0.32	0.81-11.22	0.45-2.91	1.59 - 201.83	0.02 - 1.11
El Hondo (Hondo) Alicante, Spain	7	24.2-30.6	4.3-22.0	0.15-0.29	1.31-8.96	1.4-3.26	7.3 - 149.63	0.35 - 1.10
Ebro Delta (EbroD) Tarragona, (Spain)	13	23.8-32.9	40.6-343	0.14-0.62	0.81-5.35	0.52-5.76	0.04-9.7	0.09 - 1.69
Giraud, Saintes-Maries-de-la-Mer (Camargue), France	14	19.1-30.3	0.2-194.7	0.04-0.35	2.22-6.89	n.d.	2.08-25.69	n.d.
Molentargius, Santa Guilla and Santa Catterine (Sardinia), Italy	13	25.4-33.4	2.0-238.8	0.05-0.44	0.81-11.35	0.34-4.89	6.09 - 617.41	n.d.
Sfax (Sfax) Sfax, (Tunisia)	12	24.5-29.8	40.6-220.2	0.05-0.45	2.67-40.94	0.41-3.49	1.89- 94.58	n.d.

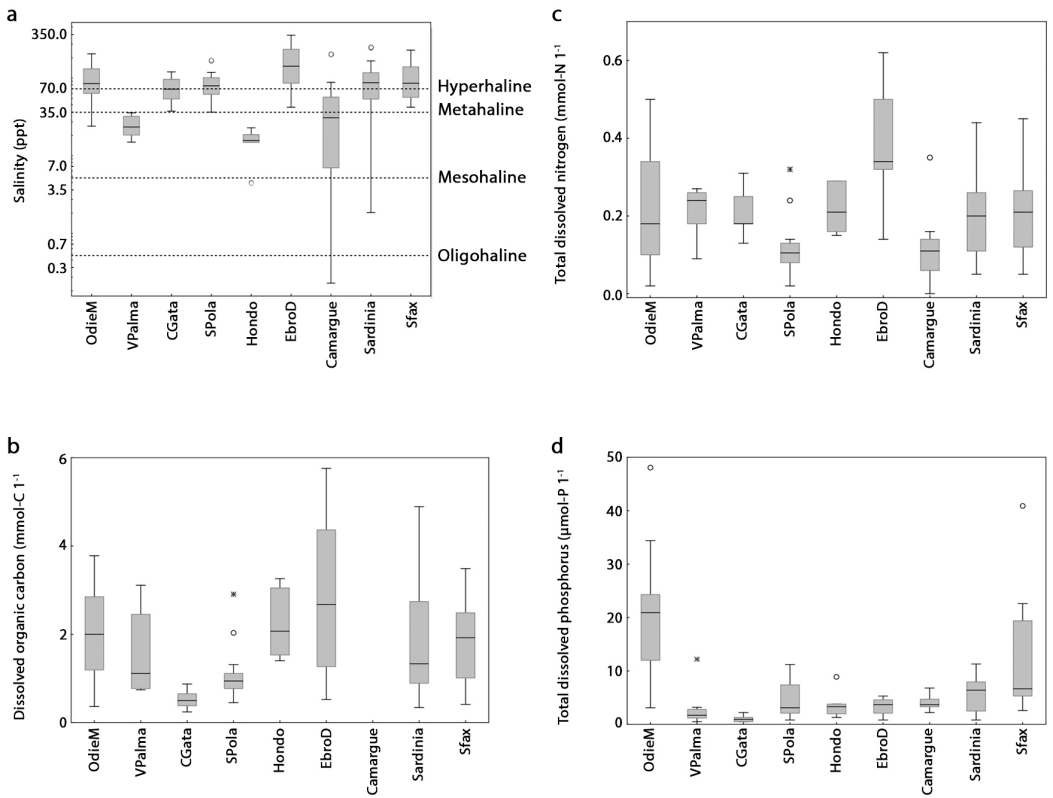


Figure 2.2. Summary of raw data for physico-chemical parameters in saline wetlands studied in the western Mediterranean basin. Values of salinity (a), total dissolved organic carbon (b), total dissolved nitrogen (c) and total dissolved phosphorus (d) for each saline wetland studied. Lines = Median values. Boxes = 25% and 75% percentils and whiskers= non-outlier range, outliers (dots) and extreme points (asterisks).

Prokaryotic heterotrophic abundance (PHA) ranged almost three orders of magnitude from 0.35×10^6 to 252×10^6 cells ml^{-1} (Table S1) with the highest median value in Sfax and the lowest one in CGata ponds (Fig. 2.3a), while cyanobacteria abundance ranged from 0.01 to $38105 (\times 10^3)$ cells ml^{-1} (Table S1; Fig. 2.3b). Bacterial heterotrophic production ranged from 18.96 pmoles of leucine $\text{l}^{-1}\text{h}^{-1}$ to 3006.80 pmoles of leucine $\text{l}^{-1}\text{h}^{-1}$ (Table S1; Fig. 2.3c), while archaeal heterotrophic production ranged from 55.72 pmoles of leucine $\text{l}^{-1}\text{h}^{-1}$ to 2289.87 pmoles of leucine $\text{l}^{-1}\text{h}^{-1}$ (Table S1; Fig. 2.3d). Chlorophyll-a concentration ranged more than 5 orders of magnitude from 0.04 to $617.41 \mu\text{g l}^{-1}$ (Table 2.1), with the highest median value at Sfax and the lowest one at DEbro (Fig. 2.3e).

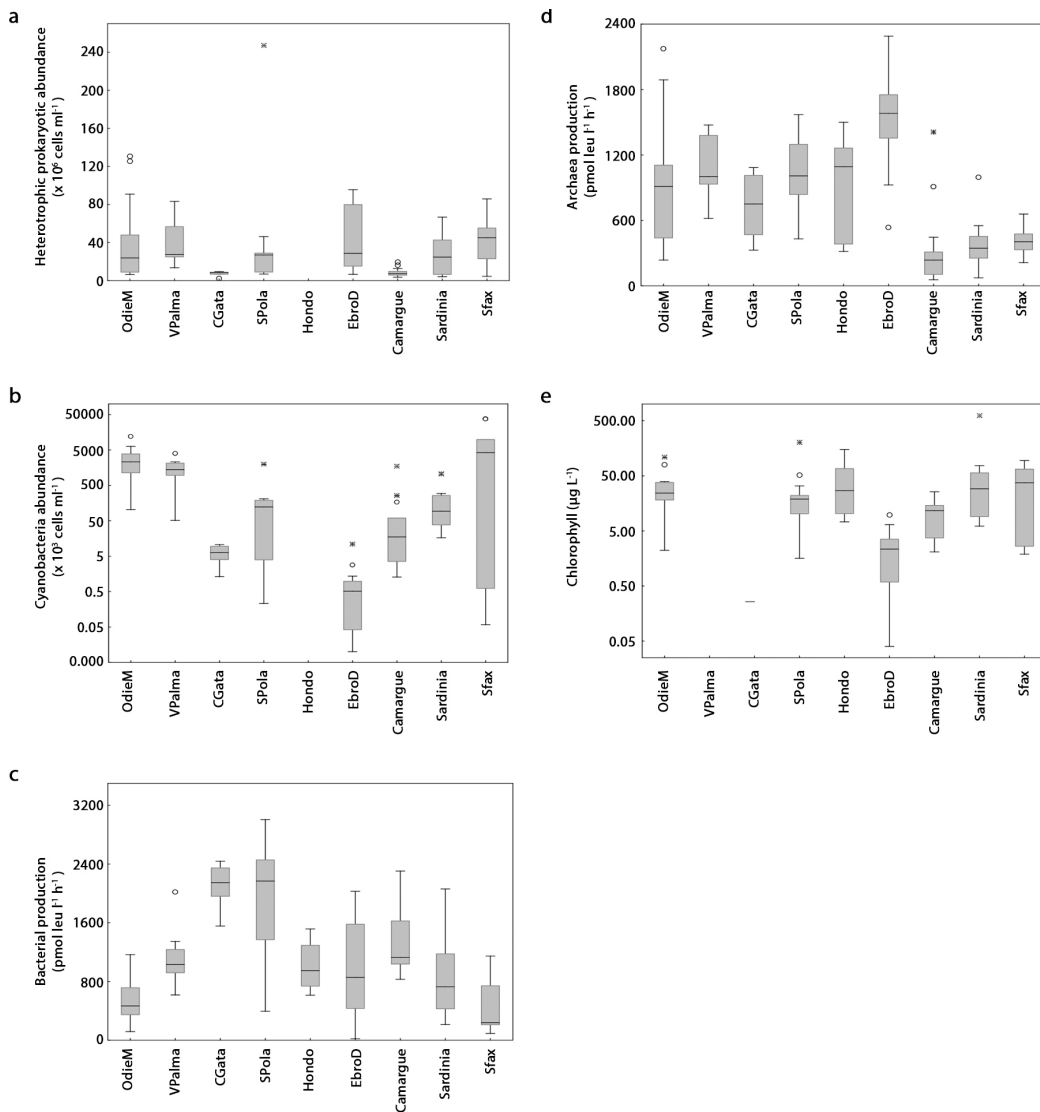


Figure 2.3. Summary of raw abundance and production of heterotrophic prokaryotes and cyanobacteria in saline wetlands studied in the western Mediterranean basin. Values of heterotrophic prokaryotic abundance (a), cyanobacteria abundance (b), bacterial production (c), archaea production (d) and chlorophyll concentration (e) for each saline wetland studied. Lines = Median values. Boxes = 25% and 75% percentils and whiskers= non-outlier range, outliers and extreme points.

In the first set of GLMs performed (Table S2 in Annex Chapter 2), we obtained that the best GLM varied for each microbial variable. For heterotrophic prokaryotic abundance, the best model includes TDN concentration and sites (categorical) as predictors (Table 2.2). The residuals of prokaryotic heterotrophic abundance (once the site was controlled) were significant and positively related to TDN concentration (Fig. 2.4a). Alternative (less significant) models also included salinity or TDP (Table S2 in Annex Chapter 2).

Table 2.2. Summary of the best-generalized linear models (GLMs) (according to AIC) selected for the prokaryotic abundance and production variables. Columns show the estimates, standard errors, Wald statistic and P values for selected predictor variables. The complete set of alternative models with $\delta AIC < 2.0$ are shown in Chapter 2 Appendix (Table S2).

Dependent Variables	Predictor Variables	Estimate	Standard Error	Wald Stat.	p-values
Prokaryotic heterotrophic abundance	Intercept	2.068672	0.013074	25035.27	0.000000
	TDN	0.109782	0.015932	47.48	0.000000
	Sites	---	---	43.76	0.000000
Cyanobacteria abundance	Intercept	1.799727	0.105138	293.0189	0.000000
	Sites	---	---	106.1193	0.000000
	TDP	-0.267744	0.080808	10.9782	0.000922
	TDN	0.181139	0.087963	4.2406	0.039468
Bacterial heterotrophic production	Intercept	3.044352	0.075297	1634.684	0.000000
	TDN	-0.492054	0.089367	30.316	0.000000
	Sites	---	---	107.336	0.000000
Archaeal heterotrophic production	Intercept	1.125856	0.021440	2757.573	0.000000
	TDN	0.139250	0.028357	24.115	0.000001
	Sites	---	---	112.124	0.000000

The best GLM for cyanobacteria abundance included sites as categorical variable and TDN and TDP as continuous variables (Table 2.2), with a significant positive relationship with TDN and negative relationship with TDP (Table 2.2). In the case of bacterial heterotrophic production, the best GLM included TDN concentration and sites as predictors (Table 2.2). The residuals of bacterial heterotrophic production (once the site was controlled) were significant and negatively related to TDN concentration (Fig. 2.4b). Indeed, the higher TDN concentration, the lower the bacterial production is, irrespectively of the site considered. Alternative (less significant) models also included salinity or TDP (Table S2 in Annex Chapter 2). For the archaeal heterotrophic production, the best GLM also included TDN concentration and sites as predictors (Table 2.2). In contrast to bacterial heterotrophic production, the residuals of archaeal heterotrophic production (once the site was controlled) were significant and positively related to TDN concentration (Fig. 2.4c). Indeed, the higher TDN concentration, the higher the archaeal production is, irrespectively of the site considered. Alternative (less significant) models also included salinity or TDP (Table S2 in Annex Chapter 2).

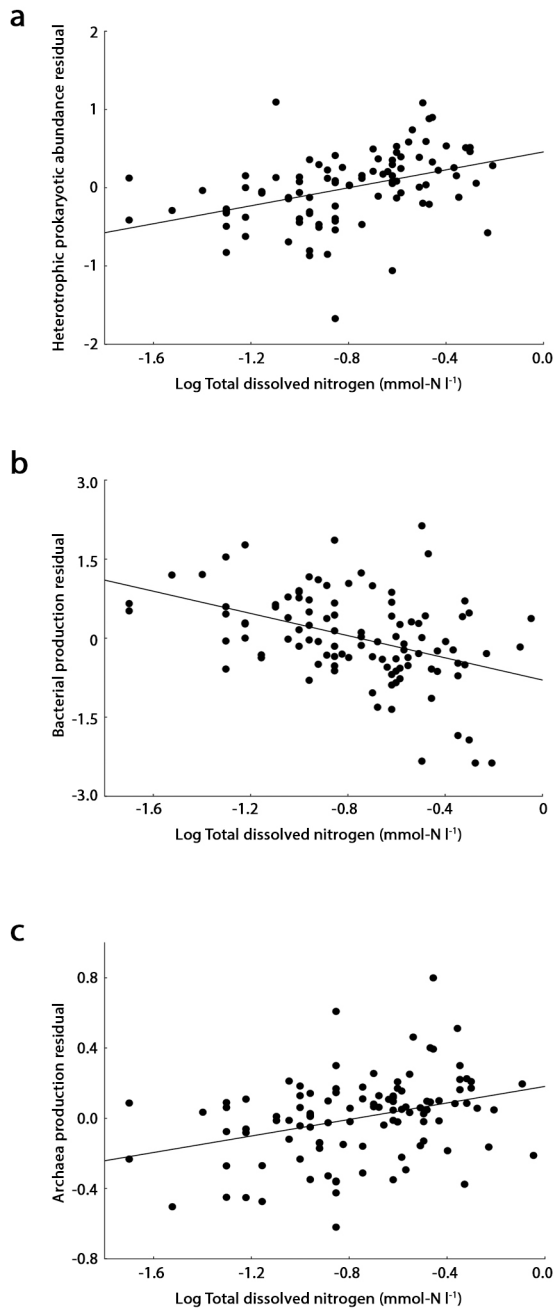


Figure 2.4. Linear regressions between heterotrophic abundance and prokaryotic production and TDN. Partial effects for relationships between (a) heterotrophic prokaryotic abundance, (b) bacterial production and (c) archaea production and TDN, based on the best models shown in Table 2. In each case the Y variable represents the residuals taken from the selected model after extraction of the X variable.

In the second set of GLMs performed, we also included the concentration of dissolved organic carbon (DOC) as a predictor variable, but Camarga site was excluded since these data were not available. This predictor variable only affected the results previously exposed for heterotrophic prokaryotic abundance and for heterotrophic bacterial production (Table S3 in Chapter 2 Appendix). In this second analysis, prokaryotic heterotrophic abundance was driven negatively by salinity and positively by DOC concentration. DOC concentration, depending on sites, controlled bacterial heterotrophic production negatively.

In a third set of GLMs we determined the best GLM exclusively for the virus abundance excluding nutrients as predictors (Table 2.3). This model included salinity as a continuous predictor and site as categorical predictor. We observed a positive relationship between the residuals of virus abundance (once site influence was considered) and the salinity (Figure 2.5). Alternative (less significant) models also included heterotrophic prokaryotic and cyanobacteria abundances (Table S4 in Annex Chapter 2).

Table 2.3. Summary of the best-generalized linear model (according to AIC) selected for the virus abundance in the sites: Odiel M, VPalma, CGata, SPola, Hondo, and EbroD. Columns show the estimates, the standard errors, the Wald statistics, and the p-values for the predictor variables. The complete set of alternative models with $\delta AIC < 2.0$ are shown in Chapter 2 Appendix (Table S4).

<i>Dependent Variables</i>	<i>Predictor Variables</i>	<i>Estimate</i>	<i>Standard Error</i>	<i>Wald Stat.</i>	<i>p-values</i>
Virus abundance	Intercept	1.316355	0.053246	611.1956	0.000000
	Salinity	0.204842	0.028806	50.5662	0.000000
	Site	---	---	117.4885	0.000000

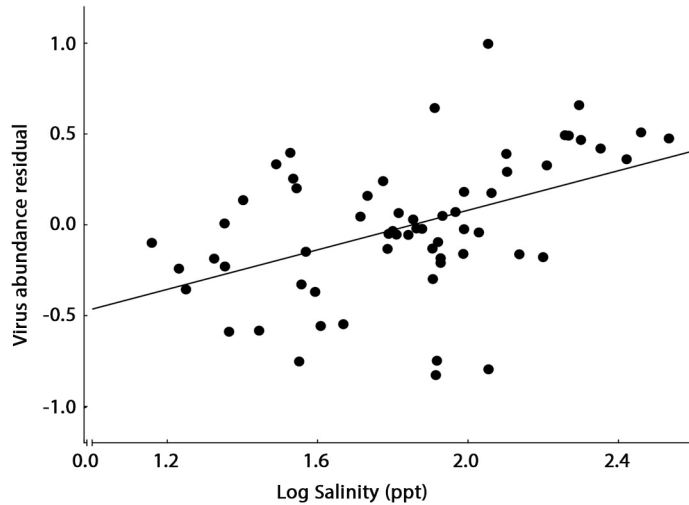


Figure 2.5. Partial effect for relationship between virus abundance and salinity based on the best models shown in Table 2.3.

Finally, we performed a four set of GLMs now including also the virus abundance as predictor of bacterial and archaeal heterotrophic production (Table S5 in Annex Chapter 2) but considering only the sites: Odiel M, VPalma, CGata, SPola, Hondo, and EbroD. The best GLM for bacterial heterotrophic production included salinity and virus abundance as predictors (Table 2.4). Once the site effect was considered, we observed a negative and significant relationship between the bacterial heterotrophic production and the salinity (Figure 2.6a) and the virus abundance (Figure 2.6b).

Table 2.4. Summary of the best-generalized linear model (GLM) (according to AIC) selected for bacterial production. Columns show the estimates, standard errors, Wald statistics, and p-values for the selected predictor variables. The complete set of models with $\delta AIC < 2.0$ are shown in Table S4.

Dependent Variables	Predictor Variables	Estimate	Standard Error	Wald Stat.	p-values
Bacterial heterotrophic production	Intercept	5.249544	0.334563	246.2003	0.000000
	Site	---	---	36.5871	0.000001
	Salinity	-0.436568	0.120411	13.1453	0.000288
	VA	-0.187402	0.066857	7.8570	0.005062

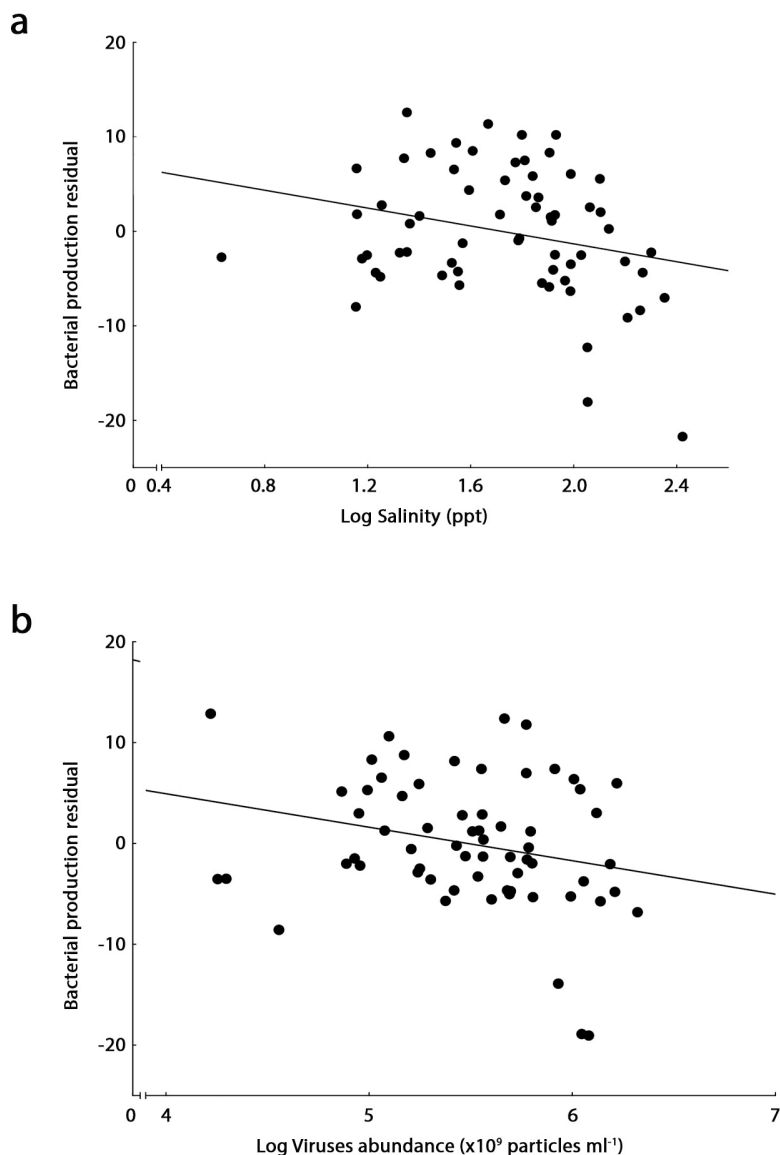


Figure 2.6. Linear regressions between bacterial production and their biological and physico-chemical predictors. Partial effects for relationships between (a) salinity (b) virus abundance, based on the best models shown in Table 2.4. In each case the Y variable represents the residuals taken from the selected model after extraction of the X variable.

On the other hand, the best GLM for archaeal heterotrophic production was coherent with the first set of GLMs performed, which included all the saline wetlands, and the best GLM for archaeal heterotrophic production included TDN and site as predictors (Annex Chapter 2, Table S5).

2.4. DISCUSSION

The best GLMs including all the study sites indicate that total dissolved nitrogen (TDN) is the main driver of the abundance of heterotrophic prokaryotes, bacterial heterotrophic production, and archaeal heterotrophic production. Total dissolved nitrogen consistently promoted archaeal heterotrophic production even considering the alternative GLMs that included dissolved organic carbon (DOC) and virus abundance (VA) as predictor variables. In contrast, bacterial heterotrophic production was negatively to TDN. This result changed when DOC and VA were also considered. The negative relationship between TDN and bacterial heterotrophic production appear to be mediated by salinity and virus abundance. Bacterial heterotrophic production declines as salinity and viruses increase. There is an alternation of the bacterial heterotrophic production (BP) by archaeal heterotrophic production (ArP) as salinity and virus abundance increase.

Archaeal species were considered, until the last decades, extremophiles usually associated to inhospitable environments such as salterns ponds where salt concentration is close to saturation (Oren, 1994, 2011; Antón *et al.* 1999). However, in this study, salinity does not seem to affect significantly ArP, whereas TDN resulted the most consistent predictor variable. Coastal wetlands provide the optimal conditions for denitrification such as a low oxygen concentration, high organic matter concentration and nitrate supply (Seitzinger, 1988; Seitzinger *et al.* 2006), being also the main process removing nitrogen excesses in these ecosystems (Saunders & Kalf 2001). Recent studies have also detected ammonia-oxidizing archaea in a wide range of environments (Wuchter *et al.* 2006; Sims *et al.* 2012), being even more dominant than ammonia-oxidizing bacteria in some ecosystems as the ocean (Lam *et al.* 2007) or lakes (Jiang *et al.* 2009). In addition, Orsi *et al.* (2016) have recently demonstrated the organo-heterotrophic nature of some archaeal groups up taking dissolved proteins that have high nitrogen content. Therefore, our results emphasize that archaeal species appear to play a key role in nitrogen dynamics in coastal wetlands, not just via denitrification.

On the other hand, bacterial production (BP) appears to be controlled by virus abundance (VA) providing a potential explanation for the negative correlation between TDN and BP. The results show that, regardless of the study site, VA increased significantly with salinity (Table 2.3, Fig. 2.5) and they affected negatively to BP (Table 2.4, Fig. 2.4), whereas VA did not have effect on ArP (Annex Chapter 2, Table S5). Based on these findings it seems that the majority of viruses could be bacteriophages, being an important cause of bacterial mortality in these saline wetlands. Thus, external factors such as evaporation would trigger an increase in VA concentration, which would in turn increase bacterial mortality, while archaea communities would be more resilient to such changes. Another complementary explanation is that sa-

linity increases are coupled to reduction in oxygen solubility promoting suboxic conditions perhaps more energetically favourable for some halophilic archaeal groups (Oren, 2001).

Traditionally, earlier works (Cole *et al.* (1999)) focused on the importance of organic carbon availability as regulators of bacterial production in different types of aquatic ecosystems. However, there was no difference between the best GLM in archaea production with and without the inclusion of dissolved organic carbon (DOC) data, indicating that DOC did not appear to be a relevant predictive variable for archaeal production. This is likely to be related to the high DOC concentrations in these saline wetlands due to both evapoconcentration in hypersaline waters (Pedrós-Alió *et al.* 2000a, 2000b; Gasol *et al.* 2004; Clementino *et al.* 2008) and mixing processes when river water with fresh organic matter concentration flows into the oligo-eusaline wetlands (Walton, *et al.* 2015), ensuring the unlimited DOC for the microbial metabolism. On the other hand, previous studies also considered the phosphorous concentration as limiting factor for prokaryotic activity in freshwaters (Smith and Prairie 2004) and oceanic waters (Hoppe *et al.* 2002; Zaccone *et al.* 2003). However, our results showed that TDP was not included as predictor variable in the best GLMs for the different microbial variables, except for the abundance of cyanobacteria (CyA). This result suggests that the study coastal wetlands were not limited by phosphorous. Cotner *et al.* (2010) demonstrated that bacteria exhibit high flexibility in their P content and stoichiometry. Neither phosphorus nor dissolved organic carbon affected prokaryotic activity in the wide range of saline wetlands studied.

2.5. REFERENCES

- Álvarez-Salgado, X.A. and Miller, A.E.J. 1998. Simultaneous determination of dissolved organic carbon and total dissolved nitrogen in seawater by high temperature catalytic oxidation: conditions for precise shipboard measurements. *Marine Chemistry* 62: 325–333. doi: 10.1016/S0304-4203(98)00037-1.
- American Public Health Association (APHA). 1992. Standard methods for the examination of water and 357 wastewater, 18th ed. American Public Health Association.
- Antón J., Llobet-Brossa, E., Rodríguez-Valera, F. & Amann, R. (1999). Fluorescence in situ hybridization analysis of the prokaryotic community inhabiting crystallizer ponds. *Environ Microbiol* 1, 517–523.
- Athearn, N. D., Takekawa, J. Y., & Shinn, J. M. (2009). Avian response to early tidal salt marsh restoration at former commercial salt evaporation ponds in San Francisco Bay, California, USA. *Natural Resources and Environmental Issues*, 15(1), 14.
- Bass-Becking, L. G. M. (1931). Historical notes on salt and salt-manufacture. *The Scientific Monthly*, 32(5), 434-446.
- Batanero, G.L., León-Palmero, E., Li, L., Green, A.J., Rendón-Martos, M., Suttle, C.A., Reche, I. (2017). Flamingos and drought as drivers of nutrients and microbial dynamics in a saline lake. *Scientific Reports*, 7 (1), art. no. 12173. <https://doi.org/10.1038/s41598-017-12462-9>.
- Battye, W., V. P., Aneja and W. H., Schlesinger (2017). Is nitrogen the next carbon?, *Earth's Future*, 5, 894–904, doi:10.1002/2017EF000592.
- Brussaard, C. P. D., Payet, J. P., Winter, C. & Weinbauer, M. G. (2010). Quantification of aquatic viruses by flow cytometry. *Manual of Aquatic Viral Ecology* (ed. Wilhelm, S. W., Weinbauer, M. G. Suttle C. A.) 11, 102–109 (Association for the Sciences of Limnology and Oceanography).
- Canfield, D. E., Glazer, A. N. & Falkowski, P. G. (2010). The evolution and future of earth's nitrogen cycle. *Science* 330, 192–196.
- Casamayor, E. O., R. Massana, S. Benlloch, L. Ovreas, B. Diez, V. J. Goddard, J. M. Gasol, I. Joint, F. Rodríguez-Valera, and C. Pedros-Alío. (2002). Changes in archaeal, bacterial and eukaryal assemblages along a salinity gradient by comparison of genetic fingerprinting methods in a multi-pond solar saltern. *Environ. Microbiol.* 4:338–348.

- Casamayor, Emilio & Triadó-Margarit, Xavier & Castañeda, Carmen. (2013). Microbial biodiversity in saline shallow lakes of the Monegros Desert, Spain. *FEMS microbiology ecology*. 85. 10.1111/1574-6941.12139.
- Chmura, Gail & Anisfeld, Shimon & Cahoon, Donald & Lynch, James. (2003). Global carbon sequestration in tidal, saline wetland soils. *Global Biogeochem. Cycles*. 17. 10.1029/2002GB001917.
- Clementino, M.M., Vieira, R.P., Cardoso, A.M., Nascimento, A.P.A., Silveira, C.B., Riva, T.C., *et al.* (2008). Prokaryotic diversity in one of the largest hypersaline coastal lagoons in the world. *Extremophiles* 12: 595–604.
- Cole, J. J. (1999). Aquatic microbiology for ecosystem scientists: New and recycled paradigms in ecological microbiology. *Ecosystems* 2: 215–225.
- Cotner JB, Hall EK, Scott JT, Haldal M. (2010). Freshwater bacteria are stoichiometrically flexible with a nutrient composition similar to seston. *Front Microbiol* 1: 132.
- Deegan, Linda & Johnson, David & Warren, R & J Peterson, Bruce & W Fleeger, John & Fagherazzi, Sergio & Wollheim, Wilfred. (2012). Coastal eutrophication as a driver of salt marsh loss. *Nature*. 490. 388-92. 10.1038/nature11533.
- DeLong, E. F. (1992). Archaea in coastal marine environments. *Proc. Natl. Acad. Sci. USA* 89:5685–5689.
- Eiler, A., A. H. Farnleitner, T. C. Zechmeister, A. Herzig, C. Hurban, W. Wesner, R. Krachler, B. Velimirov, and A. K. T. Kirschner. (2003). Factors controlling extremely active prokaryotic communities in shallow soda pools. *Microb. Ecol.* 46:43–54.
- Ferrarin C, Bergamasco A, Umgieser G, Cucco A. (2013). Spatial zonation of transitional waters derived from modelled water renewal times. *J Mar Syst* 117–118:96–107.
- Francis, C. A., Beman, J. M. & Kuypers, M. M. (2007). New processes and players in the nitrogen cycle: The microbial ecology of anaerobic and archaeal ammonia oxidation. *ISME J.* 1, 19–27.
- Franklin, R.B., Morrissey, E.M., Morina, J.C. (2017). Changes in abundance and community structure of nitrate-reducing bacteria along a salinity gradient in tidal wetlands. *Pedobiologia* 60, 21–26.
- Fuhrman, J. A., K. McCallum, and A. A. Davis. (1992). Novel major archae-bacterial group from marine plankton. *Nature (London)* 356:148–149.

- García-Vargas, E. A., & Martínez Maganto, J. (2006). La sal de la Bética romana: Algunas notas sobre su producción y comercio. *Habis*, 37, 253-274.
- Gasol JM, Casamayor EO, Join I, Garde K, Gustavson K, Benlloch S *et al.* (2004). Control of heterotrophic prokaryotic abundance and growth rate in hypersaline planktonic environments. *Aquat Microb Ecol* 34: 193–206.
- Gasol JM, del Giorgio PA. (2000). Using flow cytometry for counting natural planktonic bacteria and understanding the structure of planktonic bacterial communities. *Scientia Marina* 64:197–224
Geophys Res 108(C9):8117.
- Geertz-Hansen *et al.* (2011) Ecosystem metabolism in a temporary Mediterranean marsh (Doñana National Park, SW Spain).
- Ghai R., Pašić L., Fernández A. B., Martín-Cuadrado A.-B., Megumi Mizuno C., McMahon K. D., Papke R. T., Stepanauskas R., Rodríguez-Brito B. *et al.* (2011). New abundant microbial groups in aquatic hypersaline environments. *Sci Rep* 1: 135.
- Gruber, Nicolas & Galloway, James. (2008). An Earth-system perspective of the global nitrogen cycle. *Nature* 451: 293-296. *Nature*. 451. 293-6. 10.1038/nature06592.
- Guixa-Boixereu, N., Calderon-Paz, J.I., Heldal, M., Bratbak, G. And Pedroñs-Alio C. (1996) Viral lysis and bacterivory as prokaryotic loss factors along a salinity gradient. *Aquat. Microb. Ecol.* 11, 215-227.
- Hahn MW. (2006). The microbial diversity of inland waters. *Current Opinion in Biotechnology* 17: 256-261.
- Herbert, E.R., P. Boon, A.J. Burgin, S.C. Neubauer, R.B. Franklin, M. Ardón, K.N. Hopfensperger, L.P.M. Lamers, *et al.* (2015). A global perspective on wetland salinization: Ecological consequences of a growing threat to freshwater wetlands. *Ecosphere* 6: 1–43.
- Herndl GJ, Reinthaler T, Teira E, van Aken H, Veth C, Pernthaler A *et al.* (2005). Contribution of archaea to total prokaryotic production in the deep atlantic ocean. *Appl Environ Microbiol* 71: 2303–2309.
- Hoppe HG, Arnosti C, Herndl GJ (2002) Ecological significance of bacterial enzymes in the marine environment. In: Burns RG, Dick RP (eds) *Enzyme in the environment: activity ecology and application*. Marcel Dekker, New York, pp 73–108.

- Ingalls AE, Shah SR, Hansman RL, Aluwihare LI, Santos GM, Druffel ERM *et al.* (2006). Quantifying archaeal community autotrophy in the mesopelagic ocean using natural radiocarbon. *Proc Natl Acad Sci USA* 103: 6442–6447.
- Jiang H, Dong H, Yu B, Lv G, Deng S, Berzins N, Dai M. (2009). Diversity and abundance of ammonia-oxidizing archaea and bacteria in Qinghai Lake, Northwestern China. *Geomicrobiol J* 26(3):199–211.
- Justice NB, Pan C, Mueller R, Spaulding SE, Shah V, Sun CL *et al.* (2012). Heterotrophic archaea contribute to carbon cycling in low-pH, suboxic biofilm communities. *Appl Environ Microbiol* 78: 8321–8330.
- Karner, M., E. F. DeLong, and D. M. Karl. (2001). Archaeal dominance in the mesopelagic zone of the Pacific Ocean. *Nature* 409:507–509.
- Lam, P., Jensen, M.M., Lavik, G., McGinnis, D.F., Muller, B., Schubert, C.J., Amann, R., Thamdrup, B., Kuypers, M.M.M. (2007). Linking crenarchaeal and bacterial nitrification to anammox in the Black Sea. *Proceedings of the National Academy of Sciences of the United States of America* 104 (17), 7104e7109.
- Lazar CS, Baker BJ, Seitz K, Hyde AS, Dick GJ, Hinrichs K-U *et al.* (2016). Genomic evidence for distinct carbon substrate preferences and ecological niches of Bathyarchaeota in estuarine sediments. *Environ Microbiol* 18: 1200–1211.
- Li Y, Zhang C, Wang N, Han Q, Zhang X, Liu Y, Xu L, Ye W. (2017). Substantial inorganic carbon sink in closed drainage basins globally. *Nat Geosci* 10:501–506.
- López-Archilla *et al.* (2004). Ecosystem metabolism in a Mediterranean shallow lake (Laguna de Santa Olalla, Doñana National Park, SW Spain) *Wetlands* 24: 848-858.
- Luo, Z., Feng, W., Luo, Y., Baldock, J., Wang, E. (2017). Soil organic carbon dynamics jointly controlled by climate, carbon inputs, soil properties and soil carbon fractions. *Global Change Biology*. <http://dx.doi.org/10.1111/gcb.13767>. 00.
- Messenger, M. L. Mathis Lörcher Messenger, Bernhard Lehner, Günther Grill, Irena Nedeva & Oliver Schmitt. (2016). Estimating the volume and age of water stored in global lakes using a geo-statistical approach. *Nat. Commun.* 7, 13603 doi: 10.1038/ncomms13603.

- Moffat, A. S. (1998). Global nitrogen overload problems grows critical. *Science* 279:988-989.
- Mosier, A.C., Francis, C.A. (2008). Relative abundance and diversity of ammonia-oxidizing archaea and bacteria in the San Francisco Bay estuary. *Environmental Microbiology* 10 (11).
- Murphy, J. & Riley, J. P. (1962). A modified single solution method for the determination of phosphate in natural waters. *Analytica Chimica Acta*. 27, 31–36. *Rev. Sci. Eau*, 15, 123–135.
- Offre, A. Spang, C. Schleper. (2013). Archaea in biogeochemical cycles. *Annu. Rev. Microbiol.*, 67 pp. 437-457.
- Oren, A. (1994). The ecology of the extremely halophilic archaea. *FEMS Microbiol Rev* 13, 415–440.
- Oren, A. (2001). The bioenergetic basis for the decrease in metabolic diversity at increasing salt concentrations: implications for the functioning of salt lake ecosystems. *Hydrobiologia* 466:61–72.
- Oren A. (2011). Ecology of halophiles. *Extremophile Handbook* (Horikoshi K ed), pp. ,10.1007/978-4-431-53898-1_16, (343-361). Springer, Tokyo.
- Orsi,R.H;Wiedmann,M.(2016).CharacteristicsanddistributionofListeria spp.,including Listeria species newly described since 2009. *Appl. Microbiol. Biotechnol.*, 100, 5273–5287.
- Ortega-Retuerta, E; Pulido-Villena, E. & Reche, I. (2007). Effects of Dissolved Organic Matter Photoproducts and Mineral Nutrient Supply on Bacterial Growth in Mediterranean Inland Waters. *Microbial Ecology*, 54 (1): 161-169.
- Pedrós-Alió C, Calderón-Paz JI, Gasol JM. (2000b). Comparative analysis shows that bacterivory, not viral lysis, controls the abundance of heterotrophic prokaryotic plankton. *FEMS Microbiol Ecol* 32:157–165.
- Pedrós-Alió C, Calderón-Paz JI, MacLean MH, Medina G, Marrasé C, Gasol JM, Guixa-Boixereu N (2000a). The microbial food web along salinity gradients. *FEMS Microbiol.*
- Razinkovas-Baziukas, A., Povilanskas, R. (2012). Introducing transitional waters. In: *Respiration in Aquatic systems*. Oxford: Oxford University Press. pp 83–102.
- Roehm (2005). Respiration in wetland ecosystems. In: del Giorgio PA, Williams PJ, le B, Eds.

- Sanchez, M.I., Green, A.J. & Castellanos, E.M. (2006) Temporal and spatial variation of an aquatic invertebrate community subjected to avian predation at the Odiel salt pans (SW Spain). *Archiv Fur Hydrobiologie*, 166, 199-223.
- Sanchez, M.I., Green, A.J. & Castellanos, E.M. (2006) Temporal and spatial variation of an aquatic invertebrate community subjected to avian predation at the Odiel salt pans (SW Spain). *Archiv Fur Hydrobiologie*, 166, 199-223.
- Saunders, D.L and Kalff J. (2001). Nitrogen retention in wetlands, lakes and rivers. doi: 10.1023/A:1017506914063.
- Schlesinger, William. (2009). On the Fate Anthropogenic Nitrogen. *Proceedings of the National Academy of Sciences of the United States of America*. 106. 203-8. 10.1073/pnas.0810193105.
- Schuerch, M., Spencer, T., Temmerman, S., Kirwan, M. L., Wolff, C., Lincke, D., *et al.* (2018). Future response of global coastal wetlands to sea-level rise. *Nature* 561, 231–234. doi: 10.1038/s41586-018-0476-5.
- Seitzinger S, *et al.* (2006) Denitrification across landscapes and watersheds. *Ecol Applic* 16:2064 –2090.
- Seitzinger, S.P., (1988). Denitrification in freshwater and coastal marine ecosystems Ecological and geochemical significance, *Limnol.Oceanogr.*, 33, 702-724.
- Sims, A., Horton, J., Gajaraj, S., McIntosh, S., Miles, R.J., Mueller, R., Reed, R., Hu, Z., (2012). Temporal and spatial distributions of ammonia-oxidizing archaea and bacteria and their ratio as an indicator of oligotrophic conditions in natural wetlands. *Water Research* 46 (13), 4121e4129.
- Smith, D.C and Azam,F. (1992). A simple, economical method for measuring bacterial protein synthesis 546 rates in seawater using 3H-leucine. *Mar Microb Food Webs* 6:107–114.
- Sorokin DY, Berben T, Melton ED, Overmars L, Vavourakis CD, Muyzer G. (2014). Microbial diversity and biogeochemical cycling in soda lakes. *Extremophiles*. 2014;18:791–809. doi: 10.1007/s00792-014-0670-9.
- Verhoeven JTA, Arheimer B, Yin CQ, Hefting MM. (2006). Regional and global concerns over wetlands and water quality. *Trends Ecol Evol* 21: 96–103.

- Walton, M.E.M., Vilas, C., Coccia, C., Green, A.J., Canavate, J.P., Prieto, A., van Bergeijk, S.A., Medialdea, J.M., Kennedy, H., King, J. & Le Vay, L. (2015) The effect of water management on extensive aquaculture food webs in the reconstructed wetlands of the Donana Natural Park, Southern Spain. *Aquaculture*, 448, 451-463.
- Weston, N. B., Vile, M. A., Neubauer, D. C. & Velinsky, D. J. (2011). Accelerated microbial organic matter mineralization following salt-water intrusion into tidal freshwater marsh soils. *Biogeochemistry* 102, 135–151.
- Wuchter, C., Abbas, B., Coolen, M.J.L., Herfort, L., van Bleijswijk, J., Timmers, P., Strous, M., Teira, E., Herndl, G.J., Middelburg, J.J., Schouten, S., Damste, J.S.S. (2006). Archaeal nitrification in the ocean. *Proceedings of the National Academy of Sciences of the United States of America* 103 (33), 12317e12322.
- Wurtsbaugh WA, Miller C, Null SE, DeRose RJ, Wilcock P, Hahnenberger M, Howe F, Moore J. (2017). Decline of the world's saline lakes. *Nat Geosci* 10:816–821. <https://doi.org/10.1038/NGEO3052>.
- Yokokawa, T., Sintès, E., De Corte, D., Olbrich, K., and Herndl, G.J. (2012). Differentiating leucine incorporation of Archaea and Bacteria throughout the water column of the eastern Atlantic using metabolic inhibitors. *Aquatic microbial ecology*. Vol. 66: 247–256. doi: 10.3354/ame01575.
- You, J., Das, A., Dolan, E.M., Hu, Z., (2009). Ammonia-oxidizing archaea involved in nitrogen removal. *Water Research* 43 (7), 1801e1809.
- Zaccone R, Monticelli LS, Seritti A, Santinelli C, Azzaro M, Boldrin A, La Ferla R, Ribera d'Alcalà M. (2003). Bacterial processes in the intermediate and deep layers of the Ionian Sea in winter 1999: vertical profiles and their relationship to the different water masses. *J.*



Chapter 3

Flamingos and drought as drivers of nutrients and microbial dynamics in a saline lake

Flamingos and drought as drivers of nutrients and microbial dynamics in a saline lake

3

Gema L. Batanero, Elizabeth León-Palmero, Linlin Li, Andy J. Green, Manuel Rendón-Martos, Curtis A. Suttle & Isabel Reche

Scientific Reports, volume 7, Article number: 12173 (2017)

<https://doi.org/10.1038/s41598-017-12462-9>

3.1. INTRODUCTION

Since Hutchinson's seminal work in 1950 on the importance of guano on marine productivity, many studies have analyzed the inputs of nutrients associated with waterbird feces in inland waters (Manny *et al.*, 1994, Kitchell *et al.*, 1999, Hahn *et al.*, 2007; 2008, Dessborn. *et al.*, 2016). This process is termed guanotrophication (Leentevaar, 1967) and appears to be particularly important in arid regions (Post *et al.*, 1998), systems with long water residence times (Huang and Isobe, 2012), and inland waters used as roosts by non-breeding birds or as breeding sites by colonial waterbirds, where birds import nutrients from foraging areas (Hahn *et al.*, 2007 and 2008, Baxter and Fairweather, 1994, Kameda *et al.*, 2006, Signa *et al.*, 2012). Guanotrophication affects wetland quality and primary productivity, as shown in studies by Kitchell *et al.*, 1999, in which chlorophyll increased with the density of geese, and in experiments with phytoplankton (Van Geest *et al.*, 2007). On the other hand, large waterbirds cause sediment bioturbation with consequences for nutrient release and methane fluxes (Rodríguez- Pérez and Green, 2006; Bodelier *et al.*, 2006). Although bacterial production and diversity are known to change under pulses of nutrients (Smith *et al.*, 2004; Simek *et al.*, 2006; Reche *et al.*, 2009), no studies have directly addressed changes in aquatic microbial communities associated with guanotrophication and sediment bioturbation by waterbirds, despite the key role of microbial processes in biogeochemical cycles and greenhouse gas fluxes in wetlands and lakes.

Insights into the effects of waterbirds on microbial communities are crucial to enable integrative wetland management and the measures required to support waterbird diversity and their effects on guantrophication, nutrient recycling, microbial-derived processes and water quality in general (Huang and Isobe, 2012; Verhoeven *et al.*, 2006). This is even more important given the consequences of climate change that is affecting hydrological regimes in contrasting ways in different biomes (Erwin, 2009). Projected changes suggest an increase in wetland areas in tropical or polar latitudes; whereas temperate and Mediterranean wetlands and lakes may reduce their hydroperiod or dry out completely (Tranvik *et al.*, 2009; Nielsen *et al.*, 2009), with major implications for species diversity (McMenamin *et al.*, 2008). In the Mediterranean biome, extended droughts could reduce runoff and increase evaporation, causing salinization of many wetlands and lakes (Nielsen *et al.*, 2009; Moss *et al.*, 2009; Jeppesen *et al.*, 2015). This reduction in wetland surface or in hydroperiod length may promote the overcrowding of waterbirds in arid or semiarid regions during breeding or wintering periods (Post *et al.*, 1998; Huang and Isobe, 2012), which may reduce water quality through guano inputs and sediment bioturbation (Manny *et al.*, 1994). Similar effects may be caused by other kinds of global change such as increasing water extraction or the increase in bird populations resulting from exploitation of anthropogenic habitats (e.g. agricultural fields or fish farms) or protection from disturbance and hunting. For example, numbers of flamingos and other wading birds have increased markedly in southern Spain in recent decades due to increased protection and exploitation of artificial habitats, such as ricefields and fish ponds (Rendón *et al.*, 2008; Ramo *et al.*, 2013).

Flamingos represent a major fraction of the waterbird biomass in saline lakes in Africa (Vareschi, 1978; Tuite, 2000), and have profound effects on the limnology of Andean salt lakes (Hurlbert and Chang, 1983). In the Western Mediterranean region, their abundance and movements are particularly well monitored (Rendón-Martos *et al.*, 2000; Amat *et al.*, 2005; Balkiz *et al.*, 2009; Geraci *et al.*, 2012; Sanz-Aguilar *et al.*, 2012). Here, we studied the influence of flamingos on nitrogen, phosphorus, and microbial dynamics in a saline lake that holds the largest flamingo colony in the Western Mediterranean. Flamingos can increase N and P concentrations by guano inputs from mass aggregations during breeding periods, and by sediment bioturbation during feeding and trampling in the lake. We hypothesized that in this lake (i) dissolved nitrogen and phosphorus concentrations would be related with flamingo abundance due to guantrophication and sediment bioturbation and used correlation and regression analysis to test it; (ii) dissolved nutrients from guano would boost heterotrophic prokaryotic production affecting microbial dynamics and performed two experiments and cross-correlations to test it; (iii) drought would concentrate nutrients and microbial cells by evaporation, and therefore intensify the effects of flamingos and we compared the nutrient and microbial dynamics in two well-contrasted (wet and dry) hydrological years to test it. Finally, we discuss the implications of our findings given ongoing climate change and the effects of conservation policies on waterbird densities.

3.2. MATERIAL AND METHODS

Study site, water level and flamingo abundance

This study was performed in Fuente de Piedra, an athalassohaline lake located in an endorheic basin of karstic origin in the south of Spain (37° 6' N, 4° 44' W) (Figure 3.1a). Its hydrology is mainly linked to inputs from rainfall, two intermittent streams (Santillán and Humilladero) and ground water, and outputs mainly by evaporation (Rodríguez-Rodríguez *et al.*, 2006; Kohfahl *et al.*, 2008). This large saline lake covers a maximum area of 1350 ha and supports one of the most important breeding colonies of the greater flamingo (*Phoenicopterus roseus*) in the Western Mediterranean (Geraci *et al.*, 2012; Rendón *et al.*, 2001). Breeding adults fly within a radius of 350 km to feed in other wetlands, returning to feed their chicks at Fuente de Piedra (Rendón–Martos *et al.*, 2000; Amat *et al.*, 2005; Rendón *et al.*, 2014).

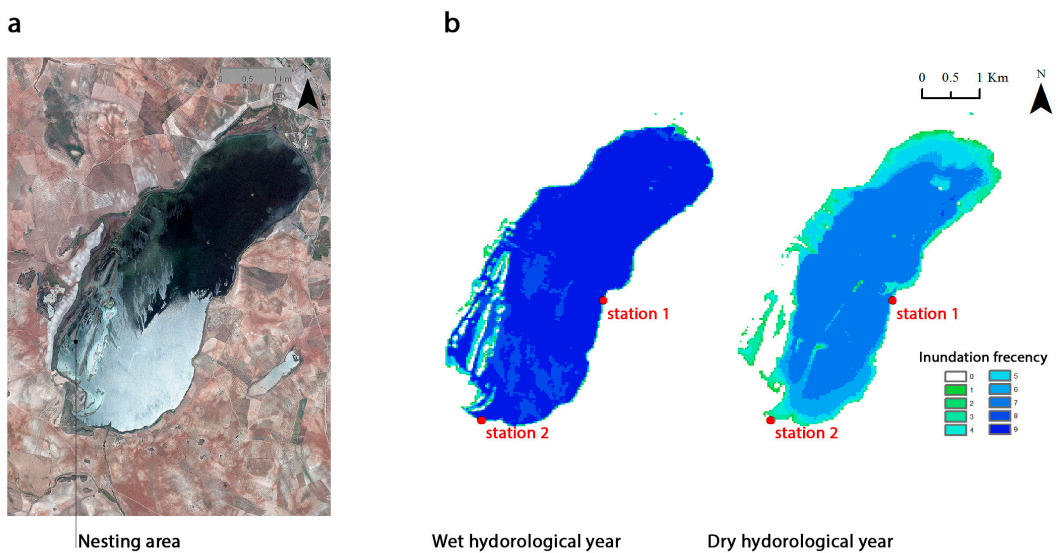


Figure 3.1. Images of the saline lake studied (Fuente de Piedra, Málaga, Spain). (a) Orthophoto (<http://ws041.juntadeandalucia.es/medioambiente/dlidar/index.action>) showing the flamingo nesting area, and (b) frequency of inundation area of the lake obtained from Landsat imagery (<https://earthexplorer.usgs.gov/>) for the wet and the dry hydrological years. Images of similar dates were used to calculate the inundation frequency for each pixel, which ranged from 0 (i.e. lake surface dry in all 9 images) to 9 (i.e. inundated in all 9 images). The location of the two sampling stations is shown by in red dots.

We sampled this lake during more than two hydrological years. The first hydrological year between September 2010 and August 2011 was considered to be wet as the lake was inundated for most time of the year (Figure 3.1b); it was similar to the previous hydrological year that was only partially sampled. In contrast, the second hydrological year (i.e. from September 2011 to August 2012) was relatively dry because the lake dried out during the summer (Figure 3.1b). Each hydrological year had two phases. The first phase comprises water filling during fall and winter (September-March); whereas, the second phase consists of water evaporation during spring and summer (April-August).

The different hydrological conditions cause intense changes in the water level of the lake (García and Niell, 1993; García *et al.*, 1997). The water level in Fuente de Piedra was measured daily using a limnigraph that registers water level variations on a paper graph through movements of a floating sensor that is located in an open shallow well in the lagoon. Changes in the inundation area were obtained with multi-temporal Landsat imagery. We collected for each hydrological year nine images with similar dates from the USGS EarthExplorer (<https://earthexplorer.usgs.gov/>). The nine images (for each hydrological year) were classified as water and non-water (Li *et al.*, 2015) and then added up to calculate the inundation frequency for each pixel using ArcGIS 10.4 software. The resulting inundation frequency was ranged from 0 (i.e. the lake was dry in all 9 images) to a maximum of 9 (i.e. the lake was inundated in all 9 images).

Samples were taken from the water column (ca. 10 cm below the surface) at two stations (red dots in Figure 1b). Station 1 is less affected by wind and turbidity and is a flamingo foraging area, whereas Station 2 is located nearer the nesting area and is more exposed to wind, evaporation and turbidity. Samples were collected biweekly from July 2010 to November 2012, except when the lake was dry from June to October of 2012. Flamingos on the lake were counted one to seven times per week during the breeding period and monthly the rest of the year, using binoculars (8 x 30) and a spotting scope (20 - 60 x 60). Birds were counted one by one for small groups, or in groups of five individuals for big aggregations. The abundance of chicks during breeding was obtained from aerial pictures. Rainfall, water level and flamingo data were provided by the “Consejería de Medio Ambiente y Ordenación del Territorio” of Junta de Andalucía, Spain.

Physico-Chemical analyses

Salinity, pH and temperature were measured using a multi-parameter probe (HANNA HI 9828). Total nutrient concentrations were measured in unfiltered water, while samples for dissolved nutrient analysis were filtered through 0.7 μ m pore-size Whatman GF/F glass-fiber filters. Soluble reactive phosphorus (SRP), total phosphorus (TP) and total dissolved phosphorus (TDP) concentrations were measured using the molybdenum blue method (Murphy

and Riley, 1962), the latter as SRP, after digestion with a mixture of potassium persulphate and boric acid at 120° C for 30 min (APHA, 1992). Total nitrogen (TN) and total dissolved nitrogen (TDN) were analysed by high-temperature catalytic oxidation (Álvarez-Salgado and Miller, 1998) using a total nitrogen analyzer (TNM-1, Shimadzu TOC-V CSH). Samples for dissolved organic carbon (DOC) were collected from surface waters in a combusted (> 2 h at 500 °C) flask, filtered through pre combusted GF/F filters, acidified with phosphoric acid (final pH < 2) and stored at 4°C in the dark until analysis. DOC concentration was measured by high-temperature catalytic oxidation in a Shimadzu total organic carbon (TOC) analyzer (Model TOC-V CSH). The instrument was calibrated using a four-point standard curve of potassium hydrogen phthalate. Samples were purged with phosphoric acid for 20 min to eliminate any dissolved inorganic carbon. Three to five injections were analysed for each sample. .

C, N and P content in chick flamingo guano

Fresh flamingo chick feces were collected during banding operations in the Fuente de Piedra colony, immediately frozen in liquid nitrogen and stored at -80 °C until analysis. Feces were thawed and classified as either pink or brown, reflecting differences in diet. Prior to analysis, feces were dried at 60 °C for at least 24h to obtain dry weight. They were then diluted in a known volume of Milli-Q water, and TN, TDN, TP, TDP, TOC and DOC concentrations were determined as explained above.

Per capita N and P loads associated with flamingo guano were estimated as functions of body mass and the N and P contents per g of dry feces (Eq. 4 in Hahn *et al.*, 2008). The average body mass of an adult flamingo male is 3579 g and of an adult female is 2525 g (Cramp and Simmons, 1977), so we took 3052 g as average body mass for adults and assumed all feces produced were deposited in the lake. Daily N and P inputs were obtained by multiplying per capita excretion by flamingo abundance, and annual loadings by summing all daily values over the year. Lake volume was calculated by integrating the area beneath the hypsographic curve (i.e. surface area vs. water level; Rodríguez-Rodríguez *et al.*, 2016).

Biological analyses

Chlorophyll a concentrations were determined by collecting the particulate material from 100 to 700 ml of water by filtering through 0.7µm pore-size Whatman GF/F glass-fiber filters, then extracting the filters with 95% methanol in the dark at 4 °C for 24 h (APHA, 1992) . Pigment absorption was measured using a Perkin Elmer UV-Lambda 40 spectrophotometer at wavelengths of 665 nm and 750 nm.

The abundances of prokaryotes (PA) and viruses (VA) were determined in triplicate samples using flow cytometry in a FACScalibur flow cytometer (excitation 448nm), and

analysed in bivariate plots of Side scatter (SSC) vs. FL1 (Green fluorescence; Gasol and Giorgio, 2000; Brussaard *et al.*, 2010). For PA, samples were collected and fixed with a mixture of 1% paraformaldehyde and 0.05% glutaraldehyde for 30 min in the dark at 4 °C, frozen in liquid nitrogen, and stored at -80 °C until analysis. In the laboratory, the samples were thawed and diluted ≥ 10 -fold with Milli-Q water to avoid coincidence of cell counts. Samples were stained with a 10 μM DMSO solution of SYBR Green I (Molecular Probes) for 10 min in the dark. Yellow-green 0.92 μm latex beads (Poysciences) were used as an internal standard. For VA, samples were fixed with glutaraldehyde 0.5 % for 15-30 min at 4 °C in the dark, flash frozen in liquid nitrogen and stored at -80°C until analysis (Brussaard *et al.*, 2010). Prior to analysis, samples were diluted ≥ 100 -fold with TE-buffer pH 8.0 (10 mM Trishydroxymethyl-aminomethane; 1 mM ethylenediaminetetraacetic acid) to avoid the coincidence in virus particle counts. VA samples were stained with a working solution (1:200) of SYBR Green I (10,000X concentrate in DMSO, Molecular Probes) for 10 min in the dark and then kept at -80° until counting. Fluorescent microspheres (FluoSpheres carboxylate modified yellow-green fluorescent microspheres; 1.0 μm diameter) were added as an internal standard. Data were analyzed using BD CellQuest Pro software.

Prokaryotic heterotrophic production (PHP) was estimated from 3H-Leucine- incorporation following the microcentrifugation technique (Smith and Azam., 1992). Three 1.5 ml replicates and two trichloroacetic acid (TCA)-killed blanks were prepared for each sampling station and day. In each sample, 5 μl of (4,5-3H)-L-Leucine was added to a final concentration of 54.6 nM and then incubated for 2-5 h at in situ temperature. Adding TCA at a final concentration of 10% terminated the incubations. In the laboratory, the samples were centrifuged (10 min at 14000 rpm), rinsed with 5% TCA, vortexed, and centrifuged again. For each sample, 1.5 ml of liquid scintillation cocktail (Ecoscint A) was added, and the radioactivity determined using an autocalibrated scintillation counter (Beckman LS 6000 TA).

Experiments with guano

To determine the effects of guano on prokaryote growth, we carried out two experiments in the laboratory using previously frozen feces from flamingo chicks collected during the ringing operations in August 2010. Chicks are fed with a secretion produced by their parents that fly to forage in other wetlands (Rendón *et al.*, 2014; 2012) and represent most of the individuals present constantly in the lake during breeding periods. The first experiment (Exp.1) was carried out using lake water on October 10th 2010 when there were approximately 34000 flamingos in the lake and a water level of 79 cm, and the second experiment (Exp. 2) was performed using lake water on May 5th (2011 year) when there were approximately 23000 flamingos in the lake and a water level of 130 cm (Figure 3.2).

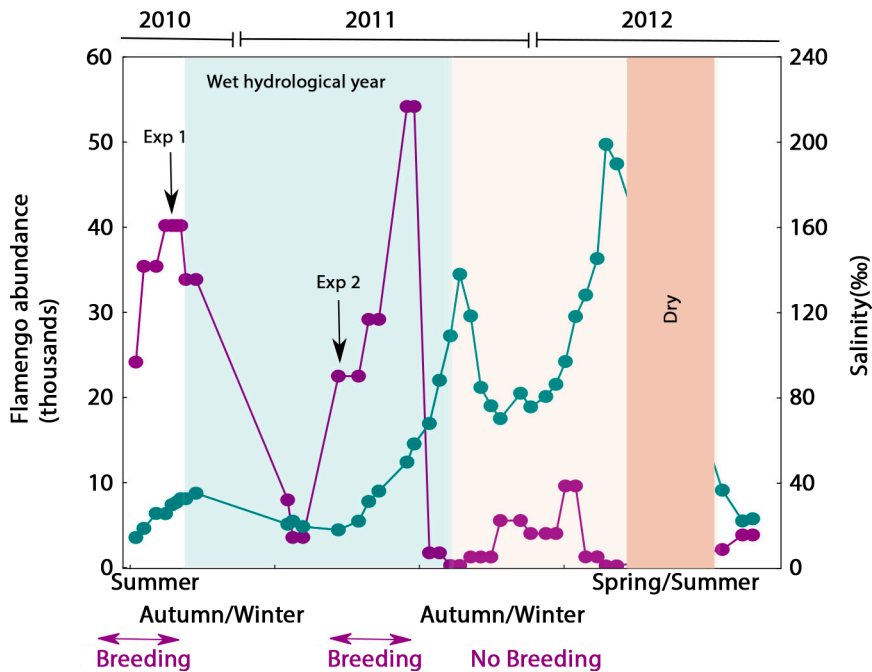


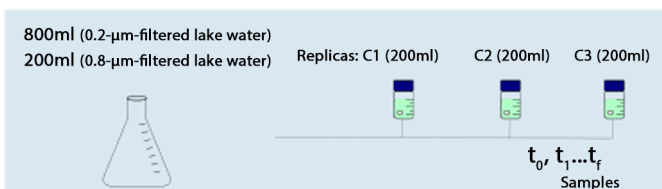
Figure 3.2. Changes in salinity and abundance of flamingos.

Flamingo abundance is shown by the purple line and salinity by the blue-green line. The wet hydrological year is shaded in blue and the dry hydrological year in cream. The lake dried out completely during the period shaded in brown. The periods of flamingo breeding are marked on the x-axis.

Each experiment consisted of two treatments and each treatment had three replicates. Controls consisted of 800 ml of 0.2- μm -filtered lake water, plus 200 ml of water filtered through a 0.8 μm pore-size Whatman GF/F filter that allowed most bacteria to pass through, but removed bacterivorous flagellates. The +Guano treatment was the same as the control, with the addition of sterilized chick feces (Figure 3.3). All the experimental (1 litre Pyrex) bottles were incubated in the dark at in situ temperature using a culture chamber. From each treatment, triplicate subsamples were collected and prokaryotic abundance and production were quantified every 12 h to during the 84 h incubation period, and samples for dissolved nutrients were taken at the initial (t_0) and final (t_f) sampling time. We determined prokaryotic abundance and production, and the concentration of dissolved nutrients, as described above for lake samples. Changes in prokaryotic abundance and production throughout the incubations were fitted to exponential or logistic functions. The fits and growth parameters (specific growth rates and carrying capacities) were obtained using nonlinear estimations. More details on the estimation procedure can be found in Pulido-Villena and Reche *et al.*, 2003.

Experiments with Guano

Control (no feces addition)



+Guano (feces addition)

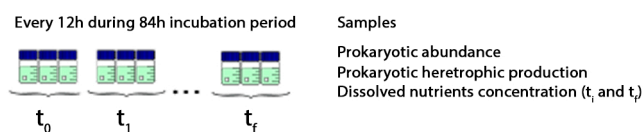
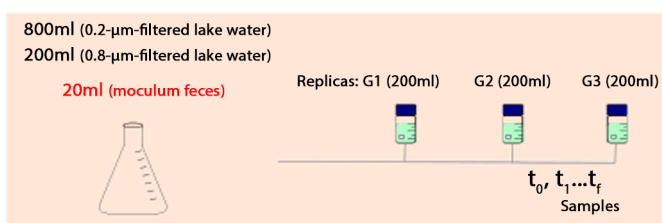


Figure 3.3. Experimental design consisted of two treatments using water from the Fuente de Piedra lake and sterilized samples of flamingo feces: Control (with no feces addition) and + Guano (with feces addition).

Statistical Analysis

We performed multiple regression analysis to assess the main drivers of SRP and TDN including flamingo abundance (proxy for guano inputs) and water level (proxy for sediment bioturbation and evaporation) and correlation analyses were performed to assess the relationships between major nutrients and microbial variables with flamingos and salinity. Finally, we used a two-way cross-correlation to analyse the sequential effects of flamingos on microbial and nutrient components in more detail. The cross-correlation coefficient (k) represents the correlation between two time series (i.e., microbial and nutrient parameters $[X]$ vs. flamingo abundance $[Y]$), where X is lagged forward or backward by ($k, 10$) observations. For this analysis we sampled every two weeks between August 2011 and May 2012 at station 1. All statistical analyses were performed using Statistica (v.7.0).

3.3. RESULTS

Nutrient dynamics in the lake

The first hydrological year was wet with an annual rainfall of 563.3 mm, a salinity of ~30 ppt, water levels ranging from 44 cm to 130 cm, and an average lake surface area of 992 ha with more than 50000 flamingos during the breeding period (blue period in Figure 3.2); it was similar to the previous hydrological year that was only partially sampled. In contrast, the second hydrological year was dry with an annual rainfall of 345.1 mm, a salinity that was always above 70 ppt, a water level that ranged from 52 cm to 0 cm when the lake dried up, an average surface area of 522 ha, and a maximum of only 12000 flamingos with no breeding (brown period in Figure 3.2) (Table 3.1).

Nutrient concentrations varied dramatically over the course of the study. DOC concentration ranged more than an order of magnitude from 1.00 mmol-C l⁻¹ to 13.59 mmol-C l⁻¹, with the highest values during the dry year (Table 3.1). Changes in DOC concentration and salinity were tightly correlated (n=73, r=0.97, p<0.0001) and coupled with the filling (autumn/winter) and evaporation (spring/summer) phases (Figure 3.4a). The TP concentration varied almost 30-fold from 1.38 μmol-P l⁻¹ to 38.60 μmol-P l⁻¹ (Table 3.1), reached the maximum during the evaporation phase of the dry year, and consequently, was strongly correlated with salinity (n=75, r=0.79, p<0.0001) (Figure 3.4b). TN concentration varied 20-fold from 0.06 to 1.17 mmol-N l⁻¹ (3. 1), reaching maximum values during the dry year. TN also showed a tight correlation with salinity (n=65, r=0.90, p<0.0001) (Figure 3.4c). TDP concentration varied from 0.73 to 22.23 μmol-P l⁻¹, and reached its maximum during the dry year, coupled with salinity (Figure 3.4d). As well as evapoconcentration, there was evidence that sediment interactions influenced TDP concentration, as TDP increased linearly as the water level (WL) decreased below 80 cm (TDP = 15.7-0.18 WL, r²=0.38, p<0.001, Figure 3.5). In contrast, SRP varied from 0.18 to 1.63 μmol-P l⁻¹ (3. 1), was not significantly correlated with salinity, and showed a first peak during the wet year, concomitant with a major increase in the abundance of flamingos (3.4e). TDN concentrations also ranged more than ten-fold from 0.06 mmol-N l⁻¹ to 0.80 mmol-N l⁻¹ (3. 1), showed dynamics time-lagged with the abundance of flamingos, and was not influenced by salinity during the dry year (n= 30, r=0.013, p =0.944) (Figure 3.4f). To explore in more detail the relevance of water level (indicative of sediment influence and evaporation) and guantrophication by flamingos on SRP and TDN concentrations in the water, we performed multiple regression analysis (Table 3.2). Both variables significantly affected SRP concentrations, although the contribution of water level was stronger (higher partial correlation coefficient) than that of flamingo abundance. TDN concentration was also significantly affected by the water level, and not directly by the flamingo abundance.

Table 3.1. Mean values and ranges (in parentheses) of basic physicochemical and biological variables in the two sampling stations during the wet and dry hydrological years.

Station Localization	Hydrological year	Rain (mm)	Temperature (°C)	Salinity (ppt)	pH	DOC (mmol-C l ⁻¹)	TN (mmol-N l ⁻¹)	TP (µmol-P l ⁻¹)	TN:TP (Molar)	TDN (mmol-N l ⁻¹)	SRP (µmol-P l ⁻¹)	Chl a (µg/L)
Station 1 37°06'19.8"N 4°45'44.5"W	2010-2011 Wet	563.3	19.1 (8.3 - 29.4)	38.3 (18.1 - 88.3)	9.03 (8.04 - 9.94)	1.99 (1.07 - 4.72)	0.22 (0.08 - 0.48)	5.12 (1.38 - 11.52)	52 (30 - 93)	0.18 (0.06-0.48)	0.41 (0.18 - 1.61)	44.2 (2.4 - 111.9)
	2011-2012 Dry	345.1	17.6 (9.3 - 25.6)	112.5 (70.3 - 199.0)	8.96 (7.46 - 9.06)	6.19 (3.85 - 13.59)	0.60 (0.32 - 1.17)	13.82 (5.78 - 38.60)	49 (24-85)	0.28 (0.07-0.80)	0.57 (0.18 - 1.63)	44.9 (14.5 - 73.3)
Station 2 37°05'07.4"N 4°47'08.3"W	2010-2011 Wet	563.3	19.7 (8.2 - 33.5)	41.6 (21.4 - 91.8)	9.03 (8.04 - 9.94)	1.98 (1.00 - 4.73)	0.22 (0.06 - 0.49)	4.57 (1.59 - 10.20)	50 (32 - 79)	0.18 (0.06-0.46)	0.47 (0.18 - 1.54)	20.7 (3.9 - 50.0)
	2011-2012 Dry	345.1	19.7 (8.3-33.5)	109.9 (67.7 - 188.0)	8.26 (7.61 - 8.99)	6.03 (3.79 - 10.02)	0.57 (0.35 - 0.83)	11.40 (5.60 - 23.93)	55 (30 - 98)	0.28 (0.07-0.74)	0.90 (0.22 - 0.91)	58.4 (23.1 - 116.1)

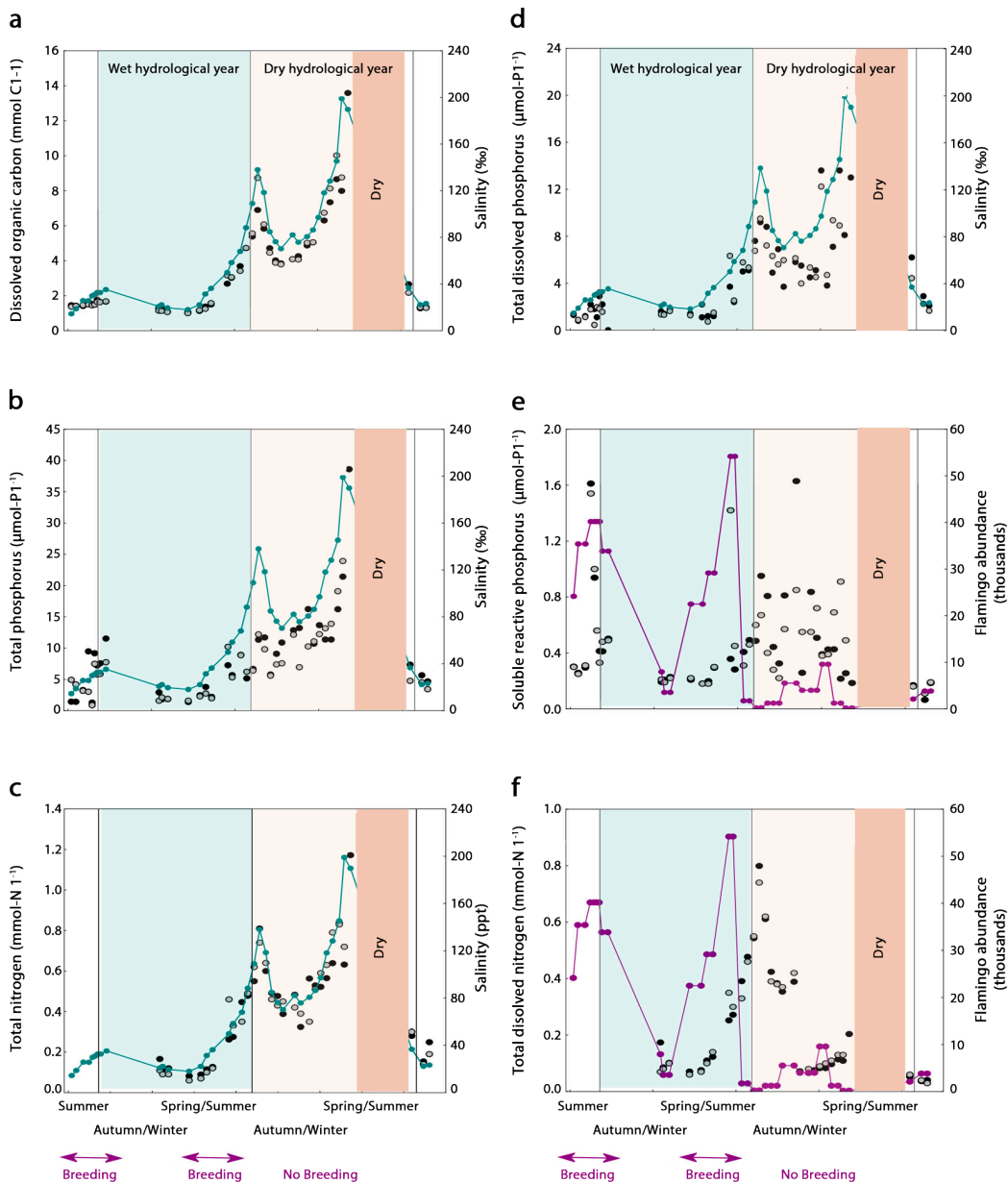


Figure 3.4. Nutrient dynamics during two hydrological years. Changes in the concentration of (a) dissolved organic carbon, (b) total phosphorus, (c) total nitrogen, (d) total dissolved phosphorus, (e) soluble reactive phosphorus and (f) total dissolved nitrogen at station 1 (black dots) and station 2 (grey dots). Salinity (blue-green line) or flamingo abundance (purple line) are shown for reference.

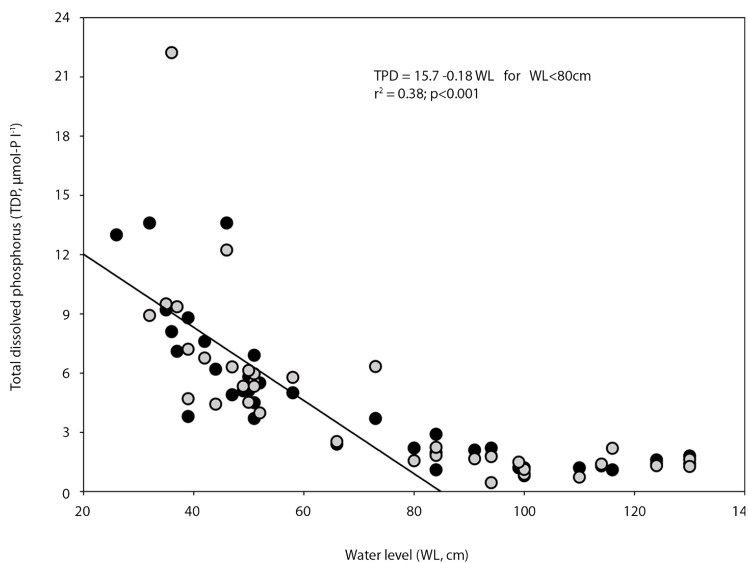


Figure 3.5. Linear negative relationship between the total dissolved phosphorus and the water level for depths lower than 80cm.

Table 3.2. Results of multiple regression analyses to assess the influence of flamingo abundance and water level on the concentrations of soluble reactive phosphorus and total dissolved nitrogen. The *r* values are partial correlation coefficients, *b* is the non-standardized regression coefficients.

Independent Variables	Soluble Reactive Phosphorus ($\mu\text{mol-P l}^{-1}$)			Total Dissolved Nitrogen (mmol-N l^{-1})		
	<i>r</i>	<i>b</i>	p-level	<i>r</i>	<i>b</i>	p-level
Flamingos	0.368787	0.000007	0.002964	---	---	---
Water level (cm)	-0.422263	-0.004579	0.000746	-0.422129	-0.002525	0.000868
Intercept		0.681651	0.000000		0.390625	0.000000

Microbial dynamics

Chlorophyll-a ranged over two orders of magnitude from $2 \mu\text{g l}^{-1}$ to $256 \mu\text{g l}^{-1}$. During the wet year at Station 1 (black dots), chlorophyll-a showed maximum values concurrent with two peaks in flamingo abundance (Figure 3.6a). Indeed, in this station we observed a significant and positive correlation between the abundance of flamingos and chlorophyll-a concentration ($n=38$, $r=0.34$, $p<0.05$). In contrast, during the dry year, when flamingos were less abundant, the highest values of chlorophyll-a were observed during the filling phase (lower salinity) in winter (Figure 3.6a). Prokaryotic heterotrophic production (PHP) ranged 40 fold from $0.05 \text{ nmoles of leucine l}^{-1}\text{h}^{-1}$ to $2.25 \text{ nmoles of leucine l}^{-1}\text{h}^{-1}$ with maximum values synchronous and correlated with the peaks in flamingo abundance (Figure 3.6b) at both Station 1 (black dots, $n=37$, $r=0.48$, $p<0.05$) and Station 2 (grey dots, $n=36$, $r=0.36$, $p<0.05$). Prokaryote abundance ranged over three orders of magnitude from 3 to $296 (\times 10^6)$ cells ml^{-1} (Figure 3.6c), while virus abundance ranged from 0.3 to $1.5 (\times 10^9)$ particles ml^{-1} (Figure 3.6d). The peak in the prokaryote abundance also coincided with the highest abundance of flamingos, while viral abundance (VA) was similar in both years. VA dynamics appeared time lagged with respect to the abundance of flamingos in the wet year. In contrast, in the dry year the maximum VA coincided with the highest salinity, during the evaporation phase (Figure 3.6d). To explore in more detail the influence of flamingos and salinity on the abundance of viruses in the water column, we performed a multiple regression analysis (Table 3.3). Both variables significantly affected viral abundance, although the contribution of flamingos was slightly greater.

Table 3.3. Results of multiple regression analyses to assess the influence of flamingo abundance and salinity on the concentration of viruses in Fuente de Piedra lake. The r-values are partial correlation coefficients, b is the non-standardized regression coefficients.

<i>Independent Variables</i>	<i>Virus abundance (ml⁻¹)</i>		
	<i>r</i>	<i>b</i>	<i>p-level</i>
Flamingos	0.548973	12.7	0.002028
Salinity (ppt)	0.506379	4634.3	0.004089
Intercept		243837.9	0.180274

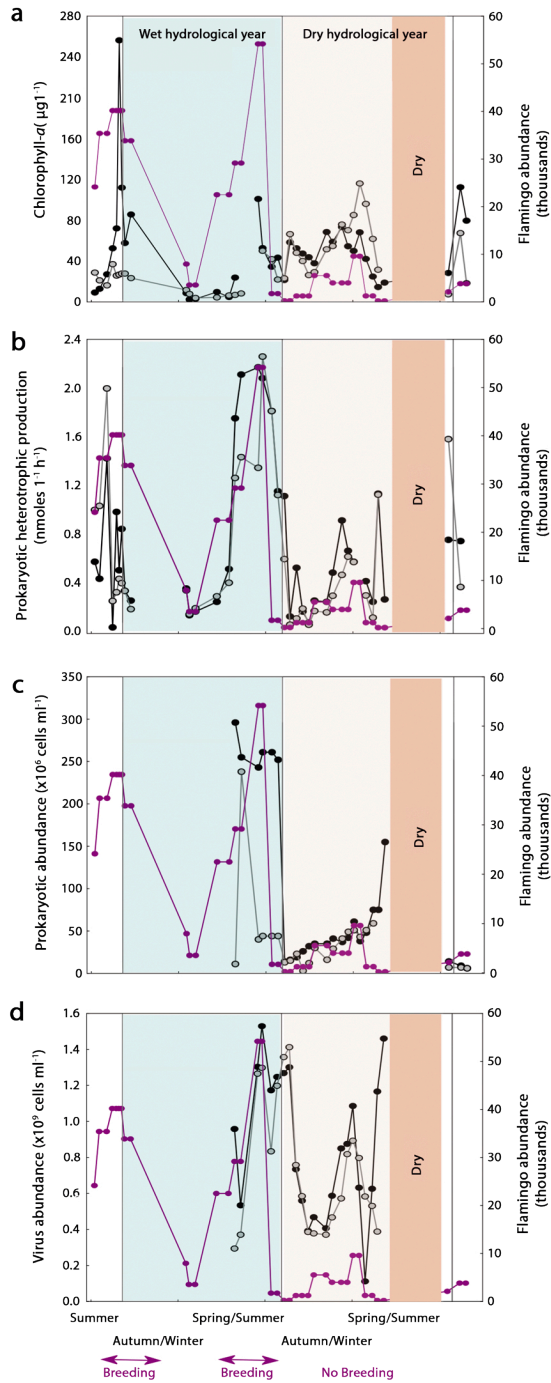


Figure 3.6. Microbial dynamics during two hydrological years. Changes in (a) chlorophyll *a* concentration, (b) prokaryotic heterotrophic production, (c) prokaryotic abundance, and (d) virus abundance at station 1 (black dots) and station 2 (grey dots). Flamingo abundance (purple line) is shown for reference.

Cascading effects of flamingos

Prokaryotic heterotrophic production and abundance appeared to be synchronized with the abundance of flamingos (Figure 3.6b and Figure 3.6c), whereas the abundances of viruses (Figure 4d) and total dissolved nitrogen concentration (Figure 3.4f) showed different time lags. To explore the existence of potential links among these synchronous or time-lagged variables associated with flamingo abundance, we performed cross-correlation analyses. Flamingo abundance (y) was significantly cross-correlated with prokaryote activity (x) at lag=0 ($r_{xy}=0.70$) and lag=-1 ($r_{xy}=0.66$) (Figure 3.7a), with prokaryote abundance (x) at lag =0 ($r_{xy}=0.46$), lag =-1 ($r_{xy}=0.65$) and lag=-2 ($r_{xy}=0.70$) (Figure 3.7b), and with total dissolved nitrogen (x) at lag =-4 ($r_{xy}=0.56$) and lag=-5 ($r_{xy}=0.67$) (Figure 3.7d). Cross-correlations with virus abundance (x) were not significant, but the coefficient was highest at lag =-4 (Figure 3.7c).

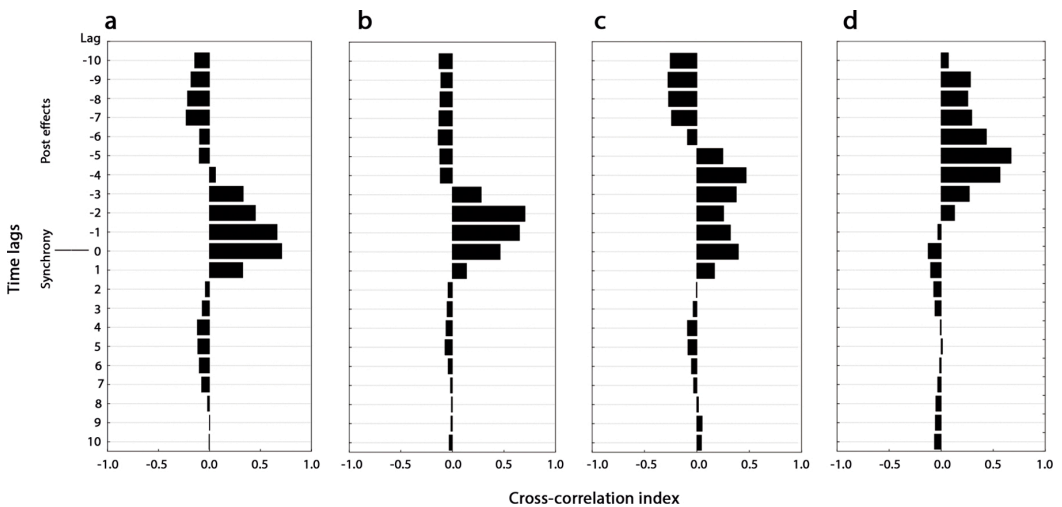


Figure 3.7. Cross-correlations of flamingos and the microbial and total dissolved nitrogen dynamics. The zero line represents a synchronous effect and the negative numbers represent time-lag effects at different intervals. The analyses were performed for (a) prokaryotic heterotrophic production, (b) prokaryotic heterotrophic abundance, (c) virus abundance and (d) total dissolved nitrogen. Significant positive effects are represented by black bars that exceed the 0.5 level on the x axis.

Nutrients delivered by flamingo guano

The nutrient content of flamingo chick feces ranged from 28.7 to 45.1 mg N g⁻¹ dry weight, and from 2.1 to 3.4 mg P g⁻¹ dry weight depending on food sources (Table 3.4). Almost all the nitrogen in flamingo chick feces was soluble, with TDN averaging 74 % of TN. In contrast, TDP only averaged 19 % of TP (Table 3.3). The molar TN:TP ratio in flamingo chick feces was 29, above the Redfield ratio and higher than found in the feces of other waterbirds

(Table 3.3). Assuming the average values of N and P content in flamingo droppings (i.e. TN = 36.9 mg N g⁻¹ and TP = 2.75 mg P g⁻¹ dry weight), we estimated that the average per capita delivery in the lake per day was 1.978 g N (141.2 mmol of N) and 0.147g P (4746.52 μmol of P). Given the abundance of flamingos, the total delivery of N to the lake was of 16.54 tonnes during the wet year (i.e. 16.7 Kg N ha⁻¹ y⁻¹) and 1.67 tonnes during the dry year (i.e. 3.2 Kg N ha⁻¹ y⁻¹). Taking into account the water volume, the annual N input during the wet year was 3.372 mg N l⁻¹ y⁻¹, and during the dry year was 1.342 mg N l⁻¹ y⁻¹. The total delivery of P to the lake was of 1.23 tonnes (i.e. 1.24 Kg P ha⁻¹ y⁻¹) during the wet year and 0.12 tonnes (i.e. 0.23 Kg P ha⁻¹ y⁻¹) during the dry year. The annual P input was 0.251 mg P l⁻¹ y⁻¹ during the wet year, and 0.100 mg P l⁻¹ y⁻¹ during the dry year.

Table 3.4. Means and standard deviations (\pm SD) of total nitrogen (TN), total dissolved nitrogen (TDN), total phosphorus (TP), total dissolved phosphorus (TDP), total organic carbon (TOC), and dissolved organic carbon (DOC) in mg per g of feces in dry weight and the molar TN: TP ratios in the feces of the greater flamingo (*Phoenicopterus roseus*) and other waterfowl. Two types of feces (brown and pink) were analyzed and are likely to be associated with different food sources. Dissolved nutrient solubilized from feces (TDN, and TDP) were calculated as the percentage (%) of the total (TN and TP).

	TN mg-N g ⁻¹ (mmol-N g ⁻¹)	TDN mg-N g ⁻¹ (mmol-N g ⁻¹)	TP mg-P g ⁻¹ (mmol-P g ⁻¹)	TDP mg-P g ⁻¹ (mmol-P g ⁻¹)	TOC mg-C g ⁻¹ (mmol-C g ⁻¹)	DOC mg-C g ⁻¹ (mmol-C g ⁻¹)	TN: TP (Molar)	Reference
Waterbirds								
Phoenicopterus roseus (brown feces) Soluble	28.78 \pm 1.42 (2.05 \pm 0.10)	24.83 \pm 4.53 (1.77 \pm 0.32) (86%)	2.06 \pm 0.98 (0.07 \pm 0.03)	0.45 \pm 0.05 (0.01 \pm 0.00) (19 %)	125.77 \pm 0.55 (10.48 \pm 0.04)	106.97 \pm 0.76 (8.91 \pm 0.06)	29	This study
Phoenicopterus roseus (pink feces) Soluble	45.15 \pm 1.80 (3.22 \pm 0.12)	29.55 \pm 5.41 (2.11 \pm 0.38) (66%)	3.38 \pm 0.37 (0.11 \pm 0.01)	0.77 \pm 0.03 (0.02 \pm 0.00) (20%)	127.25 \pm 3.15 (10.60 \pm 0.26)	112.97 \pm 0.14 (9.41 \pm 0.01)	29	This study
Branta leucopsis Barnacle goose	11 \pm 2 (0.8 \pm 0.1)	---	3.3 \pm 0.2 (0.1 \pm 0.0)	---	450.5 \pm 3.5 (37.5 \pm 0.3)	---	7.5	Van Gueest <i>et al.</i> , 2007
Anous minutus Bo. Black noddy	182.5 (13.03)	---	37.5 (1.21)	---	---	---	10.7	Smith & Johnson, 1995.
Phalacrocorax carbo L. Great cormorant	32.8 (2.3)	---	143.2 (4.6)	---	---	---	0.6	Marion <i>et al.</i> , 1994.
Ardea cinerea L. Grey heron	42.1 (3.0)	---	114.7 (3.7)	---	---	---	0.8	Marion <i>et al.</i> , 1994.
Pelecanus thagus Peruvian pelican	241.3 (17.2)	---	20.9 (0.7)	---	---	---	25	Hutchinson, 1950.

Experiments with flamingo guano

We tested if nutrients delivered by guano directly promote microbial growth in two laboratory experiments (Figure 3.8). In experiment 1 (Figure 3.8a), prokaryote abundance in re-growth cultures fitted exponential growth. The specific growth rate (μ) in the treatment with guano was almost twice as high ($\mu = 0.46 \pm 0.16 \text{ d}^{-1}$; $r^2=0.39$) as in the control treatment ($\mu = 0.27 \pm 0.01 \text{ d}^{-1}$, $r^2 = 0.35$), a significant difference. Prokaryote heterotrophic production did not fit exponential or logistic growth curves. In experiment 2 (Figure 3.8b), only the control treatment fitted exponential growth ($\mu = 0.21 \pm 0.07 \text{ d}^{-1}$, $r^2=0.30$) and the specific growth rate (μ) was similar to the control in the previous experiment. Prokaryote heterotrophic production, however, fitted logistic growth curves in both treatments. Both the carrying capacity (K) and the specific growth rates for protein synthesis (b) were higher in the treatment with guano ($K = 0.797 \text{ nmoles l}^{-1}\text{h}^{-1}$, $b = 295 \text{ d}^{-1}$, $r^2 = 0.72$) than in the control treatment ($K = 0.366 \text{ nmoles l}^{-1}\text{h}^{-1}$, $b = 11 \text{ d}^{-1}$, $r^2 = 0.71$). At the beginning and end of the experiments, we also monitored the changes in dissolved nutrients. DOC and TDN did not change significantly over the incubation period in any of the experimental treatments (Table 3.5). However, SRP decreased significantly in all treatments at the end of the incubation time (Figure 3.8a and 3.8b), likely due to its assimilation by heterotrophic prokaryotes during their growth, indicating a high P-demand by these microorganisms.

Table 3.5. Conditions of the water level and abundance of flamingos in the lake when the experiments with guano addition were performed. Results of the concentrations of dissolved organic carbon (DOC) and total dissolved nitrogen (TDN) at the beginning (t_0) and the end (t_f) of the two experiments.

Water level (cm)	Flamingo Abund.	Treatment	DOC (mmol-C l ⁻¹)		TDN (mmol-N l ⁻¹)	
			t_0	t_f	t_0	t_f
79	33849	Exp. 1				
		Control	2.00 ± 0.02	2.21 ± 0.12	0.20 ± 0.00	0.18 ± 0.00
		High	1.94 ± 0.05	2.09 ± 0.15	0.27 ± 0.00	0.24 ± 0.00
		Exp. 2				
130	22490	Control	1.17 ± 0.09	1.12 ± 0.03	0.07 ± 0.00	0.07 ± 0.01
		High	1.26 ± 0.02	1.19 ± 0.10	0.09 ± 0.01	0.09 ± 0.01

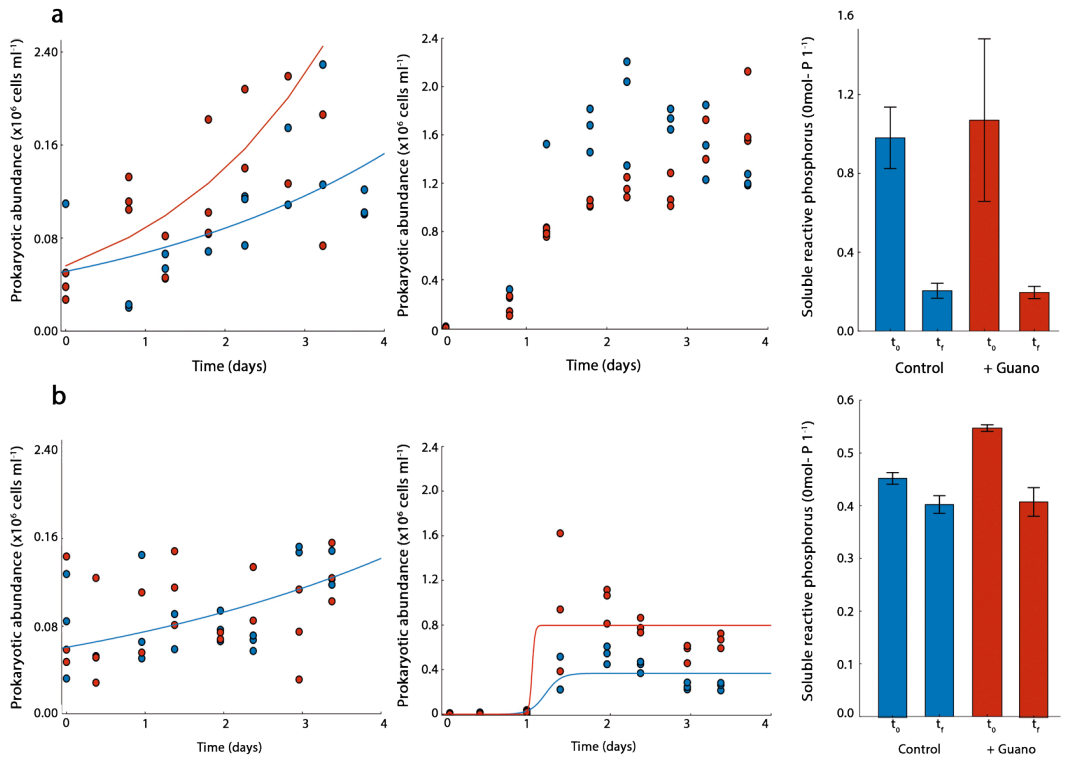
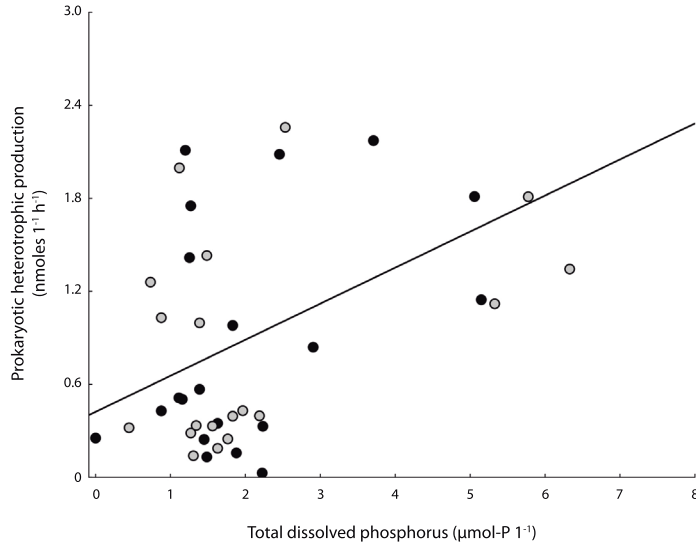


Figure 3.8. Experiments on the growth of heterotrophic prokaryotes with addition of flamingo guano. Changes in heterotrophic abundance and production during the period of incubation, and the concentration of soluble reactive phosphorus at the beginning (t_0) and end (t_f) of (a) experiment 1 and (b) experiment 2. Blue represents the treatment with the control conditions and red the treatment with addition of fresh guano from flamingo chicks.

3.4. DISCUSSION

We observed a robust, direct and synchronous influence of flamingos on heterotrophic prokaryotic production and abundance, that appears to be mediated by an increase in P availability associated with inputs from guano and sediment bioturbation, instead of by organic substrates derived from primary producers. This direct influence of flamingos on heterotrophic prokaryotic activity appears to trigger cascading effects on heterotrophic prokaryotes, virus abundance and total dissolved nitrogen. The addition of feces and sediment bioturbation when the water level was low affected the availability of dissolved phosphorus and nitrogen, whereas DOC, total nitrogen and total phosphorus were mainly driven by the hydrological phases (evaporation vs. precipitation).

In Fuente de Piedra Lake, heterotrophic prokaryotic production and primary production (with chlorophyll-a as a proxy) were both affected by the abundance of flamingos. Similar results on primary production were reported by Kitchell *et al.*, 1999, who showed a positive correlation between geese density and chlorophyll-a concentrations, which increased eight-fold in ponds with high bird densities. Chlorophyll-a increases have been linked to N and P inputs from waterbird feces (Manny *et al.*, 1994; Dessborn *et al.*, 2016), and also experimentally demonstrated (Van Geest *et al.*, 2007). In our study, this effect was even more dramatic at Station 1, where chlorophyll-a increased by up to 25 times during the flamingo-breeding season. On the other hand, prokaryotic heterotrophic production was synchronously correlated to flamingo abundance at both sampling stations (Figure 3.6b) and to total dissolved phosphorus (Figure 3.9). Different mechanisms could explain these synchronous dynamics between heterotrophic prokaryotes and flamingo abundance (Figure 3.6b and Figure 3.6c). On the one hand, heterotrophic prokaryotes could have been indirectly stimulated via phytoplankton exudation of organic carbon, which responded to the nutrients delivered by flamingos. On the other hand, flamingos may have a direct effect on prokaryotes through the inputs of limiting nutrients via guano deposition and sediment bioturbation as they move. The first possibility seems unlikely in this study since the relationship between flamingo abundance and chlorophyll-a was only significant in one of the stations and was weaker than the relationship between flamingo abundance and the PHP and prokaryote abundance. In fact, we found a positive and significant correlation between prokaryotic heterotrophic production and TDP during the wet year when flamingos reached maximum abundance ($n=39$, $r=0.39$, $p<0.01$, Figure 3.9), suggesting P-limitation of the heterotrophic prokaryotes during this period.



of sediments from Fuente de Piedra lake. In fact, SRP concentration was more affected by water level than by the flamingo abundance itself (Table 3.2), suggesting a major influence of sediments on SRP concentration in the water column of Fuente de Piedra. SRP dynamics in this system is complex and also affected by wave action and by physicochemical processes in sediments, such as adsorption/absorption, precipitation, solubilisation and redox reactions. Clavero *et al.*, 1990 performed several experiments in this lake showing that phosphate release from sediments was stimulated at salinities above 70 ppt. Therefore, the dissolved phosphorus in the system results from a combination of flamingo aggregations with fecal inputs and sediment bioturbation, along with an increase in the influence of sediments during the evaporation phase.

On the other hand, the fecal inputs from flamingo chicks contained comparatively more nitrogen than phosphorus with N:P molar ratios above the Redfield ratio (Table 3.3). These high ratios have several potential explanations which are not mutually exclusive: the feeding of chicks with N-rich food, efficient P retention by the chicks, the a wide-range of N:P ratios among waterbird feces, and the use of fresh, not dried, feces in this study. Flamingo adults make regular movements during breeding from the Fuente de Piedra colony to nitrogen-enriched feeding sites such as rice fields and fishponds in the Doñana wetland complex (Rendón-Martos *et al.*, 2000; Amat *et al.*, 2005). Our data for flamingo feces were similar to those of Hutchinson, 1950 for the Peruvian pelican that has a fish diet rich in proteins. We collected the chick feces during ringing operations and they were immediately frozen, preventing significant N losses related to ammonium volatilization, a common process in nature where feces are deposited and exposed to the atmosphere for days (Mizutani *et al.*, 1985; Gross *et al.*, 1999). Finally, we were only able to sample feces from growing chicks, and it is possible that adult flamingos have feces with a lower N:P ratio, since cloacal microbiota appears to differ with age (Van Dongen *et al.*, 2013) and chick retain P (Bougouin *et al.*, 2014) which could modify the N:P ratio in feces. However, the evidence from this study suggests flamingo fecal inputs influence also the dissolved nitrogen in the study lake (Figure 3.4f, Figure 3.7d).

Previous studies have emphasized the importance of waterbirds as nutrient vectors in aquatic ecosystems with high water retention times in arid and semiarid regions (Post *et al.*, 1998; Huang and Isobe, 2012). However, in Fuente de Piedra Lake, total N and P inputs were more than 5-fold higher during the wet year than in the dry year. During the wet year, the flamingo population size was substantially larger than in the dry year, as were their corresponding N and P inputs ($16.7 \text{ Kg N ha}^{-1} \text{ y}^{-1}$ and $1.24 \text{ Kg P ha}^{-1} \text{ y}^{-1}$). These values were higher than those reported for herbivorous ($1.07 \text{ kg N ha}^{-1} \text{ y}^{-1}$ and $0.10 \text{ kg P ha}^{-1} \text{ y}^{-1}$) or carnivorous ($0.26\text{-}0.65 \text{ kg N ha}^{-1} \text{ y}^{-1}$ and $0.12\text{-}0.16 \text{ Kg P ha}^{-1} \text{ y}^{-1}$) waterbirds in the Netherlands (Hahn *et al.*, 2007; 2008), or in Lake Mattamuskeet ($0.2 \text{ kg N ha}^{-1} \text{ y}^{-1}$) in North Carolina (Winton *et al.*, 2016). On the other hand, these allochthonous inputs of N and P from flamingo guano were higher than the atmospheric inputs of $5.89 \text{ Kg N ha}^{-1} \text{ y}^{-1}$ and $0.18 \text{ Kg P ha}^{-1} \text{ y}^{-1}$ reported for the study

region (Morales-Baquero *et al.*, 2013). These results underline the importance of waterbirds as nutrient vectors and how extreme conditions, such as the drying of the lake and the resulting crash in the numbers of flamingos, can reduce them.

The links between dissolved nutrients and flamingo abundance, however, do not appear to be simple. TDN was time lagged with flamingo abundance (Figure 3.4f, Figure 3.7d) and was also affected by water level (Table 3.2). This time lagged correlation between TDN and flamingo abundance could be partially related to a cascading effect of flamingos on the microbial community (Figure 3.7). The high flamingo abundance during the breeding season stimulates heterotrophic prokaryotic activity, which leads to an increase in the heterotrophic prokaryotic abundance with a subtle time lag (Figure 3.7 a, b). Higher bacterial abundance facilitates contact between viruses and prokaryotes and may enhance bacterial lysis, leading to more viruses (Figure 3.7c) and the release of nutrients (Figure 3.7d). There is evidence that viruses affect heterotrophic prokaryote mortality in saline systems (Guixa-Boixereu *et al.*, 1996), and that viral lysis releases soluble nitrogen and phosphorus (Wilhem and Suttle, 1999; Shelford *et al.*, 2012). Then, TDN concentration, with a time lag relative to the peak of virus abundance (Figure 3.7d), may partially be a by-product of viral lysis. Unlike the dissolved P that is quickly incorporated by prokaryotes, the non-limiting nutrients, such as dissolved nitrogen, might be retained longer in the water column and be detected at higher concentrations. However, despite the absence of N-limitation in the studied system, TDN concentration decreased during the evaporation phase of the dry year (Figure 3.4f), presumably as the result of other microbial processes such as denitrification, N_2O production or ammonium volatilization. These processes seem to be promoted in sites with important inputs of N from wastewater, agricultural lands or atmospheric deposition (Poach *et al.*, 2003, Beaulieu *et al.*, 2011; McCrackin and Elser, 2010). Since wetlands are considered efficient ecosystems for removing nitrogen and improving water quality (Verhoeven *et al.*, 2006), the influence of waterbirds on these processes of N loss should also be included in future studies. In fact, Winton and Richardson, 2017) recently found that overgrazing by waterfowl had consequences for methane and nitrous oxide emissions. Waterfowl herbivory led to increases in methane emissions but prevented nitrification.

In this study, we demonstrated that flamingos stimulated the production of heterotrophic prokaryotes and produced a series of cascading effects on virus abundance and dissolved nitrogen. This stimulus was related to the inputs of dissolved nutrients from feces and sediments. Soluble phosphorus from feces was quickly incorporated into prokaryote biomass in experiments, and sediments appear to release soluble P at high salinity when water levels are low, allowing flamingo wading. The comparatively high inputs of N delivered by flamingos appeared to be time-lagged, but the processes involved in this lag, and particularly in its subsequent loss, are complex; other microbial processes such as ammonium volatilization, denitrification and nitrous oxide emissions should be considered in future research. N and P inputs by flamingos were higher during the wet hydrological year than during the

dry hydrological year, suggesting that extreme conditions such as drought control the abundance of flamingos in this system and consequently their effects on dissolved nutrients and microbial production.

Overall, the study lake appears to have two levels of control of nutrients and microbial dynamics. At the ecosystem level, the climatic conditions (rainfall and environmental temperature) determine the hydrological budget, affecting the evapo-concentration of total nutrients (TN and TP), dissolved organic carbon, the water level and the abundance and breeding of flamingos. At a second level, there is a flamingo top-down control on dissolved nutrients (SRP and TDP) by inputs of guano and sediment bioturbation. These dissolved nutrients affect primary and heterotrophic production. Flamingos provide a major ecosystem service to humans through their cultural value and here we show that they also provide an ecosystem service by providing bioavailable nutrients that boost microbial production directly. Microbial activity facilitates the processing of organic carbon, and probably organic nitrogen, improving water quality in wetlands (Verhoeven *et al.*, 2006). Nevertheless, further work should explore shifts in the composition of the microbial communities and functional groups to unravel the impact of flamingos and weather patterns and to obtain more precise information with predictive value on functional potential of wetlands.

Future scenarios of intense droughts in the Mediterranean biome could lead to increases in total nutrients in wetlands by evapo-concentration, but the biological (autotrophic and heterotrophic) activity might be constrained by the availability of dissolved phosphorus and nitrogen, which is more dependent on the water level and presence of waterbirds. Here, we show that flamingo abundance decreased during the dry hydrological year, as did the primary and the microbial production. These facts suggest, unlike our initial hypothesis, a more active ecosystem during the wet periods than during the dry ones. Droughts can reduce biological activity in this type of Mediterranean wetland, although in less extreme systems waterbird overcrowding could occur leading to acute guantrophication. The consequences of waterbird overgrazing on biogeochemical cycles and other key processes in wetlands, such as greenhouse gas emissions, are still controversial (Winton & Richardson, 2017; Bodelier *et al.*, 2006; Dingemans *et al.*, 2011), and more field and experimental studies are needed to determine the lake-specific conditions that minimize the emissions of greenhouse gases while maintaining waterbird populations. Therefore, an integrated approach to wetlands management should determine the carrying capacity for each system, so that it houses waterbirds that promote denitrification to N_2 , but avoids the negative effects on water quality by guantrophication, and potential increases in methane and nitrous oxide emissions. that promote denitrification to N_2 , but avoids the negative effects on water quality by guantrophication, and potential increases in methane and nitrous oxide emissions.

3.5. REFERENCES

- Álvarez-Salgado, X.A. & Miller, A.E.J. (1998). Simultaneous determination of dissolved organic carbon and total dissolved nitrogen in seawater by high temperature catalytic oxidation: conditions for precise shipboard measurements. *Mar. Chem.* 62, 325–333.
- Amat, J.A., Rendón, M.A., Rendón-Martos, M., Garrido, A. & Ramírez, J.M. (2005). Ranging behaviour of greater flamingos during the breeding and post-breeding periods: Linking connectivity to biological processes. *Biol. Conserv.* 125, 183-192.
- American Public Health Association (APHA). (1992). Standard methods for the examination of water and wastewater (ed. American Public Health Association)
- Balkiz, Ö., Béchet, A. & Rouan, L. (2009). Metapopulation dynamics of the Greater Flamingo *Phoenicopterus roseus* in the Mediterranean: implication for conservation. *Flamingo Special Publication* 1, 12-16.
- Baxter, G.S. & Fairweather, P.G. (1994). Phosphorus and Nitrogen in Wetlands with and without Egret Colonies. *Aust. J. Ecol.* 19, 409-416.
- Beaulieu, J. J., Tank, J. L. & Hamilton, S. K. (2011). Nitrous oxide emission from denitrification in stream and river networks. *P. Natl. Acad. Sci. USA* 108, 214–219.
- Bodelier, P. L. E., Stomp, M., Luis Santamaría, L. Klaassen, M. & Laanbroek, H. J. (2006). Animal-plant-microbe interactions: direct and indirect effects of swan foraging behaviour modulate methane cycling in temperate shallow wetlands. *Oecologia* 149, 233–244.
- Bougouin A., Appuhamy J.A.D.R.N., Kebreab E., Dijkstra J., Kwakkel R.P., France J. (2014): Effects of phytase supplementation on phosphorus retention in broilers and layers: a meta-analysis. *Poultry Science*, 93, 1981–1992.
- Brussaard, C.P.D., Payet, J.P., Winter, C. & Weinbauer, M.G. Quantification of aquatic viruses by flow cytometry. (2010). *Manual of Aquatic Viral Ecology* (ed. Wilhelm, S.W., Weinbauer, M.G. Suttle C.A.) 11, 102–109 (Association for the Sciences of Limnology and Oceanography).
- Clavero, V., Fernández, J.A. & Niell, F.X. (1990). Influence of salinity on the concentration and rate of interchange of dissolved phosphate between water and sediment in Fuente Piedra lagoon (S. Spain). *Hydrobiologia* 197, 91-97.

- Comín, F.A., Herrera-Silveira, J.A. & Martin, M. (1997). Flamingo footsteps enhance nutrients release from the sediment to the water column. *Wetlands International publication* 43, 211-227.
- Conde-Álvarez, R.M., Bañares-España, E., Nieto-Caldera, J.M., Flores-Moya.A. & Figueroa, F. L. (2012). Submerged macrophyte biomass distribution in the shallow saline lake Fuente de Piedra (Spain) as function of environmental variables. *Anal. Jardín Bot. Madrid.* 69, 119-127.
- Cramp, S. & Simmons, K.E.L. (1977). *The Birds of the Western Palearctic, Vol. 1.* (ed. Cramp, S. & Simmons, K.E.L.) (Oxford University Press).
- Dessborn, L., Hessel, R. & Elmberg, J. (2016). Geese as vectors of nitrogen and phosphorus to freshwater systems. *Inland Waters*, 6, 111-122.
- Dingemans, B.J.J., Bakker, E.S. & Bodelier, P.L.E. (2011). Aquatic herbivores facilitate the emission of methane from wetlands. *Ecology* 92, 1166–1173.
- Erwin, k.L. (2009). Wetlands and global climate change: the role of wetland restoration in a changing world. *Wetlands Ecol. Manage* 17, 71-84.
- García, C. M, García-Ruiz, R., Rendón, M., Niell, F.X. & Lucena, J. (1997). Hydrological cycle and interannual variability of the aquatic community in a temporary saline lake (Fuente de Piedra, Southern Spain). *Hydrobiologia* 345, 131-141.
- García, C.M. & Niell, F.X. (1993). Seasonal change in a saline temporary lake (Fuente de Piedra, southern Spain). *Hydrobiologia.* 267, 211-223.
- Gasol, J.M. & Del Giorgio, P.A. (2000). Using flow cytometry for counting natural planktonic bacteria and understanding the structure of planktonic bacterial communities. *Sci. Mar.* 64, 197–224.
- Geraci, J.; Béchet, A.; Cézilly, F.; Ficheux, S.; Baccetti, N.; Samraoui, B.; Wattier, R. (2012). Greater flamingo colonies around the Mediterranean form a single interbreeding population and share a common history. *J. Avian Biol.* 43, 341-354.
- Glassom, D. & Branch, G.M. (1997). Impact of predation by greater flamingos *Phoenicopterus ruber* on the meiofauna, microflora, and sediment properties of two southern African lagoons. *Mar. Ecol. Progr. Ser.* 149, 1-12.

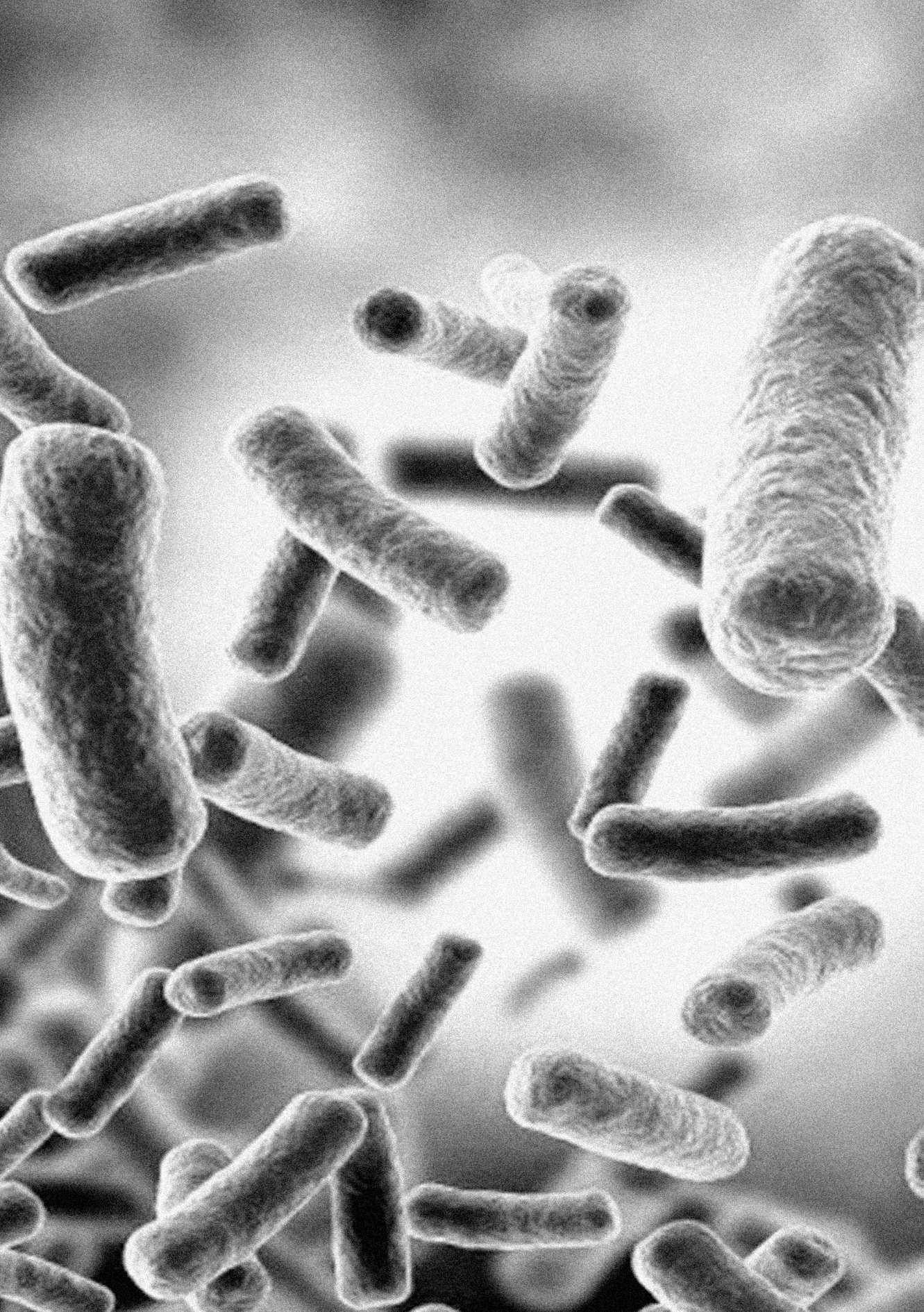
- Green, A.J. & Elmberg, J. (2014). Ecosystem services provided by waterbirds. *Biol. Rev.* 89, 105-122.
- Gross, A., Boyd, C. E. & Wood C.W. (1999). Ammonia Volatilization from Freshwater Fish Ponds *J. Environ. Qual.* 28, 793-797.
- Guixa-Boixereu, N., Calderón-Paz, J.I., Haldal, M., Bratbak, G. & Pedrós-Alió, C. (1996). Viral lysis and bacterivory as prokaryotic loss factors along a salinity gradient. *Aquat. Microb. Ecol.* 11, 215-227.
- Hahn, S., Bauer, S. & Klaassen, M. (2007). Estimating the contribution of carnivorous waterbirds to nutrient loading in freshwater habitats. *Freshwat. Biol.* 52, 2421-2433.
- Hahn, S., Bauer, S. & Klaassen, M. (2008). Quantification of allochthonous nutrient inputs into freshwater bodies by herbivorous waterbirds. *Freshwater Biol.* 53, 181-193.
- Huang, G., & Isobe, M. (2012). Carrying capacity of wetlands for massive migratory waterfowl. *Hydrobiologia* 697, 5-14.
- Hurlbert, S.H. & Chang, C.C.Y. (1983). Ornitholimnology: Effects of grazing by the Andean flamingo (*Phoenicoparrus andinus*). *Proc. Natl. Acad. Sci. U.S.A.* 80, 4766-4769.
- Hutchinson, G.E. (1950). The biogeochemistry of vertebrate excretion. *Bull. Am. Mus. Nat. Hist.* 96, 554 pp.
- Jansson, M. (1993). Uptake, exchange and excretion of orthophosphate in starved *Scenedesmus quadricauda* and *Pseudomonas K7*. *Limnol. Oceanogr.* 38, 1162-1178.
- Jeppesen, E., Brucet, S., Naselli-Flores, L., Papastergiadou, E., Stefanidis, K., Noges, T., *et al.* (2015). Ecological impacts of global warming and water abstraction on lakes and reservoirs due to changes in water level and related changes in salinity. *Hydrobiologia*, 750(1), 201-227.
- Kameda, K., Koba, K., Hobara, S., Osono, T. & Terai, M. (2006). Pattern of natural N-15 abundance in lakeside forest ecosystem affected by cormorant-derived nitrogen. *Hydrobiol.* 567, 69-86.
- Kitchell JF, Schindler DE, Herwig BR, Post DM, Olson MH, Oldham M. (1999). Nutrient cycling at the landscape scale: the role of diel foraging migrations by geese at the Bosque del Apache National Wildlife Refuge, New Mexico. *Limnol. Oceanogr.* 44, 82-836.

- Kohfahl C, Rodriguez M, Fenk C *et al.* (2008). Characterising flow regime and interrelation between surface-water and ground-water in the Fuente de Piedra salt lake basin by means of stable isotopes, hydrogeochemical and hydraulic data. *J. Hydrol.* 351, 170–187.
- Leentvaar, P. (1967). Observations in guanotrophic environments. *Hydrobiologia.* 29, 441–489.
- Li L, Vrieling A, Skidmore A, Wang T, Muñoz AR, Turak E. (2015). Evaluation of MODIS spectral indices for monitoring hydrological dynamics of a small, seasonally-flooded wetland in Southern Spain. *Wetlands* 35, 851–864.
- Manny, B.A., Johnson, W.C. & Wetzel, R.G. (1994). Nutrient additions by waterfowl to lakes and reservoirs: predicting their effects on productivity and water quality. *Hydrobiologia.* 279/280,121–132.
- Marion, L., Clergeau, P., Brient, L. & Bertru, G. (1994). The importance of avian-contributed nitrogen (N) and phosphorus (P) to Lake Grand-Lieu, France. *Hydrobiologia.* 279, 133-147.
- McCrackin, M.L. & Elser, J.J. (2010). Atmospheric nitrogen deposition alters denitrification and nitrous oxide production in lake sediments. *Ecology* 91, 528–539.
- McMenamin, S.K., Hadly, E.A. & Wright, C.K. (2008). Climatic change and wetland desiccation cause amphibian decline in Yellowstone National Park. *P. Natl. Acad. Sci. USA* 105, 16988-16993.
- Mindl, B., A. M. Anesio, K. Katrin, A. J. Hodson, J. Laybourn-Parry, R. Sommaruga, and B. Sattler. (2007). Factors influencing bacterial dynamics along a transect from supraglacial runoff to proglacial lakes of a high arctic glacier. *FEMS Microbiol Ecol.* 59, 307–317.
- Mizutani, H., Kabaya, Y. & Wada, E. (1985). Ammonia volatilization and high $^{15}\text{N}/^{14}\text{N}$ ratio in a penguin rookery in Antarctica. *Geochem. J.* 19, 323-327.
- Morales-Baquero, R., Pulido-Villena, E., & Reche I. (2013). Chemical signature of Saharan dust on dry and wet atmospheric deposition in the south-western Mediterranean region. *Tellus B* 65, 18720.
- Moss, B. *et al.* (2009). Climate change and the future of freshwater biodiversity in Europe: a primer for policy-makers. *Freshwater Reviews.* 2, 103-130.
- Murphy, J. & Riley J.P. (1962). A modified single solution method for the determination of phosphate in natural waters. *Analytica Chimica Acta.* 27, 31-36.

- Nielsen, D.L. & Rock, M.A. (2009). Modified water regime and salinity as a consequence of climate change: Prospects for wetlands of Southern Australia. *Clim. Change*. 95, 523–533.
- Poach, ME, Hunt, PGReddy, GB. (2003). Ammonia Volatilization from Marsh–Pond–Marsh Constructed Wetlands Treating Swine Wastewater. *J. Environ. Qual.* 33, 844-851.
- Post, D. M.; Taylor, J. P.; Kitchell, J. F.; Olson, M. H.; Schindler, D. E. y Herwig, B. R. (1998). The role of migratory waterfowl as nutrient vectors in a managed wetland. *Conservation Biology*, 12: 910-920.
- Pulido-Villena, E, & Reche, I. (2003). Exploring bacterioplankton growth and protein synthesis to determine conversion factors across a gradient of dissolved organic matter. *Microb. Ecol.* 46, 33–42.
- Ramo, C., Aguilera, E., Figuerola, J., Manez, M. & Green, A.J. (2013). Long-Term Population Trends of Colonial Wading Birds Breeding in Doñana (Sw Spain) in Relation to Environmental and Anthropogenic Factors. *Ardeola* 60, 305-326.
- Reche I, Ortega-Retuerta E, Romera O, Pulido-Villena E, Morales-Baquero R, Casamayor EO. (2009). Effect of Saharan dust inputs on bacterial activity and community composition in Mediterranean lakes and reservoirs. *Limnol Oceanogr* 54: 869–879.
- Reche, I., Carrillo, P., & Cruz-Pizarro, L. (1997). Influence of metazooplankton on interactions of bacteria and phytoplankton in an oligotrophic lake. *J. Plankton Res.* 19, 631-646.
- Rendón M.A., Garrido A., Guerrero J.C. Rendón-Martos M. & Amat J.A. (2012). Crop size as an index of chick provisioning in the Greater Flamingo *Phoenicopterus roseus*. *Ibis* 154, 379–388.
- Rendón M.A., Garrido A., Rendón-Martos M., Ramírez J.M. & Amat J.A. (2014). Assessing sex-related chick provisioning in greater flamingo *Phoenicopterus roseus* parents using capture–recapture models. *J. Animal Ecol.* 83, 479–490.
- Rendón-Martos, M. (1996). La laguna de Fuente de Piedra en la dinámica de la población de flamencos (*Phoenicopterus ruber roseus*) del Mediterráneo Occidental. Ph.D. thesis, University of Málaga.
- Rendón-Martos, M., Vargas, J.M., Rendón, M.A., Garrido, A. & Ramírez, J.M. (2000). Nocturnal movements of breeding greater flamingos in southern Spain. *Waterbirds* 23, 9–19.
- Rendón, M.A., Garrido, A., Ramírez, J.M., Rendón-Martos, M. & Amat, J.A. (2001). Despotism establishment of breeding colonies of greater flamingos, *Phoenicopterus ruber*, in southern Spain. *Behav Ecol Soc.* 50, 55-60.

- Rendón, M.A., Green, A.J., Aquilera, E. & Almaraz, P. (2008). Status, distribution and long-term changes in the waterbird community wintering in Doñana, south-west Spain. *Biol. Conserv.* 141, 1371–1388.
- Rodríguez- Rodríguez, M., Benavente, J. & Moral, F. (2006). High density ground-water flow, major-ion chemistry and field experiments in a closed basin: Fuente de Piedra Playa Lake (Spain). *American J. Environ. Sciences.* 1, 164–171.
- Rodríguez-Pérez, H. & Green, A.J. (2006). Waterbird impacts on widgeongrass *Ruppia maritima* in a Mediterranean wetland: comparing bird groups and seasonal effects. *Oikos*, 112, 525-534.
- Rodríguez-Rodríguez M., Martos-Rosillo S. & Pedrera A. (2016). Hydrogeological behaviour of the Fuente-de-Piedra playa lake and tectonic origin of its basin (Malaga, southern Spain). *Journal of Hydrology*, 543, 462-476.
- Sanz-Aguilar, A., Béchet, A., Germain, C., Johnson, A.R. & Pradel, R. (2012). To leave or not to leave: survival trade-offs between different migratory strategies in the greater flamingo. *J. Anim. Ecol.* 81, 1171-1182.
- Sebastian-González, E., Navarro, J., Sánchez-Zapata, J.A., Botella, F. & Delgado, A. (2012). Water quality and avian inputs as sources of isotopic variability in aquatic macrophytes and macroinvertebrates. *Journal of Limnology* 71, 191-199.
- Shelford E.J., Middelboe M., Møller E.F. & Suttle C.A. (2012). Virus-driven nitrogen cycling enhances phytoplankton growth. *Aquat. Microb. Ecol.* 66, 41-46.
- Signa, G., Mazzola, A. & Vizzini, S. (2012). Effects of a small seagull colony on trophic status and primary production in a Mediterranean coastal system (Marinello ponds, Italy). *Estuar. Coast. Shelf Sci.* 111, 27-34.
- Šimek K, Horňák K, Jezbera J, Nedoma J, Vrba J, Stralkrábová V *et al.* (2006). Maximum growth rates and possible life strategies of different bacterioplankton groups in relation to phosphorus availability in a freshwater reservoir. *Environ. Microbiol.* 8, 1613–1624.
- Smith J.S. & Johnson C.R. (1995). Nutrient inputs from seabirds and humans on a populated coral cay. *Marine Ecology Progress Series*, 124, 189–200.
- Smith, D.C. & Azam, F. A. (1992). Simple, economical method for measuring bacterial protein synthesis rates in seawater using 3H-leucine. *Mar Microb Food Webs* 6, 107–114.

- Smith, E.M. & Prairie, Y.T. (2004). Bacterial metabolism and growth efficiency in lakes: the importance of phosphorus availability. *Limnol Oceanogr.* 49, 137–147.
- Tranvik, L. *et al.* (2009). Lakes and impoundments as regulators of carbon cycling and climate. *Limnol. Oceanogr* 54, 2298-2314.
- Tuite, C.H. (2000). The distribution and density of Lesser Flamingos in East Africa in relation to food availability and productivity. *Water Birds.* 23, 52-63.
- Van Dongen, W. F. D., White, J., Brandl, H. B., Moodley, Y., Merklings, T., Leclaire, S., *et al.* (2013). Age-related differences in the cloacal microbiota of a wild bird species. *BMC Ecology* 13,11.
- Van Geest GJ, Hessen DO, Spiereburg P, Dahl-Hansen GAP, Christensen G, Faerovig PJ, Brehm M, Loonen MJJE, Van Donk E. (2007). Goose-mediated nutrient enrichment and planktonic grazer control in arctic freshwater ponds. *Oecologia.* 153, 653–662.
- Vareschi, E. (1978). The ecology of lake Nakuru (Kenya). I. Abundance and feeding of the Lesser Flamingo. *Oecologia* 32, 11-35.
- Verhoeven, J.T.A., Arheimer B., Yin C., & Hefting, M.M. (2006). Regional and global concerns over wetlands and water quality. *Trends in Ecology and Evolution* 21, 96-103.
- Waiser, M.J & Robarts, R.D. (1995). Microbial nutrient limitation in prairie saline lakes with high sulfate concentration. *Limnol. Oceanogr.* 40, 566-574.
- Wilhelm, S.W. & Suttle, C.A. (1999). Viruses and nutrient cycles in the sea. *BioScience* 49, 781-788.
- Winton R.S.; Richardson C.J. (2017). Top-down control of methane emission and nitrogen cycling by waterfowl. *Ecology* 98, 265–277.
- Winton, R. S., Moorman, M. & Richardson, C. J. (2016). Waterfowl impoundments as sources of nitrogen pollution. *Water, Air & Soil Pollution* 227, 390.



Chapter 4

Drought-reduction of lake area declines bacterial richness and increases temporal β diversity

Drought-reduction of lake area declines bacterial richness and increases temporal β diversity

4

4.1. INTRODUCTION

Large saline lakes constitute about 44% of Earth's water volume and 23% of lake surface (Messenger *et al.* 2016). Most of these lakes are located in endorheic basins in arid and semiarid regions (Meybeck, 1995; Wurtsbaugh *et al.* 2017) and play a significant role in the global carbon cycle as a large sink of dissolved inorganic carbon (Li *et al.* 2017). In addition, saline wetlands have an added value providing refuge, foraging and breeding sites for diverse migratory waterbirds (Green and Elmberg, 2014). Their environmental relevance is of particular interest due to future predictions of intense droughts as consequence of climate change and the consequent shrinking of saline lakes at global scale (Messenger *et al.* 2016; Wurtsbaugh *et al.* 2017; Wang *et al.* 2018). Projected changes suggest greater temperatures and evaporation rates and lower rainfall with a tendency to shorter hydroperiods with the subsequent severe salinization of them (Herbert *et al.* 2015; Jeppesen *et al.* 2015) or even near complete desiccation (Nielsen and Rock, 2009, Gross 2017). Concurrently with the salinization process, a reduction in waterbirds habitat is expected, causing overcrowding of waterbirds relative to lake area, particularly during breeding period (Signa *et al.* 2012; Batanero *et al.* 2017). This scenario could lead to acute eutrophication process with negative effects on wetlands quality (Manny, *et al.* 1994) that appears to be especially accentuated in systems with long water residence times in arid and semiarid regions (Huang and Isobe 2012; Post *et al.* 1998).

Since the pioneer work of MacArthur and Wilson (1967), many studies have demonstrated the importance of ecosystem area as a controlling factor in diversity patterns (Reche *et al.* 2005; Prosser *et al.* 2007; Barreto *et al.* 2014). In fact, one of the most consistent generalizations in ecology is the taxa-area relationship (TAR) as a power law. TAR states that species richness increases with the area (MacArthur and Wilson 1967; Rosenzweig 1995). This rela-

tionship has been found also at the microbial level (Bell *et al.* 2005; Reche *et al.* 2005; Martiny *et al.* 2006) both in terrestrial and aquatic environments (Drakare *et al.* 2006; Soininen *et al.* 2007; Kallimanis *et al.* 2008). Several studies, using molecular approaches, have reported positive TAR in microbial communities both in contiguous (Horner-Devine *et al.* 2004; Noguez *et al.* 2005; Zinger *et al.* 2014,) and in island-like habitats (Bell *et al.* 2005, Reche *et al.* 2005; Van de Gast *et al.* 2005. In general, a low TAR slope is consistent with (1) high dispersal rates and low local extinctions due to vast abundance (Connor and McCoy 1979) and (2) contiguous habitats, due to adjacent sites with similar species composition (Prosser *et al.* 2007). Consequently, in endorheic lakes bacterial TAR could be affected by the changes in the area over time as consequence of drought stress. Simultaneously, not only the richness, but also bacterial composition can be influenced by temporal changes of lake surface. Most studies on microbial biogeography have focused on cross-lake comparisons, measuring bacterial beta diversity in spatial contexts. However, the growing concern for preserving biodiversity underlines the need to quantify temporal change (i.e. temporal beta diversity) (Dornelas *et al.* 2013; Shimadzu *et al.* 2015). Quantification temporal beta diversity allows the determination of unidirectional changes (Dornelas *et al.* 2013) and thus, the evaluation of the consequences of severe droughts on microbial community structure and their succession patterns.

Concomitant with the lake area reduction by droughts there is an increase in salinity and major nutrients (Batanero *et al.* 2017). Salinity has been often reported as a controlling factor of the microbial community (Casamayor *et al.*, 2002; Benlloch *et al.* 2002; Oren *et al.* 2002, Henriques *et al.*, 2006; Zhang *et al.*, 2006). Salinization induces osmotic stress and can also affect microbial functions that drive elemental biogeochemical cycles (Herbert *et al.* 2015). Additionally, a massive increase of waterbirds populations can also affect microbial community structure. For instance, diversity and composition in soils enriched in seabird depositions stimulated specific groups of bacteria affecting community structure (Ramírez-Fernández *et al.* 2019).. In a recent work, Batanero *et al.* (2017) showed that the prokaryotic heterotrophic production and abundance were stimulated in the endorheic lake of Fuente de Piedra (Spain) during the periods with high abundance of flamingos.

Here, we explored the effects of changes in lake surface induced by drought on richness, diversity and composition of both free-living and particle attached bacterial assemblages in the endorheic lake of Fuente de Piedra (Spain). In addition, we monitored salinity and flamingo population to test concurrent effects. We selected Fuente de Piedra lake because is located in semiarid biome submitted to big changes in the water inundation surface and simultaneously in salinity. This lake houses during the spring-summer one of the most important colonies of breeding greater flamingos (*Phoenicopterus roseus*) in the Western Mediterranean (Rendoñ *et al.* 2001; Geraci *et al.* 2012).

We hypothesized that in this lake (i) significant differences of richness and diversity both in free-living and particle-attached bacterial assemblages will be found between two well-contrasted (wet and dry) hydrological years; (ii) bacterial community richness and diversity will be related with lake area, salinity and flamingo abundance; (iii) bacterial TAR slope will remain within the range of those reported for microorganisms with high dispersal potential and contiguous habitats; (iiii) droughts will reduce the lake area, increase salinity and water eutrophication by guano from flamingo and therefore induce changes in bacterial community composition over time. Finally, we discuss the implications of our findings given the threat of climate change and climate-linked impacts on the microbial community in saline lakes, which are key in biogeochemical cycles and wetlands functions.

4.2. MATERIAL AND METHODS

Study site, area lake and flamingo abundance

The study site is Fuente de Piedra, an athalassohaline lake located in an endorheic basin of karstic origin in southern Spain (37° 6' N, 4° 44' W). Its hydrology presents strong changes associated with its annual hydrological budget with inputs from rainfall, two intermittent streams (Santillán and Humilladero) and ground water, and outputs are mainly by evaporation (Rodríguez- Rodríguez *et al.* 2006; Kohfahl *et al.* 2008). This large saline lake covers a maximum area of 1,350 ha and houses during the summer one of the most important colonies of breeding greater flamingos (*Phoenicopterus roseus*) in the Western Mediterranean (Geraci *et al.* 2012, Rendoñ *et al.* 2001). Breeding adults fly within a radius of 350 km to feed in other wetlands, returning to feed their chicks at Fuente de Piedra (Rendón-Martos *et al.* 2000, Amat *et al.* 2005, Rendón *et al.* 2014).

Sampling period included more than two hydrological years. By using Landsat images and the Google Earth Engine platform, we mapped the extent of inundation area of Fuente de Piedra Lake during the study period (Figure 4.1). The first hydrological period between September 2010 and August 2011 is considered wet because the lake showed a more extensive inundation area, for most time of the period reaching between 75 to 100 % of lake surface (Figure 4.1) with an annual rainfall of 563 mm; the previous hydrological year, which was only partially sampled, showed also similar inundation conditions. In contrast, the second hydrological period (i.e. from September 2011 to August 2012) was comparatively drier with smaller inundation areas reaching between 1 to 25 % of lake surface during the summer (Figure 4.1). Each hydrological period comprises a filling phase during fall and winter (September-March) and a water evaporation phase during spring and summer (April-August).

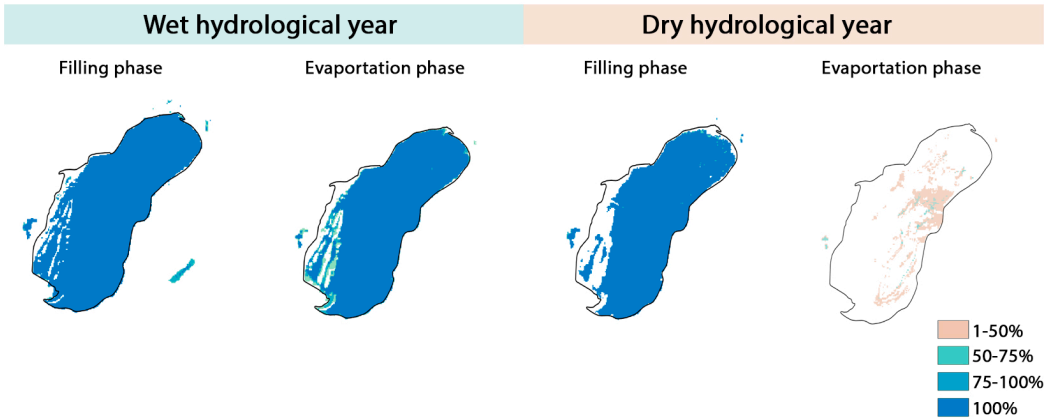


Figure 4.1. Differences in the extension of water inundation area between the wet and dry hydrological periods and between the filling and evaporation phases within each period in Fuente de Piedra lake (Spain). Frequency of inundation indicates the percentage of months that each 30 x 30 m pixel was covered by water in each period. It was computed in Google Earth Engine using the monthly history dataset of Global Surface Water produced by the Joint Research Centre (product JRC/GSW1_0/MonthlyHistory; Pekel et al. 2016). This product contains global maps of surface water extent based on a time-series of NASA's Landsat satellite images from 1984 to 2015.

Water level was daily recorded using a limnigraph and flamingo abundance data were provided by the “Consejería de Medio Ambiente y Ordenación del Territorio” of Junta de Andalucía, Spain. To get biweekly values of flamingo abundance we performed a linear interpolation of monthly data. Lake area values were computed using the hypsographic (i.e. depth – area) curve provided by Rodríguez-Rodríguez *et al.* (2016) and the water level data recorded during the study period. More details on the study site can be found in Batanero *et al.* (2017) and chapter 1. Briefly, during the wet hydrological period salinities ranged from 19.7 ppt to 90.0 ppt and the lake area ranged from 714.7 ha to 1104.9 ha with more than 50,000 flamingos during the breeding period. The previous hydrological period that was only partially sampled showed similar conditions (Table 4.1). In contrast, the second hydrological period was dry with salinities ranging from 69.0 ppt to 193.5 ppt and lake area ranging from 738.4 ha to 0 ha when the lake was completely dried up and flamingo abundance was always below 12,000 individuals (Table 4.1). Nutrient concentrations varied considerably along of the study period increasing up to 3 times during the dry hydrological period (Table 4.1).

Samples were collected biweekly from surface of the water column (ca. 10 cm) at two stations (more details on sampling and monitoring procedures can be found in Batanero *et al.* 2017). In particular, for this study, following selection of monitoring data, an aggregated mean value was calculated for the two sampling stations.

Table 4.1. Mean values and ranges (in parentheses) of basic physicochemical and biological variables in the wet and dry hydrological years.

<i>Fuente de piedra lake</i> 37°06'19.8"N 4°45'44.5"W	Temperature (°C)	pH	Rainfall (mm)	Salinity (ppt)	Flamingo Abundance	Lake area (ha)	DOC (mmol-C l ⁻¹)	TN (mmol-N l ⁻¹)	TP (µmol-P l ⁻¹)	Chl a (µg/l)
Wet hydrological year 2010-2011	19.4 (8.3 - 31.4)	9.03 (8.04 - 9.94)	563.30	39.5 (19.6 - 90.1)	28628 (3861-53579)	963.2 (714.6-1104.9)	1.8 (1.0 - 4.7)	0.2 (0.1 - 0.5)	4.41 (1.49 - 8.89)	30.0 (2.4 - 100.8)
Dry hydrological year 2011-2012	18.6 (8.8 - 29.6)	8.61 (7.53- 9.02)	345.10	117.6 (71.7 -199.0)	3379 (217-8082)	642.04 (0 -738.4)	6.3 (3.8 - 13.6)	0.6 (0.3 - 1.2)	13.52 (5.69 - 38.60)	49.8 (18.8 - 92.1)

Biological and Physico-Chemical analyses

Chlorophyll a concentration was determined by filtering determined from 100 to 700 ml of water through 0.7 µm pore-size Whatman GF/F glass-fiber filters, then extracting the pigment retained in the filters with 95% methanol in the dark at 4 °C for 24 h (APHA 1992). The absorbance of pigment was measured using a Perkin Elmer UV-Lambda 40 spectrophotometer at wavelengths of 665 nm and 750 nm.

Salinity was measured in situ using a multi-parameter probe (HANNA HI 9828). Total nutrient concentrations were measured in unfiltered water, while samples for dissolved nutrient analysis were filtered through 0.7 µm pore-size Whatman GF/F glass-fiber filters. Total phosphorus (TP) and total dissolved phosphorus (TDP) concentrations were analyzed using the molybdenum blue method (Murphy & Riley, 1962) as soluble reactive phosphorus (SRP), after digestion with a mixture of potassium persulphate and boric acid at 120 °C for 30 min. Total nitrogen (TN) and total dissolved nitrogen (TDN) were analyzed by high-temperature catalytic oxidation (Álvarez-Salgado and Miller 1998) using a total nitrogen analyzer (TNM-1, Shimadzu TOC-V CSH). Samples for dissolved organic carbon (DOC) were filtered through precombusted GF/F filters, transferred in a combusted (>2 h at 500 °C) flask, acidified with phosphoric acid (final pH < 2) and stored in the dark at 4 °C until analysis. DOC concentration was measured by high-temperature catalytic oxidation in a Shimadzu total organic carbon (TOC) analyzer (Model TOC-V CSH). Samples were purged with phosphoric acid for 20 min to eliminate any dissolved inorganic carbon. The TOC-V CSH instrument was calibrated using a four-point standard curve of potassium nitrate and potassium hydrogen phthalate for TN and DOC concentration, respectively. Three to five injections were analyzed for each sample.

Bacterial taxonomic characterization

Collection of particle-attached and free-living bacterial assemblages

For DNA characterization in Fuente de Piedra lake, DNA samples collected in two sampling stations were combined in one single sample. In consequence, DNA was extracted from a total of 67 samples across the study period. In the laboratory, the samples for analysis of the bacterial community were sequentially filtered through 3 µm and 0.2 µm filters. The fraction 0.2-3 µm was named free-living and the fraction > 3 µm was named particle-attached bacterial assemblages (i.e., discriminating between two lifestyle). Filters were covered with TES lysis buffer (40mM EDTA; 50mM Tris pH 8.3; 0.75M sucrose) and kept frozen at -80°C until ready for analysis.

Extraction of DNA

For DNA extraction, cells were resuspended from thawed filter in a TES lysis buffer and then, centrifuged (5 min at 13000 rpm). DNA were extracted from the pellets using FavorPrep™ Genomic DNA Mini Kit, following the manufacturer's instructions. The extracted DNA was separated by 0.7 % agarose gel electrophoresis with in 5X TBE (45mM Tris; 44 mM boric acid; 1mM EDTA) buffer stained with ethidium bromide at final concentration of 0.5 µg ml⁻¹. The absorbance ratio 260/280 nm was used to confirm the quality of the extracted DNA using a Nanodrop 2000 Spectrophotometer (Thermo scientific).

Construction of 16S libraries and Illumina MiSeq sequencing

Paired-end 16S Illumina sequencing libraries were constructed using a two-steps PCR amplicon approach. A first PCR was carried out using universal primers 515F and 786R with overhang partial Illumina adapters targeting the hypervariable V4 region of 16S rRNA gen. The PCR amplification were prepared using 20 µl of reagent mix containing 3 pmol of each primer (Sigma), 10 µl of Phusion flash polymerase high-fidelity PCR Master mix (Thermo Scientific), 10 ng extrated DNA and 3 µl grade water. The PCR conditions were as follows: an initial 98 °C denaturation step for 60 s, followed by 25 cycles of 98 °C for 1 s, 53 °C for 5 s, and 72 °C for 5 s and a final elongation step at 72 °C for 60 s. Then, PCR products were purification by GenElute TMPCR Clean-Up (Sigma) commercial Kit, according to the manufactures' recommendation. PCR amplicons were used to confirm successful amplification using (0.7 % w/v) agarose gel electrophoresis in 5x TBE (45mM Tris; 44 mM borate acid; 1mM EDTA) containing 0.5 µg ml⁻¹ ethidium bromide. Next, second PCR was carried out with barcoded primers by Nextera XT DNA Library Preparation Kit (Illumina), with a unique combination of barcoded primer for each sample. PCR was performed with addition of 14 ng purified DNA, 2 µl of each of barcode primers, 10 µl of phusion flash polymerase PCR Master mix and 3.2 µl grade water. This second PCR followed the same conditions as the previous 16S rRNA PCR, but carried out only in 9 cycles. After, a new purification step using a commercial kit was repeated. DNA quantification was performed employing a NanoDrop 2000 Spectrophotometer (Thermo Scientific) to achieve the normalization library concentrations. Then the 67 samples were standardized at the same final DNA concentration, pooled and multiplexed in a single tube. Finally, this pool mixture was diluted with grade water at adequate final concentration (30 µg µl⁻¹) for sequencing using the MiSeq Illumina platform. Sequencing was carried out at UGR facilities (Granada, Spain) using MiSeq Reagent Kit Preparation Guide (Caporaso et al 2012) with a paired-end read of 2x250 cycles. The insert size if the library was 252 bp with a full-length sequence amplicon of approx. 407 bases paired.

Processing and analysis of Illumina sequencing data

All steps involved in this workflow were performed separately for free-living and particle-attached bacterial assemblages to achieve a greater resolution of the bacterial community composition (Rösel *et al.* 2012). Prior data analysis, the quality of the demultiplexed sequences was assessed using FastQC (<http://www.bioinformatics.babraham.ac.uk/projects/fastqc/>), and later processed using QIIME 1.9.0 (Caporaso *et al.* 2010) and MOTHUR 1.34.3 (Schloss *et al.*, 2009) software. Briefly, paired-end reads were joined using default parameters of `join_paired_ends.py` script in QIIME. Then, we performed a quality filtering of sequences using `multiple_split_libraries.py`, with the following parameters: minimal high-quality read length = 75%, phred quality threshold = 19, maximum of consecutive low-quality calls = 3, maximum of ambiguous calls allowed = 0. PCR primer sequences were trimmed using the `trim.seqs` script within the Mothur package.

Once the sequences were quality filtered and primers trimmed, the sequences were clustered into Operational Taxonomic Units (OTU) based on the de novo OTU picking algorithm. It was performed by `pick_de_novo.py` workflow script with UCLUST (Edgar, 2010) at 99% sequence similarity. The most abundant sequence for each OTU was chosen as the OTU representative sequence using `pick_rep_set.py` script, and classified taxonomically by `assign_taxonomy.py` script, using UCLUST classifier within QIIME package, on based on the Greengenes 16S rRNA gene database (13_8 version; <http://greengenes.secondgenome.com>). Next, from the resulting OTU table, non-specific sequences (i.e. Archaea, Chloroplast and Mitochondria) were filtered out, using `filter_taxa_from_otu_table.py` QIIME script. To control for the sampling effort, datasets were standardized through rarefaction analyses at different sequencing depth (to be precise at 200, 500 and then, from 1,000 to 10,000 sequences per sample at intervals of 1,000) and 100 number of iterations. This step was carried out in QIIME for each OTU table using the script `multiple_rarefy.py`. After the normalization step, a filtering step from OTU table, was carried out to discarded all singletons (reads detected only once, which might be sequencing artifacts), using `filter_otus_from_otu_table.py` QIIME script.

Bacterial alpha diversity was determined within the QIIME pipeline at above-mentioned sequencing depths by means of the `alpha_diversity.py` script, including as metrics the number of observed OTUs richness and the Shannon diversity (Shannon - Wiener index). We found that at 2,000 sequences per sample, Shannon diversity for both free-living and particle-attached bacterial assemblages started to plateau suggesting that saturation in sequencing was achieved (Figure 4.2 b and c).

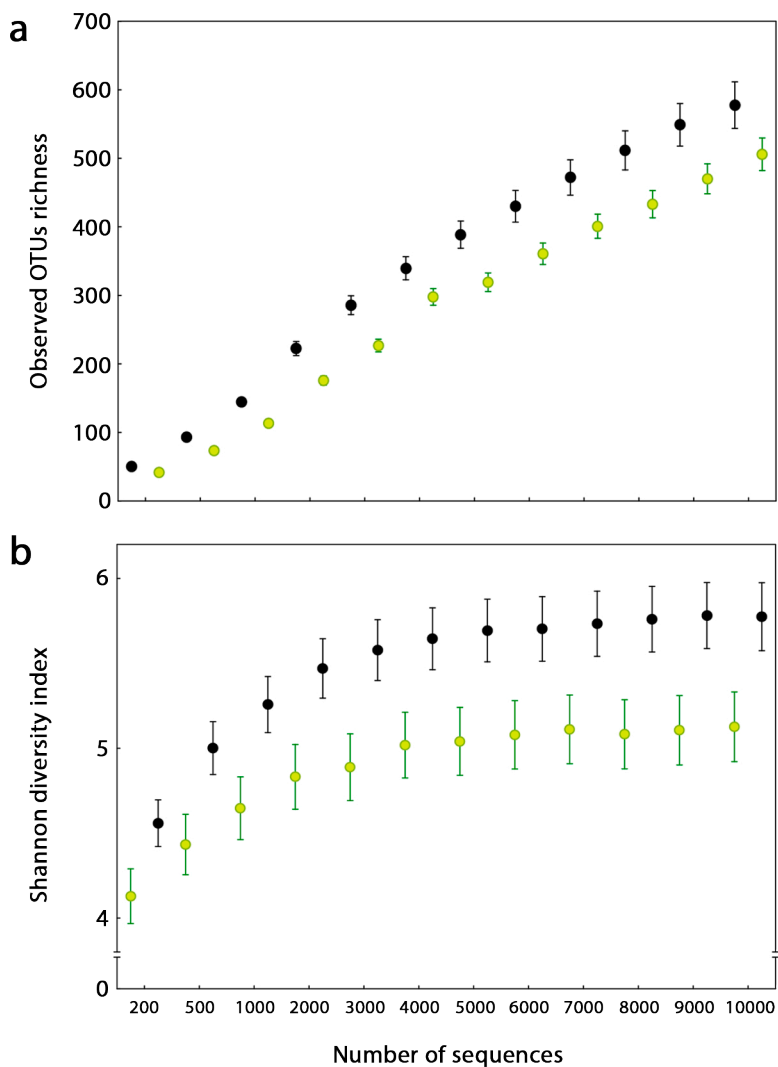


Figure 4.2. Effect of sequencing depth on observed OTUs richness (a) and the Shannon diversity index (b) trend for free-living (green circles) and particle-attached bacterial (black circles) assemblages in Fuente de Piedra Lake. The circles correspond to observed OTUs richness and Shannon diversity index average and their standard errors, respectively.

Finally, to check the differences in community composition over time we used the Bray-Curtis dissimilarity matrix (Beals, 1984) at 2,000 sequencing depth and the script `beta_diversity.py` for temporal beta diversity (Shimadzu *et al.* 2015). Simultaneously, we applied to data a second analysis at 5,000 sequences per sample, to check for effects of rarefaction depth.

Statistical analysis

Before fitting statistical models, we checked any collinearity for predictor variables using “vifstep” function provided by usdm-package (Naimi and Araújo 2016) in R (<http://www.R-project.org>). This procedure excludes the strongly correlated variables through a stepwise procedure. In our case, salinity was the only variable that had collinearity problem, resulting in its exclusion for multivariate analysis. In addition, the data were log-transformed to improve the fit to a normal distribution and to avoid heteroscedasticity.

Differences in the alpha diversity indices, including OTUs richness and Shannon diversity, between free-living and particle-attached bacterial assemblages, were analyzed using one-way ANOVA analysis of variance and statistical significance was assumed at < 0.05 . One-way ANOVA for unequal data sets was used to assess the differences in the OTUs and SW index for two size bacterial fractions between wet and dry hydrological period.

To identify the main environmental controlling factors of alpha bacterial diversity in this study lake, we performed simple regression analysis was carried out to assess the relationships between the OTUs richness and Shannon diversity as dependent variables and salinity, flamingo abundance and area lake as predictors variables. To explore in more detail controlling factors of bacterial community, we performed a multiple regression analysis to assess the interaction of predictors variables. OTUs richness and Shannon diversity index were treated as dependent variables and area lake, flamingo abundance as predictors variables, excluding salinity to avoid effects of collinearity.

Differences in the temporal beta diversity between free-living and particle-attached bacterial assemblages, were analyzed using one-way ANOVA analysis of variance was performed with statistical significance assumed at $p < 0.05$. In particular, we used as dataset in this analysis, the beta diversity measures previously calculated against the first-time point, taken directly from Bray-Curtis dissimilarity matrix. One-way ANOVA for unequal data sets was used to assess the differences in the temporal beta diversity for two size bacterial fractions between wet and dry hydrological periods. These statistical analyses were carried out using Statistica (v.7.0) software.

Finally, PERMANOVA was used to determine the correlation between the environmental controlling factors (such as salinity, area lake and flamingo abundance) and bacterial community composition over study period, using “Adonis” and “Adonis2” functions, include in the “Vegan” package (Oksanen *et al.* 2016) in R. Permutational multivariate analysis of variance were based on Bray-Curtis dissimilarity matrix. In this analysis, we used full dataset of Bray-Curtis dissimilarity matrix (as measured of temporal beta diversity (Shimadzu *et al.* 2015)

as response and covariates (salinity, lake area and flamingo abundance) as linear predictors. Contribution of each predictor variables evaluated individually using Adonis function. To explore in more detail the influence predictor variables on bacterial community composition, we assess the interaction of lake area and flamingo abundance using Adonis2 function, setting by = "margin" argument for independent variables included in the statistical model (Oksanen *et al.* 2016), excluding salinity to avoid effects of collinearity. Permutation test was based on subsets of 999 permutations for estimating statistical significance (p-values).

To assess sampling effort, all the statistical analyses were simultaneously performed using normalized dataset at 2,000 and 5,000 rarefaction depths.

4.3. RESULTS

Diversity of free-living and particle-attached bacteria

Based on metataxonomic analysis of bacterial community, we identified the OTUs present in free-living and particle-attached bacterial assemblages in each sample. Pre-processing of data sequences resulted in a total of 4,598,032 and 2,984,969 high quality sequences for 33 free-living bacteria samples and 34 particle-attached bacteria samples, respectively (Table 4.2 a and b). Total number of sequences per sample varied noticeably in both free-living and particle-attached bacteria fraction (Table 4.2 a and b), which were normalized at 2,000 sequencing depth. This sequencing depth was sufficient to describe the true species richness in the study lake, getting a balance between costs (i.e. sample losts) and required sequencing depth to generate valid results. Consequently, one sample from particle-attached bacteria dataset was excluded because the total number of sequences was below the threshold (i.e. minimum of 2000 sequences per sample; Table 4.2 b). In total, 66 samples were analyzed to calculate alpha and temporal beta diversity.

Table 4.2. Total number of sequences (not normalized), Observed OTUs richness and Shannon diversity index and temporal beta diversity (calculated against the first-time point) at 2000 sequencing depth and 99% sequence similarity for (a) free-living and (b) particle-attached bacterial assemblages for each sample in the Fuente de Piedra lake. The wet hydrological years shaded in blue and the dry hydrological year in cream.

a Free-living bacterial samples (0.2 μ m)					
After normalization at 2000 seqs/sample					
Date (dd-mm-yy)	Total number sequences post-processing	Observed OTUs richness	Shannon diversity index	Temporal beta diversity	
24-08-10	204922	225	5.59	0.00	
06-09-10	373171	267	5.99	0.36	
15-09-10	125740	164	4.75	0.59	
21-09-10	114597	173	4.83	0.55	
27-09-10	620677	244	6.16	0.47	
18-10-10	23994	159	4.42	0.60	
22-02-11	64911	196	5.13	0.53	
01-03-11	144480	177	5.59	0.71	
15-03-11	106218	194	6.08	0.74	
03-05-11	7899	220	6.18	0.82	
31-05-11	12703	186	5.96	0.80	
14-06-11	4347	196	5.58	0.65	
28-06-11	3570	117	2.75	0.78	
06-08-11	2917	205	5.99	0.87	
16-08-11	36581	135	3.59	0.91	
06-09-11	55602	199	5.55	0.80	
20-09-11	108152	197	5.67	0.69	
05-10-11	138591	143	3.59	0.84	
18-10-11	125330	140	4.10	0.84	
02-11-11	129255	118	2.78	0.90	
16-11-11	120716	135	3.32	0.89	
30-11-11	269718	151	4.02	0.91	
13-12-11	210246	155	4.69	0.89	
24-01-12	147441	200	5.62	0.63	
14-02-12	72935	222	5.49	0.66	
13-03-12	331707	115	2.30	0.93	
10-04-12	49852	184	4.59	0.57	
26-04-12	55919	141	4.17	0.75	
08-05-12	50587	135	3.90	0.84	
23-05-12	97327	116	4.44	0.77	
16-10-12	316576	202	6.09	0.80	
13-11-12	285872	171	4.96	0.84	
24-08-10	185479	218	5.59	0.73	

b <i>Particle-attached bacterial samples (3µm)</i>				
After normalization at 2000 seqs/sample				
Date (dd-mm-yy)	Total number sequences post-processing	Observed OTUs richness	Shannon diversity index	Temporal beta diversity
27-07-10	99415	154	3.77	0.00
07-08-10	30339	181	5.42	0.83
24-08-10	213813	260	5.32	0.92
06-09-10	90902	313	6.71	0.92
15-09-10	131 ^a	-	-	-
21-09-10	16649	190	5.94	0.79
27-09-10	243002	278	5.77	0.90
18-10-10	98438	191	5.52	0.88
22-02-11	124429	268	6.62	0.93
01-03-11	73519	256	6.09	0.89
15-03-11	36603	273	6.48	0.90
03-05-11	90573	349	7.15	0.93
31-05-11	29047	241	5.67	0.92
14-06-11	9942	278	6.08	0.92
28-06-11	26142	256	6.23	0.92
06-08-11	10927	154	4.96	0.88
16-08-11	16425	266	6.58	0.91
06-09-11	16509	271	6.35	0.89
20-09-11	5890	269	6.31	0.87
05-10-11	38401	195	5.27	0.86
18-10-11	20015	217	5.76	0.87
02-11-11	32387	208	4.76	0.90
16-11-11	157643	222	4.73	0.90
30-11-11	45352	143	3.90	0.93
13-12-11	96022	70	4.66	0.88
24-01-12	135757	99	2.49	0.95
14-02-12	45517	190	4.72	0.87
13-03-12	222987	225	4.89	0.89
10-04-12	118152	239	5.04	0.86
26-04-12	86344	213	4.61	0.88
08-05-12	53076	167	4.45	0.93
23-05-12	168704	197	5.44	0.84
16-10-12	123026	254	6.60	0.92
13-11-12	281167	252	6.20	0.92

After resampling the initial data and once the singletons were discarded, OTUs richness and Shannon-Wiener diversity index were calculated for each sample of free-living and particle-attached bacterial assemblages (Table 4.2 a and b). OTUs richness detected per sample ranged from 115 to 267 for free-living bacterial assemblage and from 70 to 349 for particle-attached bacterial assemblage (Figure 4.3 and Table 4.2 a and b). The Shannon diversity ranged from 2.29 to 6.18 for free-living bacteria and from 2.49 to 7.15 for particle attached-bacteria (Figure 4.4 and Table 4.2 a and b). One-way ANOVA test showed significant differences between the two size fractions for both OTUs richness ($F = 12.5$, $p < 0.001$) and Shannon diversity ($F = 5.7$, $p < 0.05$). Particle-attached bacteria showed a higher alpha diversity (in terms of OTUs richness and Shannon diversity) than the free-living fraction (Figure 4.3 and 4.4; Table 4.2 a and b).

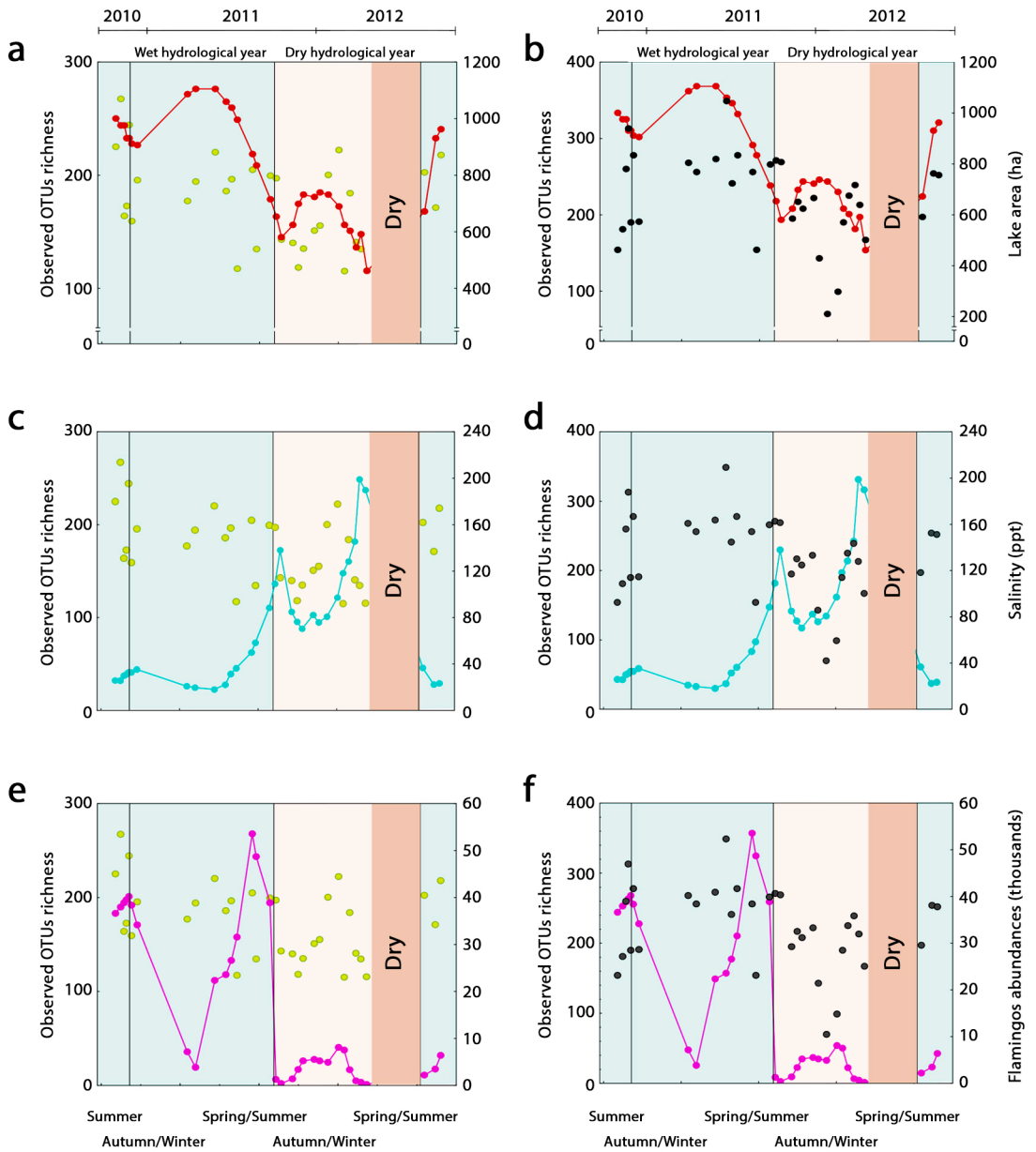


Figure 4.3. Dynamics of the bacterial operational taxonomic units during the two hydrological periods. Changes in observed OTUs richness in living-free bacteria (a, c and e; green dots) and in particle-attached bacteria (b, d and f; black dots) and the changes in salinity, abundance of flamingos and lake area. Flamingo abundance is shown by the purple line, salinity by the blue-green line and lake area by the red line. The wet period is shaded in blue and the dry period in pale brown. The lake dried out completely during the period shaded in brown.

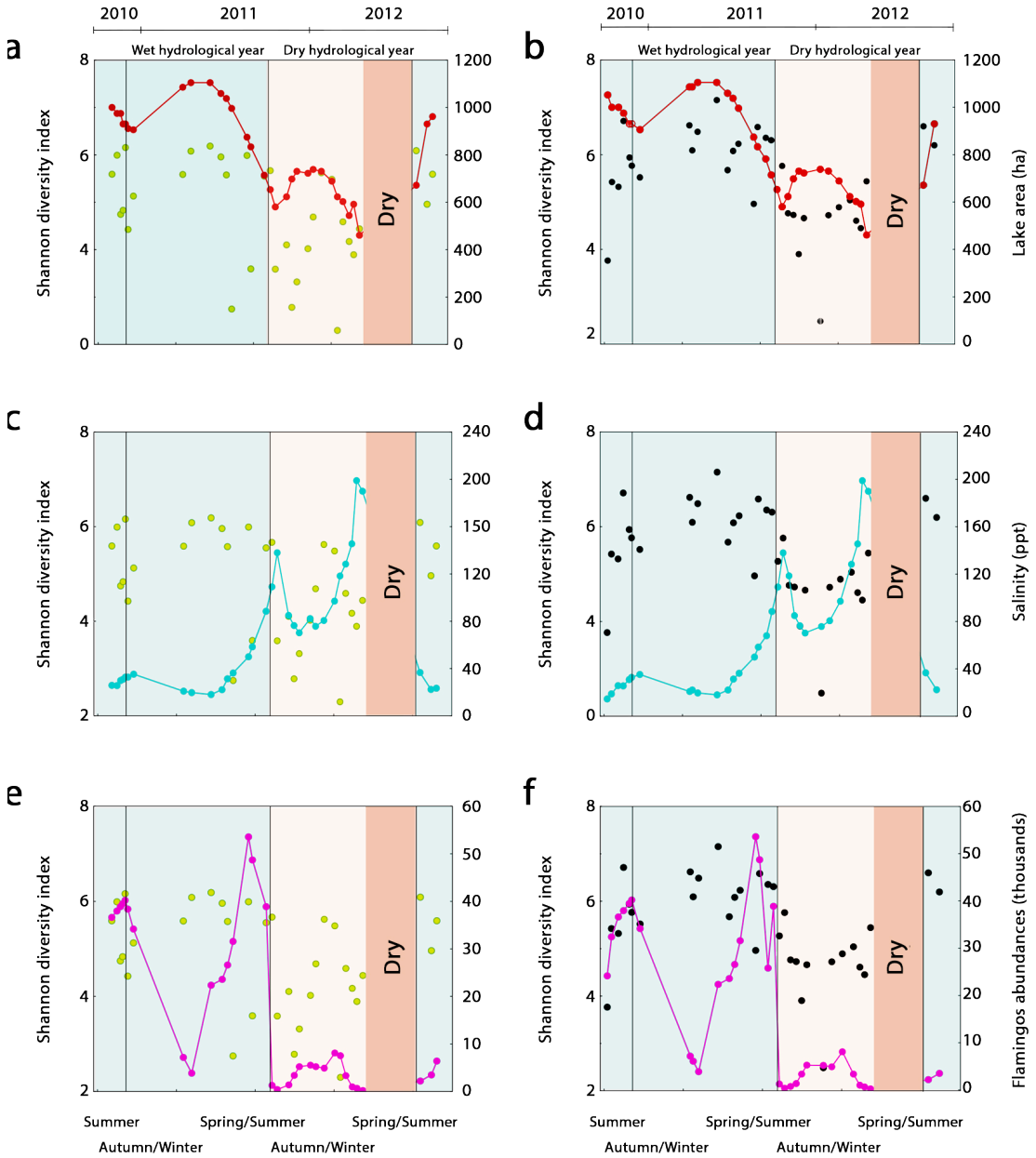


Figure 4.4. Dynamics of bacterial alpha diversity during the two hydrological periods. Changes in Shannon diversity index of living-free bacteria (a, c and e; green dots) and of particle-attached bacteria (b, d and f; black dots) and changes in salinity, abundance of flamingos and lake area. Flamingo abundance is shown by the purple line, salinity by the blue-green line and lake area by the red line. The wet period is shaded in blue and the dry period in pale brown. The lake dried out completely during the period shaded in brown.

Alpha diversity dynamics and environmental controlling factors

Bacterial alpha diversity indices significantly differed between the wet and the dry periods (one-way ANOVA), both for free-living bacteria (OTUs richness, $F = 7.9$, $p < 0.0$; Shannon diversity, $F = 8.6$, $p < 0.01$) and for particle-attached bacteria (OTUs richness, $F = 11.2$, $p < 0.001$; Shannon diversity, $F = 19.6$, $p < 0.001$). Bacterial community changes were concomitant with hydrological differences for each period, with higher OTUs richness and Shannon diversity values during the wet period than during the dry period (Figure 4.3 and Figure 4.4, respectively).

We explored the controlling factors of alpha diversity dynamics of free-living and particle-attached bacteria for the wet and dry hydrological periods. Figure 4.3 and 4.4 showed the changes of OTUs richness and Shannon diversity together with salinity dynamics, flamingo abundance and lake specific area for wet and dry years. The OTUs richness and Shannon diversity for the two bacterial fraction sizes showed synchronous dynamics with lake area during the two hydrological periods (Figure 4.3 a and b; Figure 4.4 a and b). Indeed, changes in OTUs richness and Shannon diversity were positive and significantly correlated with lake area (Figure 4.5 a and b; Table 4.3), except for particle-attached bacterial, where no significant results were obtained for OTUs richness (Figure 4.5 a; Table 4.3). Both OTUs richness and Shannon diversity of free-living bacteria and particle-attached bacteria were inversely related to salinity (Figure 4.5 c and d; Table 4.3).

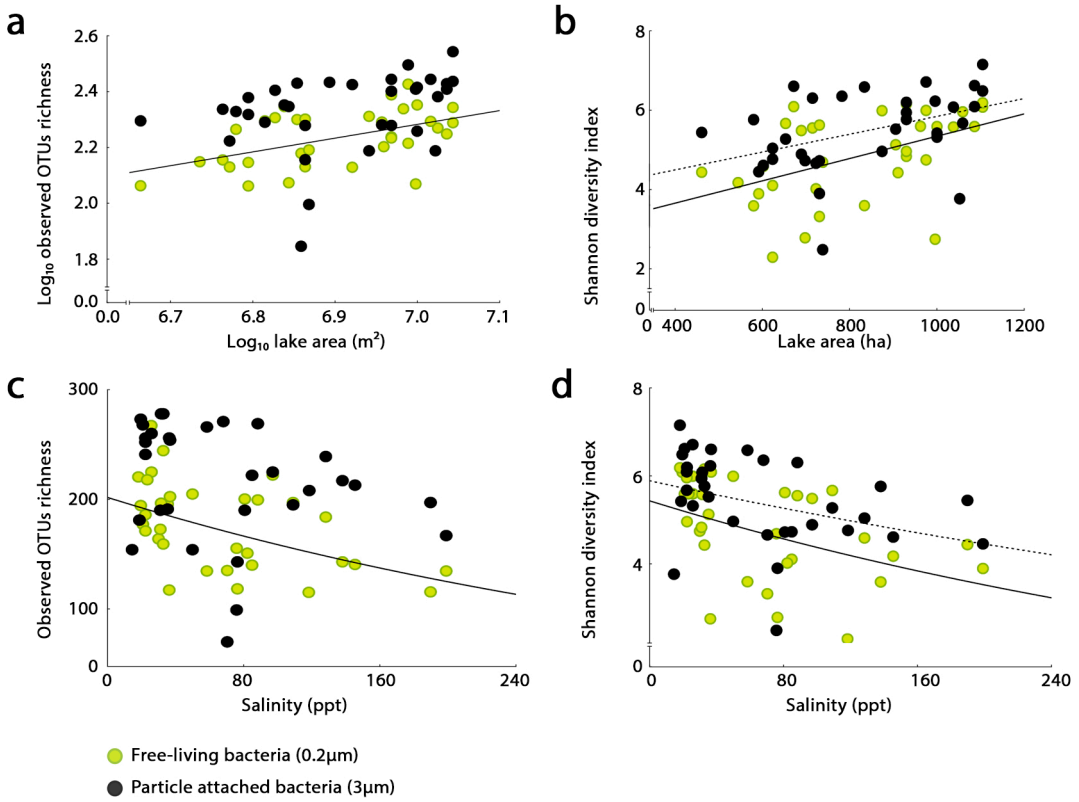


Figure 4.5. Relationships between bacterial OTUs richness and Shannon diversity index and lake area (a, b) and salinity (c, d). Free-living bacteria (green dots, continuous line) and particular-attached bacteria (black dots, discontinuous line).

Table 4.3. Results of the simple regression analyses performed to assess the influence of lake area, salinity and flamingo abundance on observed OTUs richness and Shannon diversity at 2000 rarefaction depth both free-living and attached bacteria community during study period in the Fuente de Piedra lake. Note: observed OTUs richness vs. Lake area (m²) were log transformation.

<i>Alpha diversity</i>						
Bacterial lifestyle	Dep Var	Indep Var	Fit	r ²	p-level	slope
Free-living bacteria (0.2 μm)	Log OTUS	Log Lake area	Linear	0.26	p < 0.01	0.493
	Observed OTUs richness	Salinity	Exp	0.26	p < 0.01	-0.002
		Log Flamingos	Linear	0.19	p < 0.05	25.875
	Shannon diveristy	Lake area	Linear	0.22	p < 0.01	0.002
		Salinity	Exp	0.22	p < 0.01	-0.002
		Log Flamingos	-	-	-	-
Particle attached bacteria (3 μm)	Log OTUS	Log Lake area	-	-	-	-
	Observed OTUs richness	Salinity	-	-	-	-
		Log Flamingos	-	-	-	-
	Shannon diveristy	Lake area	Linear	0.17	p < 0.05	0.002
		Salinity	Exp	0.16	p < 0.001	-0.001
		Log Flamingos	-	-	-	-

In the case of particle-attached bacteria, the Shannon diversity decreased significantly with salinity (Table 4.3). In contrast, the observed OTUs richness and Shannon diversity dynamics for both free-living bacteria and particle-attached bacteria showed no clear synchrony with flamingo abundance (Figure 4.3 e and f; Figure 4.4 e and f) with a significant and positive relationship between OTUs richness and flamingo abundance, but only for free-living bacterial assemblages (Table 4.3). Similar results were obtained for alpha diversity analysis using the normalized database at 5,000 sequencing depth (Table 1 in Annex Chapter 4). To further explore the controlling factors of bacterial community, we performed a multiple regression analysis to assess the influence of lake area and flamingo abundance as predictor variables, excluding salinity due to collinearity with lake area (Table 4.4). The results showed that lake area was the only variable that significantly affected bacterial OTUs richness and diversity index. However, OTUs richness of particle-attached bacteria was not directly affected either by the flamingo abundance or the lake area (Table 4.3 and Table 4.4).

Table 4.4. Results of the multiple regression analyses performed to assess the influence of flamingo abundance and lake area on observed otus richness and Shannon diversity both free-living and attached bacteria community during study period in the Fuente de Piedra lake.

<i>Alpha diversity</i>						
Bacterial lifestyle	Dep Var	Indep Var	r	b	p-level	
Free-living bacteria (0.2 µm)	Log OTUS richness	Log Lake area	0.51	0.49	0.002	
		Log Flamingos	-	-	-	
	Shannon diveristy	Intercept			-1.17	0.268
		Lake area	0.47	0.002	0.005	
		Log Flamingos	-	-	-	
		Intercept			2.531	0.003
Particle attached bacteria (3 µm)	Log OTUS richness	Log Lake area	-	-	-	
		Intercept			-	-
	Shannon diveristy	Lake area	0.42	0.002	0.015	
		Log Flamingos	-	-	-	
		Intercept			3.597	0.00003

Notaion: r, partial correlation coefficient; b, nonstandardized regression coefficient. Free-living bacteria (OTUs richness, n = 33; r² = 0.23; p < 0.01; Shannon div, n = 33; r² = 0.22; p < 0.01) and Attached bacteria (Shannon div, n = 33; r² = 0.17; p < 0.05).

Temporal taxon-specific patterns

A total of 21 and 22 orders were identified from top ten OTUs selected with a relative abundance (normalized) above 2 % for free-living bacteria and particle-attached bacteria, respectively (Figure 4.6 a and b). The four most representative orders were the same for free-living and particle-attached bacterial assemblages: Flavobacteriales, Puniceicoccales, Rhodobacteriales and Bacteroidales; which represented more than 50 % total bacterial community in all samples (Figure 4.6 a and b). However, the proportions of other main orders varied appreciably between free-living and particle-attached bacterial assemblages (Figure 4.6 a and b). Interestingly, we observed a clear difference in the free-living bacterial composition between the wet and the dry periods (Figure 4.6 a), whereas the changes in the composition of the particle-attached bacteria between these two periods was less apparent (Figure 4.6 b). Most sequences were linked to Flavobacteriales order, which showed a strongest preference

for free-living life styles during wet period. However, during the dry period, this order was mostly present in the particle-attached fraction (Figure 4.6 a and b). Puniceicoccales order was the second one in relative abundance and it was more abundant during dry period, particularly as attached to particles (Figure 4.6 b). In addition to the abovementioned orders, Rhodobacterales followed by Bacterioidales were the next most abundant in study lake with similar dynamic for both free-living and particle-attached life styles, which were strongly reduced on dry period (Figure 4.6 a and b). In the free-living fraction, Burkholderiales was the next most abundant order during dry period (Figure 4.6 a), while for particle-attached fraction it was Synnechococcales order during wet period and the Thiotrichales during dry period (Figure 4.6 b).

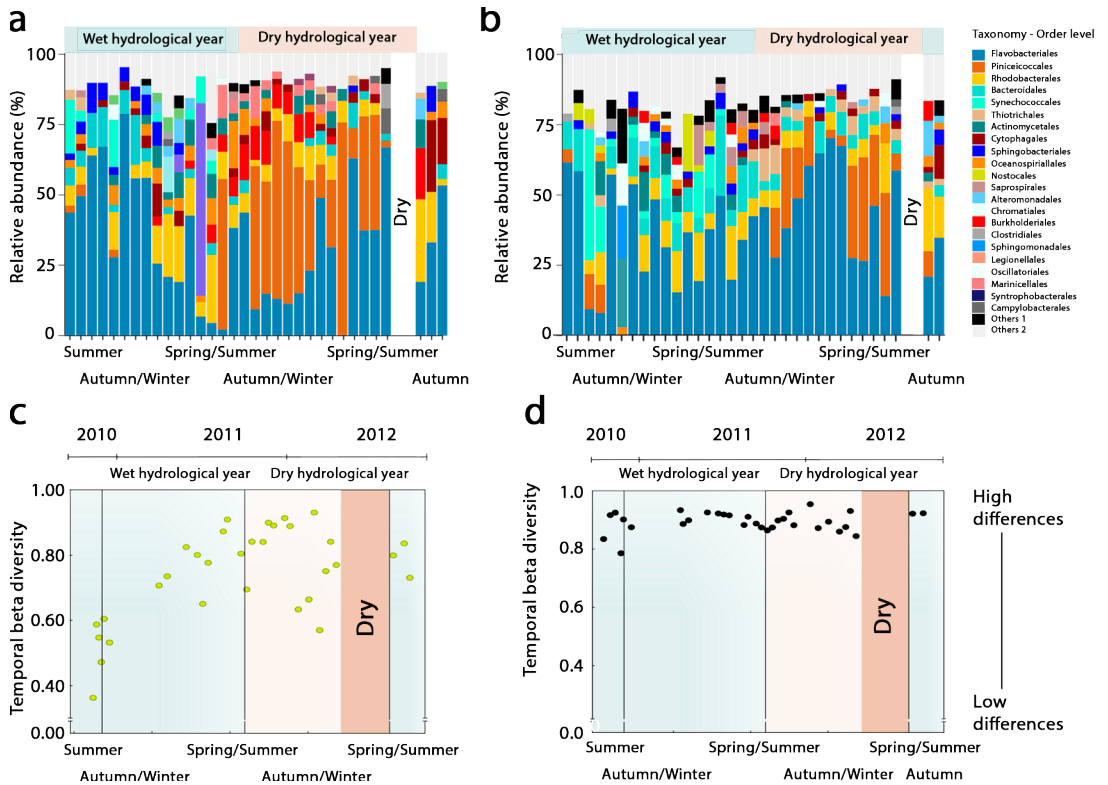


Figure 4.6. Temporal relative contribution of the top ten more abundant OTUs of bacterial community in the Fuente de Piedra lake and changes in temporal beta diversity. The relative abundances of the first ten most abundant OTUs at order level of (a) free-living bacteria and (b) particle-attached bacteria. Note “other OTUs” contribution includes different taxa for each specific sample. Temporal changes in beta diversity for (c) living-free bacteria (green dots) and for (d) particle-attached bacteria (black dots) during the two hydrological periods. The wet period is shaded in blue and the dry year in pale brown. The lake dried out completely during the period shaded in brown.

Temporal-beta diversity controlling factors

Temporal beta diversity values (calculated against the first-time point) ranged from 0.36 to 0.93 for free-living bacteria (Figure 4.6 c; Table 4.2 a) and from 0.78 to 0.95 for particle-attached bacteria (Figure 4.6 d; Table 4.2 b). One-way ANOVA test showed significant differences between the two size fractions for temporal beta diversity ($F = 34.98$, $p < 0.001$). Temporal beta diversity also differed significantly between the wet and the dry periods (one-way ANOVA) for free-living bacteria ($F = 4.9$, $p < 0.05$). In contrast, no significant differences were found between the two periods for particle-attached bacteria ($F = 0.06$, $p = 0.81$). In general, the temporal heterogeneity in particle- attached bacteria showed high beta diversity (usually above 0.8) values constantly along the two periods (Figure 4.6 b and d).

To determine the effects of the major controlling factors (such as salinity, flamingo abundance and lake area) on the changes of the bacterial community composition, we used PERMANOVA analysis. This analysis allowed determine which variables and interaction affect significantly community dissimilarities. Contribution of individual predictor variable was analyzed with Adonis function, whose results revealed that all predictor variables had a significant effect on bacterial community composition, but the best factor predicting community composition was the lake area both free-living and particle-attached bacterial (Table 4.5).

Table 4.5. Results of permutational multivariate analysis of variance (ADONIS2) of salinity and bacterial composition (Bray – Curtis distance metric) at 2000 rarefaction depth during study period in Fuente de Piedra lake.

<i>Temporal beta diversity</i>					
Bacterial lifestyle	Indep Var	Df	R ² (Adonis)	F.Model	Pr(<F) ^{a,b} .
Free-living bacteria (0.2 μm)	Log Lake area	1	0.20	8.20	p < 0.01
	Salinity	1	0.18	6.69	p < 0.01
	Log Flamingos	1	0.11	3.97	p < 0.01
Particle attached bacteria (3 μm)	Log Lake area	1	0.14	5.20	p < 0.01
	Salinity	1	0.13	4.55	p < 0.01
	Log Flamingos	1	0.11	3.85	p < 0.01

Due to collinearity, contribution of salinity was excluded from analysis and the interaction of lake area and flamingo abundance was analyzed with Adonis 2 function, whose results showed that only lake area had a significant effect with an elevated contribution on both free-living bacteria and particle-attached bacteria (Table 4.6). The results obtained for temporal beta diversity analysis using normalized dataset at 5,000 sequencing depth were similar to those obtained at 2,000 sequencing depth (Table 2 in Annex Chapter 4).

Table 4.6. Results of permutational multivariate analysis of variance (ADONIS2 function) of association between flamingo abundance and area lake and bacterial composition (Bray – Curtis distance metric) at 2000 rarefaction depth during study period in Fuente de Piedra lake.

<i>Temporal beta diversity</i>					
Bacterial lifestyle	Indep Var	Df	R ² (Adonis2)	F.Model	Pr(<F) ^{a,b.}
Free-living bacteria (0.2 μm)	Log Lake area	1	0.14	5.64	p < 0.01
	Log Flamingos	-	-	-	-
Particle attached bacteria (3 μm)	Log Lake area Salinity	1	0.06	2.22	p < 0.05
	Log Flamingos	-	-	-	-

4.4. DISCUSSION

Lake area reduction by drought led to a significant decrease in richness and diversity of both free-living bacteria and particle-attached bacteria including with a change in community composition. The negative hydrological budget increased salinity and to a lesser extent of flamingo abundance. Particle-attached bacteria had higher values of OTUs richness and Shannon diversity than the free-living counterpart. These findings point out the relevant contribution of particle-attached bacteria to ecosystem alpha diversity. This result is accordance with previous studies in marine bacteria (Zhang *et al.* 2007), the Baltic Sea (Rieck *et al.* 2015), the Southern Ocean (Milici *et al.* 2017), the Mediterranean Sea (Crespo *et al.* 2013), but in contrast with results in deep lakes (Rösel and Grossart 2012).

We also found significant differences between the wet and the dry hydrological periods with respect to bacterial alpha diversity indices in both bacterial fractions in Fuente de Piedra lake. We observed lower OTUs richness and Shannon diversity during the dry period

than during the wet period (Figure 4.3 and Figure 4.4)., Different mechanisms could explain these community changes depending on the hydrological (wet vs. dry) periods. The lake area decreased considerably during the dry period, with a concomitant increase in salinity by evapoconcentration. Surprisingly, our results showed that lake area was the main factor involved in the control of the bacterial community structure with a negative effect on OTUs richness and diversity by shrinking lake area (Figure 4.5 a and b; Table 4.3). However, according to the literature, salinity usually is a major factor controlling microbial community structure decreasing richness as salinity increases (Casamayor *et al.* 2002; Benlloch *et al.* 2002; Oren *et al.* 2002, Zhang *et al.*, 2006). Our results support a decline of OTUs richness and Shannon diversity of bacterial community with the increase of salinity (Figure 4.5 c and d; Table 4.3), but secondary as a consequence of evaporation and water level reduction.

This positive and significant relationship between OTUs richness and lake area for free-living bacteria (Figure 4.5. and Table 4.3) is consistent with the universal taxa-area relationship (TAR) established in ecology (MacArthur and Wilson, 1967). In most occasions, TAR has been governed by a power law ($S = CA^z$; Arrhenius, 1921), where A is the lake area (in square meters), S is the number of species (OTUs richness), C is a constant dependent on the taxon, biogeographical region, and population density (the intercept in the log-transformed function), and z is the rate at which new OTUs are included as the area is increasing (i.e. the slope of the log-transformed function). By performing log-transformed linear regression, we obtained a taxa-area slope coefficient of 0.49 for free-living bacteria (Table 4.3). Remarkably, this TAR slope was much higher than expected (Figure 4.7; Table 4.7;) for a contiguous habitat (Rosenzweig 1995) mostly considering the high dispersal capacity of bacteria (Finlay 2002, Bell 2001, Prosser *et al.* 2007) and it was within the range of those reported for macroorganisms (from ~0.1 to ~0.7) Drakare *et al.* 2006, Storch *et al.* 2012).

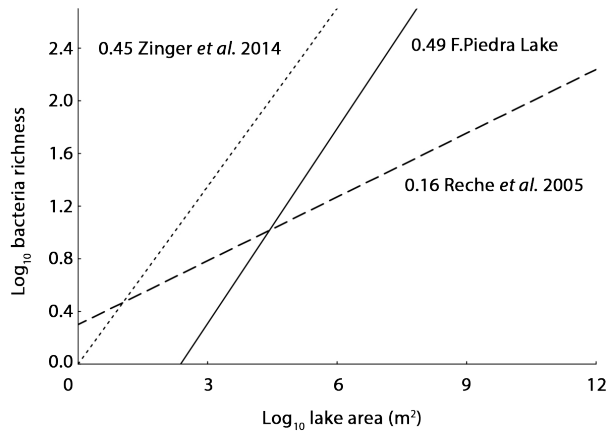


Figure 4.7. Taxa-area relationships (TAR) for free-living bacteria in several aquatic ecosystems. Comparison of the relationship between log-transformed data of bacterial richness against ecosystem size (measured in squared meters) in Fuente de Piedra Lake, freshwater lakes (Reche et al. 2005) and seawater (Zinger et al. 2014). Note that the numbers on the lines indicate the slope values.

In this study, TAR slope was higher than those ones found in previous work for microorganisms in islands habitats (Figure 4.7; Table 4.7), such as lake bacteria (Reche et al. 2005), water-filled tree holes bacteria (Bell et al. 2005) or metal-cutting fluid sump bacteria (Van de Gast et al. 2005) and similar to the slopes found for contiguous habitats in marine environments (Zinger et al. 2014) and soil tropical forest (Noguez et al. 2005).

Table 4.7. Slope-values of bacterial taxa- area relationship previously describe for different ecosystems types (Island vs. contiguous), using different molecular approach for characterize bacterial diversity (DNA fingerprint and metabarcoding). Note: Slope value was estimated with distance-decay and power law equations according to the particular study.

<i>Model type</i>	<i>Taxa-area relationship (slope-value)</i>	<i>Taxa-area relationship (distance-decay vs. power-law)</i>	<i>Molecular approach</i>	<i>Reference</i>
Island	0.16	Power-law	Fingerprint (DGGE)	Reche et al. 2005
Island	0.26	Power-law	Fingerprint (DGGE)	Bell et al. 2005
Island	0.24-0.29	Power-law	Fingerprint (DGGE)	Van Gast et al. 2005
Contiguous	0.04	Distance-decay	Sequencing (0.99% OTU)	Horner et al. 2004
Contiguous	0.009	Distance-decay	Fingerprint (T_RFLP)	Barreto et al. 2014
Contiguous	0.42 and 0.47	Power-law	Fingerprint (T_RFLP)	Noguez et al. 2005
Contiguous	ca. 0.45	Power-law	Sequencing (454)	Zinger et al. 2014
Contiguous	0.49	Power-law	Sequencing Miseg (0.99% OTU)	This study

This finding contradicts previous studies reporting higher TAR slope values in island-like habitats compared with contiguous ones (Rosenzweig, 1995; Prosser *et al.* 2007), which could be partly explained by methodological aspects. Different molecular techniques can have different resolution to determine bacterial community diversity. Although high, the TAR slope value that we found was within the expected range for meta-barcoding techniques and not for a limited resolution such as fingerprinting techniques (Angel *et al.* 2010; Ranjard *et al.* 2013). In fact, previous studies have revealed that both molecular techniques verified a significant soil bacterial TAR, but meta-barcoding method provided a higher and accurate estimation of TAR slope value, improving bacterial taxa-area relationship (Terrat *et al.* 2015). Another aspect to consider is the use TAR slope derived from distance-decay relationship, as formalized by Harte *et al.* (1999), but the validity of this approach has been highly questioned (Woodcock *et al.* 2006; Morlon *et al.* 2008; Jobe 2008; McGlinn and Hurlbert 2012), which could be underestimate TAR slope values (Prosser *et al.* 2007, Zinger *et al.* 2014). Our study supports the classic power law method for estimating TAR slope, which is

considered to be the best fit (Connor & McCoy 1979; Dengler 2009) and therefore is commonly used (Rosenzweig 1995; Dengler 2009), especially in microbial ecology (Prosser *et al.* 2007). In addition, the sequencing depth can have an effect on TAR slope values, which is a methodological issue that needed to be considered. We demonstrated here that bacterial TAR slope was weakly affected by the sequencing depth used (Figure 4.8) and we suggested that it was, after a threshold, independent of the number of sequences considered, as it was also described by Zinger *et al.* (2014). Thus, our data indicated that the integration of massive sequencing technologies reduces substantially the limitations in sequencing depth in agreement with previous studies (Zinger *et al.*, 2014; Terrat *et al.* 2015).

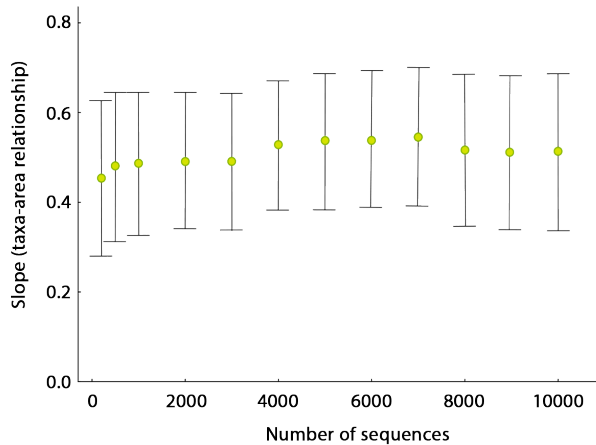


Figure 4.8. Effect of sequencing depth on taxa-area slope for free-living bacterial assemblages in Fuente de Piedra Lake.

Overall, the decline in OTUs richness and Shannon diversity as a consequence of the reduction in lake area due to drought was very consistent, emphasizing the importance of ecosystem size in endorheic, terminal lakes. Droughts reduce lake area in endorheic basins promoting their reduction in size (Messenger *et al.* 2016; Wurtsbaugh *et al.* 2017; Wang *et al.* 2018) and subsequent salinization (Herbert *et al.* 2015). Then, we have explored if concomitant effects of extreme droughts, such as high salt contents and low dissolved oxygen levels can affect bacterial community composition and life (free vs. particle-attached) style.

Our methodological procedure allowed us to distinguish between bacterial lifestyles and to achieve a greater resolution of the bacterial community composition (Rösel *et al.* 2012). However, it is important to consider that free-living and particle-associated bacterial assemblages should not be observed as unconnected entities, but rather as networking assemblages (Riemann-Winding, 2001). Previous works found general differences in com-

munity composition between two bacterial fractions linked to a high exchange between free-living and particle-attached bacteria assemblages (Hollibaugh *et al.* 2000; Ghiglione *et al.* 2007), presumably in response to environmental stress (Milici *et al.* 2017, Poli, *et al.* 2010).

We found that *Flavobacteriales* order, belonging to *Bacteroidetes* phylum, was sharply over-represented on particles during the dry period (Figure 4.6 a and b); This could be partly explained by the fact that they shifted from free-living to particle attached lifestyles to endure in an intensely reduced lake area with high salt concentrations that can eventually reach up saturation. It was not the case of *Bacteroidales* order, also within *Bacteroidetes* phylum, which was present in a higher proportion of OTUs in the wet period regardless of life style (Figure 6 a and b), suggesting a low capacity to cope droughts. *Bacteroidetes* phylum was the dominant in the study lake, which is consistent with previous observations in saline systems, such as solar salterns (Antón *et al.*, 2000, 2002), soda lakes (Vavourakis *et al.* 2007) or athalassohaline lakes (Mesbah *et al.* 2007, Jjiang *et al.* 2006; 2007). This can be explained through the adaptations of halotolerant and aerobic heterotrophs to light conditions and low dissolved oxygen level at high salts concentration (Vavourakis *et al.* 2007, Mesbah *et al.* 2007).

In the case of *Puniceicoccales* order, belonging to *Verrumicrobia* phylum, both bacterial fractions were significantly higher during the dry period than the wet period (Figure 6 a and b), indicating an extreme tolerance to droughts suggesting that they could be favored by high salinity (Choo *et al.*, 2007). The opposite trend was found for *Rhodobacteriales* order, within *Alphaproteobacteria* class, predominant bacteria in saline environments (Bouvier and Del Giorgio 2002; Cottrell and Kirchman 2005). This order was over-represented in wet period in both size fractions (Figure 6 a and b), suggesting that there was no exchange between both free-living and particle-attached life stages. Hence, moderate drought and wet conditions with higher availability of oxygen at low salt concentrations seem to be of great importance for this order, likely linked to genus that contains strictly aerobic, heterotrophic and moderately halotolerant bacteria (Pujalte *et al.* 2014). Even so, bacteria often dominant in freshwater environments were also found in the study lake, in particular *Burkholderiales* order, belonging to the class *Betaproteobacteria* (Newton *et al.* 2011; Staley *et al.* 2015). Generally, *Betaproteobacteria* decrease with increasing salinity (Demergasso *et al.* 2004, Herlemann *et al.* 2011), a finding also observed in marine habitats for *Burkholderiales* order (Aguirre *et al.* 2017). In contrast, our data showed that free-living *Burkholderiales* was well represented in the dry period (Figure 4.6 a and b), suggesting that some groups from this taxon, particularly those with free-living life style, might have a high tolerance to salinity. This is in agreement with the findings of other authors (Pumirat *et al.* 2010). In addition, many representatives are subject to microaerophilic lifestyle, growing well on low oxygen concentration (Garrity *et al.* 2005, Rosenberg *et al.* 2014).

In the *Cyanobacteria* phylum, we found a high proportion of OTUs belonging to *Synnechococcales* order, which are well known as halotolerant bacteria (Rosales *et al.* 2005). As general trend, *Cyanobacteria* are able to adapt to a wide salinity range from freshwater up to salinity levels around 100 ppt, decreasing beyond this concentration (Pedrós-Alió *et al.* 2000a). In agreement with this, our data showed that *Synnechococcales* was well represented during the wet year period (Figure 6 a and b), when salinity was below 100 ppt and was enriched with taxa of particle-attached life style. It is possible the stimulation of polysaccharides synthesis by *Cyanobacteria* as physical barrier against high-salinity stress (Brüll *et al.*, 2000) or under high ultraviolet light conditions (Callieri *et al.* 2011).

Other dominant order in the particle fraction was *Thiotrichales* that, unlike *Synnechococcales*, was present in a higher proportion under dry period (Figure 6 a and b). Many representatives are well known as large sulfur bacteria (Schulz *et al.* 1999) and though many of them show a phobic reaction even at low oxygen concentrations (Huettel *et al.* 1996), recent research has specified that they can survive under microaerophilic conditions (Schulz *et al.* 2002). Another distinctive feature of this order is its ability to hold together in aggregates covered by mucus (Salman *et al.* 2011). Our data were consistent with these observations in *Thiotrichales* order indicating that it can survive under oxygen limiting conditions during dry period grouped by a common mucus protective layer. Interestingly, there was a high proportion of OTUs belonging to *Enterobacteriaceae* order in several water samples collected, particularly in the summer of the wet period (Figure 4.6 a), coinciding with a peak of flamingo population due to massive aggregation and the establishment of an important breeding colony (>50,000 flamingos). This order is dominant in animal digestive tracts and their manifestation in natural waters could be related to fecal inputs (Benton *et al.* 1983; Green *et al.* 2011). However, our analyses indicated that the flamingo abundance played a secondary role determining diversity and composition of bacterial community in the study lake (Table 4.4).

Bacterial community was extremely responsive to environmental fluctuations, changing its composition over time (Figure 6 a and b). This fact was reflected in the temporal beta diversity dynamics; which was different in free-living and particle-attached bacteria (Figure 4.6 c and d). Turnover rate in particle-attached bacterial composition was very high regardless of the wet or dry periods (Figure 4.6 c and d). In contrast, the turnover rate in free-living bacteria showed substantial differences between both hydrological periods with the lowest turnover rates in wet period. This indicated that changes in free-living bacterial composition seemed to be shaped to a larger extent by factors related to the hydrological budget, while the dynamics of particle-attached bacteria could be more linked to key features of biofilms, with a higher level of organization and metabolic activity to cope drought stress (Flemming *et al.* 2019). This asseveration was also apparent for OTUs richness of particle-attached bacteria, whose data did not show any statistically significant relationship with salinity or lake area (Table 4.3).

Moreover, the results of Adonis analyses provided statistical evidence that temporal variations in bacterial community composition were mainly controlled by lake area and to a lesser extent by salinity (Table 4.5). Their impact was in any case distinct at the level of free-living and particle-attached bacterial assemblages, highlighting again a greater effect of the extreme environmental conditions on the free-living bacterial fraction. Although salinity must be an ultimate cause of shifts in bacterial community composition and may be important in saline and hypersaline systems (Oren, 2002a; Jiang *et al.*, 2006, Zhang *et al.*, 2012) our results showed that salinity had a limited role in controlling bacterial community (Table 4.5). This suggests that ecosystem area should be the first factor to be considered, particularly under conditions of drought stress, indicating a potential influence of the drought on bacterial succession patterns in endorheic lakes. In addition, endorheic lakes are in general systems with high hydrological retention times, which could be further accentuated by drought conditions (Mosley *et al.* 2014).

Overall, we showed that richness, diversity and time temporal beta diversity were controlled mainly by lake area. We supported the explanatory idea that ecosystem size itself limits community structure. In fact, Post *et al.* 2000 observed that more complex (longer) food-webs increases with lake area. Therefore, droughts can reduce richness and diversity of bacterial community and increase time temporal beta diversity, mostly of the free-living bacteria, in this type of endorheic wetlands as a result of shrinking ecosystem size. This result may not be an anecdotic event and could be attributable to climate change effects at regional and global levels. In fact, future predictions of intense droughts in the Mediterranean biome are expected as a result of the ongoing global warming (Giorgi and Lionello 2008; Garcia-Ruíz *et al.* 2011). These facts suggest that drier and warmer conditions related to climate change can have an influence in bacterial community structure in Mediterranean wetlands. These changes in bacterial community structure could have also a high impact on biogeochemical cycles and key processes and services of wetlands such as greenhouse gas fluxes. We suggest that further works to explore the linkages between structural and functional changes will allow to unravel the global impact of lake size changes linked to droughts and obtain complete information with predictive significance.

4.5. REFERENCES

- Aguirre M, Abad D, Albaina A, Cralle L, Goñi-Urriza MS, Estonba A, *et al.* (2017). Unraveling the environmental and anthropogenic drivers of bacterial community changes in the Estuary of Bilbao and its tributaries. *PLoS ONE* 12(6): e0178755. <https://doi.org/10.1371/journal.pone.0178755>
- Angel R, Soares MIM, Ungar ED, Gillor O (2010). Biogeography of soil archaea and bacteria along a steep precipitation gradient. *ISME J* 4: 553–563.
- Antón J, Oren A, Benlloch S, Rodríguez-Valera F, Amann R, Rosselló-Mora R. (2002). *Salinibacter ruber* gen. nov., sp. nov., a novel, extremely halophilic member of the Bacteria from saltern crystallizer ponds. *Int J Syst Evol Microbiol* 52: 485–491.
- Antón J, Rosselló-Mora R, Rodríguez-Valera R, Amann R. (2000). Extremely halophilic bacteria in crystallizer ponds from solar salterns. *Appl Environ Microbiol.* 2000, 66: 3052-3057. 10.1128/AEM.66.7.3052-3057.
- Barreto DP, Conrad R, Klose M, Claus P, Enrich-Prast A (2014) Distance-Decay and Taxa-Area Relationships for Bacteria, Archaea and Methanogenic Archaea in a Tropical Lake Sediment. *PLoS ONE* 9(10): e110128. doi:10.1371/journal.pone.0110128
- Batanero, G.L., León-Palmero, E., Li, L., Green, A.J., Rendón-Martos, M., Suttle, C.A., Reche, I. (2017). Flamingos and drought as drivers of nutrients and microbial dynamics in a saline lake. *Scientific Reports*, 7 (1), art. no. 12173. <https://doi.org/10.1038/s41598-017-12462-9>.
- Beads, E.W., 1984. Bray-Curtis ordination: an effective strategy for analysis of multivariate ecological data. *Adv. Ecol. Res.* 14, 1–55.
- Bell, G. (2001). Neutral macroecology. *Science*, 293, 2413–2418.
- Bell T, Ager D, Song JI *et al.* (2005) Larger islands house more bacterial taxa. *Science*, 308, 1884.
- Benlloch, S., Lopez-Lopez, A., Casamayor, E. O., Øvreås, L., Goddard, V., Daae, F. L., *et al.* (2002). Prokaryotic genetic diversity throughout the salinity gradient of a coastal solar saltern. *Environ. Microbiol.* 4, 349–360. doi: 10.1046/j.1462-2920.2002.00306.x
- Benton C, Khan F, Monaghan P, Richards WN, Sheddens CB. 1983. The contamination of a major water supply by gull (*Larus sp.*). *Water Res.* 17:789–798.
- Bouvier, T. C., and P. A. Del Giorgio. (2002). Compositional changes in free-living bacterial communities along a salinity gradient in two temperate estuaries. *Limnol. Oceanogr.* 47: 453–470.
- Brüll, L., Huang, Z., Thomas-Oates, J., Paulsen, B., Cohen, E. and Michaelsen, T. (2000). Studies of polysaccharides from three edible species of *Nostoc* (Cyanobacteria) with different colony morphologies: Structural characterization and effect on the complement system of polysaccharides from *Nostoc commune*. *J. Phycol.*, 36: 871–881.

- Callieri C, Lami A, Bertoni (2011) Microcolony formation by single-cell *Synechococcus* strains as a fast response to UV radiation. *Appl Environ Microbiol* 77:7533–7540
- Caporaso, J. G., Lauber, C. L., Walters, W. a, Berg-Lyons, D., Huntley, J., Fierer, N., ... Knight, R. (2012). Ultra-high-throughput microbial community analysis on the Illumina HiSeq and MiSeq platforms. *The ISME journal*, 6(8), 1621–4. doi:10.1038/ismej.2012.8
- Caporaso, J.G., Kuczynski, J., Stombaugh, J., Bittinger, K., Bushman, F.D., Costello, E.K., Fierer, N., Peña, A.G., Goodrich, J.K., Gordon, J.I., Huttley, G.A., Kelley, S.T., Knights, D., Koenig, J.E., Ley, R.E., Lozupone, C.A., McDonald, D., Muegge, B.D., Pirrung, M., Reeder, J., Sevinsky, J.R., Turnbaugh, P.J., Walters, W.A., Widmann, J., Yatsunencko, T., Zaneveld, J., Knight, R., 2010. QIIME allows analysis of high-throughput community sequencing data. *Nat. Methods* 7 (5), 335–336. <http://dx.doi.org/10.1038/nmeth.f.303>.
- Casamayor, E. O., Calderon-Paz, J. I., and Pedros-Alio, C. (2000). 5S rRNA fingerprints of marine bacteria, halophilic archaea and natural prokaryotic assemblages along a salinity gradient. *FEMS Microbiol. Ecol.* 34, 113–119. doi: 10.1111/j.1574-6941.2000.tb00760.x.
- Casamayor, E. O., R. Massana, S. Benlloch, L. Øvreas, B. Diez, V. J. Goddard, J. M. Gasol, I. Joint, F. Rodriguez-Valera, and C. Pedros-Alio. (2002). Changes in archaeal, bacterial and eukaryal assemblages along a salinity gradient by comparison of genetic fingerprinting methods in a multi-pond solar saltern. *Environ. Microbiol.* 4:338–348.
- Connor, E. F., and E. D. McCoy. (1979). The statistics and biology of the species–area relationship. *American Naturalist* 113:791–833
- Crespo BG, Pommier T, Fernández-Gómez B, Pedrós-Alió C. (2013). Taxonomic composition of the particle-attached and free-living bacterial assemblages in the Northwest Mediterranean Sea analyzed by pyro-sequencing of the 16S rRNA. *Microbiologyopen* 2:541–552. <http://dx.doi.org/10.1002/mbo3.92>.
- Crump BC, Hopkinson CS, Sogin ML, Hobbie JE. (2004). Microbial biogeography along an estuarine salinity gradient: combined influences of bacterial growth and residence time. *Appl Environ Microbiol* 70: 1494–1505.
- Choo, Y.J., Lee, K., Song, J., Cho, J.C. (2007). *Puniceicoccus vermicola* gen. nov., sp. nov., a novel marine bacterium, and description of Puniceococcaceae fam. nov., Puniceococcales ord. nov., Opiritaceae fam. nov., Opiritales ord. nov. and Opiritae classis nov. in the phylum Verrucomicrobia. *Int. J. Syst. Evol. Microbiol.* 57, 532–537.
- Demergasso, C., Casamayor, E.O., Chong, G., Galleguillos, P., Escudero, L., and Pedrós-Alió, C. (2004). Distribution of prokaryotic genetic diversity in athalassohaline lakes of the Atacama Desert, Northern Chile. *FEMS Microbiol. Ecol.* 48(1): 57–69 doi:10.1016/j.femsec.2003.12.013. PMID:19712431.
- Dengler J. (2009). Which function describes the species-area relationship best? A review and empirical evaluation. *Journal of Biogeography*, 36, 728–744.

- Dornelas M, Magurran AE, Buckland ST, Chao A, Chazdon RL, Colwell RK, Curtis T, Gaston KJ, Gotelli NJ, Kosnik MA, McGill B, McCune JL, Morlon H, Mumby PJ, Øvrea's L, Stuedeny A, Vellend M. (2013). Quantifying temporal change in biodiversity: challenges and opportunities. *Proc R Soc B* 280: 20121931. <http://dx.doi.org/10.1098/rspb.2012.1931>
- Drakare S, Lennon JJ, Hillebrand H (2006). The imprint of the geographical, evolutionary and ecological context on species- area relationships. *Ecology Letters*, 9, 215–227.
- Ewing B, Green P: Basecalling of automated sequencer traces using phred. II. Error probabilities. *Genome Research* 8:186-194 (1998).
- Finlay, B. J. (2002). Global dispersal of free-living microbial eukaryote species. *Science* 296:1061–1063.
- Finlay, B. J., and K. J. Clarke. (1999). Ubiquitous dispersal of microbial species. *Nature* 400:828.
- Flemming H-C, Wuertz S. (2019). Bacteria and archaea on Earth and their abundance in biofilms. *Nat Rev Microbiol*. <https://doi.org/10.1038/s41579-019-0158-9>.
- García-Ruiz, J.M., López-Moreno, J.I., Vicente-Serrano, S.M., Lasanta, T., Beguería, S., 2011. Mediterranean water resources in a global change scenario. *Earth Sciences Review* 105, 121–139.
- Garrity, G. M., Brenner, D. J., Krieg, N. R., Staley, J. T., & Krieg, N. R. (2005). The Proteobacteria, Part C: The Alpha-, Beta-, Delta-, and Epsilonproteobacteria. *Bergey's manual of systematic bacteriology*. Springer, New York, 647-657.
- Geraci, J.; Béchet, A.; Cézilly, F.; Ficheux, S.; Baccetti, N.; Samraoui, B.; Wattier, R. (2012). Greater flamingo colonies around the Mediterranean form a single interbreeding population and share a common history. *J. Avian Biol.* 43, 341-354.
- Ghiglione, J. F., Mevel, G., Pujo-Pay, M., Mousseau, L., Lebaron, P., and Goutx, M. (2007). Diel and seasonal variations in abundance, activity, and community structure of particle-attached and free-living bacteria in NW mediterranean sea. *Microb. Ecol.* 54, 217–231. doi: 10.1007/s00248-006-9189-7.
- Giorgi, F., Lionello, P., (2008). Climate change projections for the Mediterranean region. *Global and Planetary Change* 63, 90–104.
- Green HC, Dick LK, Gilpin B, Samadpour M, Field KG. Genetic markers for rapid PCR-based identification of gull, Canada goose, duck, and chicken fecal contamination in water. *Appl Environ Microbiol* 2012;78(2):503–10.
- Green, A.J., Elmerg, J., 2014. Ecosystem services provided by waterbirds. *Biol. Rev.* 89, 105–122.
- Grimm, N. B. *et al.* Sensitivity of aquatic ecosystems to climatic and anthropogenic changes: The Basin and Range, American Southwest and Mexico. *Hydrol. Process.* 11, 1023–1041 (1997).

- Gross, M. (2017). The world's vanishing lakes. *Curr. Biol.* 27, 43–46.
- Grossart HP, Levold F, Allgaier M, Simon M, Brinkhoff T (2005) Marine diatom species harbour distinct bacterial communities. *Environ Microbiol* 7:860–873
- Grossart, H. P. (2010). Ecological consequences of bacterioplankton lifestyles: changes in concepts are needed. *Environ. Microbiol. Rep.* 2, 706–714. doi: 10.1111/j.1758-2229.2010.00179.x
- Harte J, Kinzig A, Green J (1999). Self-similarity in the distribution and abundance of species. *Science* 284: 334–336.
- Henriques, I.S., Alves, A., Tacao, M., Almeida, A., Cunha, A., and Correia, A. (2006) Seasonal and spatial variability of free-living bacterial community composition along an estuarine gradient (Ria de Aveiro, Portugal). *Estuarine Coastal Shelf Sci* 68: 139–148.
- Herbert, E.R., P. Boon, A.J. Burgin, S.C. Neubauer, R.B. Franklin, M. Ardón, K.N. Hopfensperger, L.P.M. Lamers, *et al.* (2015). A global perspective on wetland salinization: Ecological consequences of a growing threat to freshwater wetlands. *Ecosphere* 6: 1–43.
- Herlemann, D.P., Labrenz, M., Jurgens, K., Bertilsson, S., Waniek, J.J., and Andersson, A.F. (2011). Transitions in bacterial communities along the 2000 km salinity gradient of the Baltic Sea. *ISME J.* 5(10): 1571–1579. doi:10.1038/ismej.2011.41. PMID:21472016.
- Hollibaugh JT, Wong PS, Murrell MC (2000). Similarity of particle-associated and free-living bacterial communities in northern San Francisco Bay, California. *Aquat Microb Ecol* 21:103–114.
- Horner-Devine, M. C., Lage, M., Hughes, J. B. & Bohannon, B. J. M. A taxa–area relationship for bacteria. *Nature* 432, 750–753 (2004).
- Huang, G., & Isobe, M. (2012). Carrying capacity of wetlands for massive migratory waterfowl. *Hydrobiologia* 697, 5–14.
- Huettel, M., S. Forster, S. Kloser, and H. Fossing. 1996. Vertical migration in the sediment-dwelling sulfur bacteria *Thioploca* spp. in overcoming diffusion limitations. *Appl. Environ. Microbiol.* 62:1863–1872.
- Jellison, R., Williams, W. D., Timms, B., Alocer, J. & Aladin, N. V. in *Aquatic Ecosystems: Trends and Global Prospects* (ed. Polunin, N. V. C.) 94–112 (Cambridge Univ. Press, 2008).
- Jeppesen, E., Bruce, S., Naselli-Flores, L., Papastergiadou, E., Stefanidis, K., Nøges, T., *et al.* (2015). Ecological impacts of global warming and water abstraction on lakes and reservoirs due to changes in water level and related changes in salinity. *Hydrobiologia*, 750(1), 201–227.

- Jiang H, Dong H, Zhang G, Yu B, Chapman LR, Fields MW. (2006). Microbial diversity in water and sediment of lake Chaka, an athalassohaline lake in Northwestern China. *Appl Environ Microbiol* 72: 3832–3845.
- Jobe RT. (2008). Estimating landscape-scale species richness: Reconciling frequency- and turnover-based approaches. *Ecology*, 89, 174–182.
- Kallimanis, A.S. *et al.* (2008). How does habitat diversity affect the species–area relationship? *Glob. Ecol. Biogeogr.* 17, 532–538.
- Kan, J., B. C. Crump, K. Wang, and F. Chen. 2006. Bacterioplankton community in Chesapeake Bay: predictable or random assemblages. *Limnol. Oceanogr.* 51:2157–2169.
- Kirchman DL, Dittel AI, Malmstrom RR, Cottrell MT. (2005). Biogeography of major bacterial groups in the Delaware estuary. *Limnol Oceanogr* 50: 1697–1706.
- Kohfahl *et al.* (2008). Characterising flow regime and interrelation between surface-water and ground-water in the Fuente de Piedra salt lake basin by means of stable isotopes, hydrogeochemical and hydraulic data. *J. Hydrol.* 351, 170–187.
- Li Y, Zhang C, Wang N, Han Q, Zhang X, Liu Y, Xu L, Ye W (2017) Substantial inorganic carbon sink in closed drainage basins globally. *Nat Geosci* 10:501–506.
- Lindström, E. S., Kamst-Van Agterveld, M. P., and Zwart, G. (2005). Distribution of typical freshwater bacterial groups is associated with pH, temperature, and lake water retention time. *Appl. Environ. Microbiol.* 71, 8201–8206. doi: 10.1128/AEM.71.12.8201-8206.2005
- MacArthur, R. H., and E. O. Wilson. 1967. *The theory of island biogeography*. Princeton University Press, Princeton, New Jersey, USA.
- Magurran AE (1988) *Ecological Diversity and Its Measurement*. Princeton University Press, Princeton, New Jersey.
- Manny, B.A., Johnson, W.C. & Wetzel, R.G. (1994). Nutrient additions by waterfowl to lakes and reservoirs: predicting their effects on productivity and water quality. *Hydrobiologia.* 279/280,121–132.
- Martiny, J. B. H., Bohannan, B. J., Brown, J. H., Colwell, R. K., Fuhrman, J. A., Green, J. L., ... & Morin, P. J. (2006). Microbial biogeography: putting microorganisms on the map. *Nature Reviews Microbiology*, 4(2), 102.
- McGlenn DJ, Hurlbert AH. (2012). Scale dependence in species turnover reflects variance in species occupancy. *Ecology*, 93, 294–302.
- McMenamin, S. K., Hadly, E. A. & Wright, C. K. (2008). Climatic change and wetland desiccation cause amphibian decline in Yellowstone National Park. *Proc. Natl Acad. Sci. USA* 105, 16988–16993.

- Mesbah, N. M., Abou-El-Ela, S. H., and Wiegel, J. (2007). Novel and unexpected prokaryotic diversity in water and sediments of the alkaline, hypersaline lakes of the Wadi an Natrun, Egypt. *Microb. Ecol.* 54, 598–617. doi: 10.1007/s00248-006-9193-y.
- Messenger, M. L. Mathis Lóic Messenger, Bernhard Lehner, Günther Grill, Irena Nedeva & Oliver Schmitt. (2016). Estimating the volume and age of water stored in global lakes using a geo-statistical approach. *Nat. Commun.* 7, 13603 doi: 10.1038/ncomms13603.
- Meybeck (1995). Global distribution of lakes, in *Physics and Chemistry of lakes* Springer pp. 1-35.
- Milici M, Vital M, Tomasch J, Badewien TH, Giebel HA, Plumeier I, Wang H, Pieper DH, Wagner-Döbler I, Simon M (2017). Diversity and community composition of particle-associated and free-living bacteria in mesopelagic and bathypelagic Southern Ocean water masses: evidence of dispersal limitation in the Bransfield Strait. *Limnol Oceanogr* 62(3):1080–1095. <https://doi.org/10.1002/lno.10487>.
- Morlon, H., Chuyong, G., Condit, R., Hubbell, S., Kenfack, D., Thomas, D., Valencia, R. & Green, J.L. (2008). A general framework for the distance-decay of similarity in ecological communities. *Ecology Letters*, 11, 904–917.
- Mosley, L. M. (2015). Drought impacts on the water quality of freshwater systems: Review and integration, *Earth Sci. Rev.*, 140, 203–214, doi: 10.1016/j.earscirev.2014.11.010.
- Naimi, B. *et al.* 2014. Where is positional uncertainty a problem for species distribution modelling? – *Ecography* 37: 191–203.
- Newton RJ, Jones SE, Eiler A, McMahon KD, Bertilsson S. (2011). A guide to the natural history of freshwater lake bacteria. *Microbiol Mol Biol Rev* 75: 14–49.
- Nielsen, D. L. & Rock, M. A. (2009). Modified water regime and salinity as a consequence of climate change: Prospects for wetlands of Southern Australia. *Clim. Change.* 95, 523–533.
- Noguez AMM, Arita HTT, Escalante AEE, Forney LJJ, Garcia-Oliva F, *et al.* (2005). Microbial macroecology: highly structured prokaryotic soil assemblages in a tropical deciduous forest. *Glob Ecol Biogeogr* 14: 241–248.
- Oksanen J, Blanchet FG, Kindt R, Legendre P, Minchin PR, O’Hara R, *et al.* *Vegan: community ecology package.* R package version 2.3–3. 2016; Available from: <https://CRAN.R-project.org/package=vegan>
- Oren, A. (2002a) Molecular ecology of extremely halophilic Archaea and Bacteria. *FEMS Microbiol Ecol* 39: 1–7.
- Oren, A. 2002. Diversity of halophilic microorganisms: environments, phylogeny, physiology, and applications. *J. Ind. Microbiol. Biotechnol.* 28:56–63.
- Pedrós-Alió C, Calderón-Paz JI, MacLean MH, Medina G, Marrasé C, Gasol JM, Guixa-Boixereu N (2000a) The microbial food web along salinity gradients. *FEMS Microbiol*

- Pekel, J. F., Cottam, A., Gorelick, N. & Belward, A. S. (2016). High-resolution mapping of global surface water and its long-term changes. *Nature* 540, 418–422.
- Poli A, Anzelmo G, Nicolaus B (2010). Bacterial exopolysaccharides from extreme marine habitats: production, characterization and biological activities. *Mar Drugs* 8:1779–1802.
- Post, D. M., M. L. Pace, and N. G. Hairston, Jr. 2000. Ecosystem size determines food-chain length in lakes. *Nature* 405:1047–1049.
- Post, D. M.; Taylor, J. P.; Kitchell, J. F.; Olson, M. H.; Schindler, D. E. y Herwig, B. R. (1998). The role of migratory waterfowl as nutrient vectors in a managed wetland. *Conservation Biology*, 12: 910-920.
- Prosser, James & Bohannon, Brendan & Curtis, Tom & Ellis, Richard & K Firestone, Mary & P Freckleton, Rob & L Green, Jessica & Green, Laura & Killham, Ken & Lennon, Jack & Osborn, Andrew & Solan, Martin & Van der Gast, Christopher & Young, J Peter. (2007). Essay – The role of ecological theory in microbial ecology. *Nature reviews. Microbiology*. 5. 384-92. 10.1038/nrmicro1643.
- Pujalte, M. J., Lucena, T., Ruvira, M. A., Arahál, D. R., and Macián, M. C. (2014). “The family Rhodobacteraceae,” in *The Prokaryotes: Alphaproteobacteria and Betaproteobacteria*, 4th Edn, eds E. Rosenberg, E. F. De Long, S. Lory, E. Stackebrandt, and F. L. Thompson (Berlin: Springer), 439–512.
- Pumirat *et al.*, Global transcriptional profiling of Burkholderia pseudomallei under salt stress reveals differential effects on the Bsa type III secretion system *BMC Microbiology* 2010, 10:171 doi: 10.1186/1471-2180-10-171
- Ramírez-Fernández L, Trefault N, Caru M, Orlando J (2019) Seabird and pinniped shape soil bacterial communities of their settlements in Cape Shirreff, Antarctica. *PLoS ONE* 14(1): e0209887. <https://doi.org/10.1371/journal.pone.0209887>
- Ranjard L, Dequiedt S, Chemidlin Prévost-Bouré N, Thioulouse J, Saby NPA, Lelievre M *et al.* (2013). Turnover of soil bacterial diversity driven by wide-scale environmental heterogeneity. *Nat Commun* 4: 1434.
- Reche I, Pulido-Villena E, Morales-Baquero R, Casamayor EO (2005). Does ecosystem size determine aquatic bacterial richness? *Ecology*, 86, 1715–1722.
- Rendón M.A., Garrido A., Rendón-Martos M., Ramírez J.M. & Amat J.A. (2014). Assessing sex-related chick provisioning in greater flamingo *Phoenicopterus roseus* parents using capture–recapture models. *J. Animal Ecol.* 83, 479–490.
- Rendón-Martos, M., Vargas, J.M., Rendón, M.A., Garrido, A. & Ramírez, J.M. (2000). Nocturnal movements of breeding greater flamingos in southern Spain. *Waterbirds* 23, 9–19.
- Rendón, M.A., Garrido, A., Ramírez, J.M., Rendón-Martos, M. & Amat, J.A. (2001). Despotic establishment of breeding colonies of greater flamingos, *Phoenicopterus ruber*, in southern Spain. *Behav Ecol Soc.* 50, 55-60.

- Rieck, A., D. P. Herlemann, K. Jurgens, and H. P. Grossart. (2015). Particle-associated differ from free-living bacteria in surface waters of the Baltic Sea. *Front. Microbiol.* 6: 1297. doi:10.3389/fmicb.2015.01297.
- Riemann L. Winding A. (2001) Community dynamics of free-living and particle-associated bacterial assemblages during a freshwater phytoplankton bloom. *Microb. Ecol.*43.
- Rodríguez- Rodríguez, M., Benavente, J. & Moral, F. (2006). High density ground-water flow, major-ion chemistry and field experiments in a closed basin: Fuente de Piedra Playa Lake (Spain). *American J. Environ. Sciences.* 1, 164–171.
- Rosales, N., J. Ortega, R. Mora, and E. Morales (2005). Influence of salinity on the growth and biochemical composition of the *Cyanobacterium synechococcus* sp. *Ciencias Marinas* 31:349–355.
- Rösel S, Grossart H. (2012). Contrasting dynamics in activity and community composition of free-living and particle-associated bacteria in spring. *Aquat Microb Ecol* 66: 169–181.
- Rosenberg, E., DeLong, E.F., Lory, S., Stackebrandt, E., and Thompson, F., eds.(2014). *The Prokaryotes - Alphaproteobacteria and Betaproteobacteria* (Berlin, Heidelberg: Springer)
- Rosenzweig ML (1995). *Species diversity in space and time*. Cambridge University Press, Cambridge.
- Salman, V., R. Amann, A.-C. Girth, L. Polerecky, J. V. Bailey, S. Hegslund, G. Jessen, S. Par & H. N. Schulz-Vogt, 2011. A single-cell sequencing approach to the classification of large, vacuolated sulfur bacteria. *Systematic and Applied Microbiology* 34: 243–259.
- Schloss PD, Westcott SL, Ryabin T, Hall JR, Hartmann M, Hollister EB, *et al.* (2009). Introducing mothur: open- source, platform-independent, community-supported software for describing and comparing microbial communities. *Appl Environ Microbiol.* Dec; 75(23):7537–41. <https://doi.org/10.1128/AEM.01541-09> PMID: 19801464
- Schulz, H.N., Brinkhoff, T., Ferdelman, T.G., Marine, M.H., Teske, A., Jørgensen, B.B. (1999) Dense populations of a giant sulfur bacterium in Namibian shelf sediments. *Science* 284, 493–495.
- Shimadzu, H., Dornelas, M., & Magurran, A. E. (2015). Measuring temporal turnover in ecological communities. *Methods in Ecology and Evolution*, 6, 1384–1394.
- Signa, G., Mazzola, A. & Vizzini, S. (2012). Effects of a small seagull colony on trophic status and primary production in a Mediterranean coastal system (Marinello ponds, Italy). *Estuar. Coast. Shelf Sci.* 111, 27–34.
- Soininen J, McDonald R, Hillebrand H (2007) The distance decay of similarity in ecological communities. *Ecography*, 30, 3–12.

- Staley, C., Gould, T.J., Wang, P., Phillips, J., Cotner, J.B. and Sadowsky, M.J. (2015) Species sorting and seasonal dynamics primarily shape bacterial communities in the Upper Mississippi River. *Science of the Total Environment* 505, 435–445.
- Storch D, Keil P, Jetz W (2012) Universal species-area and endemics-area relationships at continental scales. *Nature*, 488, 78–81.
- Terrat, S. *et al.* (2015). Improving soil bacterial taxa–area relationships assessment using DNA meta-barcoding. *Heredity* 114, 468–475.
- Van Der Gast, C. J., Lilley, A. K., Ager, D. & Thompson, I. P. (2005). Island size and bacterial diversity in an archipelago of engineering machines. *Environ. Microbiol.* 7, 1220–1226.
- Vavourakis CD Ghau R Rodrigues-Valera F *et al.* (2016). Metagenomic insights into the uncultured diversity and physiology of microbes in four hypersaline soda lake brines *Front Microbiol.* 7 21.1.
- Wang, J., Song, C., Reager, J.T., Yao, F., Famiglietti, J.S., Sheng, Y., MacDonald, G.M., Brun, F., Schmied, H.M., Marston, R.A., Wada, Y., (2018). Recent global decline in endorheic basin water storages. *Nat. Geosci.* 11, 926–932.
- Woodcock S, Curtis TP, Head IM, Lunn M (2006). Taxa-area relationships for microbes: the unsampled and the unseen. *Ecology* 9: 805–812.
- Wurtsbaugh WA, Miller C, Null SE, DeRose RJ, Wilcock P, Hahnenberger M, Howe F, Moore J. (2017). Decline of the world's saline lakes. *Nat Geosci* 10:816–821. <https://doi.org/10.1038/NGEO3052>.
- Zhang R, Liu B, Lau SCK, Ki J-S, Qian P-Y. (2007). Particle-attached and free-living bacterial communities in a contrasting marine environment: Victoria Harbor, Hong Kong. *FEMS Microbiol. Ecol.* 61:496 –508. <http://dx.doi.org/10.1111/j.1574-6941.2007.00353.x>.
- Zhang, Y., Jiao, N.Z., Cottrell, M.T., and Kirchman, D.L. (2006) Contribution of major bacterial groups to bacterial biomass production along a salinity gradient in the South China Sea. *Aquat Microb Ecol* 43: 233–241.
- Zinger L, Boetius A, Ramette A (2014). Bacterial taxa-area and distance-decay relationships in marine environments. *Mol Ecol* 23: 954–964.

Discussion

The saline wetlands studied in this dissertation cover a wide range in salinity, nutrients, dissolved organic matter and show high variability in the values of prokaryotic heterotrophic production (Figure 1, Table 1). The highest values appear in the coastal lagoons and marshes and are related to water mixing processes with river or estuarine waters and the lowest values appear in the endorheic system during the evaporation phase and the drier period (dark pink dots).

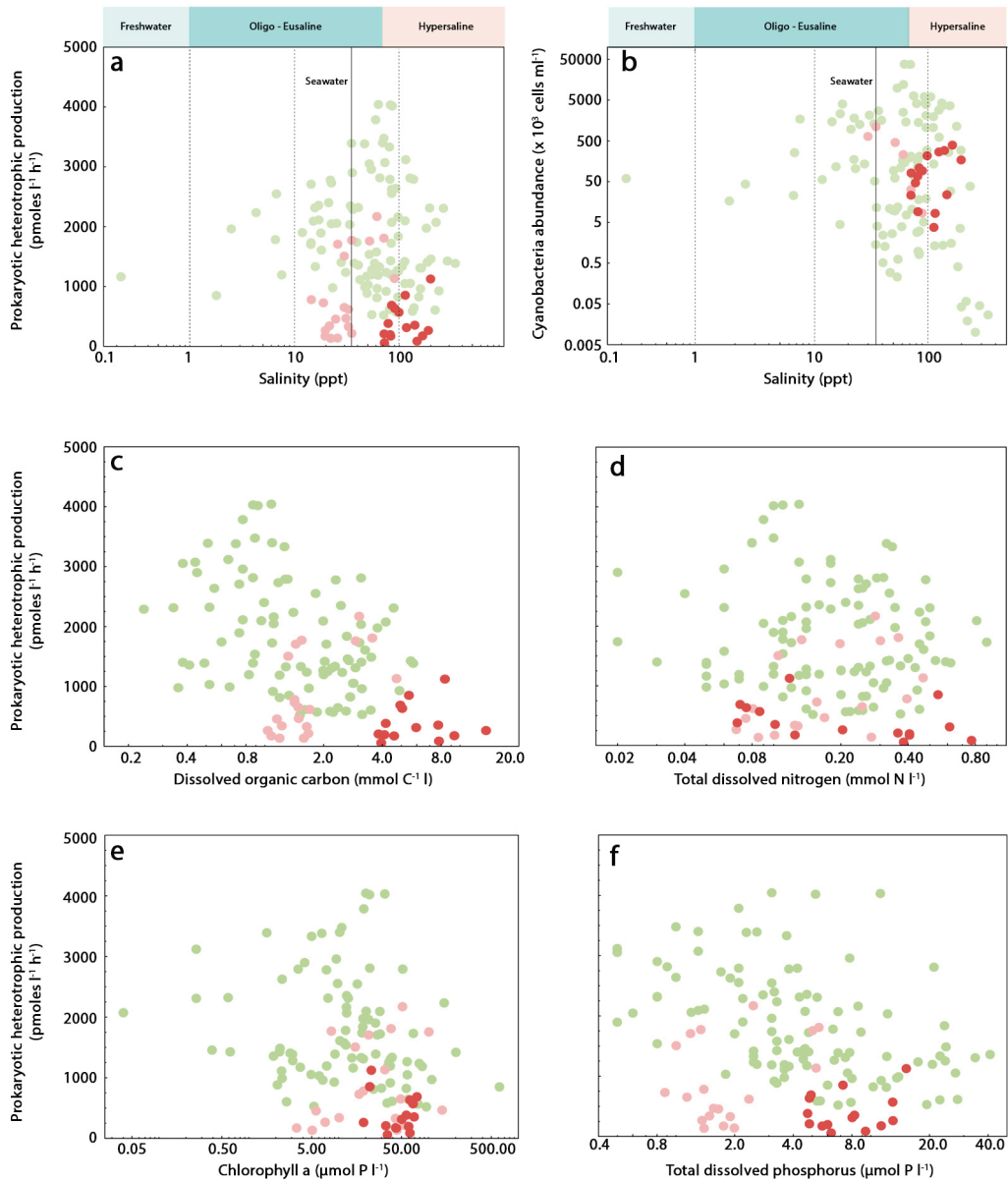


Figure 1. Prokaryotic heterotrophic production and cyanobacteria abundance in the saline. Wetlands studied in this PhD dissertation along gradients of salinity (a, b), dissolved organic carbon (c), total dissolved nitrogen (d), chlorophyll-a (e) and total dissolved phosphorus (f). The study coastal wetlands are represented in green dots and the seasonal data in the endorheic lake of Fuente de Piedra are represented in pale pink dots during the wet hydrological year and in dark pink during the dry hydrological year.

Table 1. Mean values and ranges (in parentheses) of basic physicochemical and biological variables in the wet and dry hydrological years in Fuente de Piedra lake and coastal wetlands: Salinity (ppt), Dissolved Organic Carbon (DOC mmol-C l⁻¹), Total Nitrogen (TN, mmol-N l⁻¹), Total Phosphorus (TP, μmol-P l⁻¹), chlorophyll a (Chl a, μg/l), Prokaryotic heterotrophic production (PHP, pmoles of leucine l⁻¹h⁻¹) Prokaryotic heterotrophic abundance (HA, cells ml⁻¹) and Virus abundance (VA, particles ml⁻¹).

Saline Wetlands type	Study Site	Salinity	DOC	TN	TP	Chl a	PHP	HA (x10 ⁶)	VA (x10 ⁹)
	Fuente de piedra lake	39.5	1.8	0.26	4.459	30.0	857.26	189.21	1.01
	(Wet year, 2010-2011)	(19.6 - 90.1)	(1.0 - 4.7)	(0.07 - 0.48)	(1.07 - 9.63)	(2.4 - 100.8)	134.70 - 2170.53	141.54 - 251.89	0.45 - 1.41
Endorheic lake	Fuente de piedra lake	117.6	6.3	0.60	13.48	49.8	405.32	42.06	0.76
	(Dry year, 2011-2012)	(71.7 - 199.0)	(3.8 - 13.6)	(0.36 - 1.17)	(5.69 - 38.60)	(18.8 - 92.1)	59.06 - 1124.31	13.94 - 154.78	0.35 - 1.46
Coastal lagoons and marshes	Mediterranean region	79.9	1.80	0.36	12.04	31.9	1821.96	32.02	0.59
	(9 wetlands complexes including 112 ponds)	0.22 - 343	0.24 - 5.76	0.05 - 1.2	(1.20 - 48.60)	(0.04 - 617.4)	518.89 - 4041.68	2.26 - 247.20	0.02 - 3.07

In previous studies in nearby hypertrophic and eutrophic coastal lagoons, the maximum TP concentrations, reached up to 15.21 and 5.01 $\mu\text{mol-P l}^{-1}$ in the lakes Honda and Nueva (Vicente *et al.* 2006, Cruz-Pizarro *et al.* 2003). The values obtained in this dissertation were larger in both the coastal wetlands and the endorheic lake of Fuente de Piedra during the two hydroperiods (Table 1). However, the maximum chlorophyll-a concentration found in Fuente de Piedra lake was smaller than the values found in the Honda lake (maximum: 292 $\mu\text{g l}^{-1}$) by de Vicente *et al.* (2006), while for coastal lagoons and marshes, chlorophyll-a values were almost 2-fold higher (Table 1).

Coastal wetlands appear to be more productive than Fuente de Piedra lake, reaching extremely high prokaryotic heterotrophic production and cyanobacteria abundance values particularly in the range of euhaline waters with intermediate concentrations of DOC, TDN and chl a (Figure 1, Table 1). In coastal wetlands, there is a high nitrogen demand linked to heterotrophic prokaryotes with opposing effect for archaeal and bacterial production. In our study, TDN was the main predictor variable, with a positive effect, on archaeal production (Table 2 in Chapter 2). This robust result indicates that archaea play a key role in nitrogen dynamics in these wetlands. However, the negative correlation between the bacterial production residuals and TDN could be explained by the fact that the majority of viruses are likely bacteriophages controlling bacterial production, since there was not any correlation between archaeal production and virus abundance (Table 4 in Chapter 2).

The fact that the endorheic lake of Fuente de Piedra exhibited lower prokaryotic heterotrophic production values compared with coastal wetlands could be due to fact the the heterotrophic prokaryotes in Fuente de Piedra likely are growing under P-limiting conditions (Figure 2 and Table 1).

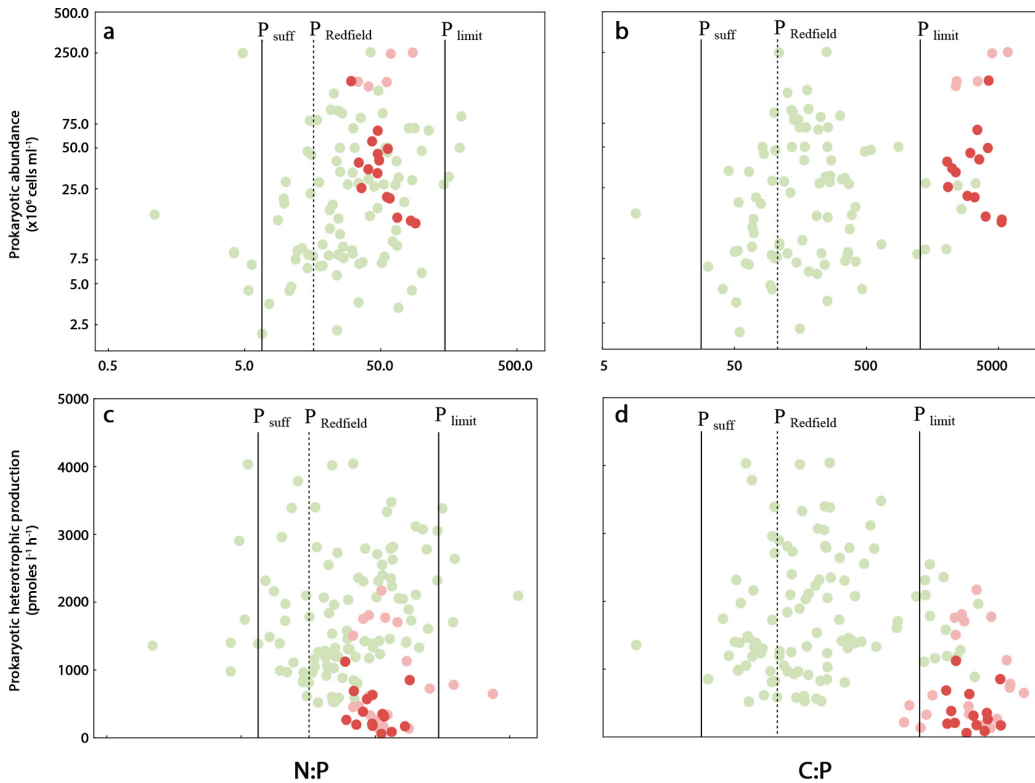


Figure 2. Prokaryotic heterotrophic abundance (a, b) and production (c, d) along gradients of the molar N:P and C:P ratios in the study saline wetlands. The molar N:P ratio of 6.7:1 stands for P-sufficient and the molar ratio 148:1 stands for P-limitation. The solid black lines are the two thresholds proposed by Cotner *et al.* (2010). The dashed line shows the Redfield N:P ratio of 16:1. The molar C:P ratio of 28:1 is considered as P-sufficient and the molar ratio of 1279:1 as P-limitation after Cotner *et al.* (2010). The dashed line shows the Redfield N:P ratio of 106:1. The study coastal wetlands are represented in green dots and the seasonal data in the endorheic lake of Fuente de Piedra are represented in pale pink dots during the wet hydrological year and in dark pink during the dry hydrological year.

In Fuente de Piedra lake, all the data of heterotrophic abundance (Fig.2 a) and production (Fig. 2c) were above the Redfield ratio of N: P (16:1) suggesting a potential P limitation. Considering all the saline wetlands, most of values of heterotrophic abundance (Fig.2 a) and production (Fig. 2c) were included inside the two thresholds (6.7-148) proposed by Cotner *et al.* (2010) given the high flexibility of the bacterial stoichiometry. In the case of the molar C: P ratio, all values of the heterotrophic abundance (Fig.2 b) and production (Fig. 2d) in Fuente de Piedra lake were clearly above the ratios of C: P established by Redfield (106:1) and by Cortner *et al.* (2010) (1279:1) for the P-limitation of the heterotrophic prokaryotes. There is a clear segregation of prokaryotic heterotrophic abundance and production in Fuente Piedra lake (pink dots) during the two hydroperiods (wet and dry) with respect to the values in the coastal wetlands, where P content appear no be not limiting (Figure 2 b and d).

Prokaryotes were more active in the endorheic lake of Fuente de Piedra during the wet period (pale pink dots in Figure 2) than during the dry one. The maximum of prokaryotic heterotrophic production and abundance was observed in eusaline waters during the wet period (dark pink dots in Figure 2) coupled temporally to flamingo dynamics (Figure 3.6 b in Chapter 3). These synchronous dynamics took place because flamingos had a direct effect on prokaryotes through the inputs of limiting nutrients by sediment bioturbation. In fact, the positive and significant correlation between prokaryotic heterotrophic production and total dissolved phosphorus during the wet year when flamingos reached maximum abundance (Figure 3.9 in Chapter 3). This P-limitation was confirmed with two experiments using guano from flamingos. In both experiments, prokaryote growth was stimulated almost twice after guano addition in comparison to the control treatments. There was a significant consumption of soluble reactive phosphorus, but not of other nutrients such as dissolved organic carbon (DOC) and total dissolved nitrogen (TDN) in the treatment with guano (Figure 3 a and b). This result confirms that the interaction between flamingos and prokaryotes was mediated by soluble phosphorus.

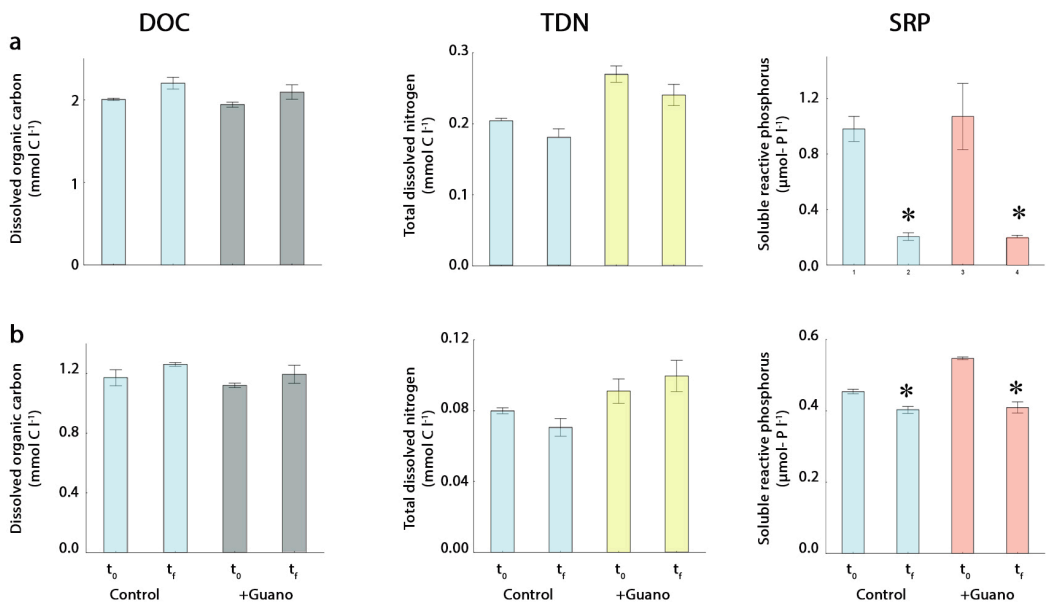


Figure 3. Experiments on the growth of heterotrophic prokaryotes with addition of flamingo guano. Changes in concentration of dissolved organic carbon (DOC), total dissolved nitrogen (TDN) and soluble reactive phosphorus (SRP) at the beginning (t₀) and the final time (t_f) of (a) experiment 1 in 2010 and (b) experiment 2 in 2011. Blue represents the treatment with the control conditions and grey (DOC), yellow (TDN) and red (SRP) the treatment with addition of fresh guano from flamingo chicks. For more details see Chapter 3.

At the ecosystem level, nutrients and microbial dynamics in Fuente de Piedra lake appeared to be controlled by the hydrological budget (evaporation vs. precipitation) that determines the water level and, ultimately, the inundation area. Therefore, changes in the inundation area during droughts in this type of endorheic lake have major implications for species diversity. In fact, we found a clear decrease in richness and diversity of bacterial community and a change in composition as result of the lake area shrinking during the dry period (Figure 4 a and b in Chapter 4). These effects were consistent for both free-living and particle-attached bacterial assemblages, indicating that lake area is a main driver of the bacterial community structure (Table 3 in Chapter 4), with a negative effect on OTUs richness and Shannon diversity. Moreover, there was also evidence that temporal variations in bacterial community composition (i.e. temporal beta diversity) were mainly driven by lake area, although the effect was higher on the free-living bacteria than on the particle-attached bacterial assemblages (Table 5 in Chapter 4). Probably, free-living bacterial assemblages are more affected by these external environmental factors such as drought, whereas the dynamics of particle-attached bacterial assemblages could be also linked to self-organization inside the biofilms (suspended particles). In fact, alpha diversity indices (i.e., OTUs richness and Shannon diversity) for particle-attached bacteria were higher than those for their free-living bacterial counterpart (Figure 4 in Chapter 4). Interestingly, turnover rate in particle-attached bacterial composition was very high regardless of wet and dry year (Figure 6 c in Chapter 4). In conclusion, the inundation area plays a key role on bacterial community structure and composition in this endorheic lake over time. This finding is even more relevant given the future predictions of severe droughts as consequence of climate change that are shrinking saline lakes inundation areas at global scale (Messenger, *et al.* 2016; Wurtsbaugh *et al.* 2017; Wang *et al.* 2018). This intense evaporation has also consequences for salinization (Herbert *et al.* 2015; Jeppesen *et al.* 2015). It could have a high global impact on microbial community in saline lakes that are key in global biogeochemical cycles and wetlands functioning, reducing their capacity to sequester carbon and remove nitrogen, and, ultimately, provoking a positive feedback to global climate change effects (Herbert *et al.* 2015). However, more studies are needed to test the effect of the changes of bacterial structure during droughts on the ecosystem functions.

The description of the microbial dynamics of saline wetlands in the Mediterranean basin will allow the scientific community to have a better knowledge of the main drivers of the microbial component depending on the saline wetland type and thus, to achieve a better understanding of climate change impact on the microbial structure in wetlands. However, continuous advances in knowledge on the microbial ecology in saline wetlands through new massive sequencing technologies suggests there is still much to be learnt. We suggest that further work should explore shifts in the functional groups of the microbial communities to unravel lake-specific conditions that minimize negative consequences linked to drought conditions on wetlands functioning and to obtain information with predictive value.

References

- Cotner JB, Hall EK, Scott JT, Heldal M. (2010). Freshwater bacteria are stoichiometrically flexible with a nutrient composition similar to seston. *Front Microbiol* 1: 132.
- Cruz-Pizarro, L., I. de Vicente, E. Moreno-Ostos, V. Amores, and K. El Mabrouki. 2003. Estudios de diagnóstico y viabilidad en el control de la eutrofización de las lagunas de la Albufera de Adra (Almería). *Limnetica* 22:135–154.
- De Vicente I, Moreno-Ostos E, Amores V, Rueda F, Cruz-Pizarro L (2006) Low predictability in the dynamics of shallow lakes: implications for their management and restoration. *Wetlands* 26:928–938.
- Jeppesen, E., Brucet, S., Naselli-Flores, L., Papastergiadou, E., Stefanidis, K., Noges, T., *et al.* (2015). Ecological impacts of global warming and water abstraction on lakes and reservoirs due to changes in water level and related changes in salinity. *Hydrobiologia*, 750(1), 201-227.
- Herbert, E.R., P. Boon, A.J. Burgin, S.C. Neubauer, R.B. Franklin, M. Ardón, K.N. Hopfensperger, L.P.M. Lamers, *et al.* 2015. A global perspective on wetland salinization: Ecological consequences of a growing threat to freshwater wetlands. *Ecosphere* 6: 1–43.
- Messenger, M. L. Mathis Loïc Messenger, Bernhard Lehner, Günther Grill, Irena Nedeva & Oliver Schmitt. Estimating the volume and age of water stored in global lakes using a geo-statistical approach. *Nat. Commun.* 7, 13603 doi: 10.1038/ncomms13603 (2016).
- Redfield, A.C. 1934. On the proportions of organic derivatives in sea water and their relation to the composition of plankton. En: James Johnstone Memorial volume: 176-192. Universidad de Liverpool.
- Wang, J., Song, C., Reager, J.T., Yao, F., Famiglietti, J.S., Sheng, Y., MacDonald, G.M., Brun, F., Schmied, H.M., Marston, R.A., Wada, Y., 2018. Recent global decline in endorheic basin water storages. *Nat. Geosci.* 11, 926–932
- Wurtsbaugh WA, Miller C, Null SE, DeRose RJ, Wilcock P, Hahnenberger M, Howe F, Moore J. (2017). Decline of the world's saline lakes. *Nat Geosci* 10:816–821. <https://doi.org/10.1038/NGEO3052>.

Conclusions

1. Saline wetlands are submitted to a high variability in salinity, nutrients and organic matter concentration with extremely variable and abundant microbial communities due to mixing processes with river or estuarine waters in the coastal wetlands and to evapoconcentration in the endorheic system, being the latter more vulnerable to drought conditions.

2. The highest prokaryotic heterotrophic production and cyanobacteria abundance in the study coastal wetlands across the Mediterranean region and in the endorheic lake Fuente de Piedra lake over time were reached particularly in eusaline waters with intermediate concentrations of dissolved organic carbon, total dissolved nitrogen and chlorophyll-a concentration.

3. In coastal wetlands heterotrophic prokaryotes had a high nitrogen demand. Total dissolved nitrogen was the only predictor variable on archaeal heterotrophic production with a positive effect indicating that archaea plays a key role in nitrogen cycling in these systems. In contrast, the decline in bacterial heterotrophic production with the increase of total dissolved nitrogen can be explained indirectly by the fact that viruses increased with salinity and they affected negatively to bacterial heterotrophic production.

4. Fuente de Piedra appears to be P-limited with a maximum of prokaryotic production and abundance in euhaline waters during the wet period and tightly coupled with flamingo dynamics. The synchronous influence of flamingos on heterotrophic prokaryotic production and abundance appears to be mediated by an increase in the P availability derived from guano inputs and mostly from sediment bioturbation.

5. Experiments with addition of flamingo guano confirmed that the growth of heterotrophic prokaryotes and that the growth was mediated by the consumption of reactive soluble phosphorus and not dissolved nitrogen or carbon.

6. Drought conditions reduced hydrological budget and, ultimately, the inundation area in the endorheic system of Fuente de Piedra lake with major implications for bacterial community structure. Lake area reduction involved a decline in the OTUs richness and diversity and an increase in temporal beta diversity.

7. The inundation area of Fuente de Piedra lake was a major controlling factor of both free-living bacteria and particle-attached bacteria, but the magnitude of this effect was higher on the free-living bacteria than on the particle-attached bacteria. Probably, free-living bacteria are more affected by environmental factors, whereas the particle-attached bacteria could be more protected due to self-organization inside the biofilm particles.

8. Coastal wetland systems were more productive than Fuente de Piedra lake. The fact that the endorheic lake of Fuente de Piedra exhibited lower prokaryotic heterotrophic production values compared with coastal wetlands could be due to heterotrophic prokaryotes growing under extreme P-limiting conditions.

9. Endorheic systems as Fuente de Piedra lake seem to be more vulnerable to changing climate conditions than coastal wetlands, especially under severe drought conditions and subsequent salinization processes that are already happening as consequences of climate change.

Conclusiones

1. Los humedales salinos están sometidos a una alta variabilidad en su concentración de salinidad, nutrientes y materia orgánica con comunidades microbianas extremadamente variables y abundantes debido a los procesos de mezcla con el agua fluvial o del estuario en los humedales costeros y debido a la evapoconcentración en el sistema endorreico estudiado, siendo este último más vulnerable a las condiciones de sequía.

2. La mayor producción heterotrófica de procariontes y la abundancia de cianobacterias en los humedales costeros de la región mediterránea estudiados y en el lago endorreico Fuente de Piedra a lo largo del tiempo se alcanzaron particularmente en aguas eusalinas con concentraciones intermedias de carbono orgánico disuelto, nitrógeno disuelto total y clorofila-a.

3. En los humedales costeros, los procariontes heterótrofos tuvieron una alta demanda de nitrógeno. El nitrógeno disuelto total fue la única variable predictiva de la producción heterotrófica de las arqueas, con un efecto positivo lo que indica que las arqueas juegan un papel clave en el ciclo del nitrógeno en estos ecosistemas. Por el contrario, la disminución de la producción heterotrófica de las bacterias con el incremento en la concentración del nitrógeno disuelto total puede explicarse indirectamente por el hecho de que los virus aumentaron con la salinidad y éstos afectaron negativamente a la producción heterotrófica bacteriana.

4. Fuente de Piedra parece estar limitada por el P, con un máximo de producción heterotrófica de procariontes y abundancia de los mismos en aguas eusalinas durante el

período húmedo y éste máximo estuvo estrechamente ligado a la dinámica de los flamencos. La influencia sincrónica de los flamencos sobre la producción y abundancia de procariontes heterotróficos parece que estuvo mediada por un aumento en la disponibilidad de P derivado de las entradas de guano y, principalmente, desde los sedimentos por bioturbación.

5. Experimentos con adición de guano de flamenco confirmaron que el crecimiento de los procariontes heterotróficos fue mediado por el consumo de fósforo soluble reactivo y no de compuestos de nitrógeno o carbono disueltos.

6. Las condiciones de sequía redujeron el presupuesto hidrológico y, en última instancia, el área de inundación en el sistema endorreico de la laguna de Fuente de Piedra, con importantes implicaciones para la estructura de la comunidad bacteriana. La reducción de la superficie de la laguna implicó una disminución en la riqueza y diversidad de las OTUs y un aumento de la beta diversidad temporal.

7. El área de inundación de la laguna de Fuente de Piedra fue un importante factor de control tanto para las bacterias de vida libre como para las bacterias adheridas a las partículas, pero la magnitud de este efecto fue mayor sobre las bacterias de vida libre que en las bacterias adheridas a las partículas. Probablemente, las bacterias de vida libre se ven más afectadas por factores ambientales, mientras que las bacterias adheridas a partículas podrían estar más protegidas debido a la autoorganización dentro de las partículas de biopelículas.

8. Los humedales costeros fueron más productivos que la laguna de Fuente de Piedra. El hecho de que el lago endorreico de Fuente de Piedra exhibiera valores más bajos de producción heterotrófica de procariontes en comparación con los humedales costeros puede deberse a que los procariontes heterótrofos crecen en condiciones extremas de limitación de P en la misma.

9. Los sistemas endorreicos como el lago Fuente de Piedra parecen ser más vulnerables a las condiciones climáticas cambiantes que los humedales costeros, especialmente en condiciones de sequía severa y los procesos de salinización subsiguientes que ya están ocurriendo como consecuencia del cambio climático.

ABBREVIATION INDEX

ArP: Archaea production

BP: Bacterial production

chl a: Chlorophyll a

CyA: Cyanobacteria abundance

DOC: Dissolved organic carbon

HA: Prokaryotic heterotrophic abundance

OTU: Operational Taxonomic Units

PA: Prokaryotic abundance

PHP: Prokaryotic heterotrophic production

SRP: Soluble reactive abundance

TAR: universal taxa-area relationship (Rosenzweig, 1995)

TDN: Total dissolved nitrogen

TDP: Total dissolved phosphorus

TN: Total nitrogen

TP: Total phosphorus

VA: Virus abundance

Annex Chapter 1

Annex Chapter 1

1

Analysis of Metagenomic Data

The analysis of the sequence data was processed using the open software, Quantitative Insights into Microbial Ecology (QIIME) version 1.9.0 by Caporaso et al. (2010) and MOTHUR software (version 1.34.3). Here, we explain all steps of this workflow, including sequence pre-processing, sequence processing, and data analysis (alpha and beta diversity calculation). We used default parameters for each Qiime and Mothur scripts, unless otherwise specified.

1. PRE-PROCESSING OF SEQUENCES:

First, the quality of the pair-end Illumina reads (MiSeq) was assessed using FastQC software (<http://www.bioinformatics.babraham.ac.uk/projects/fastqc/>). Pre-processing consisted basically in joining and filtering paired-end reads and the removal of primer sequences:

1.1. Multiple joining of paired ends

This step in Qiime allowed us to combine paired end reads (R1-forward and R2-reverse) into single sequences per sample using the following script:

```
multiple_join_paired_ends.py  
  
-i Sequences_FP (name of input directory of the paired-end reads)  
-o Joined_R1_R2_FP (name of the directory to place output files)
```

The output directory (Joined_R1_R2_FP) includes a directory per sample. Each directory contains three fastq files, a joined file and two unjoined files (for R1-*forward* and one other for R2-*reverse*).

1.2. Multiple Split Libraries

This step consists of a quality filtering of output.fastq files from the previous step. This Qiime script merges all the sequences into a single FASTA file named *seqs.fna*.

```
multiple_split_libraries_fastq.py

-i Joined_R1_R2_ (name of input directory of fastq files)
-o Split_FP (name of the directory to place output files)
-p qiime_parameters.txt
--read_indicator .join. (This option indicated that only joined reads
must be processed
--include_input_dir_path (Incorporate the input directory name in the
output sample name)
```

By default, this script uses Qiime settings for quality filtering, which are described by Bokulich et al. (2013). These parameters are: minimal high-quality read length = 75%, Phred score = 19, maximum of consecutive low-quality calls = 3, maximum of ambiguous calls allowed= 0.

```
# Parameters file
# script_name:parameter_name value
split_libraries_fastq.py:phred_quality_threshold 19
split_libraries_fastq.py:barcode_type 'not-barcoded'
split_libraries_fastq.py:max_bad_run_length 3
split_libraries_fastq.py:min_per_read_length_fraction 0.75
split_libraries_fastq.py:sequence_max_n 0
```

1.3. Trimming primers

This step trims off the primer sequences from full length sequences using the following command in Mothur:

```
mothur > trim.seqs(fasta=seq.fna, oligos=oligos.txt)

fasta=seq.fna (ouput FASTA file from Split_library.py)
oligos=oligos.txt (contain sequences of trim forward and reverse primers)
```

```
#oligos.txt
forward GTGCCAGCMGCCGCGGTAA
reverse GGACTACHVGGGTWTCTAAT
```

This command creates two FASTA files: `seqs.trim.fasta` that contains the sequences without primers and `seqs.scrap.fasta` that contains the original untrimmed sequences.

2. PROCESSING SEQUENCES INTO AN OTU TABLE

2.1. Clustering the sequences in OTUs

All of the sequences from each sample were clustered into operational taxonomic units (OTUs) and assigned to bacterial taxa. We used the *pick_de_novo_otus.py* workflow. In this process, the sequences were aligned one against another without any external reference database. In addition to clustering, this script also includes taxonomy assignment, sequence alignment, and tree-building steps.

```
pick_de_novo_otus.py

-i seqs.trim.fasta (fasta file that was created by multiple split
libraries, without primer seqs.)
-o pick_otus_99 (name of the directory to place output files)
-p parameter0.99.txt (This option indicated that sequences that are 99%
similar should be considered the same OTU)
```

The most important file created during the novo otu picking was “Otu table” in biom format; which provides the number of sequences of each OTU and their taxonomic affiliations for each sample. The steps were as follows:

1. `pick_otus.py` – This step joins similar sequences in OTUs: the sequences were clustered into Operational Taxonomic Units (OTUs) using Uclust (Edgar, 2010) following the default method implemented in QIIME with a sequence similarity threshold of 99%.
2. `pick_rep_set.py` – This step selects a representative sequence set, the most abundant sequence per OTU. This OTU representative sequence is used for taxonomic identification. The relevant file (`seqs.trim_rep_set.fasta`) is found in the “`otus_0.99/rep_set/ directory`”.
3. `assign_taxonomy.py` – This step assigns taxonomies to the representative sequences set comparing them with the reference database Greengenes (<http://greengenes.secondgenome.com>). The default classification system in QIIME was uclust. The relevant file (`seqs.trim_rep_set_tax_assignments.txt`) is found in the “`otus_0.99/uclust_assigned_taxonomy/ directory`”
4. `make_otu_table.py` This step creates a matrix of OTU abundance for each sample (Step 1) and adds the OTU taxonomy (the taxonomy file is obtained in the Step 3). The relevant file (`otu_table.biom`) is found in the “`otus_0.99 directory`”.

2.2. Curating the OTU table at the taxa-Level:

Once we have generated the OTU table, the next step was to perform a negative filtering of taxa, removing taxonomic levels of Archaea, Chloroplast and Mitochondria. This can be done using the following script:

```
filter_taxa_from_otu_table.py
-i otu_table.biom
-o otu_table_non_arch_Chlo_Mit.biom
-n k_Archaea,c__Chloroplast,f__Mitochondria
```

2.3. Division of the database in two subsets

Filtered OTU table contains both the 0.2 μm -free-living and the 3 μm -particle-attached bacteria (i.e. the complete database). For this reason, two OTU table files (one for 0.2 μm and one for 3 μm) in .biom format were generated from the filtered OTU table (otu_table_non_arch_Chlo_Mit.biom). First, it is necessary to convert the biom OTU table into a text table, allowing the manipulation of database, and its later conversion to .biom format again. This step uses the following scripts:

To convert biom format to tab-delimited table format:

```
biom convert
-i otu_table_non_arch_Chlo_Mit.biom
-o otu_table_non_arch_Chlo_Mit.txt
--to-tsv
--header-key taxonomy
```

After this step, we can open in an excel file and divide the database into two subsets and we generate an OTU table file in .biom format for each subset:

```
otu_table_non_arch_Chlo_Mit_0.2micras.txt
otu_table_non_arch_Chlo_Mit_3micras.txt
```

All the subsequent steps were performed for the two OTU tables in .biom format separately to convert tab-delimited format to biom table format:

```
biom convert
-i otu_table_non_arch_Chlo_Mit.biom
-o otu_table_non_arch_Chlo_Mit.txt
--to-tsv
--header-key taxonomy
```


2.4. Rarefaction analysis

To control for the sampling effort, the datasets were standardized by rarefaction analyses at different sequencing depth at 200, 500 and then at 1000 intervals of from 1000 to 10000 sequences and 100 iterations. In Qiime, this step was carried out using filtered OTU tables (Step 2.3) as input using the following script:

```
multiple_rarefactions_even_depth.py

-i otu_table_non_arch_Chlo_Mit_0.2micras
-o rarefied_otu_tables (directory to place rarefied output tables files)
-d 200, 500, from 1000 to 10000 at intervals of 1000 (seqs/samples to
subsampled)
-n 100 (num. iterations to perform at each depth)
```

These new rarefied tables in .biom format (100 otu tables from each rarefaction depth) were saved in a directory called “rarefied_otu_tables”.

2.5. Singleton filtering from the OTU table

After the normalization step, a filtering step from OTU table, was carried out to discard all singletons (sequences detected only once to reduce the noise due to a potential high ratio of artifacts/real OTUs using following QIIME script:

```
filter_otus_from_otu_table.py

-i rarefied_otu_tables (directory to place rarefied tables files)
-o otu_tables_no_singletons (directory to place output tables without singletons
files)
```

These new tables without singletons in .biom format were saved in a directory named “otu_tables_no_singletons”, which later was utilized as input for both the alpha and the beta diversity calculations.

2.6. Alpha diversity

The Qiime script that allows calculate alpha diversity is named `alpha_diversity.py`. Among all the available options of alpha diversity metrics, the number of observed OTUs and the Shannon-Wiener diversity index were selected. Alpha diversity analysis was executed for `OTU_table` at each corresponding sequencing depth.

```
alpha_diversity.py

-i otu_tables_no_sigletons
-m observed_otus,shannon
-o alpha_div
```

To concatenate all the generated files into a single file for further analysis we used the `collate_alpha.py` script.

```
collate_alpha.py

-i alpha_div
-o alpha_div_collated
```

Within a new output directory named “`alpha_div_collated`” two files are generated (`observed_otus.txt` and `Shannon.txt`), which contain the diversity values for each sample and rarefaction depth. We found that at a depth of 2000 sequences per sample the Shannon diversity index started the saturation plateau in free-living and particle-attached bacterial assemblages.

2.7. Beta diversity

A beta diversity metric calculates a dissimilarity value between a pair of samples. From all the available options in Qiime, we selected the Bray-Curtis dissimilarity matrix using the `beta_diversity.py` script. The output for this script was two `.txt` files, each file contains a matrix at two different rarefaction depths containing the distance values for each pairwise comparison. The input directory was the multiple rarefied OTU tables (step 2.4). Beta diversity analysis was executed for OTU_table of 0.2 and 3 μm -attached at 2000 sequencing depth.

```
beta_diversity.py
-i otu_tables_no_sigletons_2000_sequencing_depth
-o beta_div_2000_sequencing_depth
-m bray_curtis_2000_sequencing_depth
```


Annex Chapter 2

Table 1. Raw data of physicochemical and microbial variables: Temperature (Tem, °C), salinity (salin., ppt), Total Dissolved Nitrogen (TDN, mmol-N l⁻¹), Total Dissolved Phosphorus (TDP, μmol-P l⁻¹), Dissolved Organic Carbon (DOC, mmol-C l⁻¹), and chlorophyll a (Chl a, μg l⁻¹), Prokaryotic heterotrophic abundance (HA, cells ml⁻¹), cyanobacteria abundance (CA, cells ml⁻¹), Bacterial production (BP, pmoles of leucine l⁻¹h⁻¹), Archaeal Production (ArP, pmoles of leucine l⁻¹h⁻¹) and Virus abundance (VA, particles ml⁻¹) for each ponds in the study wetlands.

Odiel Marshes (Odiel/M) Huelva, Spain	Sampling Date (dd/mm/yy)	Tem	Salin.	TN	TDN	TP	TDP	DOC	Chl a	HA (x10 ⁶)	CA (x10 ⁷)	BP	ArP	VA (x10 ⁷)
E1 37°13'08.3"N 06°59'56.7"W	28/05/12	24.7	23.15	n.d.	0.05	7.16	3.66	0.36	n.d.	8.29	103.99	713.94	266.62	0.17
E2 37°12'40.8"N 06°59'43.1"W	29/05/12	21.0	39.27	0.10	0.02	6.26	3.12	0.60	18.21	6.37	1599.42	824.58	916.08	0.29
E3 37°12'40.8"N 06°59'43.1"W	29/05/12	21.2	37.07	0.31	0.05	12.36	7.88	0.87	25.79	8.88	2719.25	468.01	922.51	0.48
E4 37°13'31.2"N 06°59'46.1"W	29/05/12	20.8	61.62	0.31	0.12	20.07	13.62	1.68	108.99	32.58	11968.78	463.24	506.13	0.60
E5 37°13'46.6"N 07°00'48.5"W	28/05/12	23.1	27.84	n.d.	0.03	7.16	4.20	0.38	n.d.	8.42	135.50	1165.86	235.57	0.18
E6 37°13'46.6"N 07°00'48.5"W	28/05/12	25.4	61.15	0.14	0.11	12.72	12.00	1.19	24.34	21.2	2508.49	476.79	336.36	0.50
E7 37°13'46.5"N 07°00'48.5"W	28/05/12	24.9	64.57	0.17	0.10	17.56	12.18	1.28	14.03	19.70	1456.49	888.20	439.43	0.60
E8 37°13'46.5"N 07°00'48.5"W	28/05/12	22.2	80.46	0.21	0.14	39.45	27.97	1.61	39.25	n.d.	4103.46	285.08	329.40	0.50
E9 37°14'07.3"N 07°00'13.8"W	29/05/12	22.1	75.56	0.79	0.23	25.45	17.56	1.64	79.28	26.45	6354.18	276.40	959.76	0.64
E10 37°15'11.9"N 06°59'45.0"W	30/05/12	20.1	83.30	0.56	0.16	25.19	20.79	2.00	35.49	17.61	1423.58	341.11	856.78	0.54
E11 37°15'24.5"N 06°59'31.6"W	30/05/12	20.4	97.72	0.75	0.20	34.33	24.11	2.10	36.20	n.d.	3862.42	346.54	904.76	0.64

E12	37°14'42.5"N 06°59'33.4"W	21.1	106.98	0.44	0.37	41.06	22.76	2.29	39.25	n.d.	5975.27	388.52	946.67	0.61
E13	37°14'07.4"N 07°00'13.9"W	21.9	127.24	0.37	0.32	45.37	27.25	2.85	4.95	n.d.	615.58	495.36	556.67	1.32
E14	37°14'22.7"N 06°59'49.3"W	24.4	n.d.	0.51	n.d.	27.79	24.38	3.51	2.22	n.d.	n.d.	379.84	1106.08	1.81
E15	37°15'21.7"N 06°59'19.6"W	23.3	158.44	1.22	0.43	48.60	34.42	2.20	37.85	29.72	3650.70	396.14	910.86	0.45
E16	37°14'42.5"N 06°59'33.4"W	20.6	97.64	1.04	0.50	32.27	23.97	2.63	18.59	47.89	2109.00	725.69	1112.40	1.02
E17	37°14'42.5"N 06°59'33.4"W	23.5	126.68	0.56	0.29	23.03	21.15	3.11	22.23	90.88	2832.28	636.43	2173.49	1.66
E18	37°14'09.8"N 06°59'41.8"W	22.7	181.48	1.02	0.35	n.d.	48.06	3.78	18.63	130.68	1134.79	115.67	1860.65	2.10
E19	37°14'07.2"N 07°00'13.8"W	21.7	197.80	0.59	0.34	26.08	20.97	3.30	6.00	125.56	293.95	n.d.	1888.60	3.07

Vetla Palma, Doñana
(VPalma)
Sevilla, Spain

	Sampling Date	Temp	Salin.	TN	TDN	TP	TDP	DOC	Chl a	HA (x10 ⁶)	CA (x10 ⁶)	BP	ArP	VA (x10 ⁶)
G3	26/06/12	33.5	34.29	0.59	0.24	9.04	2.88	2.45	n.d.	47.42	51.20	1346.34	1003.16	0.82
G4	26/06/12	29.3	30.90	0.53	0.26	9.81	2.53	2.49	n.d.	83.24	2126.28	615.37	617.96	0.99
A7	26/06/12	31	33.73	0.56	0.24	17.81	12.27	3.11	n.d.	65.91	1314.23	656.83	1378.58	1.14
B6	26/06/12	31.2	14.42	0.38	0.26	n.d	11.30	0.74	n.d.	28.75	1480.18	1234.22	1474.39	0.36
B3	27/06/12	27	17.05	0.42	0.27	4.20	1.48	0.77	n.d.	n.d.	2309.43	917.73	1193.58	0.26
D6	27/06/12	29.4	22.55	0.22	0.18	8.43	1.70	1.17	n.d.	n.d.	175.35	2018.31	712.51	0.47
C2	27/06/12	29	22.57	0.35	0.09	4.35	0.61	1.11	n.d.	25.12	1801.25	1046.37	1001.69	0.27
C3	27/06/12	29.2	17.79	0.42	0.10	4.74	0.51	0.74	n.d.	13.44	3965.91	961.33	932.40	0.20
C6	27/06/12	30.8	21.14	0.41	0.21	7.27	3.27	0.99	n.d.	26.00	960.64	1014.36	1385.32	0.30
A1	27/06/12	31.8	25.27	0.49	0.25	6.58	1.20	n.d.	n.d.	24.68	1273.53	1076.62	980.81	0.63

Cabo de Gata (CGata) Almeria, Spain	Sampling Date	Temp	Salin.	TN	TDN	TP	TDP	DOC	Chl <i>a</i>	HA ($\times 10^6$)	CA ($\times 10^3$)	BP	ArP	VA ($\times 10^3$)
1 36°46'05.6"N 02°13'36.7"W	04/07/12	27.2	36.08	n.d	0.18	n.d.	0.51	0.24	0.26	2.26	4.01	1960.29	327.38	0.04
2 36°46'02.3"N 02°13'38.6"W	04/07/12	24.9	51.8	0.23	0.18	1.58	1.05	0.38	n.d.	9.51	9.51	2185.20	866.06	0.09
3 36°45'40.4"N 02°13'01.3"W	04/07/12	25.4	65.46	n.d.	0.31	3.55	1.35	0.87	n.d.	6.74	7.58	2347.09	468.45	0.09
4 36°45'40.4"N 02°13'01.2"W	04/07/12	25.9	73.02	0.23	0.13	2.04	0.97	0.44	n.d.	8.75	10.58	2438.50	634.15	0.07
5 36°45'17.7"N 02°12'51.9"W	04/07/12	27.6	92.76	0.34	0.25	1.74	0.58	0.55	n.d.	8.05	5.10	1554.77	1084.31	0.09
6 36°45'17.7"N 02°12'51.9"W	04/07/12	26.3	115.66	n.d.	0.18	1.20	2.28	0.65	n.d.	8.78	1.33	2107.50	1012.07	0.12

<i>El Hondo (Hondo) Alicante, Spain</i>	<i>Sampling Date</i>	<i>Temp</i>	<i>Salin.</i>	<i>TN</i>	<i>TDN</i>	<i>TP</i>	<i>TDP</i>	<i>DOC</i>	<i>chl a</i>	<i>HA (x10⁶)</i>	<i>CA (x10⁶)</i>	<i>BP</i>	<i>AVP</i>	<i>AV (x10⁶)</i>
Laguna35 38°11'25.1"N 00°45'00.7"W	12/06/12	24.7	14.33	0.45	0.19	2.37	2.05	2.07	26.95	n.d.	n.d.	612.22	1092.28	0.40
Reserva 38°11'25.2"N 00°45'00.7"W	12/06/12	26.3	15.15	0.81	0.23	1.40	1.31	1.99	28.68	n.d.	n.d.	913.68	1179.17	0.37
Levante 38°11'25.1"N 00°45'00.7"W	12/06/12	26.9	4.3	0.45	0.16	6.76	3.40	1.40	149.63	n.d.	n.d.	735.01	1499.63	0.86
Poniente 38°10'15.3"N 00°44'25.9"W	12/06/12	24.6	14.49	0.90	0.29	9.73	8.96	3.05	67.54	n.d.	n.d.	1268.27	460.93	1.10
Norte 38°11'22.1"N 00°45'09.6"W	12/06/12	24.2	15.83	0.27	0.15	2.55	2.50	1.53	17.86	n.d.	n.d.	948.05	382.72	0.35
Claudio 38°12'12.5"N 00°46'01.8"W	12/06/12	28.9	18.03	0.47	0.29	n.d	3.85	3.26	10.33	n.d.	n.d.	1292.39	316.25	0.36
Balserones 38°11'41.2"N 00°46'46.8"W	12/06/12	30.6	22.03	0.48	0.21	3.98	3.85	2.31	7.30	n.d.	n.d.	1515.10	1263.47	0.60

<i>Santa Pola (Spola)</i> <i>Alicante, Spain</i>	<i>Sampling Date</i>	<i>Temp</i>	<i>Salin.</i>	<i>TN</i>	<i>TDN</i>	<i>TP</i>	<i>TDP</i>	<i>DOC</i>	<i>Chl a</i>	<i>HA</i> ($\times 10^6$)	<i>CA</i> ($\times 10^3$)	<i>BP</i>	<i>ArP</i>	<i>VA</i> ($\times 10^6$)
Calderones 1 38°11'48.1"N 00°36'04.9"W	13/06/12	22.7	69.52	n.d.	0.08	4.50	1.37	1.09	10.24	27.43	190.08	2409.02	990.15	0.10
Seca 1 38°11'53.1"N 00°36'13.1"W	13/06/12	22	71.5	n.d.	0.10	1.37	1.00	0.89	10.79	n.d.	208.72	2003.72	1473.45	0.12
Seca 2 38°12'01.0"N 00°36'19.6"W	13/06/12	25.3	85.62	0.14	0.10	5.86	5.24	0.92	21.98	27.86	208.10	2720.63	1297.21	0.13
Teniente 38°11'51.8"N 00°36'01.9"W	13/06/12	23.6	63.06	0.14	0.13	4.08	3.12	1.08	20.04	8.99	145.74	2828.60	1213.08	0.10
Charco-Lis 38°10'59.0"N 00°37'06.5"W	13/06/12	26.4	35.06	n.d.	0.08	5.06	2.66	0.51	1.59	n.d.	1.44	2456.66	935.08	0.18
Canalets 38°11'11.3"N 00°36'49.3"W	13/06/12	26.1	54.16	0.08	0.06	7.96	7.81	0.77	9.41	28.89	0.23	2121.86	837.72	0.16
Calderones 2 38°11'12.6"N 00°36'49.0"W	13/06/12	25.4	59.48	0.15	0.09	11.33	2.16	0.77	19.05	14.66	3.94	2215.22	1569.87	0.19
Museo Sal 1 38°11'50.1"N 00°34'07.4"W	14/06/12	24.9	81.58	0.22	0.14	5.24	4.21	1.31	51.62	8.19	156.48	1368.96	1421.40	0.49
Museo Sal 2 38°11'50.1"N 00°34'07.4"W	14/06/12	23	113.16	0.53	0.32	6.22	2.58	2.03	201.83	247.20	1970.10	392.70	1025.08	1.11
Loma 1 38°10'08.5"N 00°37'26.9"W	14/06/12	25.2	97.3	0.14	0.12	15.94	8.64	1.11	12.23	6.87	19.12	1458.89	702.75	0.08
Loma 2 38°10'15.7"N 00°37'13.5"W	14/06/12	27.3	162.12	0.25	0.24	8.01	7.45	2.91	18.75	22.96	1.54	879.09	430.48	0.24
Charco Nuevo 38°10'13.3"N 00°37'40.7"W	14/06/12	25.9	35.6	n.d.	0.02	4.13	0.81	0.45	4.17	26.93	11.60	2335.95	565.39	0.02
Raspa 38°10'13.7"N 00°37'40.7"W	14/06/12	26.9	82.24	n.d.	0.11	14.22	11.22	0.87	32.70	46.30	111.81	3006.80	1025.79	0.02
Real 38°10'24.8"N 00°37'46.9"W	14/06/12	25.6	113.54	n.d.	0.11	7.20	n.d.	0.96	20.26	n.d.	134.72	1235.89	860.48	0.02

Ebro Delta (EbroD)		Sampling Date	Temp	Salin.	TN	TDN	TP	TDP	DOC	chl <i>a</i>	HA ($\times 10^6$)	CA ($\times 10^9$)	BP	ArP	VA ($\times 10^9$)
Tarragona, Spain															
0	40°35'13.3"N 00°40'09.9"E	23/07/12	24.7	84.64	n.d.	0.33	3.74	0.81	1.82	9.7	26.70	0.88	780.22	1772.99	0.34
1	40°34'30.7"N 00°39'34.8"E	23/07/12	23.8	46.62	0.42	0.32	2.66	2.20	0.71	6.49	15.46	10.95	2028.50	1354.13	0.15
2	40°34'5.20"N 00°39'41.5"E	23/07/12	25.0	137.16	n.d.	0.24	3.39	1.97	1.27	3.54	n.d.	1.37	930.59	1859.58	0.36
3	40°34'29.3"N 00°40'20.0"E	23/07/12	28.7	80.7	0.47	0.34	7.70	4.51	1.26	5	15.07	2.82	1579.53	1752.18	0.26
4-1	40°35'13.3"N 00°40'10.0"E	23/07/12	24.8	40.58	0.34	0.14	n.d.	3.74	0.52	0.59	7.08	0.51	1787.79	533.72	0.15
4-2	40°34'54.6"N 00°39'08.0"E	23/07/12	29.5	84.74	0.37	0.24	5.50	2.12	n.d.	2.34	29.51	0.82	1049.38	1576.57	0.32
5	40°34'23.7"N 00°40'33.5"E	23/07/12	30.1	82.78	0.40	0.33	7.50	2.35	2.70	0.62	95.54	0.98	n.d.	1581.64	0.09
6	40°34'41.3"N 00°41'26.2"E	23/07/12	32.9	185.68	n.d.	0.59	6.73	4.89	3.12	2.89	6.51	0.40	431.96	973.47	1.62
9	40°35'07.7"N 00°41'56.7"E	23/07/12	27.7	289.1	0.60	0.53	14.42	3.35	5.59	2.19	27.80	0.05	n.d.	1616.00	1.69
10	40°35'07.5"N 00°41'56.6"E	23/07/12	27	343	0.66	0.62	13.96	4.66	5.76	3.06	47.09	0.03	n.d.	1581.72	1.57
C1	40°35'02.5"N 00°41'59.8"E	23/07/12	27	200.12	0.46	0.40	7.20	4.66	2.65	0.39	83.43	0.04	532.63	925.43	1.54
C3	40°35'07.9"N 00°41'56.4"E	23/07/12	28.1	225.6	0.51	0.48	10.04	4.66	4.16	0.04	79.48	0.02	346.83	1726.65	1.38
C4	40°35'15.7"N 00°41'54.6"E	23/07/12	27.8	264.64	0.54	0.50	13.31	5.35	4.57	0.26	80.22	0.01	18.96	2289.87	1.21

Giraud, Saintes-Maries-de-la-Mer (Camargue), France		Sampling Date	Temp	Salin.	TN	TDN	TP	TDP	DOC	Chl a	HA (x10 ⁶)	CA (x10 ³)	BP	ArP	VA (x10 ³)
Enfres		26/07/11	19.1	2.48	n.d.	0.13	5.27	3.12	n.d.	21.60	4.40	43.63	1051.65	908.91	n.d.
43°26'47.7"N 04°37'00.2"E															
Galabert		26/07/11	20.8	6.58	0.12	0.11	7.43	6.49	n.d.	11.96	3.53	23.02	1472.41	310.19	n.d.
43°27'04.0"N 04°35'03.0"E															
Vaccares_1		27/07/11	26.5	11.84	0.13	0.11	n.d.	2.22	n.d.	25.69	5.69	56.52	1672.42	229.02	n.d.
43°32'40.0"N 04°37'54.2"E															
Vaccares_2		27/07/11	26.9	16.94	0.19	0.16	5.09	4.73	n.d.	12.31	8.17	4.48	2142.63	213.83	n.d.
43°33'27.4"N 04°29'26.5"E															
Launes		27/07/11	30.3	6.72	0.11	0.04	4.92	3.12	n.d.	16.13	6.95	257.81	2304.25	242.15	n.d.
43°28'12.0"N 04°24'35.0"E															
Plemason		28/07/11	21.5	7.52	0.14	0.07	3.93	3.65	n.d.	7.34	6.47	1720.68	1073.26	120.12	n.d.
43°21'46.3"N 04°47'46.7"E															
Verdier		27/07/11	25.4	0.22	0.08	0.05	4.56	3.83	n.d.	14.54	3.59	59.78	903.87	257.38	n.d.
43°31'55.6"N 04°41'59.0"E															
Fangassier		26/07/11	24.3	194.75	0.39	0.35	7.43	4.38	n.d.	7.63	16.16	3.58	902.74	1409.63	n.d.
43°26'23.9"N 04°36'53.4"E															
P. Rascallion		28/07/11	21.8	54.74	0.10	0.14	4.74	4.56	n.d.	3.07	9.35	11.93	1182.88	97.19	n.d.
43°24'26.4"N 04°39'38.5"E															
G. Rascallion		27/07/11	22.2	49.4	0.13	n.d.	4.56	3.30	n.d.	2.08	9.72	9.90	828.7	55.72	n.d.
43°25'05.6"N 04°37'18.3"E															
Dame		28/07/11	21.6	48.9	0.14	0.13	n.d.	4.74	n.d.	3.73	12.73	2.65	1069.27	105.13	n.d.
43°23'09.7"N 04°47'30.3"E															
Cincs Francis		28/07/11	22.1	60.65	0.14	0.06	4.56	3.30	n.d.	11.43	7.57	166.92	1290.54	287.33	n.d.
43°22'33.2"N 04°48'08.6"E															
Ursule		28/07/11	22.4	84.95	0.15	0.14	7.25	6.89	n.d.	12.27	19.51	3.09	1624.8	445.49	n.d.
43°21'17.9"N 04°46'59.3"E															
Quentin		28/07/11	22	42.34	0.08	0.07	6.53	3.62	n.d.	2.31	6.78	1.29	1037.35	74.99	n.d.
43°21'17.7"N 04°46'59.3"E															

<i>Molentargius, Santa Guilla and Santa Catherine (Sardinia), Italy</i>	Sampling Date	Temp	Salin.	TN	TDN	TP	TDP	DOC	chl <i>a</i>	HA ($\times 10^6$)	CA ($\times 10^7$)	BP	Ar/P	VA ($\times 10^7$)
Bianca_S23 39°12'33.8"N 09°08'39.3"E	09/07/13	29.5	75.2	n.d.	0.14	6.04	3.20	1.10	37.49	6.53	67.69	843.84	73.34	n.d.
Bianca_S20 39°12'35.9"N 09°08'43.2"E	09/07/13	28.8	50.36	0.12	0.11	2.04	1.89	0.52	6.09	4.14	93.02	921.97	108.43	n.d.
Bianca_S21 39°12'37.9"N 09°08'45.6"E	09/07/13	31.7	58.24	0.13	0.11	8.96	6.81	0.49	9.09	5.58	109.47	1131.45	256.86	n.d.
Quarto_S16 39°13'30.8"N 09°11'55.9"E	10/07/13	25.4	99.32	0.19	0.16	10.66	7.93	2.24	76.19	40.82	294.50	211.84	354.61	n.d.
Minore_S04 39°14'26.0"N 09°09'10.9"E	10/07/13	27.8	1.79	0.11	0.04	n.d.	6.09	1.33	617.41	54.19	16.61	299.71	551.67	n.d.
Maggiore_1 39°14'19.0"N 09°09'02.4"E	10/07/13	28.3	112.6	0.14	0.07	23.8	7.66	2.83	58.27	66.65	1055.02	504.18	546.84	n.d.
Maggiore_2 39°14'14.8"N 09°09'23.6"E	10/07/13	28.1	97.56	0.08	0.05	26.95	10.39	2.74	56.56	58.61	1054.89	370.45	453.26	n.d.
Quarto_S18 39°13'07.3"N 09°09'55.9"E	10/07/13	31.4	238.84	0.39	0.35	34.49	11.35	4.89	8.95	24.73	38.25	n.d.	995.17	n.d.
Culatica 39°13'44.3"N 09°12'53.2"E	10/07/13	31.1	154.2	n.d.	0.14	12.09	n.d.	2.73	29.87	30.65	259.24	482.05	345.07	n.d.
Quarto_S17 39°13'24.6"N 09°11'34.3"E	10/07/13	32.7	160.12	0.13	n.d.	20.57	8.08	3.14	6.67	42.66	29.09	611.26	351.98	n.d.
Santa Guilla_1 39°11'01.5"N 09°02'55.5"E	10/07/13	33.8	83.96	0.14	0.13	11.27	4.89	1.09	28.95	5.43	18.05	1502.96	221.18	n.d.
Capoterra 39°09'42.0"N 09°01'35.7"E	10/07/13	31.2	15.64	0.14	0.06	6.58	0.81	0.34	12.78	7.29	116.52	2060.27	254.17	n.d.
Santa Guilla_2 39°10'20.2"N 09°01'49.9"E	10/07/13	33	51.68	0.15	0.14	4.2	0.85	0.89	12.03	8.56	61.07	1219.99	317.84	n.d.

<i>Sfax</i> (<i>Sfax</i>) <i>Sfax</i> , (Tunisia)	Sampling Date	Temp	Salin.	TN	TDN	TP	TDP	DOC	Chl <i>a</i>	HA ($\times 10^6$)	CA ($\times 10^6$)	BP	ArP	VA ($\times 10^6$)
Tyna 34°38'16.3"N 10°40'05.6"E	12/06/13	24.5	40.56	0.05	0.05	45.76	40.94	0.41	1.89	4.51	2.43	1145.99	211.76	n.d.
AVP_11 34°38'43.1"N 10°42'51.9"E	12/06/13	25.6	54.2	0.20	0.10	7.58	2.67	0.83	37.42	26.29	9882.82	740.2	455.90	n.d.
PE_C1_1 34°38'14.5"N 10°40'07.9"E	12/06/13	25.9	95.48	0.34	0.20	18.11	6.59	1.99	57.89	49.09	4202.70	806.08	459.60	n.d.
AVP_15 34°38'24.4"N 10°41'0.89"E	12/06/13	26.6	62.76	0.37	0.14	17.42	3.14	1.19	84.85	35.21	38105.50	632.76	554.42	n.d.
PE_C3 34°38'43.0"N 10°42'51.6"E	12/06/13	28.3	134.16	0.66	0.25	24.72	5.57	2.60	66.16	85.83	3550.32	212.1	376.68	n.d.
AVP_4 34°40'47.9"N 10°44'43.8"E	12/06/13	28	47	0.12	0.09	n.d.	13.96	0.66	2.35	6.15	0.29	690.84	300.06	n.d.
AVP_17 34°40'50.6"N 10°44'36.1"E	12/06/13	27.5	70.84	0.44	0.15	23.49	6.83	1.51	94.58	55.24	37281.13	238.58	280.31	n.d.
PE_C2 34°40'49.9"N 10°44'44.0"E	12/06/13	28.8	134.12	0.51	0.24	14.65	5.30	2.16	34.52	68.48	4187.92	91.26	493.02	n.d.
PE_C5_F 34°40'53.2"N 10°44'36.6"E	12/06/13	29.6	138.6	0.63	0.28	n.d.	n.d.	2.37	59.87	n.d.	n.d.	219.01	426.46	n.d.
PE_C5_B 34°38'30.8"N 10°41'0.96"E	12/06/13	29.8	94.08	0.59	0.22	n.d.	n.d.	1.85	n.d.	45.13	6074.59	209.07	362.04	n.d.
PI_C3_1 34°38'50.3"N 10°42'37.7"E	12/06/13	27.9	220.16	0.49	0.45	n.d.	22.63	3.49	2.63	22.96	0.06	n.d.	658.26	n.d.
PI_C3_2 34°38'49"N 10°42'50.0"E	12/06/13	27.9	54.88	0.46	0.37	n.d.	19.41	3.15	5.32	50.83	0.62	147.81	382.28	n.d.

Table 2. List of the best models ($\Delta AIC < 2$) of GLM analysis for prokaryotic heterotrophic abundance, cyanobacteria abundance, bacterial production and archaeal production. The models included as continuous predictors: Salinity, Total Dissolved Nitrogen (TDN) and Total dissolved phosphorus (TDP) and as categorical variable: Site. The symbols + and – denotes the positive or negative effects, respectively.

Dependent Variable	Pred. Var. 1	Pred. Var. 2	Pred. Var. 3	Pred. Var. 4	Degrees Freedom	AIC	L.Ratio Chi^2	p-values
Prokaryotic Heterotrophic Abundance	(+) TDN	Site	---	---	8	57.36916	62.91673	0.000000
	(+) Salinity	(+) TDN	Site	---	9	58.42106	63.86484	0.000000
	(+) TDN	(-) TDP	Site	---	9	58.99624	63.28966	0.000000
Cyanobacteria Abundance	(+) TDN	(-) TDP	Site	---	9	278.0048	90.12917	0.000000
	(-) Salinity	(+) TDN	(-) TDP	Site	10	279.4223	90.71176	0.000000
Bacterial Production	(-) TDN	Site	---	---	9	689.1308	89.31962	0.000000
	(-) TDN	(-) TDP	Site	---	10	691.0294	89.42101	0.000000
	(-) Salinity	(-) TDN	Site	---	10	691.1135	89.33690	0.000000
Archaeal Production	(+) TDN	Site	---	---	9	-3.55629	93.84983	0.000000
	(+) TDN	(-) TDP	Site	---	10	-3.47724	95.77078	0.000000
	(-) Salinity	(+) TDN	Site	---	10	-2.39585	94.68939	0.000000
	(-) Salinity	(+) TDN	(-) TDP	Site	11	-2.19648	96.49001	0.000000

Table 3. List of the best models ($\Delta AIC < 2$) of GLM analysis for virus abundance. The models included as continuous predictors: Salinity, prokaryotic heterotrophic abundance (HA) and cyanobacteria abundance (CA) and as categorical variable: Site. The symbols + and - denotes the positive or negative effects, respectively.

Depen. Var.	Pred. Var. 1	Pred. Var. 2	Pred. Var. 3	Pred. Var. 4	Degrees Freedom	AIC	L.Ratio	p-values
Virus abundance	(+)Salinity	Site	---	---	5	17.99998	73.00712	0.000000
	(+)Salinity	(+) HA	Site	---	6	19.84163	73.16548	0.000000
	(+)Salinity	(-) CA	Site	---	6	19.99492	73.01218	0.000000

Table 4. List of the best models ($\Delta AIC < 2$) of GLM analysis for bacterial and archaea production. The models included as continuous variables: Salinity, Virus abundance (VA), Total dissolved nitrogen (TDN) and as categorical variable: Site. The symbols + and – denotes the positive or negative effects, respectively.

Depen. Var.	Pred. Var. 1	Pred. Var. 2	Pred. Var. 3	Pred. Var. 4	Degrees Freedom	AIC	L.Ratio	p-values
Bacterial production	(-) Salinity	(-) VA	Site	---	7	428.1875	80.68874	0.000000
	(-) Salinity	(-)TDN	(-)VA	Site	8	430.0998	80.77642	0.000000
Archaeal production	(+) TDN	Site	---	---	6	-18.0085	27.73965	0.000105
	(+)TDN	(+)VA	Site	---	7	-17.2916	29.02279	0.000143
	(+)Salinity	(+)TDN	Site	---	7	-16.3576	28.08880	0.000212

Table 5. List of the best models ($\Delta AIC < 2$), of GLM analysis for prokaryotic heterotrophic abundance, cyanobacteria abundance, bacterial production and archaeal production. The models included as continuous variables: Salinity, Total Dissolved Nitrogen (TDN) and Total Dissolved phosphorus (TDP), Dissolved Organic Carbon (DOC), and as categorical variable: Site. The symbols + and – denotes the positive or negative effects, respectively. Since DOC data for Camargue were not available this site was removed.

Dependent Variable	Pred. Var. 1	Pred. Var. 2	Pred. Var. 3	Pred. Var. 4	Deg. Freed	AIC	L.Ratio	p-values
Prokaryotic Heterotrophic Abundance	(-)Salinity	(+)DOC	---	---	2	35.62344	54.11647	0.000000
	(-)Salinity	(+)TDN	(+)DOC	---	3	37.35688	54.38303	0.000000
	(-)Salinity	(-)TDP	(+)DOC	---	3	37.54945	54.19046	0.000000
Cyanobacteria Abundance	(+)TDN	(-)TDP	Site	---	8	236.0618	81.42007	0.000000
	(+)Salinity	(+)TDN	(-)TDP	Site	9	237.8034	81.67845	0.000000
	(+)TDN	(-)TDP	(+)DOC	Site	9	237.9371	81.54473	0.000000
	(-)TDP	(+)DOC	Site	---	8	238.0458	79.43604	0.000000
Bacterial Production	(-) DOC	Site	---	---	8	528.7949	99.1869	0.000000
	(+) Salinit	(-) DOC	Site	---	9	528.9185	101.0633	0.000000
	(+) TDP	(-) DOC	Site	---	9	530.7291	99.2527	0.000000
	(-) TDN	(-) DOC	Site	---	9	530.7479	99.2339	0.000000
Archaeal Production	(+)TDN	Site	---	---	8	-18.8662	74.01701	0.000000
	(+)TDN	(-)TDP	Site	---	9	-18.2427	75.39355	0.000000
	(+)TDN	(+)DOC	Site	---	9	-17.5807	74.73155	0.000000
	(+)TDN	(-)TDP	(+)DOC	Site	10	-17.4558	76.60666	0.000000

Table 6. List of the best models of GLM analysis selected according to AIC including the data of dissolved organic carbon (DOC). Camargue was removed since DOC data were not available for this site. Columns show the estimates, standard errors, Wald statistic and P values for selected predictor variables. Site was a categorical variable representing each study wetland.

Dependent Variables	Predictor Variables	Estimate	Standard Error	Wald Stat.	p-values
Heterotrophic Prokaryotic abundance	Intercept	2.081045	0.050571	1693.429	0.000000
	DOC	0.174741	0.031442	30.886	0.000000
	Salinity	-0.061829	0.028704	4.64	0.031241
Cyanobacteria abundance	Intercept	1.866811	0.109208	292.2093	0.000000
	TDN	0.250653	0.094568	7.0252	0.008037
	TDP	-0.299521	0.084389	12.5974	0.000386
	Sites	----	----	98.4199	0.000000
Bacterial production	Intercept	3.451823	0.026299	17226.95	0.000000
	DOC	-0.727185	0.094472	59.25	0.000000
	Sites	----	----	79.28	0.000000
Archaea production	Intercept	1.140738	0.018052	3993.18	0.000000
	TDN	0.141189	0.024873	32.22	0.000000
	Sites	----	----	115.71	0.000000

Annex Chapter 4

Table 1. Results of the simple regression analyses performed to assess the influence of area lake, salinity and flamingos on observed otus richness and Shannon diversity at 5000 rarefaction depths both free-living and attached bacteria community during study period in the Fuente de Piedra lake. Note: observed OTUs richness vs. Lake area were log transformation.

Alpha diversity- at 5000 sequencing depth						
Bacterial lifestyle	Dep Var	Indep Var	Func fit	r ²	p-level	slope
Free-living bacteria (0.2 µm)	Log OTUs	Log Lake area	Linear	0.30	p < 0.01	0.535
	Observed OTUs richness	Salinity	Exp	0.32	p < 0.001	-0.002
		Log Flamingos	Linear	0.22	p < 0.01	52.56
	Shannon diversity	Area lake	Linear	0.32	p < 0.01	0.003
		Salinity	Exp	0.30	p < 0.001	-0.002
		Log Flamingos	Linear	0.11	p < 0.01	0.535
Particle-attached bacteria (3 µm)	Log OTUs	Log Lake area	---	---	---	---
	Observed OTUs richness	Salinity	---	---	---	---
		Log Flamingos	---	---	---	---
	Shannon diversity	Area lake	Linear	0.18	p < 0.05	0.002
		Salinity	Exp	0.16	p < 0.001	-0.001
		Log Flamingos	---	---	---	---

Table 2. Results of permutational multivariate analysis of variance (ADONIS2) of salinity and bacterial composition (Bray – Curtis distance metric) at 5000 rarefaction depth during study period in Fuente de Piedra lake.

Temporal - beta diversity (at 5000 sequencing depth)					
Bacterial lifestyle	Indep Var	Df	R ² (Adonis)	F.Model	Pr (<F) ^{a,b}
Free-living bacteria (0.2 µm)	Lake area		0.21	7.79	p < 0.01
	Salinity		0.18	6.34	p < 0.01
	Log Flamingos		0.11	3.59	p < 0.01
Particle-attached bacteria (3 µm)	Lake area	1	0.14	5.20	p < 0.01
	Salinity	1	0.12	4.49	p < 0.01
	Log Flamingos	1	0.09	3.07	p < 0.01

Table 3. Results of permutational multivariate analysis of variance (ADONIS) of salinity and bacterial composition (Bray – Curtis distance metric) at 5000 rarefaction depth during study period in Fuente de Piedra lake.

Time - beta diversity -5000 depth					
Indep Var	Filter pore size	Df	R ² (Adonis)	F.Model	Pr (<F) ^{a,b}
Salinity	Free-living bacteria (0.2 μm)	1	0.18	6.33	p < 0.01
	Attached bacteria (3 μm)	31	0.99	3.03	p < 0.05

Annex photos Cerdeña

Credit F. Perfectti

























Annex photos Camarga

Credit F. Perfectti & H. Hote

























Gema Laura Batanero Franco

Tesis Doctoral

Julio 2019